THE STABILITY OF THIN SHELLS

by

P.J. MOSS, B.E.(N.Z.), D.I.C.

A Thesis submitted for the Degree of
Doctor of Philosophy in the Faculty
of Engineering of the University of
London

Civil Engineering Department,
Imperial College of Science and Technology,
London.

December 1964

ABSTRACT

Some concepts of stability and buckling are first considered. Previous work concerning the stability of thin shells of cylindrical, spherical, and conical shapes is reviewed and discussed.

The case of the complete circular cylindrical shell acted upon by an axial load is treated in detail. The theory is developed in terms of a stress function and a displacement function. The resulting non-linear equations are solved for the case of a displacement function containing five arbitrary parameters.

The experimental study of the axially loaded cylindrical shell is described. The cylindrical shells were formed from "Darvic" polyvinylchloride plastic. The tests showed that the nature of the material used to bond the shells on to the end caps was a significant factor in influencing the development of the buckling process for the cylinder. In the case of those cylinders where it was possible to measure the minimum load carried in the buckled state, the experimental load-end shortening curve was similar to the theoretical curve over the same range of load and end-shortening. However, the experimental value for the lowest post-buckling load was approximately 0.20 of the calculated classical buckling load, as against the value of 0.3012 predicted by the theory. Thus it would seem that further terms are required in the displacement function in order to fit the theory to the experimental results.

ACKNOWLEDGEMENTS

The author has been privileged in conducting this research under the general guidance of Professor A.L.L. Baker, D.Sc., M.I.C.E., M.I.Struct.E.

Detailed guidance and general assistance was given by Dr. J. Munro and Mr. J.C. de C. Henderson, for which the author is indebted to them both.

The experimental work, which was carried out in the Concrete Structures Laboratory, would have been impossible without the generous assistance of Dr. C.W. Yu and the laboratory staff of the Civil Engineering Department, and their help is gratefully acknowledged. Mr. R.W. Loveday has given many helpful suggestions and advice concerning the design of the testing frame and the use of equipment. Mr. N.D. Scott has also given many useful suggestions for the design and fabrication of the testing frame, and its fabrication was ably supervised by him.

The digital computing was carried out by the University of London Institute of Computer Science and the author wishes to thank the staff for their assistance and their generous allocation of computing time.

The kindness of Professor J. Kempner in suppling a copy of his numerical results for comparison is greatly appreciated.

Special thanks are due to Mr. S.Z. Uzsoy, both for assistance with the experimental work and the checking of the typescript of this thesis. Mr. D. Gunesekera has also assisted with the experimental work and his help is much appreciated.

The author is grateful to the New Zealand Ministry of Works for their consent to carry out this research and for their financial support during this time.

CONTENTS

	page
Abstract	2
Acknowledgments	3
Contents	5
List of Figures	9
List of Plates	11
List of Tables	12
Notation	13
1) INTRODUCTION	
1.1 The definition of thin shells	20
1.2 Concrete shells	21
1.3 Scope of research	24
2) GENERAL BACKGROUND TO THE CONCEPTS OF STABILITY AND BUCKLING	
2.1 Introduction	25
2.2 Buckling	25
2.3 Stability theories	28
2.4 Methods of determining stability	31

page

3) CYLINDRICAL SHELLS

3.1 Introduction 35

3.2 External Pressure 39

3.3 Torsion 55

3.4 Axial Compression 72

3.5 Bending 99

3.6 The effect of internal pressure 102

3.7 Combined loadings 115

3.8 Discussion 118

4) SPHERICAL SHELLS

4.1 Introduction 120

4.2 Experimental work 121

4.3 Complete spherical shells 124

4.4 Spherical segments 127

4.5 Dynamic analysis 136

5) CONICAL SHELLS

5.1 Introduction 139

5.2 External pressure 140

5.3 Axial compression 145

5.4 Torsion 147

5.5 Combined loadings 147

page

6) GENERAL APPROACH TO THE DERIVATION OF THE EQUATIONS GOVERNING STABILITY, AND THE METHODS OF SOLUTION

6.1 General 149

6.2 Calculus of variations 151

6.3 The principle of total potential energy 156

6.4 Rayleigh-Ritz method of solution 157

6.5 Galerkin's method 159

6.6 Solutions of systems of nonlinear equations 161

6.7 Numerical methods for minimising a function 166

7) DERIVATION OF THE NONLINEAR STABILITY EQUATIONS FOR THE CYLINDRICAL SHELL

7.1 Basic equations 169

7.2 Equilibrium equations 173

7.3 Choice of displacement functions 175

7.4 Five parameter function 178

7.5 Six parameter function 189

7.6 Seven parameter function 192

7.7 Ten parameter function 195

page

8) THEORETICAL RESULTS

8.1 Introduction 200

8.2 Previous methods 200

8.3 Partial elimination method - based on Thielemann's method 202

8.4 Newton-Raphson method 205

8.5 Rosenbrock method 207

8.6 Fletcher-Powell method 209

8.7 Numerical results - five parameter case 211

8.8 Numerical results - other cases 224

8.9 Discussion 225

9) EXPERIMENTAL WORK

9.1 Introduction 227

9.2 Testing frame 227

9.3 Dynamometers 231

9.4 Cylinders 236

9.5 Method of testing 238

9.6 Results 240

9.7 Discussion 255

10) DISCUSSIONS AND CONCLUSIONS

10.1 Discussion 258

10.2 Conclusions 261

REFERENCES 262

ADDITIONAL REFERENCES 280

LIST OF FIGURES

page

2.1 Post buckling behaviour of structural elements in compression 27

3.1 Typical post buckling functions for cylindrical shells under various loading conditions 37

3.2 Comparison of experimental results with theory for circular cylindrical shells 44

3.3 Increments of potential energy versus deflection parameter 54

3.4 Potential energy barriers separating buckled and unbuckled forms for circular cylindrical shells under external pressure 54

3.6 Comparison of test data with theory for circular cylindrical shells under torsion 58

3.7 Postbuckling behaviour of cylindrical shells under torsion with varying geometric parameter 59

3.8 Loo's comparison of his theory with results of pure torsion tests 66

3.9 Diagrammatic representation of variation of axial stress with end shortening 84

3.10 Buckling in an elastic testing machine 84

3.11 Theoretical behaviour of axially compressed cylindrical shell 85

3.12 Column supported laterally by nonlinear spring 86

3.13 The effect of initial imperfections on the stress-shortening diagram for an axially compressed cylindrical shell 87

3.14 Donnell's plot of peak value of stress ratio against R/t with results of axial compression tests 95

3.15 Post buckling functions for internally pressurised cylinders 106

page

3.16	Effect of internal pressure	106
4.1	Modes of initial deformation	125
4.2	Theoretical and experimental results for buckling of shallow spherical caps	135
7.1	Cylinder and coordinate system	170
8.1	Flow diagram - generalised Newton-Raphson method	206
8.2	Flow diagram - Rosenbrock's steepest descent method	208
8.3	Flow diagram - Fletcher-Powell method	210
8.4	Load-end shortening diagram (linear plot)	215
8.5	Load-end shortening diagram (log.-linear plot)	216
8.6	Variation of total potential energy	217
8.7	Variation of strain energy	218
8.8	Variation of parameter values for five parameter deflection function	219
8.9	Variation of radial displacement with stress	220
8.10	Variation of radial displacement with end-shortening	221
9.1	Details of testing frame	228
9.2	Dynanometer details	232
9.3	Wiring diagram for 5^T dynamometer to make four arm bridge	233
9.4	Results for test 3/3	245
9.5	Results for test 3/8	246
9.6	Results for test 5	247
9.7	Results for test G3	248

LIST OF PLATES

		page
3.1	Typical buckling patterns for cylindrical shells	38
9.1	Testing frame	229
9.2	5^T dynamometer	234
9.3	Buckle pattern - cylinder 5	249
9.4	Buckle pattern - cylinder 9	250
9.5	Buckle pattern - cylinder G/4	251

page

TABLES

3.1	Interaction formulae	117
8.1	Numerical results for five parameter case	213
9.1	Experimental data	241
9.2	Experiment results	242

NOTATION

The notation used in Chapters 3, 4 and 5 is not fully listed below, but is generally defined where it is first used.

A_{ij} Fourier coefficients for stress function

D flexural rigidity $= \frac{Et^3}{12(1-\nu^2)}$

E modulus of elasticity

L length of cylinder

K_x, K_y, K_{xy} axial, circumferential and torsional curvatures

M_x, M_y, M_{xy} axial, circumferential and torsional bending moments

N applied average axial compressive shell action

Ncl classical buckling shell action

N_x, N_y, N_{xy} axial, circumferential and shear middle surface shell actions

$N^* = \frac{N}{Ncl} = \frac{\sigma}{\sigma cl}$

R radius of cylinder, or sphere, average radius for cone (i.e. $= \frac{R_1 + R_2}{2}$)

R_1 larger end radius of cone

R_2 smaller end radius of cone

W_1 elastic strain energy for extensional forces

W_2 elastic strain energy in bending

W_3 potential energy of axial load

W_4 potential energy of pressure loading

Z, Z_L geometric parameter

a_o, a, b, c, d, e deflection function parameters

a_{ij} Fourier coefficients for deflection function

c_p pressure parameter $= \frac{pRL^2}{D\pi}$

l_x, l_y axial and circumferential halfwavelengths

m, n number of axial and circumferential buckles

p pressure (external or internal)

t wall thickness

u, v, w axial, circumferential and radial displacements

w_o radial displacement of imperfect surface

x, y, z axial, circumferential and radial coordinates on the middle surface of the shell

suffixes cl, cr refer to the classical buckling and critical values of the particular parameter.

$\beta = \frac{\pi^2 R}{ly}$ parameter of the total potential energy expression

E_x, E_y, E_{xy} middle surface axial and circumferential normal strains and shear strain

ε end shortening

ε_{cl} = $\dfrac{1}{3(1-\nu^2)}$ $\dfrac{t}{r}$

ε^* = $\varepsilon/\varepsilon_{cl}$

λ geometric parameter = ρ

μ ratio of half wavelengths, ly/lx

ν Poisson's ratio

ξ, ξ_o constants, coordinate values

π total potential energy

π^* $\pi \div (1/4\ \pi r l)$

ρ geometric parameter = $\dfrac{R}{t}\ \sin^2\alpha\ \sqrt{12(1-\nu^2)}$

σ applied average axial compressive stress

σ_x, σ_y middle surface axial and circumferential stresses

σ_{cl} classical buckling stress = $\dfrac{1}{\sqrt{3(1-\nu^2)}} \cdot \dfrac{Et}{r}$

τ shear stress

ϕ stress function

∇^2 = $\dfrac{\partial^2}{\partial x^2} + \dfrac{\partial^2}{\partial y^2}$

∇^4 = $\nabla^2 . \nabla^2$

∇^8 = $\nabla^4 . \nabla^4$

CHAPTER 1

INTRODUCTION

Thin shell structures have been used for a considerable time now in building construction, as well as in applications in astronautics and aeronautics. They have the general properties: they are three-dimensional, and their thickness is small compared to their other dimensions; the major part of the load coming on them is carried by forces acting in the middle-surface of the shell; and the same members are used for load-carrying and for enclosing the desired space.

In spite of the increasing amount of attention that is being given to the problem of stability of thin shells, much less is known here than is the case for the separate problem of the stress analysis of shells. This thesis considers some of the problems that relate to the stability of thin shells.

1.1 The definition of "thin" shells

While there is frequent reference to the term "thin shell", throughout the literature, there does not seem to be any definition to go with it that draws the line between "thick" and "thin" shells. Novozhilov [150] arbitarily limits thin shells to those whose t/R ratio is less than 1/20. Vlasov [163] restricts thin shells to those for which the t/R ratio is less than 1/30.

Another limitation introduced for the theoretical and experimental work described in this thesis, is that the shells were to be sufficiently thin that the buckling stress was below the elastic limit for the particular material. By limiting the stresses and strains to those within the elastic range, the material properties could be specified by two parameters only, viz. Young's modulus (E), and Poisson's ratio (ν).

1.2 Concrete Shells

From time to time, it has been said that the stability of large thin, concrete shells will become a problem as shells are built to cover larger and larger areas. So far, little has been done to check the validity of these suggestions. The considerable amount of experimental work that has been carried out on concrete shells, has been almost exclusively to check stress theories and not stability theories. In some of these tests, it has been stated that the final failure of the shell was due to "buckling", though it has seldom been made clear just what this implied.

A series of six tests carried out by Lundgren in 1943, and reported in 1945 [158] appear to be the only tests that have been carried out to investigate the stability of concrete shells. The shells were cylindrical ones, and were loaded on four regions only as it was hoped that this would provide the worst loading distribution for the shell. Under these loading conditions, it is not surprising that a "wave"

developed in the surface as the loads were increased, and the explanation that this "wave" was due to "buckling" - and seemingly implying a change in the stability of the shell - does not seem warranted.

In discussing the stability of thin, concrete shells generally, it is recognised that there are other problems that occur in addition to those for metal shells. One factor here is the physical nonlinearity of the material (i.e. in the stress-strain relationship), which must be taken into account at all stages of loading. Other factors are cracking, and creep. Morice (1951) [159] suggested that for the buckling failure of a shell roof, the solutions will be much the same as those of a curved plate or the complete tube in bending. This, he suggested, was because failure is localised within the region of maximum stress where it is little affected by the shell boundary conditions. This may be true for some types of shells, but for many types of concrete shell roof it is well known now that boundary conditions do affect the distribution of stress throughout the entire shell. Also, it appears that even for complete shells - such as the cylindrical shells - whose stability is reviewed in Chapter Three - the influence of the end boundary conditions is significant. Hence it seems reasonable to consider the buckling behaviour of concrete shells to be influenced by the boundary conditions.

The most recent attempt to discuss the stability of concrete shells appears to be that of Bradshaw (1963) [150]. He took the theoretical and experimental results for metal and plastic (material)

shells, and sought to apply them to concrete shells. At the present time, this is still an unsatisfactory thing to do on account of several factors:-

1) Both the theoretical and experimental work that have been carried out to date to investigate stability (for shells other than spherical), have been with reference to complete shells, and not segments of complete shells as used in building structures. As Bradshaw himself recognised, boundary conditions will almost certainly complicate the analysis for the shells used in buildings.

2) The actual properties of concrete cannot be described with just the same parameters as metal. The inelastic behaviour of concrete is not the same as plasticity in metals. It is not satisfactory to allow for the inelastic behaviour of concrete merely in terms of Poisson's ratio and the modulus of elasticity. Both of these are difficult to measure accurately, and in any case their values will be affected by variations in the amounts of reinforcing steel used.

3) The use of interaction formulae to allow for the effects of combined stresses is satisfactory, providing the formulae give reasonable results. As far as is known, none of the proposed interaction formulae for isotropic shells have been checked experimentally for concrete, and consequently they are of doubtful value.

The full investigation of the stability of concrete shell roofs can be broken down into two parts, viz. the structural aspect and the material aspect. Both these parts of the problem are involved in

themselves, and further work needs to be done in connection with each before reliable conclusions can be reached concerning the combined effect.

The work reported in this thesis is an attempt to summarise the present state of knowledge concerning the stability of thin shells, and to contribute towards a better understanding of the stability of the axially compressed cylindrical shell. Knowledge gained from these would then be of value in determining how best to treat the stability of the structural shapes used for concrete shells.

1.3 Scope of Research

a) To review the literature concerning the stability of cylindrical, spherical and conical shells;

b) To investigate the stability of the axially compressed cylindrical shell both experimentally and theoretically.

CHAPTER TWO

GENERAL BACKGROUND TO THE CONCEPTS OF STABILITY AND BUCKLING

2.1 Introduction

Throughout the literature, there is widespread use of the terms "stability" and "buckling".

Stability is a term that is reasonably well understood, for consider a device of some sort that operates under certain general conditions. These conditions are changed slightly. Does the change have little or considerable effect upon the device? In the first case it is considered to be stable, and in the second as unstable. The term "buckling" on the other hand, is used in many different ways and requires definitions when used in a particular instance.

In this Chapter, a definition of buckling is given, and the various ideas of stability and buckling are considered. In addition, the various methods that are useful in evaluating stability are considered.

2.2 Buckling

For the purposes of this thesis, the buckling load is defined as the load at which large nonlinear deflections are initiated in the structure. The usefulness of this definition in relation to the different buckling behaviour of the different members, is illustrated

by the four cases that follow. This is illustrated diagramatically in Figure 2.1. In what follows, the "critical" load referred to in each case is the eigenvalue of the boundary-value problem as described in Section 2.3.1.

(a) slender column

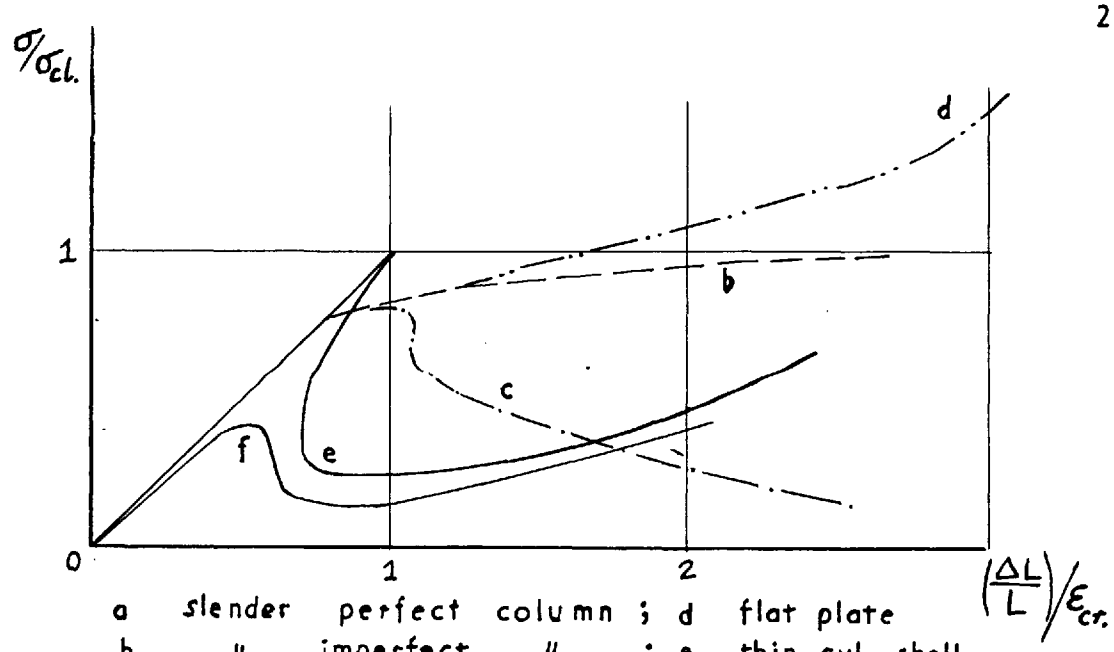
For a slender perfect column, the lateral deflection of the column is infinitesimal up until the critical load, when it becomes indefinitely large. For the imperfect column there is a more gradual transition with the deflection tending to infinity as the critical load is approached.

(b) thin, rectangular plate

Here the deformation process takes place so gradually that the "collapse" load (which is taken to be the load at which the deformation becomes greater than acceptable), is all that can be determined experimentally or practically. This collapse load is usually found to be several times greater than the critical load.

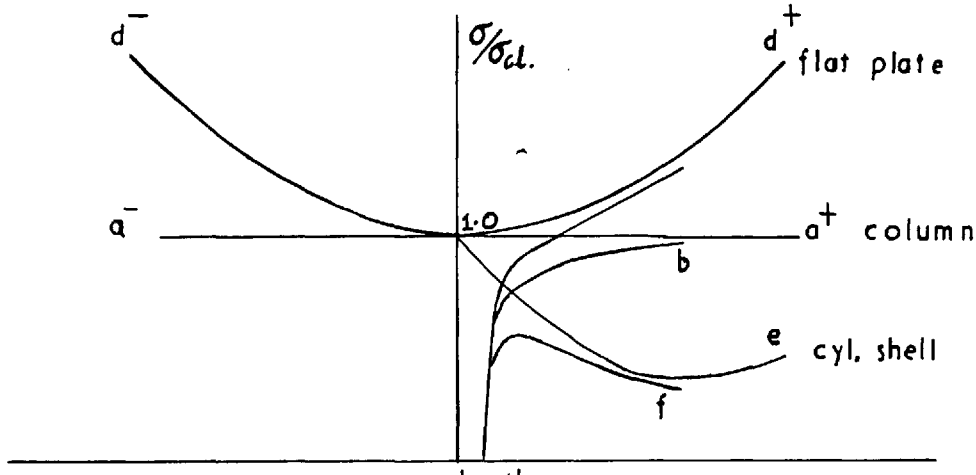
(c) cylindrical shell

This buckles at a load which is very much smaller than the critical load with deformation being linear only up until buckling takes place. The buckled form has a deflection normal to the surface that is of the same order as, or greater than, the thickness. The shell behaviour is governed by nonlinear differential equations.



a slender perfect column ; d flat plate
b " imperfect " ; e thin cyl. shell
c col. of medium slenderness ; f thin imperfect cyl. shell

STRESS RATIO AS A FUNCTION OF BUCKLING STRESS RATIO.



BUCKLING STRESS RATIO AS A FUNCTION OF BUCKLE WAVELENGTH.

FIG. 2.1 : POST BUCKLING BEHAVIOUR OF STRUCTURAL ELEMENTS IN COMPRESSION.

(d) hyperbolic paraboloid shell

The experimental work of Batchelor [7] shows that as the load on the hyperbolic paraboloid shell was increased, the load-displacement relation became nonlinear and the maximum vertical displacement was very much greater than its thickness. At this stage the shell was "buckled" according to the definition given, though the particular stage in loading at which this occurred was not as obvious as in the case of the axially loaded cylindrical shell.

For the case of thin shells, some discrepancies have arisen over the use of the term - "buckling load". This has occurred particularly for the case of external pressure loadings on cylindrical and conical shells where some researchers have taken the buckling load as the load at which the first buckle appeared, while others have given it as the load that was carried when the buckling pattern became fully developed. It seems preferable to define the "buckling load" as at the beginning of this Section, and to use other expressions to describe any additional experimental features.

2.3 Stability Theories

The various theories used to predict or describe the phenomenon of stability are based on assumptions that are made concerning the magnitudes of strains and displacements. The complete theory making no assumptions at all, would appear impossible to solve, and so requires to be simplified in one way or another, in order to reduce its

complexity. The various assumptions have given rise to a number of descriptions for the various approaches, and these are outlined in this Section.

2.3.1 Classical Theory

This is based on the assumption that a given state of equilibrium becomes unstable when there are equilibrium positions infinitesimally near to that state of equilibrium and under the same external load. The classical stability criterion is concerned with a continuous load-deformation process involving prescribed loads, unlike a dynamic criterion which may consider rapidly varying loads. The reasoning underlying the classical criterion for stability is that at very small displacements under a load slightly less than the critical load, the shell will return to its original position; at a load that is slightly greater than the critical load, the shell on being given a very small displacement may move away to a new position of equilibrium. Hence at the critical load, the shell is assumed to remain displaced and for this to be the case there must be an adjacent equilibrium position under this same load.

The classical stability theory assumes both the strains and the displacements to be infinitesimal, and in this case the strains can be expressed as linear functions of the displacements. The result is that the governing equations for the shell stability become linear differential equations in terms of either the stresses or the displacements. Thus the classical buckling load is obtained as the

critical, characteristic, or eigenvalue, solution of the differential equation and for this reason it is generally referred to as the critical load.

2.3.2 Finite Displacement Theory

Here, both the strains and the displacements are considered to be finite, and it is necessary to take geometrical nonlinearity in the strain-displacement relations into account. It is possible that even when both strains and displacements are infinitesimal, they may be connected by a nonlinear relation due to physical nonlinearity, but this is not considered as a feature of this Section or of this thesis.

In order to simplify the strain energy and potential energy expressions, it is usual in most problems to neglect terms involving powers higher than the fourth in the displacements and their derivatives.

This simplification does place a limit on the usefulness of these expressions where they are used. For those cases where the strains and displacements are large, and the above simplification is not valid, then it is preferable to refer to a "large displacement theory".

2.4 Methods of determining Stability

The methods used to treat elastic stability problems are:-

(a) equilibrium method

(b) energy method

(c) imperfection method

(d) dynamic (vibration) method.

2.4.1 Equilibrium Methods

The basis of the general theory of the stability of mechanical systems was developed by Poincaré (1885) [94] in his study of the stability of rotating masses of fluid. When the load on the mechanical system increases, Poincaré found that the coordinates representing equilibrium states, describe certain paths. Usually there is only one path when the load is small, but "bifurcation" points could occur at higher loads. Poincaré assumed that the unbuckled state represented by the stem of the path, becomes unstable after a bifurcation point is reached.

The eigenvalue approach to the buckling problem, by considering the equilibrium equations for the slightly deformed system, is called the equilibrium method of determining stability.

2.4.2 Energy Method

The energy theory of buckling was first formulated by Bryan [15] in 1888, and is based on the principle of minimum potential energy. Here, the total potential energy of the system is to be such that its first variation is zero.

i.e. $\pi = \text{const}$

$$\delta\pi = 0$$

Usually the Rayleigh-Ritz method of solution is used in conjunction with the total potential energy expression to give a solution in terms of the system of equations.

$$\frac{\partial\pi}{\partial a_i} = 0$$

where the a_i are arbitrary parameters.

The method is described and discussed more fully in later chapters.

2.4.3 Imperfection Method

For any mechanical system, the behaviour of the geometrically perfect system may be regarded as the limit that results if certain imperfections, eccentricities, or auxiliary loads, approach zero. When imperfections in the system are present the limit will not be reached, and the discrepancy between the buckling loads for the perfect and imperfect systems depends on the size of the initial imperfections.

This approach to stability theory is known as the "imperfection method". In effect, the stability problem is transformed into a nonlinear equilibrium problem for which a maximum load can be obtained. In some cases it has been found that the presence of even small imperfections will reduce the buckling load greatly below that for the perfect system.

A slightly different imperfection problem is that of creep. This is dependent both on the magnitude of the imposed stress, and time. Up until recently, research into the effects of creep had been mainly concerned with uniaxial stress systems, such as columns and the knowledge of creep effects for biaxial and triaxial stress systems was limited. At the present time, a great deal of research is being carried out in connection with these latter stress systems, but the picture is still far from complete. On account of this it seems premature to go to any great lengths to include this "imperfection" from the material into an analysis of the behaviour of the structure. For shells made from a material such as concrete, creep may have considerable effect on the stability, and will require to be taken into account.

2.4.4 Dynamic Method

The dynamic or vibration method for treating stability problems is based on the principle that a system undergoing infinitesimal vibrations will have a fundamental frequency that becomes zero at the critical load. For example, the fundamental frequency for

infinitesimal vibrations of a statically loaded straight column decreases as the axial load increases and becomes zero when the Euler buckling load is reached.

The "static" approaches, i.e. the imperfection, energy and equilibrium methods, are useful for those classes of problems where the applied loads are conservative, but for the general case where the loads are nonconservative then the dynamic method must be used.

For the particular problems of the axially loaded cylindrical shell and the spherical shell, the equations of motion of the shell are solved in terms of a deflection function, the arbitrary parameters of which are assumed to be functions of time. Numerical integration of the parameters is then possible, and the behaviour of the shell at buckling can be studied.

CHAPTER 3

CYLINDRICAL SHELLS

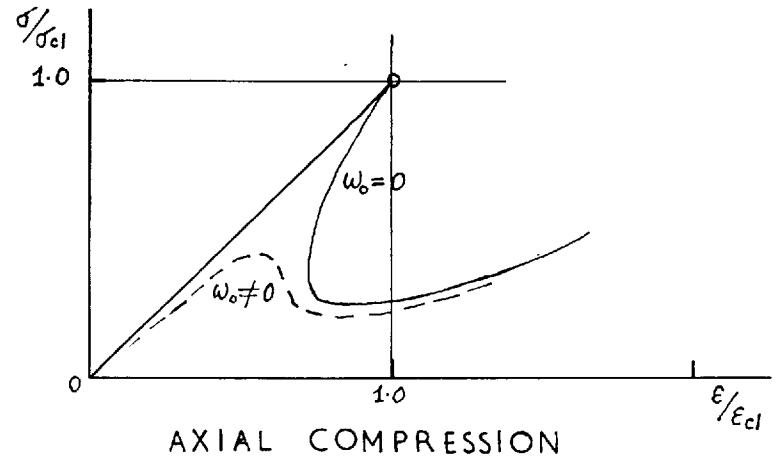
3.1 INTRODUCTION

In the development of the stability theory of thin shells, the majority of the work has been carried out in reference to shells in the form of circular cylinders, or spheres. For spheres or spherical segments, the loading conditions imposed have been those of external pressure. In the case of cylinders, the types of loading that have been considered include: torsion, external pressure, and axial compression, as well as combinations of these. The effect of internal pressure on the stability has also been considered.

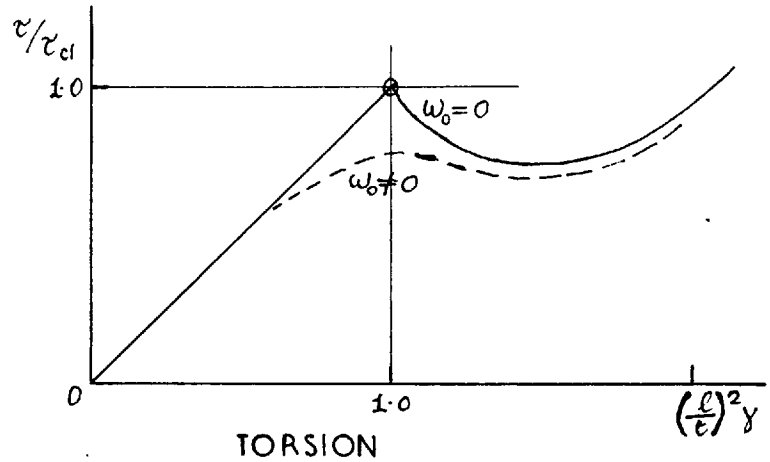
The majority of the experimental work has been carried out on tubes of aluminium, steel, or brass, though celluloid has been used to a limited extent. The end conditions under which the cylinders have been tested have ranged from simply supported to the clamped case. For the case of cylindrical shells under axial compression, Kanemitsu and Nojima [149] (1942), working at Cal. Tech., California, concluded that the end conditions of the shell have no influence on the stability of cylindrical shells providing $L > 1.5\ R$. This result appears to have been accepted by

many subsequent researchers, and has been taken as a basis for neglecting end conditions in both theory and experiment, not only for this same loading case but others as well. However the work of Hoff [57, 89,155] shows that a "free" edged cylindrical shell can buckle at less than the classical load due to instability of the "free" edge. The importance of this edge instability has not been widely accepted and it seems that the effect of end conditions on the buckling load is an open question at the present time.

Initially, all the theoretical investigations of the stability of cylinders were based on the classical (linear) theory. However, it was found that there was a discrepancy between the theoretical buckling load and the experimentally observed buckling load, this discrepancy being considerable in the case of axial compressive loading. Recent post buckling (finite deflection) analyses of the stability of cylinders have helped to give an understanding of the nature of this discrepancy. Figure 3.1 shows the postbuckling functions for the axial compression, torsion, and external pressure loading cases. This shows the considerable decrease in axial load that can be sustained by the axially compressed cylindrical shell after buckling. In the case of torsion, the decrease is not so great, while for external pressure the fall in the load carried is quite small, and may not occur at all. In Figure 3.1

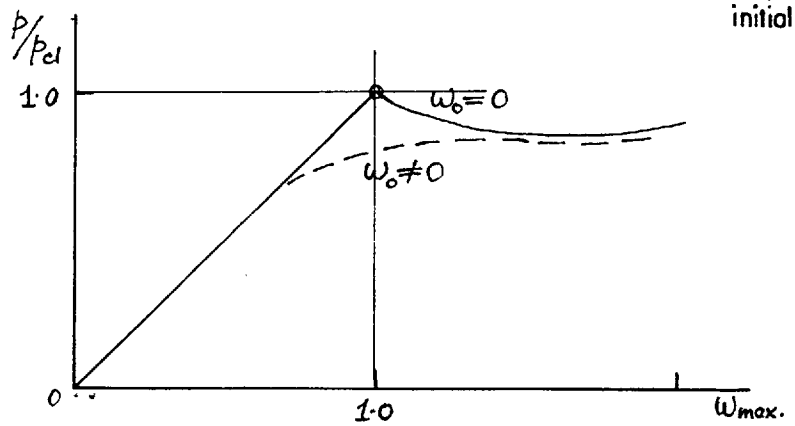


AXIAL COMPRESSION



TORSION

ω_o = amplitude of initial imperfection.



EXTERNAL PRESSURE

FIG. 3.1 : TYPICAL POSTBUCKLING FUNCTIONS FOR CYLINDRICAL SHELLS UNDER VARIOUS LOADING CONDITIONS (Diagramatic only)

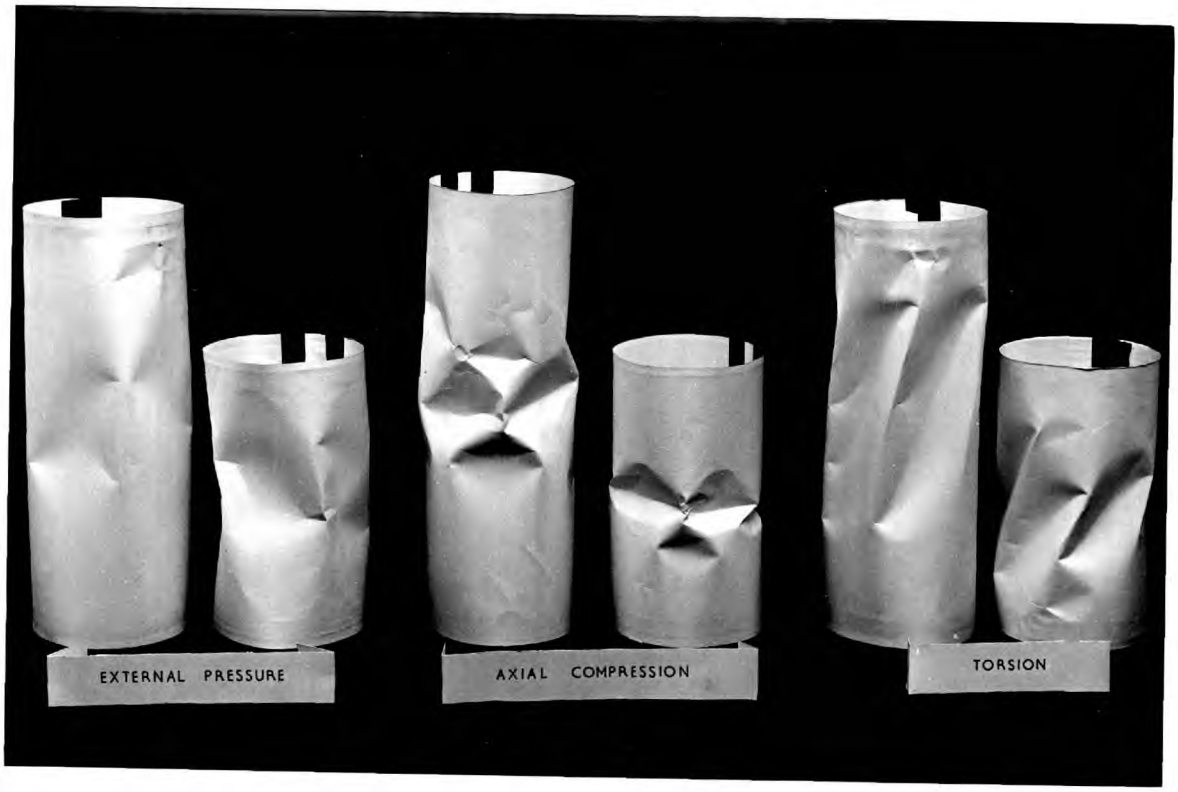


Plate 3.1. Typical buckling patterns for cylindrical shells.

the full line corresponds to the post buckling function of a perfect cylindrical shell, while the dashed line represents the trend of the post buckling function when the shell has initial imperfections. Some idea of the displacement pattern for the main loading cases can be gained from Plate 3.1.The model shells were made of paper for the purposes of demonstration.

In what follows in this Chapter, the terms "cylindrical shell" and "cylinder" both refer to a "circular cylindrical shell".

3.2 EXTERNAL PRESSURE

3.2.1 Introduction

For the buckling of circular cylindrical shells under external pressure, there are two cases to consider. Firstly, there is the case of radial pressure acting on its own, and secondly, there is the case of hydrostatic pressure. Hydrostatic pressure consists of the radial pressure acting on the walls of the cylinder, together with the same pressure acting axially on the ends of the cylinder.

Sturm's work has shown that the effect of an axial load up to the value reached under hydrostatic pressure, does not greatly alter the buckling mode of the cylinder from that which would be found if the lateral pressure were acting alone.

3.2.2 Experimental Work

From Sturm's tests (1941) [121], it can be seen that circular cylindrical shells when subject to radial or hydrostatic pressures, buckle into a fluted form. The number of lobes or flutes into which the cylinder buckles, depends to a large extent on the length of the cylinder. In general, the smaller the L/R ratio of the cylinder, the more flutes will form when the cylinder buckles. It would appear that for $L/R > 10$, the simply-supported cylinder buckles into a form with two flutes, while below this value the number of flutes formed increases as the L/R ratio decreases, reaching about six for $L/R = 2$. For fixed-end cylinders, the number of flutes formed is one more than in the case of simply-supported ends, at any value of L/R.

Windenberg and Trilling (1934) [143] carried out tests on the buckling of thin cylinders acted on by hydrostatic pressure.

3.2.3 Classical Approach

The earliest work on the stability of cylinders acted upon by external pressure is given by the work of Levy (1884), in connection with the buckling of circular rings. Levy considered a unit width circular ring which was deformed from the circular shape under action of a uniform pressure, p. The calculation for the moments of this deformed ring, which arise from both the external pressure and the membrane load, showed that the

moment went to infinity at a value of p given by:

$$p_{cr} = \frac{3EI}{R} \tag{3.1}$$

If the ring were considered to be a unit section out of an infinitely long cylinder, then $I = \frac{t^3}{12(1-\nu^2)}$. Therefore, the critical external radial pressure for such an infinitely long cylinder (with no axial load on the cylinder), is:

$$p_{cr} = \frac{E}{4(1-\nu^2)} \left(\frac{t}{R}\right)^3 \tag{3.2}$$

This formula only applies to the case of an infinitely long cylinder, where end conditions have no effect and so need not be considered.

Bryan (1888) [15] applied the buckling of rings to the stability of long cylinders. Lorenz (1908) [79] and Southwell (1913) [119] considered the case of short cylinders where the constraint at the edges provides a stiffening effect to the shell.

In 1914, von Mises [84] developed a more accurate formula for the critical pressure of a short cylinder. He introduced an assumed deflection pattern which reduced the deflection and moments at the cylinder ends to zero (i.e. to simple support). The analysis was a small-displacement one. Since the length was taken into consideration, the pressure, p, is

a function not only of the modulus of elasticity of the material (E) and the R/t ratio, but also of the L/R ratio. The resulting equation is:

$$\frac{(1-\nu^2)\, p_{cr}\, R}{Et} = \frac{1-\nu^2}{(n^2-1)(1+n^2L^2/\pi^2R^2)} + \frac{t^2}{12R^2}\left\{n^2-1+\frac{2n^2-1-\nu}{1+n^2L^2/\pi^2R^2}\right\} \qquad (3.3)$$

Von Mises and others have also considered the case of hydrostatic pressure where the axial load has to be taken into account.

Sturm (1941) [121] not only carried out experimental work on the buckling of cylinders under external pressure, but also carried out an analytical investigation of their behaviour up to the "collapse" load, i.e. up to the buckling load. In this analysis, he not only considered the effects of the end supports, i.e. fixed and simply supported ends, but also extended his analysis to cover the plastic behaviour of the material, the "out-of-roundness" of the cylinder, and the stiffening effects of ring-stiffeners. In taking into account the initial "out-of-roundness" of the cylinder, it was assumed that this would correspond to the actual configuration at collapse. Sturm's tests show that this was not always the case, for the tests were in better agreement with his analytical results for perfect

cylinders rather than those that allowed for the "out-of-roundness".

In 1947, Batdorf [8] applied the Donnell equations to the cases of a cylinder under radial pressure and hydrostatic pressure. The results were presented in terms of two parameters, viz.

a pressure parameter $$C_p = \frac{pRL^2}{D\pi^2}$$

and

a geometric parameter $$Z_L = \left(L^2/Rt\right)\sqrt{1-\nu^2}$$

Figure 3.2 shows the graph of the pressure parameter against geometric parameter and shows Sturm's experimental results for comparison, for the cases of radial pressure acting alone and for hydrostatic pressure.

The theoretical curves show reasonable agreement between theory and experiment, except for values of $Z_L < 100$ in the case of hydrostatic pressure. It seems probable that these discrepancies at low values of Z_L are due to the fact that for these cases, the axial stress predominates. In Section 3.4.2 it is pointed out that for the axially loaded cylinder, the experimental results are much lower than the theoretical values, and it is more than likely that the ratio of radial stress to axial stress is important in determining the

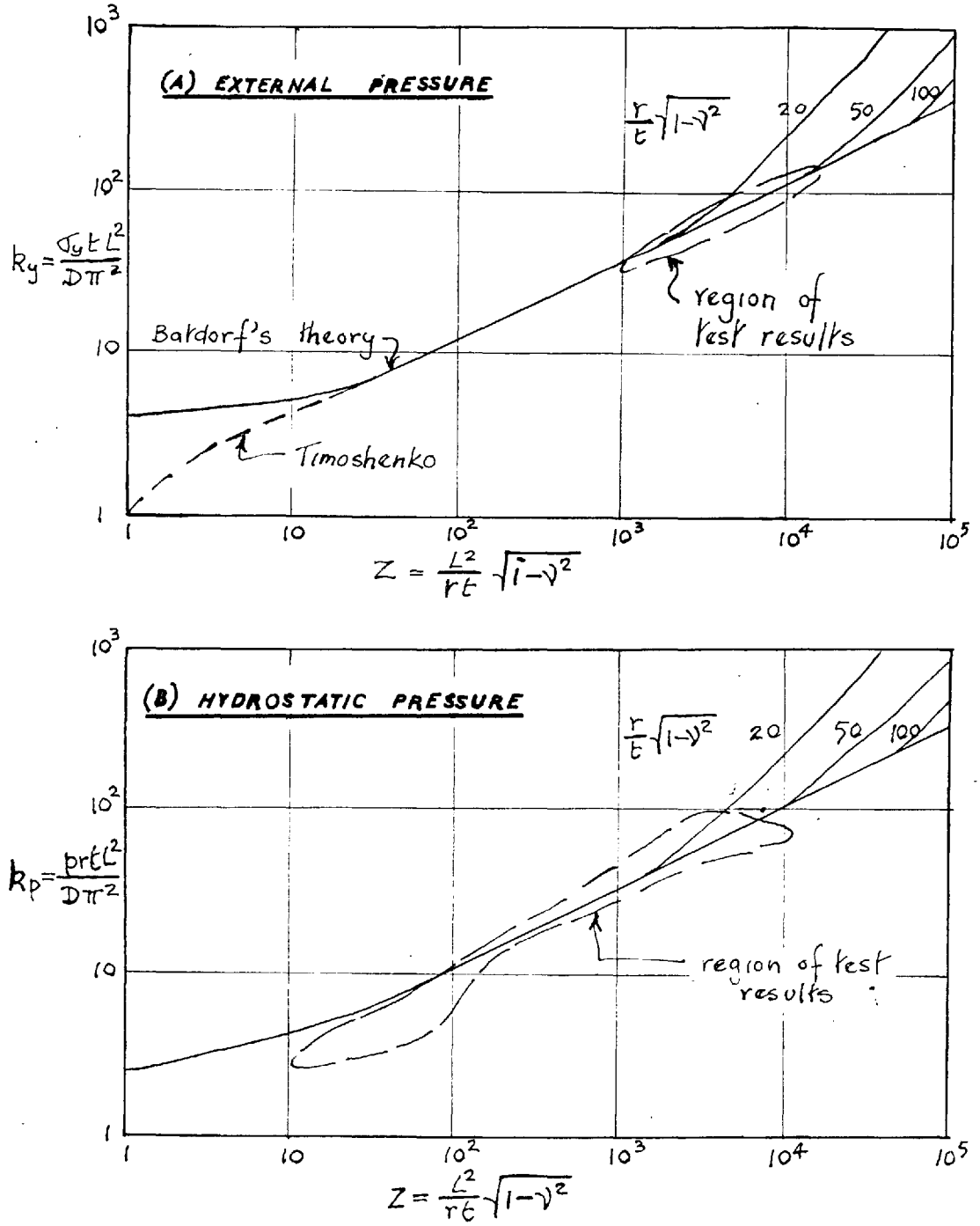


FIG. 3.2: COMPARISON OF EXPERIMENTAL RESULTS WITH THEORY FOR CIRCULAR CYLINDRICAL SHELLS (after Batdorf [8])

behaviour of the hydrostatically loaded cylinder.

Gerard and Becker (1957) [44] suggest that the discrepancy between experimental and theoretical loads for $Z_L < 100$ in Figure 3.2(b) is due to plasticity effects, as against the suggestion made above, that it is due to the effects of the axial load.

3.3.4 Non Linear Theories

As can be seen from Figure 3.2(b) cylindrical shells under hydrostatic pressure show reasonable agreement between theoretical and experimental results, unlike the case of cylindrical shells under axial compression. However, the discrepancy was sufficient for Nash (1955) [90] to study the post-buckling behaviour of such cylinders and to consider the effect of the initial imperfections as well. In doing so, he followed the method used by Donnell and Wan (1950) [27] for the case of axial compression (see Section 3.4.3.2). The Rayleigh-Ritz method was used to obtain the non-linear equations, with the assumed deflection function being taken as:

$$w = at \left[\text{Sin} \frac{my}{R} \quad \sin \frac{n\pi x}{L} \quad + d \left(1-\cos \frac{2n\pi x}{L}\right) \right] \qquad (3.4)$$

where the first term here is the only one that had been used by von Mises in his small-displacement analysis. The total potential energy was minimised with respect to two parameters.

Following Donnell and Wan, and Loo, Nash uses an "unevenness" parameter, U_o, where:

$$U_o = a_o \left[\frac{t(L+2\pi R)}{2\pi RL}\right]^2 = \frac{V}{2}\left[\frac{t(L+2\pi R)}{2\pi RL}\right]^2 = \frac{t^2 V}{8\pi^2 R^2 L^2}(L+2\pi R)^2 \qquad (3.5)$$

As a result of a comparison of his analysis with experimental results, Nash suggests a value of $U_o = 3 \times 10^{-4}$ as giving reasonable agreement between the theory and experiment. This is higher than Donnell and Wan, and Loo suggested as a result of their investigations for the cases of axial compression and torsion. Nash also found that the number of circumferential waves around the cylinder is predicted sufficiently closely by the small displacement theory (i.e. n = 8).

For a particular shell, Nash showed that the critical pressure was dependent upon the value of U_o and that there was a post-buckling drop in the pressure.

Nash suggested that deflection functions other than he had used should also be tried, since Equation (3.4) does not fit the boundary conditions exactly.

Donnell (1956) [25] carried out an analysis for thin "hinged edge" cylinders under hydrostatic pressure, using the method that he and Wan had previously used in the case of the axially loaded cylinder. In this way he also showed how the pressure-volume relationships were dependent upon the initial imperfections present in the cylinders. As previously, it was assumed that the initial imperfections of the cylinder formed a regular geometric displacement pattern that was identical with the post-buckling mode of the cylinder, and that the most important component of the initial imperfection was that which was similar to the post-buckling mode.

Donnell obtained the partial differential equations for the problem, in terms of a stress function, ϕ. This was obtained from the compatibility equation once a particular form had been assumed for the deflection function, w.

The displacement function chosen by Donnell was:

$$w = at\left[\cos\frac{ns}{r}\cos\frac{mnx}{r} + b\left(\cos\frac{mnx}{r} + 0.3\cos\frac{3mnx}{r}\right)\right]$$

$$\text{for } -L/2 < x < L/2 \qquad (3.6)$$

Here n = number of circumferential waves and

$m = m'\pi r/nL = ly/lx$

This assumes that $lx = L$.

Substituting for m in the function, and translating the origin of the axes to one end of the cylinder, we obtain:

$$w = at\left[\sin\frac{ns}{r}\sin\frac{m'\pi x}{L} + b\left\{\cos\frac{2m'\pi x}{L} + 0.3\cos\frac{6m'\pi x}{L}\right\}\right]$$

$$\text{for } 0 < x < L \qquad (3.7)$$

In either case (Equation (3.6) or (3.7)) the first term represents the small (linear) deflection term, while the second term represents the inward deflection of the cylinder and (according to Donnell), has a shape approximately proportional to the squares of the primary deflection. Donnell justified the use of the factor 0.3 on one or two grounds, but it seems to have been introduced primarily in order to permit the use of another term in the deflection function without increasing the number of unknown parameters.

Donnell's results are expressed in terms of the following parameters:

$$\text{pressure parameter} : \quad \bar{p} = \frac{R^{3/2}Lp}{t^{5/2}E}$$

$$\text{length} : \quad \bar{L} = \frac{L}{\sqrt{Rt}} \qquad (3.8)$$

$$\text{initial displacement} : \quad \frac{UR}{t} = \frac{\pi^2 a_o Rt}{\sqrt{(1x)^3(1y)}}$$

where $a_o t$ = amplitude of initial displacement,

lx,ly = halfwavelengths of primary buckling waves in axial and circumferential directions,

volume change parameter : $V = \frac{\text{vol. decrease}}{(Rt)^{3/2}}$ (3.9)

Using these parameters, Donnell has presented the results for cylinders with **hinged** ends. Comparing theoretical results with experimental data, good agreement between them can be brought about using values of U of the order of 0.0001 to 0.0003.

At about the same time, Kempner (1956) [69] sought to solve the case of the cylinder acted upon by hydrostatic pressure, also. Like Nash, and Donnell, he used a finite-deflection theory and considered initial imperfections. He used the deflection function:

$$w = \zeta t \left[\left(a - \cos \frac{ny}{\lambda c} \right) \cos \frac{nx}{L} + c \right] \tag{3.10}$$

where λ_c = halfwavelength determined from small-displacement theory for circumferential buckles.

Initial imperfections were taken as:

$$w_o = \zeta_o t \left[\left(a - \cos \frac{ny}{\lambda c} \right) \cos \frac{nx}{L} \right] \tag{3.11}$$

On account of the numerical difficulties involved in the

Rayleigh-Ritz solution, Kempner gave only one solution of the problem.

Following on from this, Kempner et al. (1957) [71] sought to solve the same problem. In this investigation, initial imperfections were ignored, and a different form was assumed for the deflection function. In this case:

$$w = \xi t \left[(a - \cos \frac{\pi y}{ly}) (\cos \frac{\pi x}{L} + b \cos \frac{3\pi x}{L}) + e \right]$$

$$= \xi t \left[- \cos \frac{\pi y}{ly} \cos \frac{\pi x}{L} + a \cos \frac{\pi x}{L} + ab \cos \frac{3\pi x}{L} \right.$$

$$\left. - b \cos \frac{\pi y}{ly} \cos \frac{3\pi x}{L} + e \right] \qquad (3.12)$$

Kempner et al. minimised the total energy with respect to five parameters, but in order to obtain solutions to these non-linear equations, they made several approximations in turn, using each approximation to guide them in solving the next more difficult equation. In other words, they built up the complete solution in the following manner:

<u>1st approximation:</u> a = b = 0 - this gives the classical solution. They then used the simplification, $\alpha = \alpha_{crit}$, where $\alpha = \left(\frac{\lambda y}{L}\right)^2$

<u>2nd approximation:</u> b = 0 - also considered was the case when $\alpha = \alpha_{crit}$

complete solution: with and without $\alpha = \alpha_{crit}$

In this way, they were able to show, as Nash and Donnell had done, that pressures less than critical existed in the region where Batdorf had found a considerable discrepancy between experimental and theoretical (small-deflection) results. However, in spite of their careful analysis, the calculated minimum value of the post-buckling load was found to be only 3 per cent less than the classical, while experimental values were some 70 - 80 per cent of the classical. While this discrepancy can in part be due to the need for more accurate strain-displacement relations, or more extensive assumed deflection parameters, the main error could be due to neglecting initial imperfections. Nash, who considered initial imperfections in his analysis, had earlier found that his results agreed reasonably well with experimental ones.

Kempner et al. found that with the deflection function they assumed, finite-displacement equilibrium configurations existed for pressures greater than, as well as less than the classical critical pressure. However, these pressures less than critical were found to exist only in a small range, and outside this, pressures greater than critical were required, even in the post-buckling range.

In 1958, Donnell [15] presented a further report dealing with the buckling of thin cylinders acted upon by hydrostatic pressure. This time the analysis was for the case of fixed edges. The method he used was the same as that of the previous report [25]. From this new analysis it is found that there is no drop-off in resistance after buckling takes place. For the case of hinged edges, Donnell had found that there could be a small drop-off in resistance for shells of a particular range of geometry.

For the case of fixed edges, Donnell assumed the deflection function in the form:

$$w = at\left(\cos\frac{ns}{r} + b\right)\left(1 + \cos\frac{2mnx}{r}\right) \qquad (3.13)$$

Initial imperfections were also taken into account, and values for U of between 0.0001 and 0.0008 were required to cover the range of the experimental results.

Langhaar and Boresi (1958) [75] have analysed the cylinder under radial and hydrostatic pressures, though they considered only geometrically perfect shells, neglecting all imperfections. In their analysis they considered an axial force variable between zero and that for the case of hydrostatic pressure. Their results are presented in a series of tables for the solution of the buckling equations, for both fixed-ended and simply-supported cylinders. They also give tables of coefficients that enable the

"Euler" and "Tsien" critical pressures to be calculated. Here, the "Euler critical pressure" is the value of the buckling pressure obtained from the classical theory, while the "Tsien critical pressure" is the pressure at which the shell can snap from a stable unbuckled equilibrium position, to a stable buckled equilibrium position. The latter is discussed in Section 3.4.3.1., and is the same as Tsien's "lower buckling load".

In the development of their theory, Langhaar and Boresi derive equations in terms of the axial, circumferential, and radial components of the middle surface displacement. As a result of using a parameter W_o, which is chosen so as to minimise the buckling pressure, they derive an expression for the increment of total potential energy on buckling, as a function of W_o^2:

i.e. $$\frac{\Delta V}{ERtL} = (B_1 - Ka_1)\, W_o^2 + (B_2 + Ka_2)\, W_o^4 + B_3\, W_o^6 \qquad (3.14)$$

If for a given shell, $\frac{\Delta V}{ERtL}$ is plotted against W_o, different curves are obtained for different values of pressure, p (see Figure 3.3). The minima on the curves represent stable equilibrium configurations, while the maxima represent unstable equilibrium configurations.

The maxima on the curve corresponding to p_2, represents a potential energy barrier that the shell must cross in order to buckle, if the pressure is exactly equal to the Tsien critical

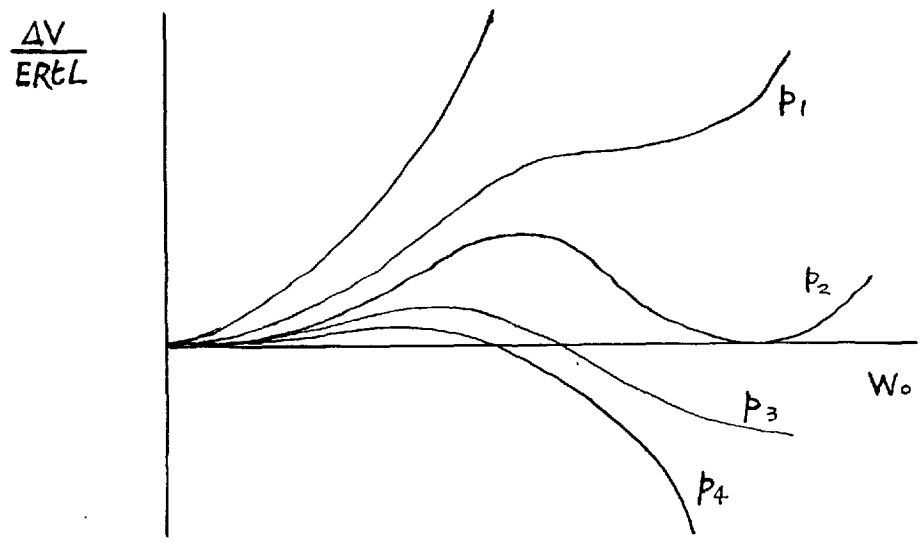


FIG. 3·3 : INCREMENTS OF POTENTIAL ENERGY VERSUS DEFLECTION PARAMETER

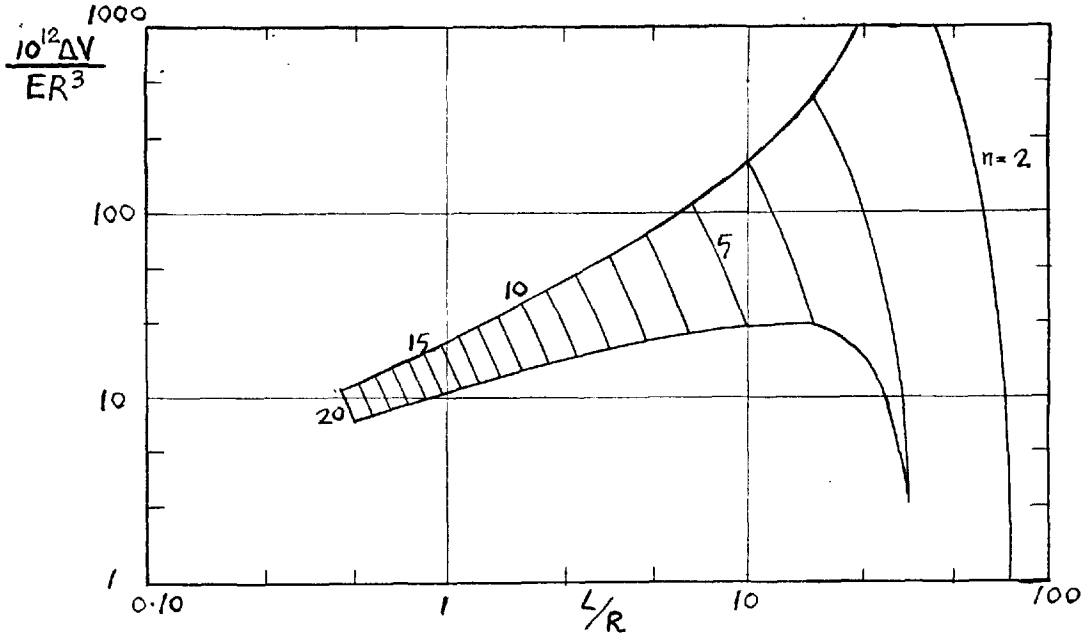


FIG. 3.4 : POTENTIAL ENERGY BARRIERS SEPARATING BUCKLED AND UNBUCKLED FORMS FOR CIRCULAR CYLINDRICAL SHELLS UNDER EXTERNAL PRESSURE. (DIAGRAMATIC)

pressure. It therefore serves as a rough indication of the immenance of snapthrough. The value of this maximum can be obtained from the equation (3.14):

$$\text{i.e.} \qquad \left(\frac{\Delta V}{ER^3}\right)_{max} = \frac{4}{27} \cdot \frac{tL}{R^2} \cdot B_3 \bar{W}_o^6 \qquad (3.15)$$

where $\bar{W}_o$ is the root that corresponds to the point of tangency with the x-axis (see Figure 3.3) (for pressure p_2).

Equation (3.15) is plotted in Figure 3.4 for an R/t = 1000, for the number of circumferential wavelengths, n = 2 - 20, and the case of hydrostatic pressure.

Using this graph, Langhaar and Boresi calculate that a shell, for which L/R = 0.6, and R/t = 1000, will buckle with n = 17, for which $10^{12}\ \Delta V/ER^3 = 11.5$. Therefore, if R = 20", and $E = 30 \times 10^6$ p.s.i., $\Delta V = 2.76$ inlb = 0.23 ftlb, and it is quite possible that accidental disturbances might supply this amount of energy and so cause the cylinder to snapthrough into a buckled configuration.

3.3 TORSION

3.3.1 Introduction

It was in relation to the torsional buckling of thin-walled cylinders that Donnell (1933) [23] introduced his simplified theory, deriving a single 8th order partial differential equation. This approach has been used widely, and has become the basis of

the present linear theories (cf. Batdorf [3]), not only for the case of torsion, but also for external pressure and axial compression. Donnell's theory has also become the basis for the linear stress analysis of thin shells.

More recently, Yoshimura and Niisawa (1957) [146] have shown that there are two extremes of loading that must be considered. For constant torsional moment, buckling will take place at a "lower buckling load", while for constant angle of twist, buckling will only take place at the "upper buckling load", i.e. the buckling load of the classical linear theory.

3.3.2 Experimental Investigations

A summary of the experimental work that has been carried out, has been given by Gerard and Becker [44]. The first experiments were carried out by Lundquist (1932) [82], and Donnell (1933) [23], using brass and steel as materials.

Experimental results have been shown to lie between 70 - 80 per cent of the theoretical results predicted by the classical theory. The fairly wide scatter of results (see Figure 3.6) is perhaps due to the fact that cylinders tested under constant torsional angle (i.e. in a rigid testing machine), buckle at the classical buckling load, while under constant torsional moment buckling occurs at a somewhat lower load. Since testing machines are not truly rigid, it is probable that in the experimental work the

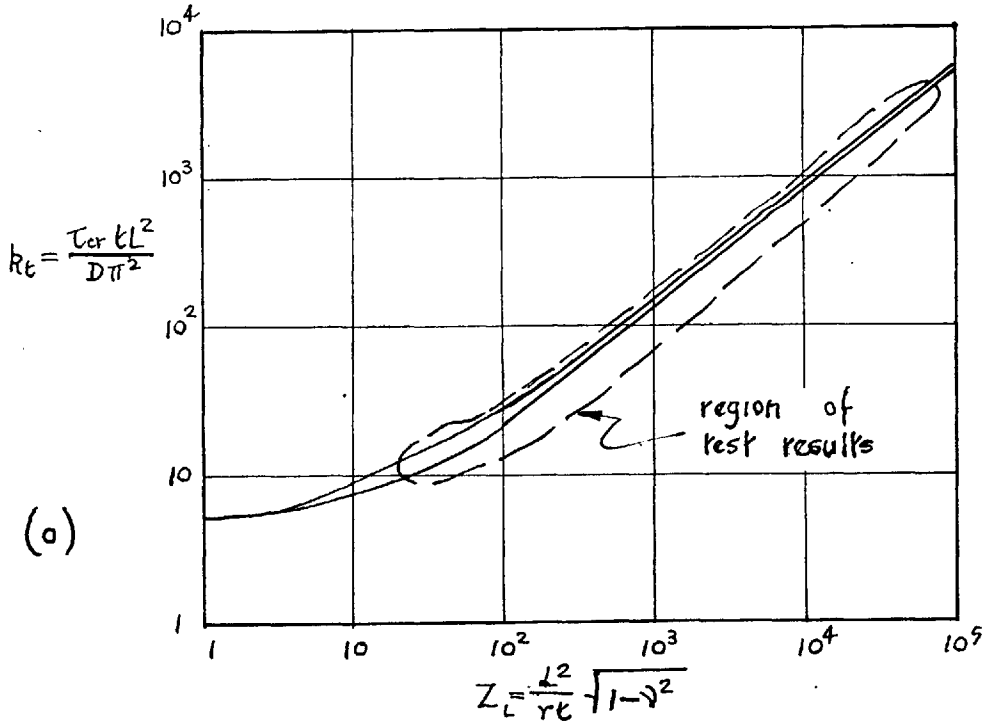
cylinders are tested under conditions somewhere between the two extremes.

The most recent investigation of the torsional buckling of a cylinder has been that carried out by Weingarten (1962) [139] though in the main he was using internally pressured cylinders.

Weingarten compared his experimental results with the theoretical analyses of Loo and Nash, and found that the results were in qualitative agreement but not quantitative agreement.

Figure 3.7 illustrates the experimental behaviour of cylinders under torsion with varying geometric parameter. This shows that for at least one value of L^2/Rt there is close agreement between the results for steel and Mylar (plastic) cylinders. The small discrepancy between the results for the two materials is probably explained by the slightly different buckle patterns that occurred, as shown in the photographs presented in the report.

For small values of L^2/Rt, the load increases with angular rotation in the post buckled region, while for large values the load decreases with increasing angular rotation. In the case of a perfect specimen of $L^2/Rt = 2000$, Loo found only a 12 per cent decrease in strength in the buckled region, while Nash found it to be 26 per cent. However, Weingarten found from his experimental results for $L^2/Rt = 3200$, that there is a 72 per cent decrease in strength. An explanation for this difference can be found by studying the buckling pattern of the unpressurised cylinder. It



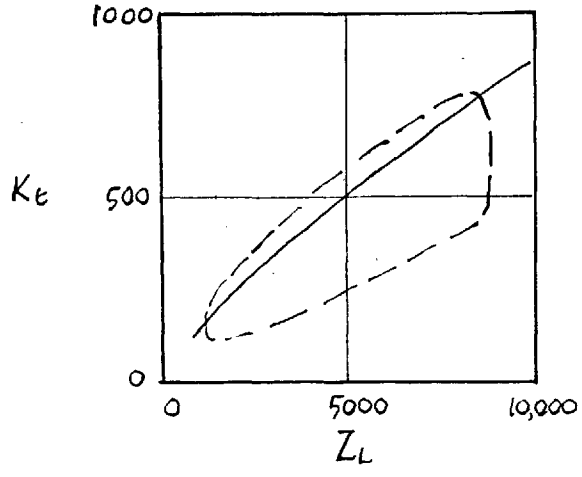


FIG. 3·6: COMPARISON OF TEST DATA WITH THEORY FOR CIRCULAR CYLINDRICAL SHELLS [44] UNDER TORSION (a) LOGARITHMIC SCALE (b) LINEAR SCALE.

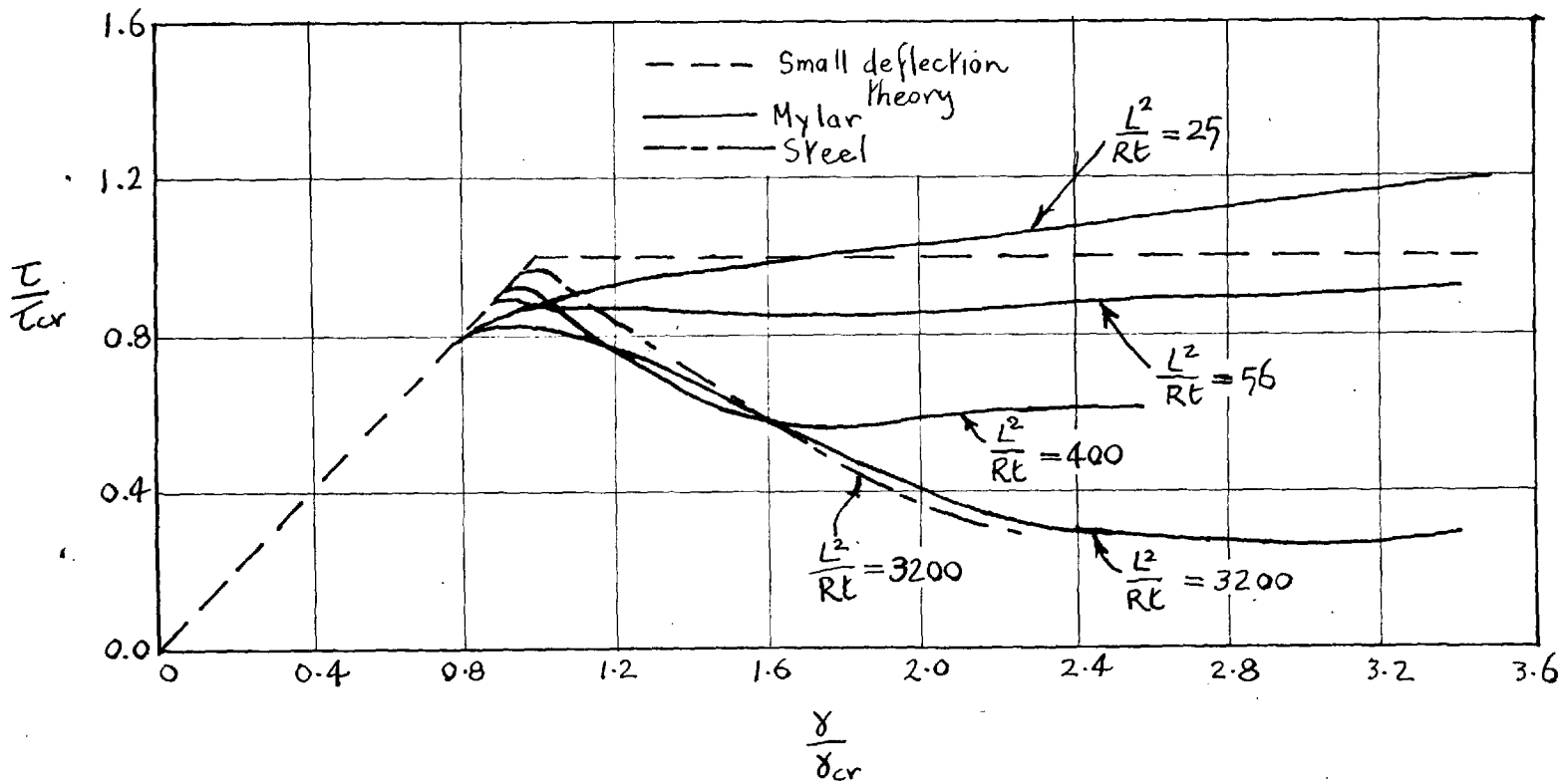


FIG. 3.7 : POST BUCKLING BEHAVIOUR OF CYLINDRICAL SHELLS UNDER TORSION WITH VARYING GEOMETRIC PARAMETER. [139]

can be seen that the angle crests and troughs of the buckles are not parallel, whereas the deflection functions assumed by Loo and Nash assume that these are parallel.

3.3.3 Linear Approach

The earliest analytical investigation of the buckling of thin-walled cylindrical shells under torsion was carried out by Schwerin (1924). A similar investigation has been carried out by Flügge (1934). These investigations were for very long cylinders where the end support conditions did not affect the stability. As a result, they obtained a critical torsional shear stress equation for the infinitely long cylinder, in the form:

$$\tau_{cr} = \frac{T_{cr}}{2\pi R^2 t} = \frac{E}{3\sqrt{2}(1-\nu^2)^{3/4}} \left(\frac{t}{R}\right)^{3/2} \qquad (3.16)$$

In this case the number of waves into which the surface buckles, is two.

For $\nu = 0.3$, we have:

$$\tau_{cr} = \frac{T_{cr}}{2\pi R^2 t} = 0.255\ E \left(\frac{t}{R}\right)^{3/2} \qquad (3.17)$$

For tubes of very large L/R ratio, another mode of buckling is the deformation of the tube axis into a helix. According to Fung and Sechler [40], Schwerin's analysis is applicable to this

case, and predicts a critical shearing stress given by:

$$\tau_{cr} = \frac{2\pi E}{(1-\nu)} \frac{R}{L} \left[1 - \frac{t}{2R} + \frac{1}{12} \left(\frac{t}{R}\right)^2 + ... \right] \qquad (3.18)$$

For this case the tube must be very long (L/R very large) before critical shearing stresses less than the material yield point are found, so that buckling is elastic.

For short cylinders, the end conditions can no longer be disregarded, and the probelm of determining the critical shear stress becomes very complex. Donnell (1933) [23] introduced a number of simplifications into the shell equations, and also simplified the boundary conditions that require to be fulfilled. In this way, Donnell derived the 8th order differential equation:

$$D\nabla^8 w + \frac{Et}{R^2} \frac{\partial^4 w}{\partial x^4} + 2\,St\nabla^4 \frac{\partial^2 w}{\partial x \partial y} = 0 \qquad (3.19)$$

As a result of these simplifications, Donnell obtained the following formulae for the critical shearing stress for short and moderately long cylinders:

for clamped ends:

$$\tau_{cr} = \frac{E}{1-\nu^2} \left(\frac{t}{L}\right)^2 \left[4.6 + \sqrt{7.8 + 1.67 \left(\sqrt{1-\nu^2} \cdot \frac{L^2}{Rt} \right)^{3/2}} \right] \qquad (3.20)$$

and for simply supported ends:

$$\tau_{cr} = \frac{E}{1-\nu^2}\left(\frac{t}{L}\right)^2\left[2.8 + \sqrt{2.6 + 1.40\left(\sqrt{1-\nu^2}\cdot\frac{L^2}{Rt}\right)^{3/2}}\right] \quad (3.21)$$

When the experimental results are plotted, they lie just below Donnell's two theoretical formulae.

Timoshenko [129] reports that Kromm (1940) carried out a more detailed investigation in the case of simply-supported ends, and arrived at the following formula:

$$\tau_{cr} = 4.39\ \frac{E}{1-\nu^2}\left(\frac{t}{L}\right)^2\sqrt{1 + 0.0297\,(1-\nu^2)^{3/4}\left(\frac{L^2}{Rt}\right)^{3/2}} \quad (3.22)$$

which is claimed to agree slightly better with test results.

Batdorf et al. [8, 10] using the simplified Donnell theory, have presented the results in terms of two parameters as they have done for the other loading cases on the cylinder.

Using these parameters, the resulting curve is shown in Figure 3.6(a). From this it can be seen that the experimental values average some 15 - 20 per cent below those given by the theory. The discrepancy is even more clearly seen in Figure 3.6(b) where, instead of using the log-log plot as in Figure 3.6(a), the same results are plotted on a linear scale. Part of the discrepancy may be explained by the fact that Donnell, and Lundquist, reported failure loads and not just initial buckling loads.

3.3.4 Nonlinear Approach

The first application of nonlinear theory to the case of torsional buckling of a cylinder, was carried out by Loo [78] in 1954. In addition, he took into account the initial imperfections inherent in the cylinders. Donnell and Wan's [27] assumptions regarding the shape of the deformed surface, and the magnitude of the initial imperfections, were considered to be not general enough to be applicable to the case of torsional buckling. As a result, Loo chose to make more general assumptions that could be applied to the case of torsion, as well as axial compression. By comparing his results (for the case of axial compression) with those of Donnell and Wan, Loo was able to show that his differing assumptions did produce similar results.

Loo used a Rayleigh-Ritz approach, expressing the strain energy in terms of the deflection function, w, and the membrane stress function, ϕ. On assuming the deflection function to be of the form:

$$w = at\left[\sin\frac{n}{R}(y+\psi x)\sin\frac{\pi x}{lx} + \frac{d}{2}\left(\cos\frac{2\pi x}{lx} - 1\right)\right] \qquad (3.23)$$

and the initial imperfection to be:

$$w_o = a_o t\left[\sin\frac{n}{R}(y+\psi x)\sin\frac{\pi x}{lx} + \frac{d}{2}\left(\cos\frac{2\pi x}{lx} - 1\right)\right] \qquad (3.24)$$

where:

$\gamma = \tan\theta$, $n = \pi r/ly$, $m = ly/lx$

θ = angle between buckling waves

at = amplitude of radial deflection

$a_o t$ = amplitude of initial imperfection

a,d = constants

then a particular solution can be found for ϕ. A complementary solution for ϕ is also found, of the form:

$$\phi = c_1 x^2 + d_2 xy + c_3 y^2 \qquad (3.25)$$

Strictly, the strain energy should be minimised with respect to the four unknown parameters a, d, n and γ. However, in order to reduce the mathematical work, Loo assumes that the values for γ and n are not very different from those found from Donnell's small-deflection theory. Loo's grounds for making this assumption are that the small deflection values agree reasonably with the experimental values. As a result, Loo only minimises the energy expression with respect to the two parameters a and d.

Loo plots $(L/t)^2 \frac{\sigma_{xy}}{G}$ versus $(L/t)^2 \gamma_{xy}$ for various values of an imperfection parameter V (= $0.5a$), which show that for $L/R > 20$, there is a post-buckling fall in shearing strength. The strength is shown to increase again provided $20 \leq L^2/Rt \leq 2\times10^3$,

while for $L^2/Rt > 2x10^4$, the strengths of the cylinders decrease continuously. An approximate formula for the peak shearing stress was found to be:

$$1 - \frac{(\sigma_{xy})}{(\sigma_{xy_{cr}})_{peak}} = 0.75 \left[\frac{V}{(L^2/Rt)^{0.3}} \right]^{0.6} = 1.14 \left[\frac{a_o}{(L^2/Rt)^{0.3}} \right]^{0.6} \tag{3.26}$$

The imperfection magnitude is assumed to be of the form:

$$a_o = U_o \left[\frac{lx\,ly}{lx + ly} \cdot \frac{1}{t} \right]^{\delta} \tag{3.27}$$

Loo chooses a value of $U_o = 0.5x10^{-4}$ and $\delta = 2$, which he shows are reasonable for the case of buckling of a column, and the axial compression of a cylinder. Here $lx \simeq L$, and $ly \approx mlx \approx mL$.

This equation (3.26) is shown to agree with the general trend of the experimental results, passing roughly through the middle of the region in which the experimental results lie (Figure 3.8).

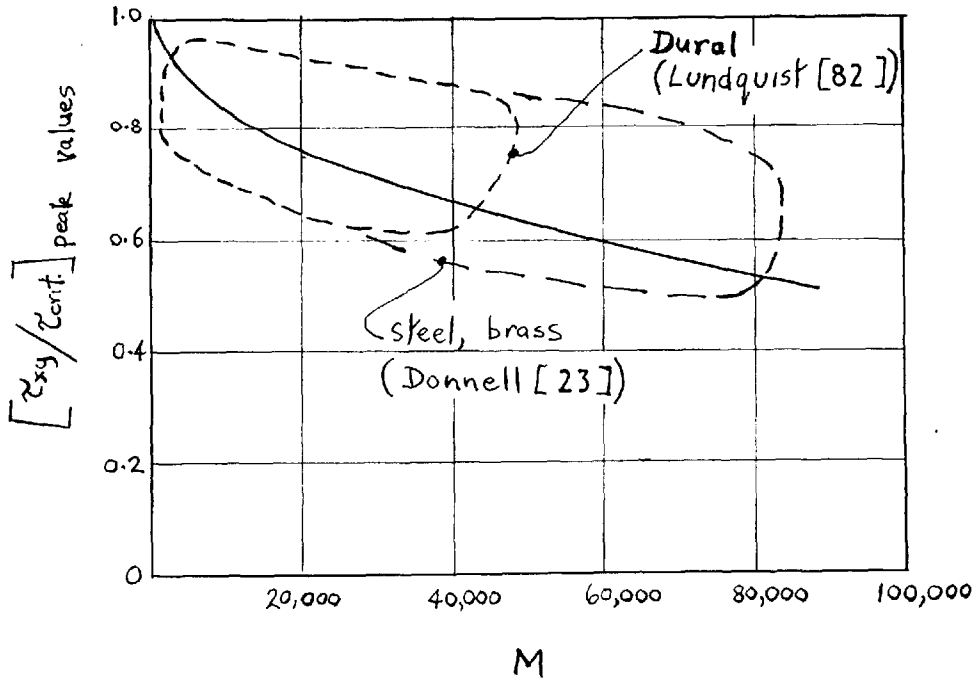


FIG. 3.8: LOO'S COMPARISON OF HIS THEORY FOR $\delta = 2$, $U = 0.50 \times 10^{-4}$ WITH RESULTS OF PURE TORSION TESTS

The next analysis of the torsion problem, was carried out by Yoshimura and Niisawa [146] (1957), who stated that torsional buckling was a Durchschlag problem, as was axial compressive buckling. For this to be so, the existence of the stable state after buckling depends on whether there exists an intensely buckled surface which is approximately applicable to the undeformed surface. Like Loo, they used the finite-deflection theory, solving it by means of a Rayleigh-Ritz method. For this case, the assumed deflection function is:

$$w = af_o \left(1 + \cos \frac{\pi x}{L}\right) + af_1 \left\{\cos \frac{1}{R} (\lambda_1 x + ny) + \cos \frac{1}{R} (\lambda_2 x + ny)\right\} \tag{3.28}$$

where af_o, af_1 are the amplitudes.

$\frac{2\pi R}{\lambda_1}$, $\frac{2\pi R}{\lambda_2}$ are the wavelengths in the axial and circumferential directions

2L = length of the cylinder,

n = number of circumferential waves.

Yoshimura and Niisawa are assuming here that the surface deforms into a one-sheet hyperboloid (1st term) and that the helical wave pattern (2nd term) is superimposed on this surface, and not on the initial cylindrical surface. Equation (3.28) does not satisfy the boundary conditions for either fixed ends

or simply-supported ends. However, Donnell [23] has stated that the end conditions do not significantly affect the buckling stress, but this has in no way been proved.

The total potential energy expression, after being put into a non-dimensional form, is then minimised with respect to four parameters, with a fifth parameter being assigned different values. In this way it is shown that there are post-buckling equilibrium states with lower loads and larger deflections than those obtained just at buckling. This drop in load is smaller than is found with axially loaded cylinders, but larger than that found for cylinders loaded by external pressure. This agrees quantitatively with the experimental results in the three different loading cases. Yoshimura and Niisawa point out also that the amount of post-buckling fall-off is dependent on the type of testing procedure used. There is found to be a distinct lower buckling stress for the case of constant torsional moment, but no lower buckling stress for the case of constant angle of twist.

At almost the same time as Yoshimura and Niisawa, Nash (1957) [91] also carried out an analysis of the post-buckling deflection of cylinders loaded in torsion. Nash carried on from the work of Loo, and sought as rigorous an analysis as possible. Hence, in order to improve the accuracy of the

analysis, Nash minimised the total potential energy with respect to all the arbitrary deflection parameters, with no results being assumed from the small-deflection theory. By considering the periodicity of the circumferential displacements, Nash showed that there was a decrease in the number of waves as the load is increased, i.e. m became larger instead of remaining constant at the small-deflection theory value. By assuming slightly different deflection functions, Nash separated the cases of clamped and simply-supported ends.

The deflection functions that Nash assumed in connection with the Rayleigh-Ritz solution of the differential equations were - for clamped ends:

$$w = at\left[\sin\frac{n}{R}(y+\gamma x)\left\{1-\cos\frac{2\pi x}{L}\right\}+d\left(\cos\frac{2\pi x}{L}-1\right)+c\right] \qquad (3.29)$$

and for simply-supported ends:

$$w = at\left[\sin\frac{r'}{R}(y+\gamma' x)\sin\frac{\pi x}{L}+d'\sin\frac{\pi x}{L}+e'\right] \qquad (3.30)$$

where e and e' are terms introduced to correspond to a uniform radial displacement so that membrane stresses that are present may be those due entirely to torsion. e and e' are, however, shown to have only a negligible effect on the results.

The deflection functions given above do not accurately fit

the end conditions, particularly for small-deflections. However, the second terms do, and as Nash shows, these become the most important terms for large displacements, and the functions then become more exact.

Instead of minimising the total potential energy in the usual manner, i.e. with respect to the four parameters a, n, δ and d in this case, to obtain the four partial differential equations that must be solved in order to obtain solutions for the four parameters, Nash used another approach. His method was to assume a value of L^2/Rt; then for various values of $(L/t)^2 \gamma_{xy} \in V$, values for a, d, δ, n, were chosen, and adjusted to make the total potential energy a minimum. In this way, curves of $(L^2/Rt)\,\gamma_{xy}$ versus $(L/t)^2 \frac{\sigma_{xy}}{G}$ were plotted for varying V, and for different (L^2/Rt) ratios.

The resulting curves show a greater drop in post-buckling resistance, than that found by Loo. Nash also found that m and δ varied with a (the amplitude), and were not constant as assumed by Loo; in fact m increased considerably. Like Loo, Nash suggested empirical formulae for the peak value of torsional resistance, taking the initial imperfections into account.

These were:

for clamped ends: $$1 - \frac{(\sigma_{xy})}{(\sigma_{xy_{cl}})_{peak}} = 4.25 \left[\frac{V}{H^{0.3}} \right]^{0.6} \qquad (3.31)$$

for simply-supported ends: $$1 - \frac{(\sigma_{xy})}{(\sigma_{xy_{cl}})_{peak}} = 3.10 \left[\frac{V}{H^{0.3}} \right]^{0.6} \qquad (3.32)$$

where: $$a_o = U_o \left[\frac{l_x \, l_y}{l_x + l_y} \cdot \frac{1}{t} \right]^{\delta} = (1/2)V \; ; \quad m = l_y/l_x$$

$$l_x = L/2 \quad ; \quad l_y = (m/2)L$$

In these formulae, Nash suggests using average values for m. The value for U_o was 0.17×10^{-6}, which was based on the tests of Lundquist, and Donnell.

To date, Nash's analysis is the most accurate that has been carried out for this case of the torsional buckling of thin walled cylinders. It can reasonably explain the lower than classical buckling by assuming appropriate values for the initial imperfections.

3.4 AXIAL COMPRESSION

3.4.1 Introduction

The experiments made to verify the theoretical results of the classical and small displacement (linear) theories have shown that, unlike other structural elements such as bars and plates, the elastic buckling of thin-walled circular cylinders under axial compression differs greatly from the predicted results of the classical linear theory.

For axially loaded cylinders, test results give about 20 - 30 per cent of the classical buckling load, while for cylinders under torsion and external pressure tests give about 70 - 80 per cent of the buckling loads predicted by classical theory.

Also, the experimental results for cylinders loaded under axial pressure show considerable scatter, which is much greater than found in tests on cylinders loaded by torsion or external pressure.

For these reasons, considerable attention was given to the problem of the buckling of cylindrical shells loaded under axial compression. Insights into the problem of buckling for this case have enabledus to gain a better understanding of buckling in other particular cases, and of the whole process of buckling of thin shells in general.

3.4.2 Experimental Work

A summary of the experimental work has been given by Gerard and Becker [44] and Harris et al. [51, 122]. The most recent experimental work reported is that of Almroth, Holmes, and Brush (1964) [149], and they include a detailed account of their testing procedure. Evensen (1964) [30] has reported a photographic observation of the buckling of thin cylindrical shells.

The remainder of this Section is a commentary on the experimental behaviour of axially compressed cylindrical shells.

In an ordinary hydraulic, or dead-weight testing machine, the elastic buckling of thin-walled cylinders takes place with great rapidity. Such a process has been described as "snapthrough", "oilcanning" or "durchschlag". Here, the full buckling pattern develops almost at once. In a testing machine on which the rate of end shortening can be controlled, it is found that small ripples appear initially on the surface of the cylinder. Later, these develop into isolated buckles at random positions on the cylinder. As the end shortening is increased, more and more buckles develop, finally joining to form the generally observed diamond pattern.

The reasons that best explain the formation of the diamond shaped buckling pattern are as follows. For the shell, the

bending rigidity, I, is proportional to (thickness)^3, whereas the rigidity against membrane extension (or contraction) is proportional to the thickness. Hence, when the thickness is very small, the resistance to bending is much less than that due to extension and in order to seek a lower strain energy configuration, the cylinder will take up a form that entails the least amount of stretching of the middle surface. Since both a cylindrical surface and a diamond pattern formed by a regular arrangement of flat triangular surfaces are developable, it is possible for the cylindrical surface to deform into the diamond pattern without membrane extension. This assumes that the bending takes place along ideally sharp ridges.

In a real cylinder, the bending is concentrated around the ridges and, as a consequence, a small amount of stretching is introduced. The thinner the cylinder wall, the stronger the tendency to form such a developable diamond pattern. However, for cylinders with relatively thick walls it is possible for the cylinder to buckle in a sine wave form, i.e. to buckle in a series of ripples, as suggested by the linear theory. This has been shown experimentally, e.g. at Cal. Tech. (see also Reference 129).

The random, isolated character of the initial buckles has suggested to many investigators that "imperfections" of one kind

or another may be responsible for their appearance. However, they have found in their tests that initial buckles do not necessarily appear at visible imperfections. Also, a buckled cylinder when allowed to return to its unstrained position, and then tested again, does not necessarily buckle in the same places as previously. In the case of one carefully controlled experiment, it was found that there was a considerable circumferential variation of compressive stress. It is possible that this may explain the variation in the position of the initial buckles.

With this idea in mind, that imperfections of the test specimen, and disturbances in the loading system, might reduce the buckling stress, several experiments have been carried out where deliberate disturbances were introduced. These included various imperfections of the specimen, as well as disturbances in the loading process. These have shown that imperfections of a size comparable to the buckle wavelength, significantly reduce the buckling stress, but smaller imperfections have no effect, even though they may seem to be severe. On the other hand, it has been shown that with cylinders that have been manufactured as near perfect as possible, the buckling stress of the cylinder is greatly increased and buckling stresses up to 70 per cent of the

classical value have been reported [149].

From the above, it can be seen that the low buckling stresses that have been generally reported are most likely due to imperfections in the manufactured cylinders. At the same time it appears that cylinders when acted upon by axial compressive load are much more sensitive to initial imperfections than is the case when cylinders are acted upon by torsion and external pressure.

Tsien [134] in his theoretical work, considered that the characteristics of the testing machine could affect the stress at which buckling took place. This is discussed in Section 3.4.3.1, where it is pointed out that the limiting loading processes are provided by rigid and deadweight testing machines. For the former, the distance between the end plates is the parameter that can be controlled, while for the latter, the load is the parameter that can be controlled, and there is no control over the end shortening. Recent tests by Almroth, Holmes, and Brush [149] have shown that there is no difference in buckling stress for cylinders tested under rigid or deadweight conditions. There is, however, a difference in post-buckling behaviour for the two extremes, as well as all the possibilities inbetween.

Thielemann [125] has shown that the shape of the experimentally

determined load-deflection diagram, is similar in the post-buckled region to that predicted by theory, but the minimum of the curve was still much lower than that of Kempner's theory. The minimum post-buckling loads determined by Thielemann and by Almroth, Holmes and Brush were of the order of 10 per cent of the classical load.

3.4.3 Linear Theories

The classical and small displacement theory approach has been dealt with by Lorenz (1908), Timoshenko (1910), Southwell (1913) [119], Robertson (1928), Flugge (1932) [34] and others [129].

They have solved the differential equations to obtain the eigenvalues for the problem. Perfect elasticity and perfect initial shape have been assumed. They all arrive at a buckling stress of:

$$\sigma_{cr} = \frac{E}{\sqrt{3(1-\nu^2)}} \cdot \frac{t}{R} = 0.609 \frac{Et}{R} \qquad (3.33)$$

for $\nu = 0.3$.

A comparison between experimental and classical theory results is shown in Figure 3.1, taken from Donnell and Wan's paper. This shows the ratio of the experimental buckling stress to the classical buckling stress. The former is usually taken as the maximum stress sustained by the cylinder

in a testing machine, while the latter is given by Equation (3.33). The experimental results obtained by the various researchers lie within the regions indicated. In general, it can be seen that the experimental values of σ_{cr} are widely scattered and are all less than the theory calls for.

In an attempt to explain this discrepancy, Flügge (1932) [34] considered the variation between the end conditions assumed in the theoretical analysis and those realised in experimental tests. He found that the influence of the end conditions extended only to a distance of $\sqrt{Rt}$ in from the ends. He was unable to account for the discrepancy for cylinders whose length was great compared with $\sqrt{Rt}$.

No progress was made in explaining why axially loaded cylindrical shells buckled at lower than the classical load until the nonlinear theories were used.

In this Section it is convenient to mention also some of the other attempts that have been made to predict the buckling stress for the axially loaded cylindrical shell.

Batdorf [8] as in the cases of torsion and external pressure, has presented his results in terms of two parameters, e.g.:

critical stress parameter $\quad k_x = \dfrac{\sigma_x t L^2}{D\pi^2}$

geometric parameter $\quad Z = \dfrac{L^2}{Rt}\sqrt{1-\nu^2}$

For values of Z above about 5, the curve becomes a straight line of slope 1. This straight line is given by the formula:

$$k_x = \frac{4\sqrt{3}}{\pi^2} Z = 0.702\ Z \qquad (3.34)$$

For any fixed value of R/t, some value of Z always exists above which L/R is so large that the cylinder fails as a column before the cylinder walls buckle.

Gerard and Becker (1957) [44] present their results in the form used by Batdorf. In doing so, they have expanded it and shown how the influence of initial imperfections may be taken into account.

In addition, there have been several attempts to define the buckling stress by means of empirical formula, but none of these is entirely satisfactory on account of the considerable scatter in experimental results.

3.4.4 Nonlinear Theories

3.4.4.1 Energy Theory

The first real progress in explaining the discrepancy between experiment and theory, was made by Donnell (1934) [24], when he introduced a nonlinear, finite-displacement theory into the elastic stability analysis of cylinders, as well as considering the effect of initial imperfections. In this way,

Donnell sought not only to determine the bifurcation points of possible states of equilibrium, but also to examine post-buckling effects.

The full importance of the nonlinear load-displacement relationship in shell stability theory, was first shown by Karman and Tsien (1939, 1941) [65, 66]. They showed that in the case of a spherical shell under external pressure, and a cylindrical shell under axial compression, equilibrium states involving large displacements could be maintained by loads far less than the critical loads given by the linear theory. Karman and Tsien suggested that since some of these large displacement configurations closely approach the observed phenomena, the shell must "jump" suddenly from the unbuckled state to these particular equilibrium states, and the structures fail as a result of this sudden change. They were able to show that adjacent states of equilibrium occurred, even at loads below the critical. This meant that the post-buckling behaviour of the axially loaded cylinder was entirely different from that of other structural elements such as bars and plates.

If the shell is considered to "jump" from one equilibrium position to another, then it would seem more reasonable to consider the dynamic stability of the shell rather than the static stability, in order to determine the load at which the shell buckles. However, Yao (1962) [144] appears to be the first

to attempt a dynamic analysis.

It is also possible, that imperfections in the cylinder, or in the loading distribution as mentioned in Section 3.4.2 might affect the conditions of a jump. In other words, the imperfection method (as described later), and the energy theory should possibly complement each other and give a deeper insight into the buckling problem. However, the energy theory as proposed by Karman and Tsien, and further developed by Leggett and Jones (1942) [76], Michielson (1948) [83], Kempner (1954) [68] and Yoshimura (1955) [145], remains a perfect cylinder theory. The imperfection theory as used by Donnell and others has explained with considerable success the discrepancies between the theoretical and experimental buckling loads, but remains a purely static theory, except for the recent work of Yao.

Karman and Tsien (as did Donnell and Wan later) started with the nonlinear strain-displacement relations. Using these, they derived the equation of compatibility, expressing it in terms of Airy's function. The equation of equilibrium was obtained by using the equivalent variational form:

$$\delta (w_1 + w_2 + w_3) = 0$$

where w_1 = elastic strain energy for extensional stresses

w_2 = elastic strain energy in bending

w_3 = potential energy of the axial forces

In order to solve this by an approximate method, Karman and Tsien assumed that the displacement of the middle surface was given by the expression:

$$\frac{w_1}{R} = \cos^2\left(\frac{mx + ny}{2R}\right) \cos^2\left(\frac{mx - ny}{2R}\right) \tag{3.35}$$

which assumes a diamond shaped pattern, and where the squares are introduced to account for the fact that the shell has a definite preference to buckle inwards. Equation (3.35) is alternatively:

$$\frac{w_1}{R} = 1/4 + 1/2 \left[\cos \frac{mx}{R} \cos \frac{ny}{R} + 1/4 \cos \frac{2mx}{R} + 1/4 \cos \frac{2ny}{R}\right] \tag{3.36}$$

The classical theory which is applicable for infinitesmal displacement, required:

$$\frac{w_2}{R} = \cos \frac{mx}{R} \cos \frac{ny}{R} \tag{3.37}$$

As a result, Karman and Tsien used the displacement function:

$$\frac{w}{R} = \left(f_o + \frac{f_1}{4}\right) + \frac{f_1}{2}\left(\cos \frac{mx}{R} \cos \frac{ny}{R} + 1/4 \cos \frac{2mx}{R} + 1/4 \cos \frac{2ny}{R}\right) + \frac{f_2}{4}\left(\cos \frac{2mx}{R} + \cos \frac{2ny}{R}\right) \tag{3.38}$$

where f_o, f_1, f_2, m and n are the constants to be determined by the principle of minimum potential energy.

Using this assumed form of w, W_1, W_2, W_3 are expressed in terms of f_o, f_1, f_2, m and n, and these constants are determined by conditions of the form:

$$\frac{\partial}{\partial f_o} (W_1 + W_2 + W_3) = 0$$

Karman and Tsien [66] minimised the function with respect to three parameters, f_o, f_1, f_2, and assumed arbitrary values for m and n.

Leggett and Jones [76] minimised the energy function with respect to the ratio m/n as well, and showed that this varied with the overall end-shortening of the cylinder in the post-buckling region.

Michielson [83] minimised the equation with respect to the same four parameters as Leggett and Jones.

Kempner [68] made a still more rigorous calculation of the post-buckling behaviour of the perfect cylinder, by using a slightly different displacement function and minimising it with respect to five parameters.

The results of these analyses is illustrated diagramatically in Figure 3.9, where the variation of axial stress is plotted against the end shortening of the cylinder. Point A corresponds to the buckling load of the classical theory. The line OA represents

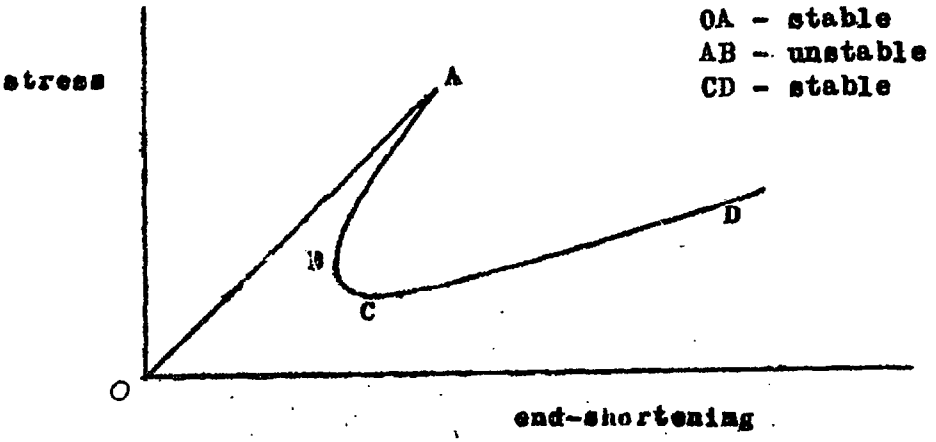


Fig. 3.9: Diagramatic representation of the variation of axial stress with unit end-shortening.

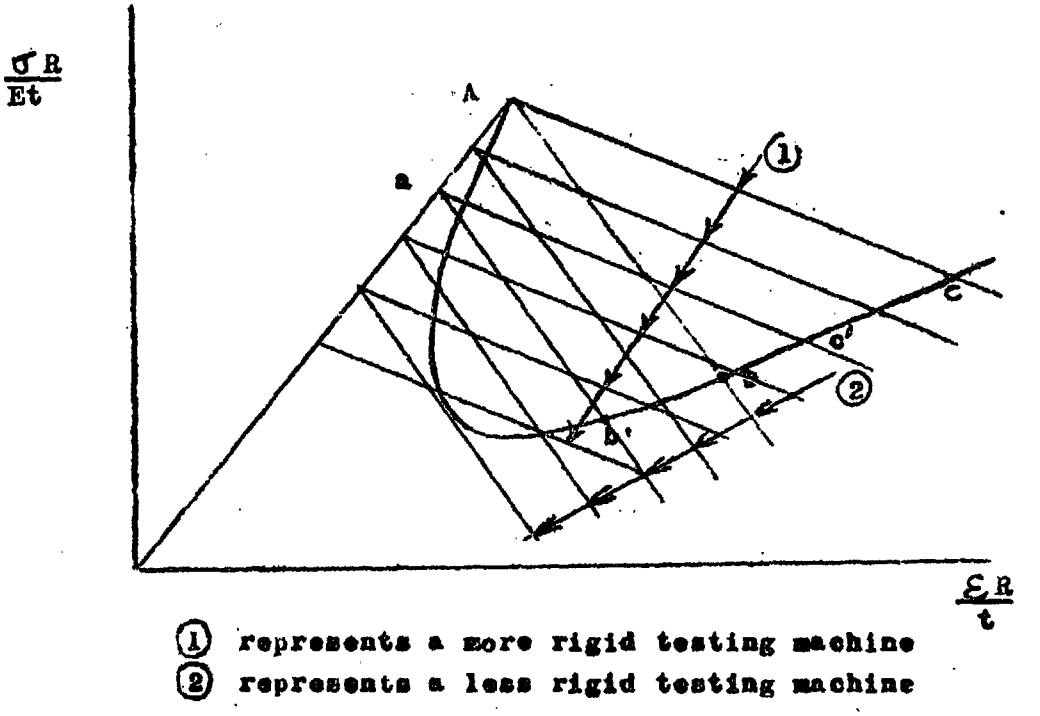
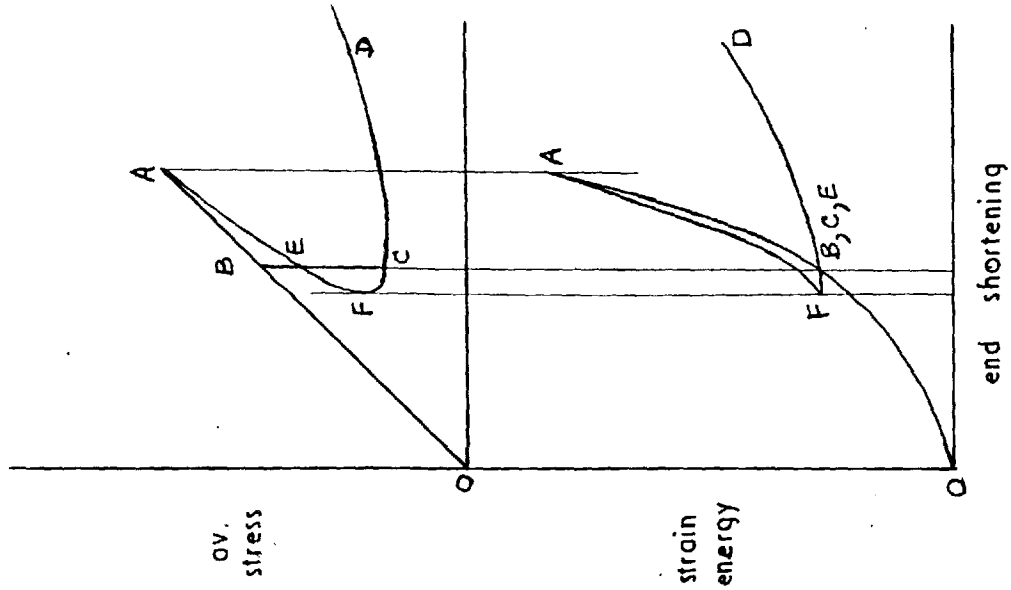
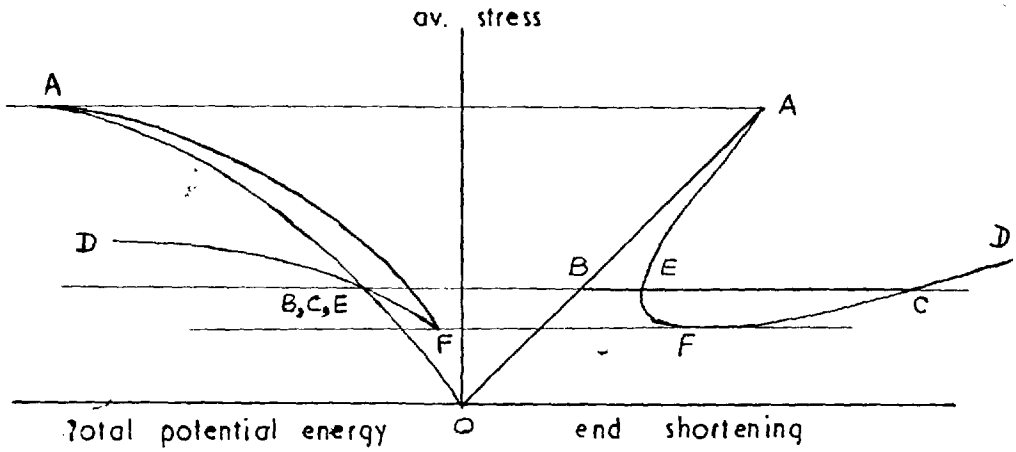


Fig. 3.10: Buckling in an elastic testing machine.



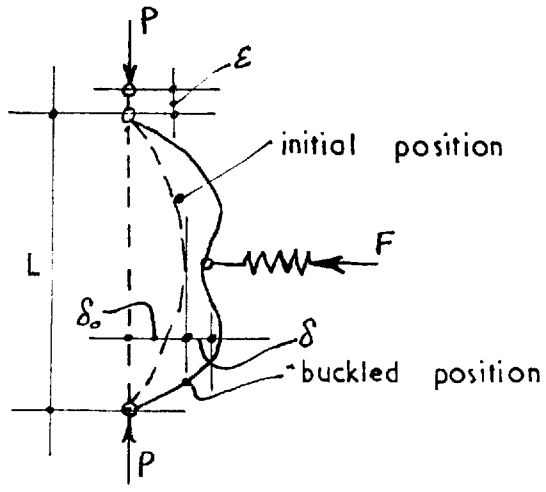
(a) RIGID TESTING MACHINE



(b) DEADWEIGHT TESTING MACHINE

FIG. 3·11: THEORETICAL BEHAVIOUR OF AXIALLY COMPRESSED CYLINDRICAL SHELL.

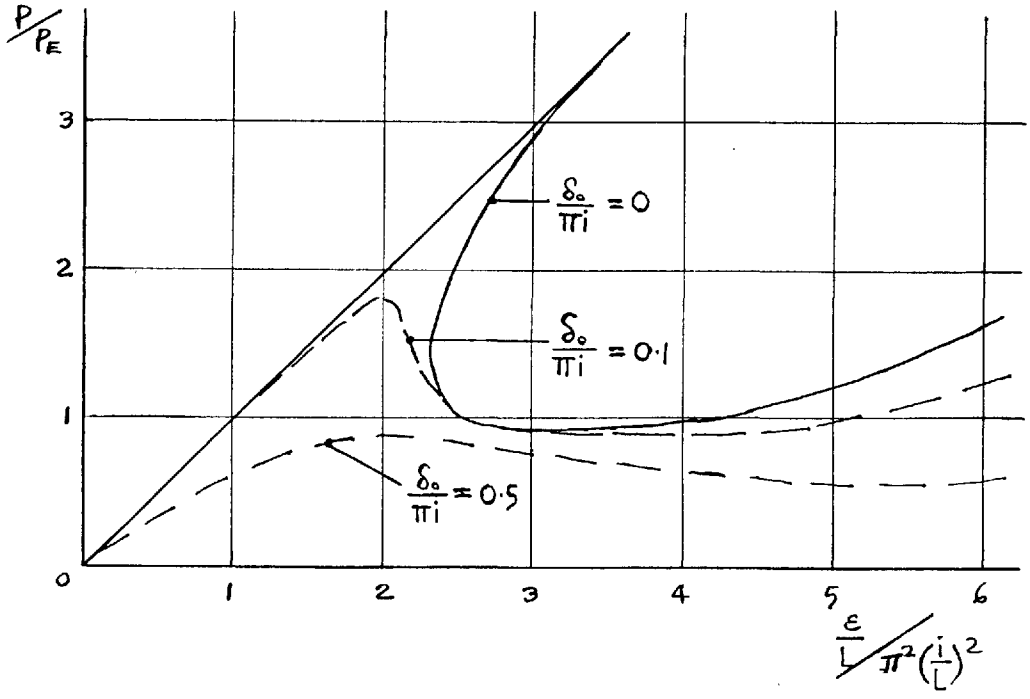
(AFTER TSIEN [134])



$$P_E = \frac{\pi^2 E I}{L^2}$$

= Euler column load

i = radius of gyration



RELATION BETWEEN LOAD P AND END-SHORTENING ε FOR COLUMNS WITH NONLINEAR LATERAL SUPPORT AND VARYING AMOUNTS OF INITIAL DEFLECTION.

FIG. 3·12 COLUMN SUPPORTED LATERALLY BY NONLINEAR SPRING [REF. 133]

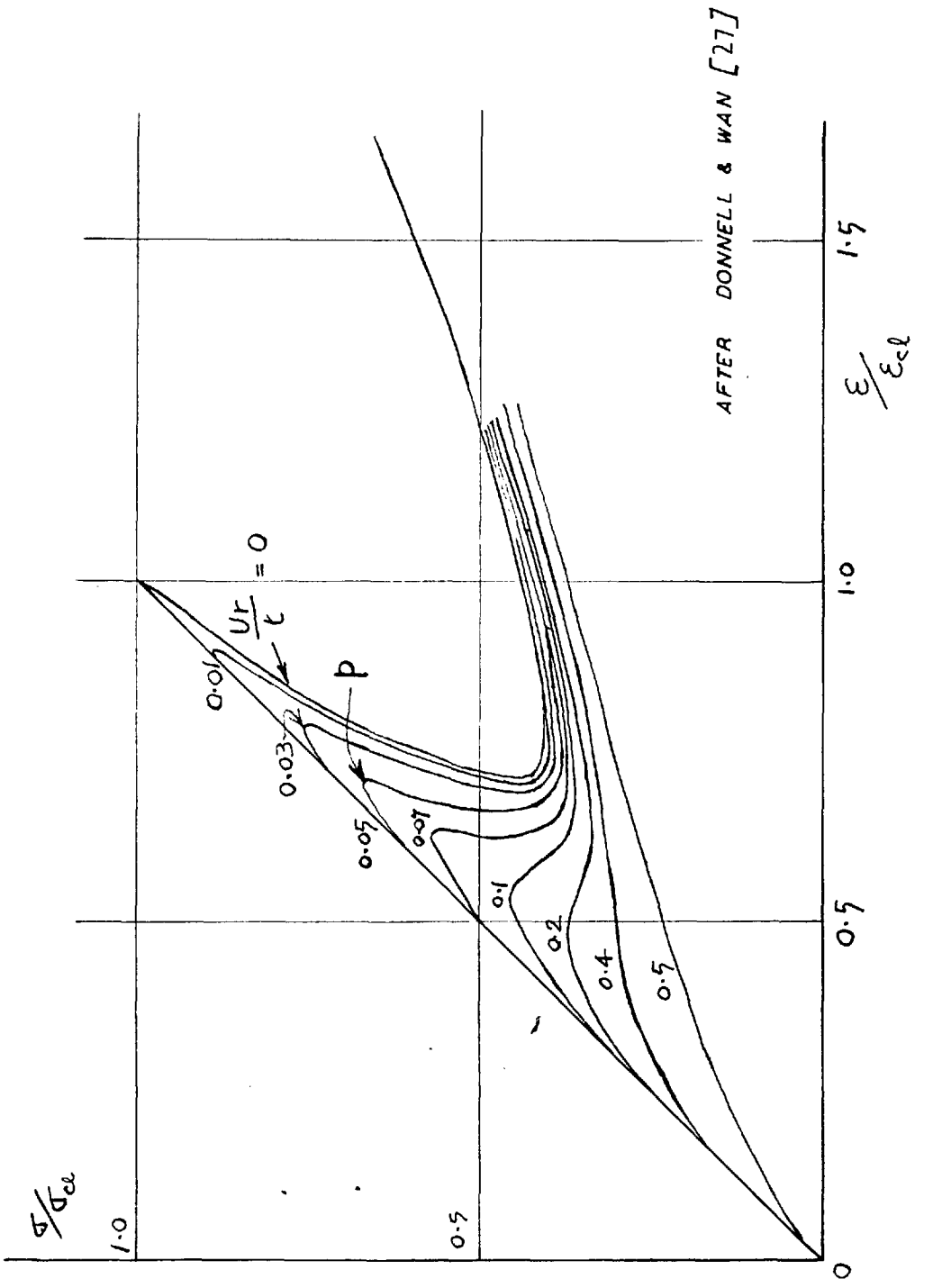


FIG. 3·13 THE EFFECT OF INITIAL IMPERFECTIONS ON THE STRESS - SHORTENING DIAGRAM FOR AN AXIALLY COMPRESSED CYLINDRICAL SHELL.

the unbuckled state while the branch ABCD represents equilibrium configurations in the post-buckled state. Equilibrium configurations represented by AB are statically unstable, while those represented by CD are stable. The stability of the equilibrium configurations represented by BC depends on the nature of the loading process being considered. For deadweight loading it represents unstable states, while for controlled end-shortening it represents stable states. For loading cases intermediate between the two extremes, the change from unstable to stable states of equilibrium will occur somewhere between B and C.

For the loading case where the distance between the end plates is controlled, a perfect cylinder should theoretically follow the line OA (Figure 3.9) up to the point A as the end-shortening is increased. At A, something drastic must happen, for after buckling starts the end shortening must decrease (i.e. the end plates have to move apart) to maintain equilibrium. If this is not done, the next possible equilibrium state lies on the curve BD in the vicinity of C.

In the case of a testing machine that will allow both the load to decrease and the end-shortening to increase when the cylinder buckles, the jump will follow the testing machine characteristic as indicated in Figure 3.10. Thus at A the

equilibrium configuration of the shell will jump to that at b or c according to the rigidity of the testing machine. Point A, which is the classical buckling load of the linear theory, is referred to as the "upper buckling load" by Tsien.

In accordance with Karman and Tsien's ideas, it is possible that if disturbances of sufficient magnitude act on the cylinder, a jump might occur at point a before the point A is reached, and end at b' or c' on the other stable branch, as shown in Figure 3.10.

In order to determine the point called the "lower buckling load" at which a jump might take place, Tsien (1942) (134) introduced a principle which is now referred to as the "energy criterion" of buckling. In it, Tsien reiterated the statement made previously by Karman and himself, that "under average and actual service conditions themost probable equilibrium state is the one with the lowest possible energy level". This assumes that disturbances of sufficient magnitude exist so that the transitions from higher energy levels to lower energy levels, may be able to take place. There are two conditions that must be met for these possible energy levels: (a) corresponding external forces andinternal stresses must be in equilibrium (b) the geometric restraint and loading conditions must be satisfied.

This second condition depends on the manner in which the specimen is loaded. Limiting loading processes are provided by a rigid testing machine and by dead weight loading. For a rigid testing machine buckling is likely to occur at a certain value of end shortening, δ, which gives equal strain energy for the unbuckled equilibrium state represented by A (see Figure 3.11(a)) and for the buckled equilibrium state (represented by B). For deadweight loading buckling will occur at a certain value of the end load which gives equal total potential energy, ϕ, before and after the jump (ϕ = S-Pδ, where S is the strain energy, P is the loading force, and δ is the end shortening of the specimen). (See Figure 3.11(b)).

Tsien applied this criterion to long, perfect, cylindrical shells under axial compression, and to perfect spherical shells under external pressure. In both cases buckling loads of the same order of magnitude as found in laboratory experiments were obtained. Some of Tsien's support for the "energy criterion" principle came from a comparison between the theoretical and experimental results for the case of a column with nonlinear elastic supports [133, 134]. However, these results (Figure 3.12) appear to support the idea of "imperfections" contributing to the lowering of the buckling load, as well as any support they provide for the energy criterion of buckling.

Since Tsien first formulated his energy criterion of buckling, there has been much criticism of it. There has been some support for it, but the greater part of the criticism is adverse. Several researchers have referred to the criterion as being a rather arbitrary approach and of little value. (e.g. see Thompson [126] and Fung and Sechler [40]) Even though the energy of the cylinder in the unbuckled and post-buckled stable states are equal at the "energy criterion" (or "equal energy") load, the probability of buckling depends on whether or not sufficient additional energy can be imparted to the cylinder to enable it to pass through the unstable post-buckles state that separates the two stable equilibrium states. The amount of energy required to pass throughthe unstable equilibrium state is given in Figure 3.11 as the difference between the lines OA and AF. While it was thought that external vibrations might be sufficient to supply the additional energy required to cause buckling at the "energy criterion" load, tests under many different conditions have instead led to the opposite view.

The "energy criterion" of buckling loses much of its usefulness when it is being used to determine the theoretical buckling stress since the values of the potential energy (or the strain energy) are dependent upon the choice of the normal-deflection function. This has been shown by Almroth [2] where

the load-potential energy curve varies according to the number of parameters in the assumed normal-deflection function.

Since Tsien used the particular case of a column with non-linear elastic supports to support his energy criterion of buckling, other researchers have suggested that the case of a transversely loaded arch should be considered as well. Fung and Kaplan [38] found that experimental snapthrough loads for the shallow arch agreed reasonably well with the classical load whereas the energy criterion of buckling led to buckling loads much too low in comparison. In another case, where buckling took place under transitional buckling modes, Gjelsvik and Bodner [45] found that the "energy criterion" load was a reasonable lower bound to other theoretical and experimental results.

While much doubt has been cast upon the energy criterion of buckling as formulated by Tsien, there may be some cases where it is useful and can provide reasonably accurate results. On the whole though, it has not become established as a buckling criterion.

3.4.4.2 Imperfection Theory

A comprehensive analysis of initially imperfect cylinders was carried out by Donnell and Wan [27]. They used the assumption that only the component of the initial deviation from the perfect shape which is of the same shape as the deflection surface, is of importance. The deflected surface expression they used contains

one more abbitrary constant than that used by Karman and Tsien.

Donnell and Wan took:

$$w = at\left(\cos \frac{mn}{R}x \cos \frac{ny}{R} + b \cos \frac{2mnx}{R} + c \cos \frac{ny}{R} + d \right) \tag{3.39}$$

Initial deviation from perfect shape, w_o, is given by:

$$w_o = a_o t\left(\cos \frac{mnx}{R} \cos \frac{ny}{R} + b \cos \frac{2mnx}{R} + c \cos \frac{ny}{R} + d \right) \tag{3.40}$$

The equation for the membrane stress function becomes:

$$\nabla^4 \phi = Ek \left[\frac{(\partial^2 w)^2}{(\partial x \partial y)} - \frac{\partial^2 w}{\partial x^2} \cdot \frac{\partial^2 w}{\partial y^2} \right] - \frac{E}{r} \cdot \frac{\partial^2 w}{\partial x^2} \tag{3.41}$$

where:

$$k = 1 + \frac{2w_o}{w} = \text{constant.}$$

Donnell and Wan derive an energy expression, solving it by the Rayleigh-Ritz method. They present their results (Figure 3.13) as a graph of stress ratio versus end shortening ratio, including the effect of an unevenness factor. U - the unevenness factor, is a constant proportional to the amplitude

of the initial imperfection, $a_o t$, which is considered as a function of the fabrication method alone, and is an assumed geometric equivalent of the various kinds of imperfection: geometric, material, service, condition, etc.

a_o is assumed to be of the form:

$$a_o = \frac{(U)}{(\pi^2)} \frac{l_x^{1.5} l_y^{0.5}}{t^2} = \frac{Ur^2}{m^{1.5} n^{0.5} t^2} \qquad (3.42)$$

Figure 3.13 shows the average stress versus end shortening for various values of the parameter Ur/t. For a cylinder with a certain value of Ur/t, say 0.05, the behaviour of the shell in a testing machine may follow the loading curve smoothly and gradually up to the peak p, and will then fail elastically in an explosive manner, ending at a point at a lower branch of the curve according to the rigidity of the testing machine as discussed previously (see Figure 3.10). It is possible that with large enough disturbances, a jump may take place before the peak p is reached, and this cannot be ruled out, but the usefulness of the idea of the energy criterion is now lessened. Donnell and Wan believe that buckling occurs at the peak p, and not before the peak is reached, unless plastic deformation sets in. With the imperfection theory, any possible jump before the peak p is reached would be explained by a larger value of the constant U.

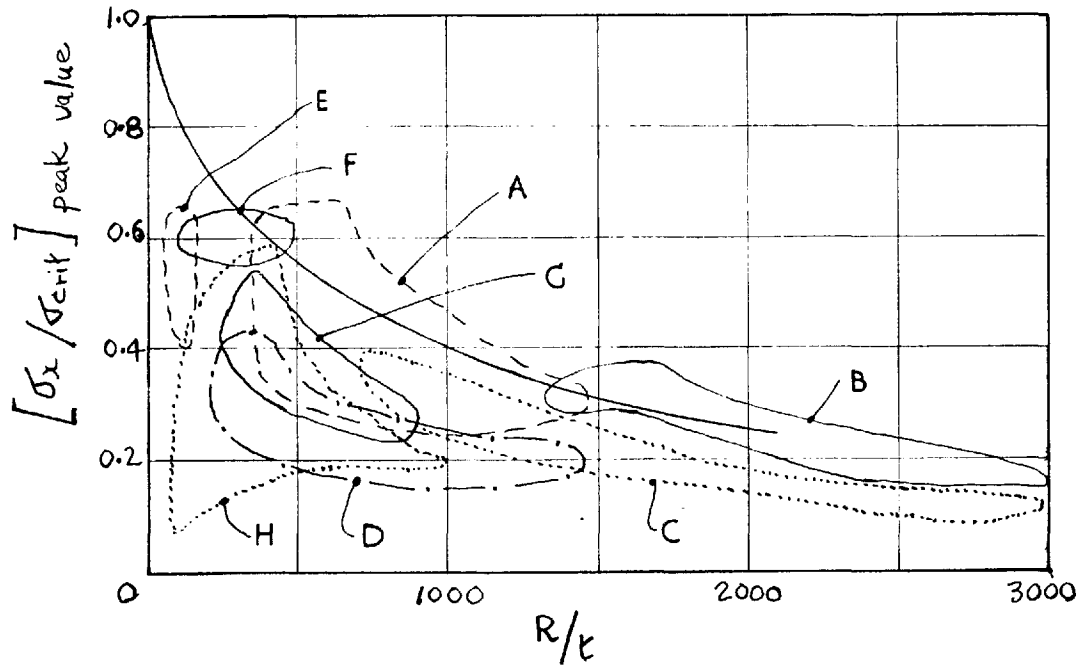


FIG. 3.14. DONNELLS PLOT OF PEAK VALUE OF STRESS RATIO [$U_0 = 0.00015$] AGAINST R/t WITH RESULTS OF AXIAL COMPRESSION TESTS.

A	LUNDQUIST	[DURAL]	[81]
B	GALCIT	[STEEL]	[49]
C	"	["]	[50]
D	DONNELL	[STEEL, BRASS]	[24]
E	FLUGGE	[CELLULOID]	[34]
F	ROBERTSON	[STEEL]	[101,102]
G	BRIDGET	[BRASS, STEEL]	[14]
H	WILSON & NEWMARK	[STEEL]	[142]

In their paper, Donnell and Wan give an example of a cylinder with U = 0.00015, and $\sigma_y/\sigma_{cr} = 5$, where σ_y is the yield stress of the material. They show that by a suitable choice of the value U, the theoretical curve can be lowered to the level found in experiments.

Figure 3.14 shows Donnell and Wan's graph of σ/σ_{cl} vs r/t.

3.4.4.3 Dynamic Theory

The only dynamic analysis that has been carried out to date is that of Yao (1963) [144]. In the analysis, the equations of motion for the cylinder were solved to give a continuous load-displacement curve for the pre- and post-buckled states. The effects of initial imperfections were also included in this. The results showed that the cylinder, in contrast to the static theory, has a vibratory motion after the cylinder loses its initial stability. When small imperfections were considered under cases of slow loading, the dynamic theory predicted a buckling stress of about the same magnitude as the classical value. Larger imperfections when taken into account, caused a significant drop in the buckling strength of the cylinder.

As they stand, Yao's numerical results are of limited use since he did not seek to give a complete picture of the buckling process. They do, however, show the possibilities of the dynamic method. Yao only considered the two cases of

initial imperfections (one large and one small) and only considered one value of the wavelength ratio, μ. In addition, the assumed expression for the initial imperfections was of the same form as the radial deflection function used by Karman and Tsien (Equation (3.36) while the expression used to represent the buckled shape was the same as that used by Kempner (i.e. Equation (3.39). Further development of the theory can be expected to make it more general in a way similar to that in which Karman and Tsien's early work has been developed.

3.4.5 Comment

All the theoretical work carried out in connection with perfect cylindrical shells sought to represent the displacement function, w, by an expression that corresponded to the experimentally observed buckling pattern. Minimising the total potential energy with respect to the undetermined parameters should then enable the buckling process to be described completely. However, it found that the minimum post-buckling load that could be reached was still considerably above that found experimentally.

The next stage was to consider more terms in the Rayleigh-Ritz solution, i.e. to take further terms in the expansion that describes the normal displacement. This has been done recently by Almroth [2] as well as in this thesis. Almroth used up to

eight undetermined parameters in the displacement function, and claimed that after this, there was negligible change in the minimum post-buckling load. At that stage also, the theoretical min. post-buckling load was of the same magnitude as Thieleman had found experimentally, and it changed only very slightly over a range of end shortening. Hence it would seem that a total of ten parameters are required to describe the post-buckling function of an axially compressed cylinder. Functions like that used by Almroth though, no longer represent a diamond shaped buckling pattern.

The most recent work appears to be that of Sobey [161]. In this, he minimises the total potential energy with respect to twenty-five parameters.

Kuranishi and Niisawa (1959) [72] have shown that the choice of a more complicated displacement pattern than that normally chosen, can reduce the upper buckling load of a perfect cylindrical shell below that of the classical value.

Even though Almroth has shown that the energy theory can predict a minimum post-buckling load that is in agreement with that of experiment, three other possibilities can also be investigated.

1) A more complicated displacement function that meets the boundary conditions can be tried.

2) More parameters can be taken in the displacement function and used in the imperfection theory.

3) Instead of using one displacement function and a stress function, three displacement functions may be used, thus allowing more accurate strain-displacement relations to be used, e.g. $1/2\ (\partial u/\partial x)^2$, $1/2\ (\partial w/\partial x)^2$ can be retained in the expression for ϵ_x.

3.5 BENDING

3.5.1 Introduction

The buckling behaviour of cylinders under bending corresponds to that of axially compressed cylinders in two respects. Firstly, linear theory predicts buckling stresses of the same order of magnitude for both these cases. Secondly, the test data are below the predictions of linear theory by approximately the same amount. As a result, Gerard and Becker have correlated test data on cylinders in bending in a manner similar to that used for axially compressed cylinders.

In addition to those factors that affect the stability of cylinders under axial compression, the stability of cylinders under bending is also affected by the linear variation of bending strain across the section. This results in a strain

gradient, and hence a stress gradient, at any location on the cylinder surface. Hence a "gradient factor" has been introduced which permits calculation of the bending-buckling stress from the axial-compressive buckling stress of a corresponding circular cylinder.

3.5.2 Linear Theories

According to Gerard and Becker [44] the first person to investigate the bending stability of cylinders, was Brazier (1927). He calculated the stress at which a circular cylinder would become unstable as a result of the flattening of the cross-section. This type of instability is comparable with Euler buckling of a very long axially compressed cylinder.

Often it has been assumed that the stress at which local buckling under bending has occurred in cylinders, is equal to the value for axially compressive buckling for the same cylinder. Flugge (1932) however, performed calculations based upon the linear theory that showed a 30 per cent increase in bending-buckling stress over the classical value for the axial case. An increase of about this magnitude is shown by the experimental results obtained by Lundquist (1935) on aluminium specimens, and Donnell (1934) on steel and brass specimens.

Gerard and Becker [44] divide the local-buckling behaviour of cylinders in pure bending into three ranges, as they do for

other cases. "In the short cylinder range, the buckling coefficient k_b approaches that of a wide compressed plate as a lower limit." k_b is expressed in the form:

$$k_b = \frac{12(1-\nu^2)}{\pi^2 E} \sigma_{cr} \left(\frac{L}{t}\right)^2 \qquad (3.43)$$

In the long cylinder range, the relation between the buckling stress and the cylinder geometry is of the form: $\sigma_{cr} = CEt/R$.

"The two limits of the local buckling region are connected by a transition curve, and throughout this entire region buckling occurs in the diamond pattern observed in axially compressed cylinders. When the cylinder is very long, the flattening of the cross-section caused by the radial components of the axial deformation in the bent cylinder leads to a large reduction of the effective section modulus of the cylinder, and instability occurs as a single transverse wave on the compression side of the shell. This is the type of instability investigated by Brazier."

3.5.3 Nonlinear Theories

To date, no finite-displacement analyses have been reported for the bending of cylinders.

3.6 THE EFFECT OF INTERNAL PRESSURE

3.6.1 Introduction

For the case of no internal pressure, the average stress in the cylinder in the circumferential direction is almost zero. However, when the cylinder is loaded under internal pressure, the circumferential stress is not zero, and changes in the buckle pattern result. Gerard and Becker [44] have shown that stability is influenced by the nature of the superimposed membrane stresses at buckling and that tensile stresses have the effect of increasing the post-buckling loads. On this basis, since the circumferential stresses induced by the internal pressure are tensile, it would be expected that internal pressure would increase the buckling loads of the cylinder. This has been shown both experimentally and theoretically to be the case.

3.6.2 Axial Compression with internal Pressure

According to the small-deflection analysis made by Flügge (1932), the effect of internal pressure on the critical load of the axially compressed cylinder was negligible. This does not agree with experimental results, however.

In order to improve the agreement between theory and experiment, Lo, Crate and Schwartz (1950) [77] carried out a large deflection analysis of the problem. The approach was to use the

nonlinear equations of Karman and Tsien, but extended to take account of the internal pressure. The internal pressure alters the expressions for total potential energy, strain energy, and the relation between the end-shortening and the average compressive stress. The same deflection function as used by Karman and Tsien, was tkken. The total potential energy was expressed in terms of the two nondimensional parameters: $\bar{\sigma}_{cr} = \frac{\sigma_{cr}}{E} \cdot \frac{R}{t}$; & $\bar{p} = \frac{p}{E} \frac{(R)^2}{(t)}$. This was differentiated with respect to four arbitrary parameters, but instead of solving the resulting four partial differential equations, to obtain the complete stress ($\bar{\sigma}_{cr}$) versus end-shortening ($\bar{\varepsilon}$) curve, Lo et al. produced a method for determining solely the buckling stress. To do this, they used Tsien's energy criterion and assumed that the end-shortening remains constant during buckling, i.e. the testing machine is rigid. The method given for determining $\bar{J}_{cr}$ was reasonably straightforward.

Their theoretical work showed that there was no possibility of increasing $\bar{J}_{cr}$ beyond the classical value of 0.605, and that this is the buckling pressure for all values of $\bar{p} \geqslant 0.169$.

From their experimental work for $\bar{p} < 0.1$, even though the results followed the trend of the theory, there was a considerable discrepancy between them.

Fung and Sechler (1957) [39] sought to extend the work of Lo et al. by carrying out a series of tests for pressures up to $\bar{p} \approx 2.0$. They found that the experimental values were much lower than theory, but did show the same trend. When the increments of $\bar{\sigma}_{cr}$ (i.e. $\Delta\bar{\sigma}_{cr} = \bar{\sigma}_{cr} - (\bar{\sigma}_{cr})_{\bar{p}=0}$) are plotted against $\bar{p}$ there is much better agreement with Lo's theory, but the results are fairly scattered even so.

A useful part of their paper is the photographs showing the changes in buckle pattern with increasing internal pressure. At zero internal pressure the diamond shaped buckles are isolated and random. With slight internal pressure there is a helical arrangement of consecutive buckles. These change to elongated diamond shaped buckles, finally becoming bellows-shaped buckles as the pressure increases further.

At about the same time, Harris, Suer, Skene and Benjamin [51] (1957), investigated experimentally the stability of thin walled cylinders under axial compression and taking internal pressure into account. They sought to extend Karman and Tsien's large deflection theory and Donnell and Wan's use of initial imperfections, to this case. At the same time, the usefulness of the idea of initial imperfections in the cylindrical shell is limited since the magnitude of the imperfections requires to be known. For cylinders used in construction, it is almost

impossible to determine these initial imperfections. As a result, Harris et al. resorted to a semi-empirical development of curves that could be used for design purposes.

Their approach had the disadvantage that there was a considerable scatter in the test results they used. It also entailed the basic assumption that the initial imperfections in test specimens were similar to those in actual structural cylinders. However, as they were mainly interested in the design curves for missile construction, they developed them from the test data as 90 per cent probability curves by correlating the experimental data statistically with theoretical parameters.

One of the most thorough investigations of the effect of pressurization on the axial compressive buckling of thin walled cylinders has been carried out by Thielemann (1958) (125). While this analysis applies to unpressurised cylinders as well, its main purpose was to consider the effects of internal pressure, not only for isotropic cylinders, but also for orthotropic ones.

Figure 3.15 shows Thielemann's post-buckling functions for the axially compressed isotropic cylinder as a function of the internal pressure parameter, $\bar{p}$. To obtain these, Thielemann solved the nonlinear partial differential equations using a computer to give an iterative solution. The post-buckling function marked $\bar{p} = 0$ is identical with the post-buckling function determined by Kempner. In this case (i.e. $\bar{p} = 0$)

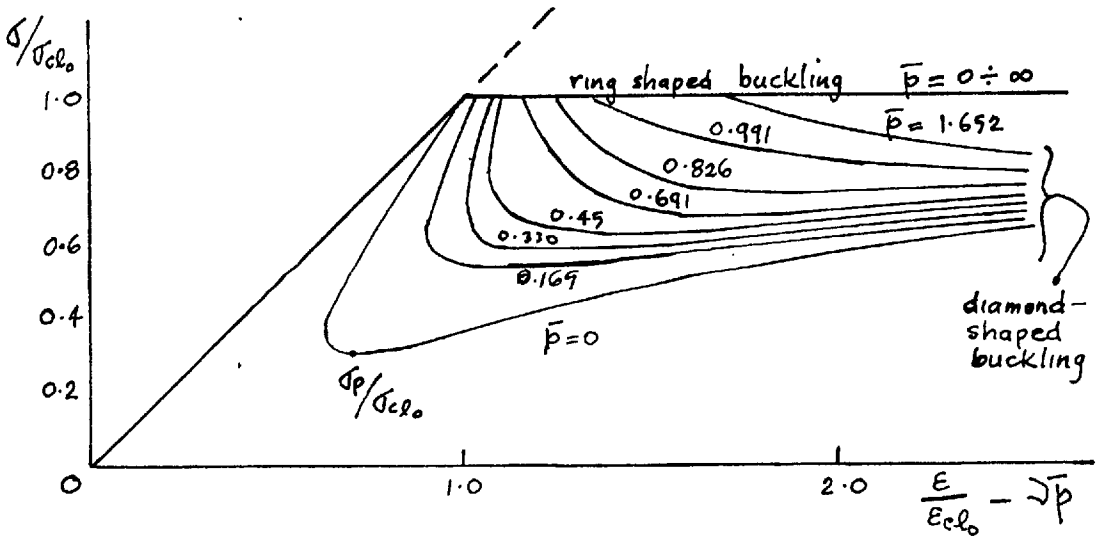


FIG. 3·15: POST BUCKLING FUNCTIONS FOR INTERNALLY PRESSURISED CYLINDERS.

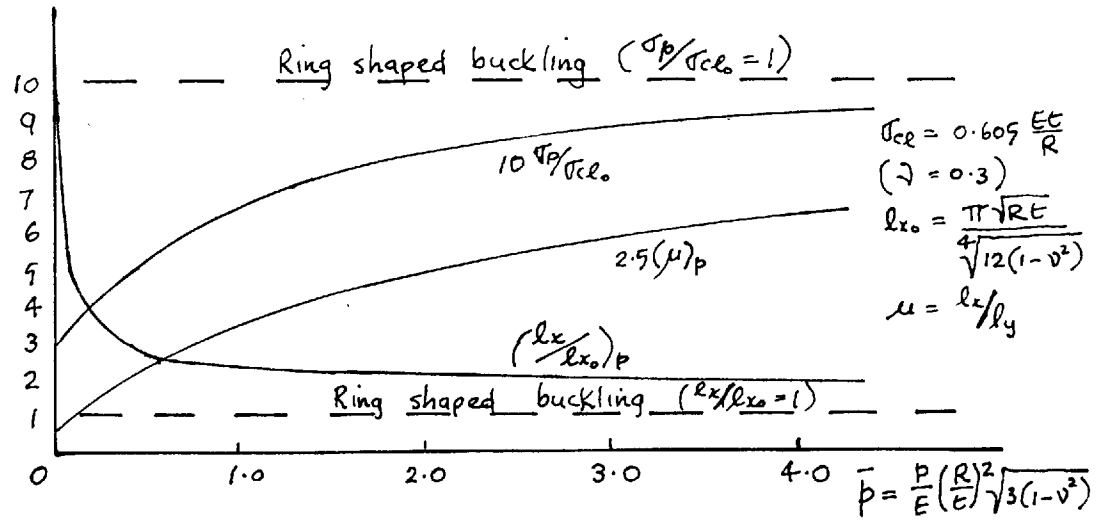


FIG. 3·16: EFFECT OF INTERNAL PRESSURE.

the first branch of the solution which is connected with diamond shaped buckling, as well as the second branch which is connected with ring-shaped buckling, bifurcate from the same point $\bar{U} = 1$ on the straight line: $\bar{U} = \bar{\varepsilon}^*$.

For the case $\bar{p} > 0$, the branch of the first solution does not bifurcate from the straight line $\bar{U} = \bar{\varepsilon}^*$ representing the prebuckling states of equilibrium, but from some part of the second solution connected with ring-buckling. As can be seen from Figure 3.15 the ring-buckling configuration becomes stable within a certain range of end-shortening before it changes into a diamond-shaped configuration. The higher the internal pressure, the larger will be the range of stable ring-buckling. The characteristic snapthrough effect that is found in unpressurised cylinders disappears for higher values of interior pressure. In agreement with these theoretical results, stable ring-buckling configurations have indeed been observed in tests.

Figure 3.15 also shows quite clearly the strong influence of the internal pressure on the post-buckling functions connected with diamond shaped buckling. In the post-buckling region, increasing internal pressure considerably increases the minimum load carried by the cylinder. However, the post-buckling function connected with ring-buckling is not influenced at all by the pressurisation; thus the buckling stress of an axially compressed cylinder cannot be increased above the classical stress.

The effects of pressurisation are also shown in Figure 3.16. The minimum values σ_p/σ_{clo} of the post-buckling loads are shown, with the classical buckling load as reference. This ratio increases from the 0.3 value of the unpressurised cylinder up to nearly unity with increased pressure. Also shown is the ratio of the half-wavelength connected with the buckling configuration at minimum of the post-buckling function, to the half-wavelength of ring-buckling. As well, there is shown the ratio μ of the circumferential to axial wavelengths, as a function of the internal pressure. It can be seen that the form of the buckling pattern is influenced greatly by the presence of even very small values of internal pressure.

3.6.3 Torsion with internal Pressure

The first paper that discusses the effects of internal pressure on the torsional buckling of circular cylinders, was by Crate et al. (1944) [22]. They derive an empirical interaction equation to match a series of experimental tests. They suggest using the equation:

$$R_t^2 + R_p = 1 \qquad (3.44)$$

where $R_t = \tau/\tau_{cr}$ and $R_p = p/p_{cr}$. This has since been quoted by both Batdorf, and Gerard. The value τ_{cr} is the experimental buckling stress, and p_{cr} is determined as the critical external pressure for hydrostatic loading as given by the approximate

equation:

$$p_{cr} = - 0.92\ E\ R/L\ (t/R)^{2.5} \qquad (3.45)$$

which is applicable in the range $15\ t/R \leq (L/2R)^2$.

Hopkins and Brown (1951) [60] used a solution of the Donnell small-deflection equation adapted to include the effect of the internal pressure. They found good agreement between experimental and theoretical values of the critical shear stress, and were able to show that a small increase in internal pressure was able to give a quite large increase in the critical torsional moment (i.e. 50 - 250 per cent increase in moment for an 8 p.s.i. internal pressure, depending on the L/R ratio). It was also found that an increase in internal pressure increased the number of circumferential buckles, and also increased the angle between the axis of the cylinder and the direction of the waves. The slight variation between the results for clamped and simply-supported ends was found to diminish rapidly with increase of internal pressure. This analysis did not consider post-buckling behaviour. Interaction formula were discussed on the basis of their theoretical and experimental work.

The most comprehensive analysis to date, both experimentally and theoretically, has been carried out by Weingarten (1962) [139]. While the theoretical work was a small displacement analysis based on a modified form of Donnell's equation, the experimental work

carried into the post-buckling region. Weingarten showed that the results given by his proposed interaction formula were in reasonable agreement with the results from his small displacement analysis.

The modified form of Donnell's equation was:

$$D(\nabla^2+1)^2 w + \frac{Et}{R}\nabla^{-4}\frac{\partial^4 w}{\partial x^4} + t(\sigma_x \frac{\partial^2 w}{\partial x^2} + \sigma_\theta \frac{\partial^2 w}{R^2 \partial^2 \theta} + \sigma_x \frac{1}{R}\frac{\partial^2 w}{\partial x \partial \theta}) = 0 \qquad (3.46)$$

and this was solved by Galerkin's method assuming that the radial deflection was of the form:

$$w = \sin n\theta \sum_{m=1}^{\infty} a_m \sin \frac{m\pi x}{L} + \cos n\theta \sum_{m=1}^{\infty} b_m \sin \frac{m\pi x}{L} \qquad (3.47)$$

Values of the critical torsion stress parameter $(\tau/\tau_{cr})_c$ were computed from the small deflection theory by varying the pressure parameter p/p_c for the cases of (a) lateral internal pressure ($\sigma_c = 0$) (b) hydrostatic internal pressure ($\sigma_c = -\frac{pR}{2t}$) (c) combined internal pressure and tension ($\sigma_c = -\frac{pR}{t}$).

Here τ = buckling shearing stress under combined loads

τ_{cr} = critical stress for unpressurised cylinders

p = uniform internal or external pressure

p_c = critical external pressure

$$= \frac{\sqrt{6}\pi}{9(1-\nu^2)^{3/4}} \cdot \frac{E}{(L/R)(R/t)^{5/2}}$$

The pressure parameter p/p_c was determined from the approximate equation:

$$p/p_c = \frac{3\sqrt{2}}{4\pi} \sqrt{Z} \cdot p^*$$

where p^* = internal pressure parameter $= \sqrt{12(1-\nu^2)} \frac{p}{E} \left(\frac{R}{t}\right)^2$

Z = geometrical parameter $= L^2/rt \cdot \sqrt{12(1-\nu^2)}$

This enabled the torsion stress parameter $(\tau/\tau_{cr})_c$ to be evaluated from the theory for small deflections.

The interaction formula:

$$(\tau/\tau_{cr})^2_{INT} = (1 - R_c)(1 - p/p_c)$$

where R_c = compression stress ratio $= \sigma_c/\bar{\sigma}_c$

with $\bar{\sigma}_c = \frac{E}{3(1-\nu^2)} \cdot \frac{t}{R}$

was also used to evaluate $(\tau/\tau_{cr})_{INT}$.

The ratio of the computed values of the torsion stress parameter obtained from the small deflection analysis to the values obtained from the interaction formula, showed a variation of less than 3 per cent.

3.6 4 Axial Compression and Torsion with internal Pressure

Harris, Suer and Skene (1958) [52] touched briefly on the effect of internal pressure on this combined loading. As far as they could judge from the very few tests carried out - and for

only two different values of the pressure parameter $\bar{p}$ at that - the same interaction formula as was suggested for the unpressurised cylinder would seem to hold.

The interaction formula $R_c + R_t^2 = 1$ was a lower bound to the experimental results. The critical stresses for the individual loading cases which appear in the denominator of the formula, were to be the values for the cylinder under the appropriate internal pressure.

i.e. for any pressure $\bar{p}$, $$\left\{ \frac{\sigma_x}{(\sigma_x)_{\bar{p}}} \right\} + \left\{ \frac{\tau}{\tau_{\bar{p}}} \right\}^2 = 1 \qquad (3.48)$$

They found that the order of application of the axial load and torsion, did not affect the magnitude of the critical stresses.

Weingarten's paper [139] also considered the effect of internal pressure on the combined torsion and axial compression (or tension) loading. It was shown that the interaction formula:

$$R_t^2 = (1 - R_c)(1 - R_p)$$

where:

$R_t = \tau/\tau_{cr}$

$R_c = \sigma/\bar{\sigma}_c$ as in Section 3.6.3

$R_p = p/p_c$

gave results that were not more than 2 per cent different from

those calculated from the accurate small deflection analysis. The experimental results are lower than those predicted by the linear theory at low pressures, where imperfections are probably significant, but approach the linear theory results as the pressure increases (i.e. as the tensile forces set up by the internal pressure increase).

3.6.5 Bending with internal Pressure

The buckling of a cylinder under bending is similar to axial compressive buckling, though the buckling stresses are slightly greater on account of the variation in the magnitude of the compressive stress around the circumference. However, unlike the case of axial compressive buckling, the critical stress of the pressurised cylinder under bending exceeds that of the small-deflection of unpressurised cylinders, i.e. the classical value.

The explanation for this behaviour is given by Stein and Hedgepath, and reported by Weingarten (1962) [138]. They found that the collapse moment under bending is twice the moment at which wrinkling starts at the outer fibre of the cylinder. Hence we must differentiate between the buckling moment at which the outer portion of the compressive zone of the cylinder first shows significant deformation and the collapse moment for which the deformation becomes infinitely large.

No large deflection analyses have been carried out to date.

This is to a large extent due to the considerable mathematical difficulties and the problem of selecting a suitable deflection function.

The first work on th. stability under bending of pressurised cylinders was carried out by Harris et al (1958) [122]. Their tests showed the increase in strength given by pressurisation. They found that the internal pressure changed the buckle pattern by decreasing both wavelengths, with the longitudinal half-wavelength decreasing more than the circumferential one.

In 1962, Weingarten [138] carried out a small-deflection analysis, the numerical results of which do show the increase in buckling strength with increasing internal pressure. He used the same modified Donnell equation as given in the previous section (Equation (3.47)).

The stresses prior to buckling were taken to be:

$$\sigma_x = \sigma_c + \sigma_b \cos \quad ; \quad \sigma_{x\theta} = 0; \quad \sigma_\theta = \frac{pR}{t}$$

The differential equations were solved by the Galerkin method, assuming the radial deflection to be given by:

$$w = \sin \frac{m\pi x}{L} \sum_{n=0}^{\infty} a_n \cos n \qquad (3.49)$$

In this way, Weingarten produced an interaction curve in the form of a graph, for the case of buckling of pressurised cylinders under bending.

He showed that for a particular cylinder, the buckling load determined experimentally was less than the small-deflection value for $p^* < 2.0$ [1] and above it for $p^* > 2.0$. Also, when axial tensile forces are present (hydrostatic case), there is a reduction in the extent of the buckled area, due to the effect of the superimposed tensile stresses.

3.7 COMBINED LOADINGS

3.7.1 Introduction

It would appear that the first investigations into the buckling of circular cylindrical shells under combined loads were experimental. Bridget, Jerome, and Vosseller (1934) [14] conducted tests on steel and brass cylinders in torsion combined with axial tension or compression, and derived empirical interaction curves from the results. Wagner and Ballerstedt (1936) constructed an interaction equation from the data obtained from tests on brass cylinders under torsion and tension.

Theoretical analyses were made by Kromm (1939) andby Leggett (1943) on the combination of torsion and axial compression, using the basic linear shell equilibrium equations. Subsequently,

---

(1) $$p^* = \frac{p}{E}\left(\frac{R}{t}\right)^2 \sqrt{12(1-\nu^2)}$$

Bruhn (1945) conducted a large number of tests on celluloid cylinders under various combinations of axial compression, axial tension, bending and torsion. He compared his results with empirical interaction relations.

More recently, Batdorf, Stein and Schildcrout (1947) investigated buckling under axial compression and torsion using Donnell's equation. They derived theoretical interaction relations which they modified for practical application by substituting empirical buckling stresses for the theoretical values in the denominators of the stress ratios.

3.7.2

The present state of knowledge regarding the effect of the interaction of various loading cases on the stability of thin-walled isotropic cylinders, is shown in Table 1. From this it can be seen that our knowledge regarding interaction effects is still limited. Even in those cases where an attempt has been made to describe the buckling by means of an interaction formula, the results are not entirely satisfactory. In nearly all cases the interaction effect is given with reference to the classical buckling criterion; the only case where the lowest buckling load of the post-buckling region is used is Terebushko's formula for the case of combined axial compression, external

TABLE 3.1 INTERACTION FORMULAE.

LOADING	INTERACTION FORMULA	REFERENCE	NOTES	
axial compression + bending	$R_c + R_b = 1$	Bruhn (Gerard[44])	all values of Z_L ; all edge restraint	
axial compr^n + torsion	$R_c + R_b^2 = 1$	Batdorf[10]	using theoretical $(\sigma_x)_{cr}$ and $(\tau)_{cr}$ $Z_L < 1$: simply-supported case $Z_L < 5$: clamped case	
			using empirical $(\sigma_x)_{cr}$ and $(\tau)_{cr}$ $1 < Z_L < 7.7\left(\frac{R}{t}\right)^2$: simply-supported $5 < Z_L < 7.7\left(\frac{R}{t}\right)^2$: clamped	
axial tension + torsion	$0.4R_c + R_t = 1$	(Gerard[44])	using theoretical values	$-1 < R_c < 0$ $30 < Z_L < 7.7\left(\frac{R}{t}\right)^2$ all edge restraints
	$0.8R_c + R_t = 0.9$	Batdorf[10]		
	$0.5R_c + R_t = 1$	Batdorf[10]	using exptl. values	
torsion + bend.	$R_t^2 + R_b^{1.5} = 1$	(Gerard[44])		
axial compr^n. + torsion + bending	uncertain, but possibly $R_c + R_b + R_t^2 = 1$	(Gerard[44])		
axial compr^n. + torsion + ext. presure	$R_c + R_p^{\frac{3}{4}} + R_t^{\frac{3}{2}} = 1$	Terebushko	based on initial buckling load	
	$R_c + R_p + R_t = 1$		based on 'lower' buckling load	

pressure and torsion. It has generally been found that to produce a suitable interaction formula, it is necessary to base it on the experimentally observed values of critical load and not on theoretical results. It has been found that agreement of the formula with experimental results is poor, especially in cases where the axial compression stress predominates.

3.8 DISCUSSION

From all this, a few observations can be made about the three main loading cases, i.e. external pressure, torsion, and axial compression. Some of these comments can be applied to the other cases as well. All throughout, the linear theory has not been sufficient to explain all features of the experimental behaviour. For the case of axial compression in particular (as well as other cases where the superimposed membrane stresses at buckling are compressive) the finite displacement theory is necessary to describe the post-buckling behaviour.

There is even then, a wide discrepancy between experimental post-buckling loads and those predicted theoretically. This might well however be remedied by considering more terms in the arbitrary function (or functions) that is (are) used in the approximate method of solution of the stability problem. This is described in later Chapters, as well as in Reference 2.

For the case of axial compression, while an attempt has been made by Tsien and by Karman and Tsien to explain buckling, in terms of changes of energy and "energy levels", it is the consideration of initial imperfections after the manner of Donnell and Wan that seems to explain best the discrepancy between theoretical and experimental buckling loads. The main drawback to the widespread use of initial imperfections to give better theoretical estimates of the buckling load lies in the difficulty of deciding on the magnitude of likely imperfections. For this reason it seems best to consider the minimum loads carried in the post-buckling region as the basis of comparison and this is followed in the subsequent comparison of theoretical and experimental work in this thesis.

Since the minimum post-buckling load is not as greatly influenced by initial imperfections as is the snapbuckling load, a theoretical approach that agrees reasonably well with test results for this seems to provide the most practical approach to the problem. In this way, the minimum post-buckling load should provide the lowest minimum to the load-carrying capacity of the cylindrical shell and as such is the base that must be used in a load factor or similar assessment of the shell strength.

CHAPTER FOUR

SPHERICAL SHELLS

4.1 INTRODUCTION

There have been two approaches to the treatment of the stability of spherical shell segments and complete spherical shells. One approach (e.g. that of Fung and Sechler [39]) is that the spherical shell segment is simpler to solve analytically than the complete sphere and can be used as a starting point for the latter. The other approach (as given by Thompson [126]) is that the sphere is simpler to deal with as it has membrane stresses only, while the clamped spherical shell segment has bending stresses introduced. Recent work by Gjelsvik and Bodner [46] favours the former approach. They point out that the use of a boundary layer treatment in the case of a clamped spherical segment does lead to a reasonable asymptotic solution. The same approach (as introduced by Friedrichs [37]) has given totally different results in the case of the complete sphere, and here the correct asymptotic behaviour is still an unresolved problem.

Several of the early theoretical papers dealing with the post buckling behaviour of the complete spherical shell, also included analyses of the clamped spherical shell segment. Here the shell segment was treated in the same manner as the complete

sphere, though not necessarily making the assumption that the segment undergoes uniform contraction before buckling as is necessary with the complete sphere. The only loading case that needs to be considered is that of uniform external pressure.

The rest of this chapter is a brief review of the work that has been carried out to date concerning the stability of spherical shells. Its main purpose is to show the development of this work up to the present time. A more detailed review and discussion of the work carried out in this field up to 1960 has been given by Thompson (1960) [126].

4.2 EXPERIMENTAL WORK

In experimental work, "critical" values of the external pressure are defined as the pressure at which snapthrough occurs. The only exception is in the case of very shallow spherical shells which do not buckle in this way, and here it is taken as the maximum value of the pressure sustained by the spherical shell.

The experimental work carried out has shown that not only does the buckling pressure, p_{cr}, depend on a geometric parameter ρ, where $\rho = R/t \sin^2\alpha \sqrt{12(1 - \nu^2)}$ but that the mode of deformation also changes with ρ; this has been clearly shown

in the work of Kaplan and Fung [64] on clamped spherical shell segments, as well as in subsequent work.

The main difficulty in all the experiments appears to be that of the manufacture of the test specimens; the manufacture of a nondevelopable surface such as a spherical one, that is of accurate geometry, uniform thickness, and free from initial stresses, presents a considerable problem. Most specimens have been made by spinning from flat sheet, and have very large residual stresses which may affect the results significantly. Kaplan and Fung [64] overcame these difficulties to some extent by hot spinning the specimens from magnesium alloy, but even so, the specimens were not of as high a quality as they would have desired. Some of their specimens showed a considerable, and irregular variation from spherical as revealed by measurements across different diameters. At Cambridge University, it has been found that the hemispherical copper shells made commercially for large diameter ball-cocks, are as accurate as can be obtained by any other means.

Perhaps the only way of obtaining perfect specimens, would be by electro-deposition on an exactly shaped mandril in the way that cylindrical shells have been formed as near perfect as possible.

In view of the initial imperfections that have existed

in all the test specimens, it is probable that the existing test results are not suitable for theoretical comparisons since the theory to date only relates to perfect spherical shells.

The experimental work that is reviewed in the following sections is considered separately for complete spheres and for spherical segments.

4.2.1 Complete Spheres

Altogether, very little experimental work has been published that relates to the stability of complete spheres under uniform external pressure. From what has been published, though, the experimental buckling pressure seems to be approximately one quarter of the classical critical pressure and the shells are reported to snap into a rotationally symmetric dimple. This local dimpling was in contrast to the more general waving over the surface that is predicted by the classical theory.

4.2.2. Spherical Segments

The considerable number of tests that have been carried out on shallow clamped domes, loaded under external pressure, fall into two groups - those carried out with the shell loaded by oil pressure, and those where air pressure was used for loading. In the former, the shells buckled under approximately constant volume conditions, while in the latter, the buckling

took place under approximately constant pressure. When the results that have been published to date are plotted against the geometric parameter, a considerable scatter appears. The general trend appears to be that the buckling pressure drops as the geometric parameter, ρ, increases.

The first tests were reported by Tsien [134], having been carried out by Crockett and Dunn. The next tests were those carried out by Köppel and Jungbluth [157] (1953), using air pressure for loading. Kaplan and Fung [64] (1954) then reported a quite detailed study of shallow shell buckling under both air and oil loadings. Their investigation showed that the pre-buckling mode of deformation changes with the geometric parameter, ρ. This is illustrated in Figure 4.1. Subsequent tests on clamped spherical domes have been reported by Homewood, Brine and Johnson [59] (1959).

4.3 COMPLETE SPHERICAL SHELLS

In their now classic work von Karman and Tsien not only dealt with cylindrical shells, but also considered spherical shells acted upon by external pressure. They carried out a nonlinear analysis for this problem as well, though some sweeping assumptions were made to simplify the analysis. It was here that they first introduced the idea of the "lower



(a) $\lambda \leq 5$. Mode I. maximum w at centre.



(b) $5 \leq \lambda < 9$. Mode II. maximum w not at centre.



(c) $\lambda \leq 9$. Mode III. a maximum of w at centre.

$$\lambda = \rho^{\frac{1}{2}} \quad \text{where} \quad \rho = \frac{R}{t} \sin\alpha \sqrt{12(1-\nu^2)}$$

Figure 4.1: Modes of initial deformation (64).

buckling load", which has been discussed already in Section 3.4.4.1.

Friedrichs [37] next showed that the simplifying assumptions of von Karman and Tsien caused an error of a factor of approximately two. On account of this, he attempted an analysis of the post buckling states of the spherical shell using an asymptotic treatment of the problem, where both t/R and β, the central angle of the dimple, tended to zero. As his analysis gave no satisfactory solution, he concluded that the assumption that the dimple angle tended to zero was incorrect. He added to Karman and Tsien's idea of the lower buckling load, by pointing out that the buckled state of the shell at the lower buckling load has a higher total potential energy than in the unbuckled state, at the same pressure. His suggestion was that an "intermediate buckling load" should be used to measure the buckling load of the shell. This "intermediate buckling load" was defined as "the lower limit of all values of pressure p for which a buckled state of equilibrium exists with an energy level below that of the unbuckled state". He claimed that this pressure was very close to the lower buckling pressure, but was much easier to evaluate.

The next contribution was by Tsien [134] who further developed Friedrichs' suggestion of the intermediate buckling

load, into his "energy criterion" of buckling. This has already been discussed in Section 3.4.3.1. with reference to axially loaded cylindrical shells. The values he obtained for the intermediate buckling load were in general agreement with the few experimental results available.

The further theoretical work that has been carried out for the buckling of complete spheres under external pressure - that of Yoshimura and Uemura [147], Mushtari and Surkin [88], Altshular [4], Feodosiev [31], Mushtari [86], and Surkin [123] - has been discussed previously by Thompson (1960) [126].

Recent work by Ho and Nash [54] concerning a dynamic analysis of complete spherical shells and shallow spherical caps is discussed in Section 4.5.

To date, no theoretical analysis has been published that deals with a spherical shell under uniform pressure and takes the effect of initial imperfections into account. It may well be that such an analysis would, as in the case of axially loaded cylindrical shells, explain the discrepancy between theory and experiment.

4.4 SPHERICAL SEGMENTS

As for complete spheres, the first work dealing with the buckling of spherical segments (also referred to as spherical caps),

was that by Karman and Tsien [65] (1939). They applied the Rayleigh-Ritz procedure to an approximate energy formulation of the problem. Friedrichs [37] (1941) pointed out that the Karman and Tsien assumption that only the vertical component of the deflection need be considered, instead of taking the deflection to be radial, was too restrictive. As a result he gave an 'improved' energy formulation of the problem. Tsien (1942) [134] then revised the equations, but even so, the results were not accurate. Murray and Wright (1961) [85] have pointed out that the Rayleigh-Ritz method involves a simplification of the equilibrium equation by assuming small angles and by omitting terms. They also state that on the basis of their work, the Rayleigh-Ritz solution is not a solution of the equilibrium equation in even an approximate sense. On the basis of subsequent experimental work, it can be seen that the form assumed by Karman and Tsien for the deflection parameter is too simple to give accurate results for any but very shallow shells. Yoshimura and Uemura (1942/3) [147] and Feodosiev (1946) [31] have carried out similar work to the above, though Feodosiev used Galerkin's method.

Following on from this, the approach has been one of finding methods for solving the governing nonlinear differential equations to determine the "upper" buckling load (i.e. the

maximum pressure of the pressure-displacement diagram). Usually, the stresses and deflections of the unbuckled state have been determined as well. The methods used have been perturbation methods, power series calculations, linearizations, and finite difference methods.

Kaplan and Fung (1954) [64] used a perturbation method taking the radial deflection at the centre of the shell as a parameter. The nonlinear equations were converted into a sequence of linear equations by expanding all dependent variables in powers of the centre deflection and then equating the coefficients of each power. However, solutions were only obtained for very shallow shells. Later, Archer (1958) [5], using similar equations to those derived by Reissner, extended and improved the perturbation technique and was able to obtain solutions for a greater range of shells.

Instead of using the perturbation technique, Simons (1956) [112] sought to solve the nonlinear equations by means of a power series solution (expanding terms in powers of the polar angle θ). This was similar to proceedings introduced by Way, and by Friedrichs and Stoker in their treatment of the buckling of circular plates. Reiss, Greenberg and Keller (1957) [98] and Weinitschke (1958/60) [140] have also used similar power series technique, making use of

electronic computers to solve the nonlinear equations. Reiss, Greenberg and Keller sought to give a complete description of the stresses and deflections over a wide range of the loading parameter Q, and the geometric parameter, ρ. Weinitschke gave results for simply supported edges as well as fixed.

With the power series technique, the method of evaluating the upper buckling load was to determine the load at which the series became divergent. This was then taken as the upper buckling load. However, in spite of the fact that it has been able to provide results over a greater range of the geometric parameter than has the perturbation method, it is open to doubt whether it does give correct results over the whole range. It is difficult to verify the exact relation between the upper buckling load of the cap and the load at which the power series begins to diverge instead of converge, for the physical and mathematical problems may not correspond at all. Weinitschke modified the approach of Reiss, Greenberg and Keller slightly, by applying analytic expansions to extend the radius of convergence. In the range $\rho < 18$, Reiss et al. and Weinitschke obtained similar results for the buckling load, but above this range Weinitschke found convergence difficulties, and doubted the results of Reiss et al.

At about the same time as the previous work, Reiss (1958) [97] attempted a different approach to the problem, by solving two linear problems. The first was the eigenvalue problem for a "membrane" segment supported in such a way that only membrane stresses were introduced before buckling; the second was the linear bending problem for the clamped segment. In this way he was able to determine the values of the geometric parameter, ρ, at which the mode of initial deformation changes. As a result, he was able to present a qualitative picture of the pressure parameter versus ρ curve which passes through the experimental points.

Von Willich (1959) [141] used an energy method, based on potential energy considerations. His energy expression was finally written in terms of two parameters only. By assuming that one of these parameters could be treated as constant during the loading process, he evaluated the maximum pressure. Chen (1959) [21] used the same method as Von Willich but without the above assumption. Chen analysed initially imperfect as well as perfect domes. He was able to show that initial imperfections in the shape of the middle surface can produce large reductions in the buckling pressure.

Keller and Reiss (1959) [67] used a new method for solving the nonlinear equilibrium problem for a clamped spherical cap. This was an iterative solution of a

finite-difference approximation of the boundary value problem. They confined their attention to caps that buckled in the first mode, and for these they evaluated the upper and lower buckling loads and confirmed that the pressure-displacement diagram has nonunique solutions when $pL < p < pu$ as had always been assumed. Budiansky(1959) [17] also tried a new approach, this being to construct the integral equations corresponding to the differential equations. These were then solved approximately, using a computer. While he considered both initially imperfect as well as initially perfect domes, he found that very large imperfections would be needed to give agreement between his maximum pressures and the experimental values for large values of ρ. For this reason, he suggested that non-symmetrical deformations must be considered for these values of ρ.

Thurston (1961) [128] has presented results which confirm the work of Weinitschke and Budiansky.

Murray and Wright (1961) [85] sought to use a different approach to solve the nonlinear equilibrium and energy equations that had been given by Karman and Tsien. Since there is a singularity at the origin, Murray and Wright use a power series expansion to move away from it and then use a step-by-step integration procedure to carry out computation throughout the desired opening angle of the shell. They were also able to

avoid making the assumption that the shell was of small angle, and so their results should be applicable to a wider range of shells. Their results are presented as a two parameter family of solutions for the equilibrium equation for a shell of given radius and wall thickness. In this way they show the behaviour of the shell in both the pre-buckling and post-buckling states. By considering the boundary conditions, they then obtain a one-parameter family of solutions which describe the possible configurations of the shell for various pressures. From these the upper and lower buckling loads are obtained. In the course of their solution, Murray and Wright show that their results depend critically on several terms which are neglected by the process of linearization in the classical theory.

In 1962, Humphreys and Bodner [62] presented a new approach to the buckling of spherical caps when they set out to determine the minimum impulse conditions for dynamic snapbuckling. Their analysis assumed a very simple deflection function, but even so, it showed new possibilities for determining the possibility of snapthrough. Their work is reviewed in more detail in Section 4.5.

Later the same year, Gjelsvik and Bodner brought out two papers dealing with the snapbuckling of arches [45] and the nonsymmetrical snapbuckling of spherical caps [46]. In the

latter, an energy procedure is used to compute the nonsymmetrical snapbuckling pressure. By this procedure, Gjelsvik and Bodner are able to show that nonsymmetrical buckling takes place when the geometrical parameter exceeds a certain value. Since they use only single term approximations to represent the initial and buckled shapes, the solutions are not fully reliable numerical values, though they should bring out the general behaviour of the shell. They also carry out a more accurate analysis that includes the development of a boundary layer in the cap, by means of which they evaluate the "equal-energy" load or "intermediate" buckling load of Friedrichs. They go on to show that the "energy" buckling load is a reasonable lower bound to the experimental values of buckling pressure. This can be seen in Figure 4.2. Gjelsvik and Bodner claim that the "energy" buckling load is a reasonable lower bound solution for buckling that is nonsymmetrical and could be applied particularly to "transitional" buckling where the mode of the intermediate equilibrium state is different from either the initial or buckled modes. Stable nonsymmetrical buckling shapes and transitional unstable nonsymmetrical buckling shapes have indeed been observed in tests.

The most recent work has been that of Feodosiev (1963) [32] who solved the problem of the axisymmetric bending of a shallow spherical dome and obtained the same results as Thurston.

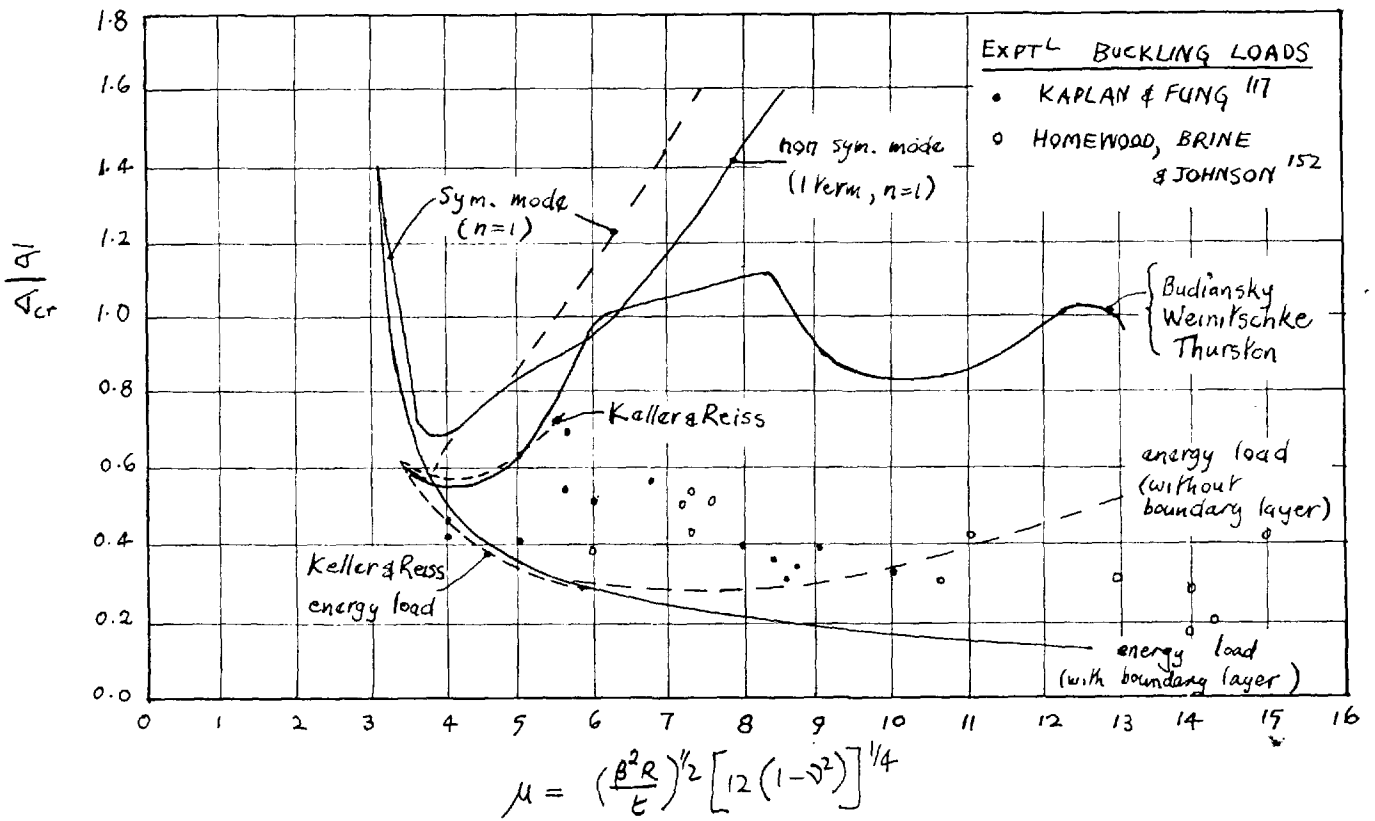


FIG. 4·2: THEORETICAL AND EXPERIMENTAL RESULTS FOR THE BUCKLING OF SHALLOW SPHERICAL CAPS.

He wrote his previously derived equations in terms of finite differences and solved them by means of a computer. On introducing time as a parameter into the differential equations, he shows that a simplification can result as regards computation. Again, more general displacement functions are required to describe the complete buckling of spherical shells including nonsymmetric buckling.

4.5 DYNAMIC ANALYSIS

It has been mentioned previously that a dynamic analysis is the more correct approach to the snapbuckling of spherical shells (as well as to other shells that buckle suddenly), instead of equilibrium and energy methods that have been in general use up to date. The straightforward approach would be to solve the governing nonlinear dynamic equations for the vibration response of the shell under rapidly applied dynamic loads. This, however, is difficult to do since more than one deformation mode has to be considered and all possible asymetric modes must also be included. Approximate solutions of the dynamic equations using a single symmetrical deflection mode have been obtained; these have been carried out by Volmir (1958) [137] and by Grigolyuk (1955) [48]. Grigolyuk's paper deals with both free and forced vibrations of shallow shells. More recently, Ho and Nash (1963) [54] have considered both complete spherical shells and shallow

spherical caps subjected to a dynamically applied uniform normal pressure. They satisfy the equation of motion approximately for the particular buckling configuration assumed.

Ho and Nash consider the load to be a dynamically applied uniform normal pressure that increases linearly with respect to time. Using finite displacement theory they establish the compatibility equation together with the equation of motion in the direction of the geometric axis of the buckled region. For an assumed buckled shape the compatibility equation can be solved, exactly, while the equation of motion can be satisfied approximately by means of the Galerkin procedure. By investigating the stability of the resulting equation, the extent of the buckled region can be established for the case of the complete spherical shell. For the case of the shallow spherical cap, buckling is assumed to be axisymmetric. As mentioned in Section 4.4, asymetrical buckling configurations also need to be considered in order to cover all cases of the buckling of shallow spherical caps, but this has not been reported to date.

While it is not a true dynamic analysis, it is convenient to consider the work of Humphrey and Bodner (1962) [62] under this heading. They treated the problem of the snapbuckling of shallow, thin spherical caps and cylindrical panels not by solving the dynamic equations, but by using the energy approach to determine the conditions under which snapbuckling could occur. Their analysis

while restricted to considering only a single symmetrical deformation, mode so that the shells could be represented as nonlinear single-degree-of-freedom systems, was able to handle different types of edge conditions. Throughout the analysis, it was assumed that the loading condition effectively imparted a uniform initial velocity, and hence kinetic energy, to the shell.

In the analysis, Friedrichs' equations, together with Tsien's assumed deflection function, were used. By assuming that under impulsive loading there is no external load acting during the motion of the shell, no external work is done on the shell. The maximum kinetic and potential energies are then equal. This assumption may or may not be justified depending on the buckling motion of the shell and whether the load can follow it or not. For instance, it has been shown [57] that for a cylindrical shell under deadweight axial loading, the snapbuckling may be so sudden that the load cannot follow the shell during the buckling process, though this may not be so with external pressure.

By obtaining an energy curve for the shell in terms of f, the ratio of the maximum deflection to the radius R, Humphrey and Bodner show that there may be a peak, which represents unstable equilibrium, at which snapthrough may occur if the initial kinetic energy is greater than the value corresponding to this peak. Arising from this, they show that for any given cap size, there is a limiting thickness ratio above which no snapbuckling can occur.

CHAPTER FIVE

CONICAL SHELLS

5.1 INTRODUCTION

Up to the present time, the stability of conical shells has not been studied to the same extent as has the stability of cylindrical and spherical shells. This is mainly due to the mathematical difficulties involved in solving the governing differential equations for the problem. It has resulted in the theoretical approach being confined to small deflection analyses, except for three published attempts at finite displacement analyses. There are also several loading conditions for which not even small deflection analyses have been attempted as yet, one case being that of pure bending. As is the case with cylindrical shells, it is known that large deformations and plastic stability are important factors for several loading conditions - such as axial compression, external pressure, and the case of both loadings acting together.

Experiment, as well as theory, has shown that more parameters influence the stability of conical shells than is the case for cylindrical shells. Variations in end restraint have been shown to have little effect on the stability of

cylindrical shells under axial compression (see Section 3.1) but for conical shells the end restraint does affect the stability. The length and angle of the conical shell have also been shown to influence the stability of the cone. These two parameters can be shown to increase greatly the algebraic and computational work required to obtain a numerical solution to the theory.

As a rough guide to the behaviour of conical shells, we can say that cones of small semi-vertex angle behave like cylindrical shells. At the other extreme, those of large angle behave more like circular flat plates, or perhaps even like spherical caps.

A survey of the work carried out on the stability of conical shells has recently been presented by Seide [110].

In the Sections 5.2 to 5.5 that follow, the behaviour of conical shells is more closely reviewed for specific loading conditions.

5.2 EXTERNAL PRESSURE

The first paper to deal with the stability of conical shells was that by Pflügger (1937) [93], wherein the differential equations governing the stability of conical shells with variable wall thickness were derived by a rigorous analysis. Only complete cones were considered, and the wall thickness was proportional to the distance from the apex. Unfortunately, the solution

itself was not of much use since the boundary conditions were not realistic.

The next approach was at the other extreme from Pflügger's solution. Here, Tokogawa (1940) [130] and also Bijlaard (1953) [11] sought to replace the conical shell by an equivalent cylindrical shell.

It was not until 1947, that Niordson [92] published a Rayleigh-Ritz type solution for conical shells subjected to a uniform external lateral pressure. The analysis is confined to a small deflection one, and even then several simplifications are made in order to obtain a solution. These simplifications restrict the solution to the case of shells of small semi-vertex angle, large L/R, and with a large number of buckling waves.

The energy solution, using the Rayleigh-Ritz method, was also used by Grigolyuk (1954) [47]. The results were based on the linear theory and were presented in the form of tables. They are applicable only for the case of a complete cone. At about the same time, Mushtari and Sackenkov (1954) [87] carried out a single term Galerkin solution to determine the upper limit of the critical loading. This is reviewed in Section 5.5.1.

Taylor (1957) [124] is reported to have derived a more accurate expression for the total potential energy than had been used up to that time, and to have given an approximate two term solution for the complete cone. This work does not appear to be

generally available though.

Radkowski (1958) [96] carried out an analysis for both single- and multi-layered conical or cylindrical shells acted upon by rotationally symmetrical stresses, i.e. by external pressure or axial compression. His method was similar to Niordson's but without some of the latter's simplifying assumptions. While he uses nonlinear strain-displacement relations, the energy expressions that are used are simplified ones. By neglecting all the powers of the displacements,and their derivatives, that are higher than quadratic, Radkowski effectively reduces his analysis to a linear one.

Radkowski, like Mushtari, Sackenkov and Seide, measured the displacement of the surface of the cone from the point of "incipient buckling".

By making use of their earlier work - Hoff (1955) [56], and Singer (1959) [113] - Hoff and Singer (1959) [58] found a solution to the differential equations governing the stability fo truncated cones. This solution is in the form of a series for each of the three displacements, u, v, and w, and applies to the case of nearly simple support for the cone. This restriction is caused by the boundary conditions that were assumed in order to obtain a solution. Both the solution and the differential equations are limited to short, thin

shells, having a small cone angle which will buckle with a large number of circumferential waves.

At about the same time as Hoff and Singer, Seide (1959) [107] carried out an analysis for external pressure loading, based on his work for axial compression loading [105]. By using nonlinear strain-displacement equations, Seide obtains the equilibrium and compatability equations from the first variation of the potential energy expression.

In addition, Seide compares his solution with those of other investigators and with the available experimental data. From this he presents a parametric solution for the stability of conical shells, after the manner of Batdorf [8] for cylindrical shells.

Of the experimental work that has been carried out, the most comprehensive is that of Singer and Eckstein (1962) [115]. Their work covered tests on seventy-one different aluminium alloy conical shells of different thicknesses, and covering three different cone angles. These test results were then compared with other experimental results and with several theoretical results. From this it was found that the theories of Singer [56] and Seide [107] were reasonably accurate in predicting loss of stability. Initial imperfections in the shells were also studied. Here it was found that their effect was mainly confined to influencing the pre-buckling behaviour,

and had only a small influence on the buckling pressure. More significant than the "maximum out-of-roundress" was the shape of the "initial circularity plot". If the shape of this was similar to the buckled shape, then buckling was likely to take place at a lower pressure than when it was less favourable.

In addition to the above, Kempner [70] and Seide [106] have derived eighth order differential equations to describe the stability of conical shells. No use seems to have been made of them in determining the loads at which conical shells lose stability.

Concerning experimental results, Seide (1962) [110] has pointed out that while they are said to agree favourably with the theory for external pressure loadings, the experimental results show considerable scatter. He suggests that this could be partly due to variations in end conditions from test to test. It has been found that for cylindrical shells under external pressure, clamping can increase the critical pressure by some forty per cent. The same may hold for conical shells, in which case variations in end conditions between the clamped and simply supported cases could account for the scatter. In one set of tests, Seide [111] noted that the low melting temperature alloy used to clamp the specimens appeared to yield, thus altering the boundary conditions.

5.3 AXIAL COMPRESSION

Very little theoretical or experimental work appears to have been done for this loading condition, unlike the case for cylindrical shells.

Experimental work has been carried out by Lackman and Penzien [73] and by Homewood, Brine and Johnson [59].

The first theoretical analysis was a linear one by Seide [104] (1956). In order to obtain a solution, he assumed that the state of stress before buckling was the membrane one. Further, he considered only rotationally symmetric deformations. This meant that the shear stress $N_{s\theta}$, and the circumferential displacement, v, could be taken as zero before and after buckling. The critical load was obtained as the solution of a stability determinant that is written in terms of Bessel functions.

Seide (1957) [105], next carried out a nonlinear analysis. He included the shearing terms, but neglected the influence of the circumferential displacement terms, v, in the bending-displacement expressions.

Compatability and equilibrium equations were then obtained by minimising the total horizontal energy expression.

Following on from these, Lackman and Penzien (1960) [73] showed how Seide's work could be generalised to give the lowest

critical load for a conical shell. This was:-

$$P_{cr} = \frac{2\pi\, Et^2 \cos^2 \alpha}{\sqrt{3(1 - \nu^2)}} \qquad (5.1)$$

They compared this result with experimental results and found that the buckling loads calculated from the formula:

$$P_{cr} = 2\pi C Et^2 \cos^2 \alpha \qquad (5.2)$$

(where C comes from Donnell and Wan's [27] work for U = 0.0003) gave good agreement.

The most recent work on the stability of conical shells under axial compression is again by Seide (1962) [111], this time taking the effects of internal pressure into account. The analysis is a linear one only. Buckling is assumed to be axisymmetric since this is the predominant buckling mode for internally pressurised cylindrical shells. It is further assumed that before buckling the meridional stress N_s is adequately represented by the membrane stress. By assuming that the slope $\partial w/\partial z$, is represented by a Fourier series, Seide obtains the stability criterion in the form of an infinite determinant, which can then be solved asymptotically. He obtains results for both simply supported and clamped edges. The available experimental results agree qualitatively, but not quantitatively, with the theoretical

results. It is probable that the discrepancy was caused by factors in the experiments that could not be taken into account in the theory.

5.4 TORSION

Only one analysis appears to have been carried out to date. This has been done by Seide (1962) [108] and is similar to his analysis for the case of external pressure [107].

Experimental work has been carried out by Singer and Eckstein (1963) [116].

5.5 COMBINED LOADINGS

5.5.1 Axial Compression and External Pressure

The first theoretical analysis for this loading case was that of Mushtari and Sackenkov (1954) [87]. Their analysis is a linear one, and makes use of Galerkin's method for solving the governing differential equations approximately. Mushtari and Sackenkov state that their initial differential equations are applicable only for the case of short and thin shells, the buckling of which produces a great number of circumferential waves. Seide [107] uses the same equations but places no explicit qualification upon their use. These governing differential equations are written in terms of the linear

membrane stresses that occur before buckling, together with the complementary stresses that occur at buckling. The complementary circumferential elongation is also considered.

Subsequent theoretical work has been carried out by Seide (1962) [109]. The results are presented in the form of interaction curves, and these show only a small variation in buckling pressure with variation in the taper ratio (= 1 - R_1/R_2) of the cone.

Experimental work has been carried out by Homewood, Brine and Johnson [59]. The results agree reasonably well with Seide's interaction curves.

5.5.2 Torsion and External Pressure

Experimental work has been carried out by Singer and Eckstein (1963) [116].

5.5.3 External Pressure, Torsion and Axial Compression

Some experimental work is reported as having been carried out by Singer, Eckstein, and Baruch (1962) [117] but the reference does not seem to be generally available.

CHAPTER 6

GENERAL APPROACH TO THE DERIVATION OF THE EQUATIONS GOVERNING STABILITY, AND METHODS OF SOLUTION

6.1 GENERAL

The fundamental problems of mechanics (of which stability is one example), have been governed both by differential equations and by what have become known as "minimal principles". In other words, the problem of solving the boundary value problem for the differential equation governing a given mechanical system generally turns out to be equivalent to the problem of finding the function which minimises the integral by which the potential energy of the system is expressed. This latter approach, based upon the principle of minimum potential energy, has been found to be very useful in determining the stability of cylindrical and conical shells.

Mathematically, the expression for the total potential energy is found to provide the most convenient means of deriving the equilibrium equations for the shell. These are obtained by writing the Euler equations of the calculus of variations for the total potential energy integral. In this case, the function that is the solution of the Euler equation, must satisfy the boundary conditions. If instead, no restriction is placed on the function initially, then the Euler equations cannot be used directly and the first variation of the total potential energy must be written in full. Here, natural boundary conditions must

be met in order that the variation of the integral be zero, i.e. that the integral be a minimum.

It is well known that many mechanical problems do not have a rigorous solution that can be easily obtained. This is particularly so for boundary-value problems where a solution to a differential equation, or a system of differential equations, is sought with prescribed boundary conditions. The same difficulty arises when "minimum principles" are used. With all these, the difficulty is not so much in finding a possible solution, than in adapting these solutions to prescribed boundary conditions. Therefore, it is often necessary to accept an approximate solution to the problem that is either not an exact solution to the differential equations, or else does not fully satisfy the boundary conditions. The former alternative provides an upper bound to the exact solution [118] while the latter one can provide a lower bound [18, 19].

While in stability theory, the derivation of the partial differential equations that describe the stability presents some difficulty, the major problem remains that of the solving the equations to obtain a numerical solution of the problem. It is for this reason that before dealing with the actual theoretical work itself, this Chapter underlines some of the principles and methods that are useful in developing the theory, and then outlines some of the ways of obtaining solutions.

6.2 CALCULUS OF VARIATIONS

This deals with the problem of finding functional forms for which given integrals assume maximum or minimum values. Expressed in other words, the calculus of variations deals with the problem of finding paths of integration for which integrals have maximum or minimum values.

Corresponding to the first and second derivatives of the differential calculus, there are the first and second variations in the calculus of variations. For any integral I, we denote the first variation I_1, and the second variation, I_2. Then for the integral I to be a maximum we must have $I_1 = 0$ and $I_2 < 0$, while for a minimum value of I we have $I_1 = 0$, $I_2 > 0$.

For the integral $I = \int_a^b F(x, s, \frac{\partial s}{\partial x}) dx$ (6.1)

whose end points are fixed, to be stationary for "weak variations" (i.e. variations that are independent of the path of the variation) then $y = s(x)$ must be a solution of the differential equation:

$$\frac{\partial F}{\partial y} - \frac{d}{dx}\left(\frac{\partial F}{\partial y'}\right) = 0 \qquad (6.2)$$

An equation of this nature that provides the minimising function, is known as the "Euler characteristic equation" or merely "Euler equation". Written in full, Equation (6.2) becomes:

$$\frac{\partial F}{\partial y} - \frac{\partial^2 F}{\partial x \partial y'} - \frac{\partial^2 F}{\partial y \partial y'} \cdot \frac{dy}{dx} - \frac{\partial^2 F}{\partial (y')^2} \frac{d^2 y}{dx^2} = 0 \qquad (6.3)$$

Solutions of Euler's equation must pass through the end points of the range of integration. A requirement of the integral I which is to be minimised is that it must have continuous first and second partial derivatives with respect to its arguments, i.e. in Equation (6.1), I must possess continuous derivatives with respect to x, s, and $\frac{\partial s}{\partial x}$.

In dealing with the second variation I_2, it is necessary to solve the Jacobi accessory equation. For the integral I of Equation (6.2) this is:

$$\left\{ F_{00} - \frac{d}{dx}\left(F_{01}\right) \right\} u - \frac{d}{dx}\left\{ F_{11} \frac{du}{dx} \right\} = 0 \qquad (6.4)$$

where $F_{00} = \frac{\partial^2 F}{\partial y^2}$, $F_{01} = \frac{\partial^2 F}{\partial y \partial y'}$, $F_{11} = \frac{\partial^2 F}{\partial (y')^2}$ and $y = s(x)$ is the solution that passes through A and B, the end points of the range of integration. The details of this are described fully by Fox [175], and by Elsgol● [216].

A summary of the Euler equations and the tests for maximum and minimum for the integrals encountered in stability theory is given in the following paragraphs.

(a) For an integral of the form:

$$I = \iint F(z,x,y;p,q)\ dxdy \tag{6.5}$$

where $p = \partial z/\partial x$ and $q = \partial z/\partial y$ and z is a function of x and y, then the integral I is stationary when z is a solution of the partial differential equation:

$$\frac{\partial F}{\partial z} - \frac{\partial}{\partial x}\left(\frac{\partial F}{\partial p}\right) - \frac{\partial}{\partial y}\left(\frac{\partial F}{\partial q}\right) = 0 \tag{6.6}$$

If at all points of the domain of integration, $\frac{\partial^2 F}{\partial p^2}$ has a constant sign, and $\frac{\partial^2 F}{\partial p^2}\cdot\frac{\partial^2 F}{\partial q^2} > \left(\frac{\partial^2 F}{\partial p \partial q}\right)^2$, then the integral I is a maximum if $\frac{\partial^2 F}{\partial p^2}$ is negative, and a minimum if it is positive.

(b) For a double integral with derivatives of the second order, i.e. for:

$$I = \iint F(x,y,z,p,q,r,s,t)\ dxdy \tag{6.7}$$

where: $p = \frac{\partial z}{\partial x}$, $q = \frac{\partial z}{\partial y}$, $r = \frac{\partial^2 F}{\partial x^2}$, $s = \frac{\partial^2 F}{\partial x \partial y}$, $t = \frac{\partial^2 F}{\partial y^2}$

Forsythe[36] **and Elsgolc**[28] have shown that there will be a stationary value when z is a solution of the characteristic equation:

$$\frac{\partial F}{\partial z} - \frac{\partial}{\partial x}\left(\frac{\partial F}{\partial p}\right) - \frac{\partial}{\partial y}\left(\frac{\partial F}{\partial q}\right) + \frac{\partial^2}{\partial x^2}\left(\frac{\partial F}{\partial r}\right) + \frac{\partial^2}{\partial x \partial y}\left(\frac{\partial F}{\partial s}\right) + \frac{\partial^2}{\partial y^2}\left(\frac{\partial F}{\partial t}\right) = 0 \tag{6.8}$$

The conditions that must be satisfied in order to determine a maximum

or minimum value for I, are that:

$$\frac{\partial^2 F}{\partial r^2}\,,\ \frac{\partial^2 F}{\partial s^2} > \left(\frac{\partial^2 F}{\partial r \partial s}\right)^2$$

$$\frac{\partial^2 F}{\partial s^2} \times \frac{\partial^2 F}{\partial t^2} > \left(\frac{\partial^2 F}{\partial s \partial t}\right)^2$$

$$\frac{\partial^2 F}{\partial t^2} \times \frac{\partial^2 F}{\partial r^2} > \left(\frac{\partial^2 F}{\partial t \partial r}\right)^2$$

must be satisfied everywhere throughout the field of integration, and $\frac{\partial^2 F}{\partial r^2}\,,\ \frac{\partial^2 F}{\partial s^2}\,,\ \frac{\partial^2 F}{\partial t^2}$ have a common sign which is positive for a minimum value for I, and negative for a maximum value.

(c) In connection with the stability of thin shells, the integral to be minimised, i.e. the total potential energy, usually contains three dependent variables - the displacements u,v,w - and in this case the Euler equations must hold for each variable.

e.g. for a minimum of the integral

$$I = \int F\left(x, y, z, \frac{\partial y}{\partial x}, \frac{\partial z}{\partial x}\right) dx \qquad (6.9)$$

then the Euler equations must hold for each variable

i.e.
$$\left.\begin{aligned} \frac{\partial F}{\partial y} - \frac{d}{dx}\left(\frac{\partial F}{\partial y'}\right) &= 0 \\ \frac{\partial F}{\partial z} - \frac{d}{dx}\left(\frac{\partial F}{\partial z'}\right) &= 0 \end{aligned}\right\} \qquad (6.10)$$

(d) In the case of an integral which is time dependent, such as:

$$I = \int_{t_0}^{t_1} F(q_1, q_2, q_3, \ldots q_n, \dot{q}_1, \dot{q}_2, \dot{q}_3, \ldots \dot{q}_n)\, dt$$

the q's must satisfy the n equations:

$$\frac{\partial F}{\partial q_m} - \frac{d}{dt}\left(\frac{\partial F}{\partial \dot{q}_m}\right) = 0 \qquad (6.11)$$

(m = 1,2,3, ... n)

6.3 THE PRINCIPLE OF MINIMUM POTENTIAL ENERGY

This principle states that a motionless conservative system is in a stable state of equilibrium, if the potential energy assumes a stationary value, and the equilibrium is stable only if the potential energy is a minimum. From the principle of virtual work it has been shown that the first variation of the potential energy vanishes (i.e. $\delta\pi = 0$) for any equilibrium configuration of the system.

In the case of small strains and displacements (which give rise to linear differential equations), the uniqueness theorem shows that there is only one equilibrium condition and any variation from it shows a positive increase in potential energy. Then in this case, the equilibrium condition is a minimum and is stable.

The Euler equations connected with the problem, π = minimum, are actually the equilibrium equations. It has been found that the method of the calculus of variations when coupled with the principle of minimum potential energy, provides the easiest way of arriving at the equilibrium equations when considering the stability problem of circular cylindrical shells and also conical shells.

6.4 RAYLEIGH-RITZ METHOD OF SOLUTION

For this, approximate stationary values of an integral of the form:

$$I = \iint F(x,y,z;p,q)\, dxdy \qquad (6.5)$$

are sought assuming:

$$z = \sum_{i=1}^{n} a_i f_i(x,y) \qquad (6.13)$$

where $f_i(x,y)$ $(i = i,2, \ldots n)$ are suitably chosen functions, and the a_i are a set of so far undetermined parameters. On substituting for z in Equation (6.5) and evaluating the integral, we obtain an expression for I in terms of the parameters, a_i. Then, for I to be stationary, the parameters must be chosen so that:

$$\frac{\partial I}{\partial a_i} = 0 \qquad (i = 1,2, \ldots n) \qquad (6.14)$$

In this way, n simultaneous equations are obtained from which the a_i can be determined, and hence z can be determined.

Most applications of this method lead to approximate solutions, with the degree of approximation and the amount of computation involved both depending on the choice of the approximating functions. It is usual to choose the arbitrary functions $f_i(x,y)$ such that they reflect any symmetry of the solution, z, and that they satisfy the same boundary conditions as z, if possible.

When it is used as above, the Rayleigh-Ritz method gives no estimate of the error in the solution to I, nor anything else regarding convergence to the exact solution. It is possible to fit bounds to the exact solution, and it has been shown (Ref. 118.) that when the solution does not minimise the integral exactly, then the solution is an upper bound. Also, Trefftz [131] has suggested that a lower bound solution can be obtained by relaxing some of the boundary conditions. Usually, the function taken to minimise the total potential energy for a cylindrical shell, does not fit the boundary conditions, and consequently little can be said about the nature of the solution.

6.5 GALERKIN'S METHOD

While it is of general application, the method when applied to the equivalent of the minimisation problem can be shown to lead to the equation:

$$I = \iint_R L(u)\ \eta(x,y)\ dxdy = 0 \qquad (6.16)$$

where:

$$L(u) = \frac{\partial F}{\partial u} - \frac{\partial}{\partial x}\left(\frac{\partial F}{\partial u_x}\right) - \frac{\partial}{\partial y}\left(\frac{\partial F}{\partial u_y}\right) = 0 \qquad (6.17)$$

is the Euler equation for the minimal problem, and $\eta(x,y)$ is an arbitrary function that must vanish on the boundary of the region R. The solution u_n, is chosen in the same form as for the Rayleigh-Ritz method, i.e.:

$$Z = u_n = \sum_{i=1}^{n} a_i f_i(x,y) \qquad (6.15)$$

Now the integral on the right hand side of Equation (6.16) must vanish for any arbitrary function, $\eta(x,y)$ and Galerkin chooses:

$$\eta(x,y) = f_i(x,y) \qquad (6.18)$$

Then it is required that:

$$\iint_R \left\{ \frac{\partial F}{\partial u_n} - \frac{\partial}{\partial x}\left(\frac{\partial F}{\partial (u_n)_x}\right) - \frac{\partial}{\partial y}\left(\frac{\partial F}{\partial (u_n)_y}\right) \right\} f_i(x,y)\, dx\, dy = 0 \qquad (6.19)$$

and these n equations are sufficient to determine the n parameters a_i.

Since $z = u_n$ is not an exact solution of the Euler equation, Equation (6.17), the integral in Equation (6.16) does not, in general, vanish for any arbitrary variation in $u(x,y)$. It vanishes only when $u(x,y)$ = the exact solution of the problem. The magnitude of the function $L(u_n)$ can therefore be used as a measure of the degree of approximation attained. Let $e_n(x,y)$ be called the error function, where:

$$e_n = L(u_n) = \frac{\partial F}{\partial u_n} - \frac{\partial}{\partial x}\left(\frac{\partial F}{\partial (u_n)_x}\right) - \frac{\partial}{\partial y}\left(\frac{\partial F}{\partial (u_n)_y}\right) \qquad (6.20)$$

Then from Equation (6.19) we have that the error function is required to be orthogonal to each of the n functions $f_i(x,y)$.

In the Galerkin method, we go directly from the Euler equations to Equation (6.19), and it is not necessary to form the energy integral I, the approximate integral I_n, and the n derivatives $\partial I_n / \partial a_m$ as in the Rayleigh-Ritz method, However, if the energy integral is used in conjunction with the principle of stationary potential energy to provide the equilibrium equations, then it is simpler to use the energy expression directly as in the Rayleigh-Ritz method.

6.6 SOLUTION OF SYSTEMS OF NONLINEAR EQUATIONS

When the Rayleigh-Ritz approach is applied to the case of the minimisation of the total potential energy of a thin shell, the resulting equations form a system of nonlinear equations. Usually with these equations, it is not possible to follow a Gaussian procedure as used in dealing with systems of linear equations, whereby variables are eliminated one by one until only a single equation in a single unknown remains. Very few methods appear to be available for the solution of systems of nonlinear equations, and different approaches may be required for different problems.

In order to illustrate the general methods, the set of nonlinear simultaneous equations are taken as:

$$f_i\ (x_1, x_2, x_3, \ldots x_n) = 0 \qquad (6.21)$$

Let the true solution be the vector $(\xi_1, \xi_2, \ldots \xi_n)$, and let $(x^o_1, x^o_2, \ldots x^o_n)$ be an approximation to the solution, such that:

$$\xi_i = x^o_i + \delta x^o_i \qquad (6.22)$$

$$(i = 1, \ldots n)$$

Then, since x^o_i is not the true solution:

$$f_i(x^o_i) = \Delta f_i \qquad (6.23)$$

where Δf_i is the residual of the equation.

6.6.1 Partial Elimination

This method is limited to those cases where the number of equations and parameters is small, and where some of the parameters can be eliminated easily. It is best illustrated with respect to the particular case of the circular cylinder under axial compression, and is discussed in Section 8.3 .

6.6.2 Relaxation

In this method, the residuals Δf_i of the set of equations f_i, are examined, and the residual of largest moduli is selected. If this is the j-th, then we seek to reduce the component of x_i in this direction, thereby reducing the residual. Put in other words, the j-th equation is solved for the j-th variable as a function of the current estimates of the other unknowns. The process is continued until the residuals are of smaller modulus than a predetermined value, or some other suitable test for the accuracy of the solution is met.

This particular method is not satisfactory for use with automatic digital computers, for as shown by Booth (Ref. 12, page 103), it is not always possible to select the coordinate of largest residual at each step, for if the coordinate x_k has just been altered, then if

$|\Delta f_k|$ is still the largest residual, further relaxation with respect to x_k will not produce any further improvement in the solution.

6.6.3 Generalised Newton-Raphson Method

From Equations (6.21) and (6.22) we have:

$$f_i(x_i + \delta x_i) = 0 \tag{6.24}$$

By Taylor's expansion this can be written as:

$$f_i(x_j + \delta x_j) = f_i(x_j) + \sum_{j=1}^{n} \delta x_j \frac{\partial f_i}{\partial x_j} + O(\delta x_j)^2 \qquad (i,j = 1, 2, \ldots n) \tag{6.25}$$

Neglecting second-order terms and above, we have:

$$\sum_{j=1}^{n} \delta x_j \frac{\partial f_i}{\partial x_j} + f_i(x_j) = 0$$

i.e.
$$\underline{\delta x_j} \times \underline{\frac{\partial f_i}{\partial x_j}} + \underline{f_i(x_j)} = 0$$

Therefore
$$\underline{\delta x_j} \times \underline{\frac{\partial f_i}{\partial x_j}} = -\underline{f_i(x_j)} = -\underline{\Delta f_i(x_j)} \tag{6.26}$$

where $\underline{\delta x_j}$, $\underline{\frac{\partial f_i}{\partial x_j}}$, $\underline{f_i(x_j)}$ and $\underline{\Delta f_i(x_j)}$ are written in matrix notation.

Letting $\underline{f_x}$ represent $\underline{\frac{\partial f_i}{\partial x_j}}$, then we have for the correction:

$$\underline{\delta x_j} = - \underline{f^{-1}_x} \; \underline{\Delta f_i}$$

If the initial solution, x°_i, is sufficiently close to ξ_i, we might expect to find that by solving the equations:

$$f_i(x^{\circ}_j) + \sum (x'_j - x^{\circ}_j) \frac{\partial f_i(x^{\circ}_j)}{\partial x^{\circ}_j} = 0 \qquad (6.27)$$

for the x'_j, we could obtain a better approximation to the solution ξ_i, than x°_i.

Therefore we can write:

$$\underline{x'_j - x^{\circ}_j} = - \underline{f_x^{-1}}(x^{\circ}_j) \, \underline{\Delta f_i}(x^{\circ}_j)$$

$$\text{i.e.} \quad \underline{x'_j} = \underline{x^{\circ}_j} - \underline{f_x^{-1}}(x^{\circ}_j) \, \underline{\Delta f_i}(x^{\circ}_j) \qquad (6.28)$$

If, as in the case of the Rayleigh-Ritz method, the f_i are the elements of a vector ϕ, then we can introduce the matrix:

$$\underline{\phi_x}(x_j) = \frac{\partial f_i(x_j)}{\partial x_j}$$

This is the Jacobian matrix of the functions f_i, evaluated at the point x_j..

Then Equation (6.27) becomes:

$$f_i(x_j^\circ) + (x_j' - x_j^\circ)\phi_x(x_j^\circ) = 0$$

Therefore $$x_j' = x_j^\circ - \phi_x^{-1}(x_j^\circ)\phi(x_j^\circ) \qquad (6.29)$$

Normally though, it is usual to solve for the correction $(x'_j - x^\circ_j)$ which is then added to the previous solution to obtain an improved solution.

6.7 NUMERICAL METHODS FOR MINIMISING A FUNCTION

The Rayleigh-Ritz method, or the Galerkin method, as mentioned previously, lead to a system of equations that must be solved in order to evaluate the unknown parameters in the function that minimises the total potential energy. An alternative method is to minimise the total potential energy expression numerically. Here, the total potential energy is expressed in terms of the unknown parameters of the assumed minimising function. These parameters are then suitably varied numerically until the potential energy takes on a minimum value. The methods normally used are all variations of what are known as "descent" methods.

6.7.1 Successive variation of parameters

Here, the unknown parameters (the components x_i of the vector x), are given assumed values. Each parameter is then varied in value in turn, such that the value of the function ϕ is reduced at each step. The parameters may be varied by a selected amount in turn, or else each parameter may be altered such that the minimum is found for each parameter in turn.

6.7.2 Method of Steepest Descent

For the function $\phi(x_i)$, we have:

$$\phi_x = \frac{\partial \phi}{\partial x} = \text{grad } \phi$$

The direction of the gradient ϕ_x is normal to the surface at any point x on the surface ϕ = const which passes through the point x.

If an approximation, x°_i, is taken that is sufficiently close to the point that minimises ϕ, then a new point can be chosen along the line of the gradient through x, such that the function ϕ is reduced in value. Hence we seek to determine a point:

$$x'_i = x^{\circ}_i - \lambda\phi x$$

The minimum of the function:

$$\phi(x^{\circ}_i - \lambda\phi_x) = \phi_1(\ ) \tag{6.30}$$

is given by:

$$\phi_x(x^{\circ}_i - \lambda\phi_x) = 0 \tag{6.31}$$

i.e.

$$\phi^T_x \phi_x(x^{\circ}_i - \lambda\phi_x) = 0 \tag{6.32}$$

Since $\phi^T_x \phi_x \neq 0$ at the point x°_i, then Equation (6.32) is not satisfied by $\lambda = 0$, unless x'_i is the minimum point represented by $\bar{y}_i$.

Once λ has been obtained, the point x'_i can be evaluated, and a new point x^2_i is sought along the gradient ϕ_x through the point x'_i.

6.7.3 Other Descent Methods

A number of variations of the method of steepest descent have been suggested, mainly to facilitate the use of automatic computers. Two of these methods - those of Rosenbrock [103] and of Fletcher and Powell [33] - are described in Chapter 8.

CHAPTER SEVEN.

DERIVATION OF THE NONLINEAR STABILITY EQUATIONS FOR THE CYLINDRICAL SHELL.

7.1 BASIC EQUATIONS.

The cylinder and co-ordinate system are as shown in figure 7.1. The cylinder has a uniform wall thickness, without stiffeners, and is subject to a compressive load fixed in the axial direction and uniformly distributed around the circumference, together with an external pressure that is uniform over the whole surface.

7.1.1. Expressions for curvatures.

These are :-

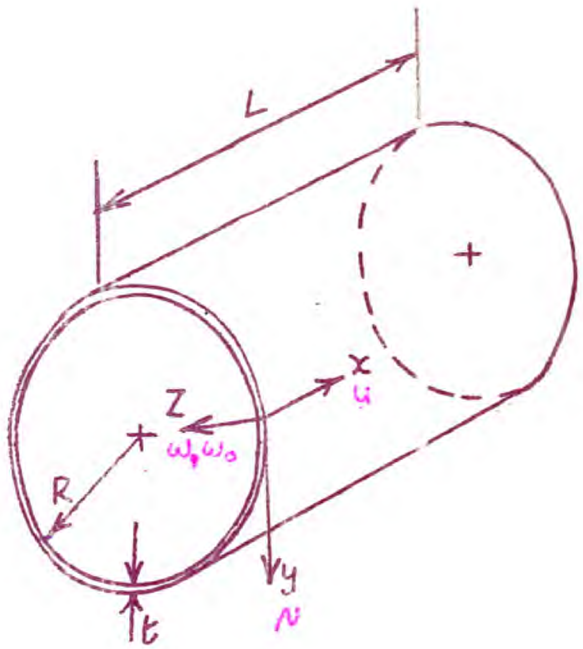
$$K_x = \frac{\frac{\partial^2 w}{\partial x^2}}{\left\{1+\left(\frac{\partial w}{\partial x}\right)^2\right\}^{3/2}}$$

$$K_y = \frac{\frac{\partial^2 w}{\partial y^2}}{\left\{1+\left(\frac{\partial w}{\partial y}\right)^2\right\}^{3/2}}$$

$$K_{xy} = \frac{\frac{\partial^2 w}{\partial x \partial y}}{\left\{1+\frac{\partial w}{\partial x}\cdot\frac{\partial w}{\partial y}\right\}^{3/2}}$$

Providing the shell is shallow, the terms involving powers of the first derivatives of the radial displacement, can be neglected in comparison to unity. The expressions for the curvatures then become :-

$$K_x = \frac{\partial^2 w}{\partial x^2} \; ; \quad K_y = \frac{\partial^2 w}{\partial y^2} \; ; \quad K_{xy} = \frac{\partial^2 w}{\partial x \partial y}$$



axes are shown in black

displacements are shown in red

Fig. 7.1. Cylinder and co-ordinate system.

7.1.2. Strain - displacement relations for the middle surface.

For the perfect cylinder, these are :-

$$\epsilon_x = \frac{\partial u}{\partial x} + \frac{1}{2}\left(\frac{\partial w}{\partial x}\right)^2$$
$$\epsilon_y = \frac{\partial v}{\partial y} + \frac{1}{2}\left(\frac{\partial w}{\partial y}\right)^2 - w/R$$
$$2\epsilon_{xy} = \frac{\partial u}{\partial y} + \frac{\partial v}{\partial x} + \frac{\partial w}{\partial x}\cdot\frac{\partial w}{\partial y}$$

where products of the terms $\frac{\partial u}{\partial x}, \frac{\partial v}{\partial y}, \frac{\partial u}{\partial y}, \frac{\partial v}{\partial x}$ have been neglected.

The displacements are measured from the position of the middle surface of the initially imperfect cylinder. The radial difference between the perfect cylinder and the initially imperfect middle surface is denoted by w_0. Therefore, the radial displacement from the perfect circular cylinder is given by :-

$$w' = w + w_0$$

For the initially imperfect cylinder, where only radial displacement is considered :-

$$\epsilon'_x = \tfrac{1}{2}\left(\partial w_0/\partial x\right)^2$$
$$\epsilon'_y = \tfrac{1}{2}\left(\partial w_0/\partial y\right)^2 - w_0/R$$
$$2\epsilon'_{xy} = \left(\partial w_0/\partial x\right)\left(\partial w_0/\partial y\right)$$

Therefore, for strains measured from the perfect cylinder :-

$$\epsilon''_x = \frac{\partial u}{\partial x} + \frac{1}{2}\left(\frac{\partial(w+w_0)}{\partial x}\right)^2$$
$$\epsilon''_y = \frac{\partial v}{\partial y} + \frac{1}{2}\left(\frac{\partial(w+w_0)}{\partial y}\right)^2$$
$$2\epsilon''_{xy} = \frac{\partial u}{\partial y} + \frac{\partial v}{\partial x} + \frac{\partial(w+w_0)}{\partial x}\cdot\frac{\partial(w+w_0)}{\partial y}$$

Therefore, the increase of strains under load is given by :-

$$\epsilon_x = \frac{\partial u}{\partial x} + \frac{1}{2}\left(\frac{\partial w}{\partial x}\right)^2 + \frac{\partial w_0}{\partial x}\cdot\frac{\partial w}{\partial x} \qquad 7.1.$$

$$\epsilon_y = \frac{\partial v}{\partial y} + \frac{1}{2}\left(\frac{\partial w}{\partial y}\right)^2 + \frac{\partial w_0}{\partial y}\cdot\frac{\partial w}{\partial y} - \frac{w}{R} \qquad 7.2.$$

$$2\epsilon_{xy} = \frac{\partial u}{\partial y} + \frac{\partial v}{\partial x} + \frac{\partial w}{\partial x}\cdot\frac{\partial w}{\partial y} + \frac{\partial w_0}{\partial x}\cdot\frac{\partial w}{\partial y} + \frac{\partial w}{\partial x}\cdot\frac{\partial w_0}{\partial y} \qquad 7.3.$$

7.1.3) Shell action - strain relations.

$$N_x = \frac{Et}{1-\nu^2}(\epsilon_x + \nu\epsilon_y) \qquad 7.4$$

$$N_y = \frac{Et}{1-\nu^2}(\epsilon_y + \nu\epsilon_x) \qquad 7.5$$

$$N_{xy} = \frac{Et}{1+\nu}\epsilon_{xy} \qquad 7.6$$

7.1.4) Moment - curvature relations.

$$M_x = D\left(\frac{\partial^2 w}{\partial x^2} + \nu\frac{\partial^2 w}{\partial y^2}\right) \qquad 7.7$$

$$M_y = D\left(\frac{\partial^2 w}{\partial y^2} + \nu\frac{\partial^2 w}{\partial x^2}\right) \qquad 7.8$$

$$M_{xy} = D(1-\nu)\frac{\partial^2 w}{\partial x \partial y} \qquad 7.9$$

7.1.5) Expressions for the Energy.

The extensional strain energy, W_1, is given by :-

$$W_1 = \frac{1}{2}\int_0^L\int_0^{2\pi r}\left[N_x\epsilon_x + N_y\epsilon_y + 2N_{xy}\epsilon_{xy}\right]dx\,dy \qquad 7.10$$

The bending strain energy, W_2, is given by :-

$$W_2 = \frac{1}{2}\int_0^L\int_0^{2\pi r}\left[M_xK_x + M_yK_y + 2M_{xy}K_{xy}\right]dx\,dy \qquad 7.11$$

The potential of the external loads is given by :-

$$W_3 = -\int_0^{2\pi r}(N_x)_{x=L}\,dy\int_0^L\frac{\partial u}{\partial x}\,dx \qquad 7.12$$

$$W_4 = -\int_0^L\int_0^{2\pi r} p w\,dx\,dy \qquad 7.13$$

The total potential energy, Π, is given by :-

$$\Pi = W_1 + W_2 + W_3 + W_4 \qquad 7.14$$

7.2 EQUILIBRIUM EQUATIONS.

In the expressions for W_1, W_2, W_3, and W_4, the terms $\epsilon_x, \epsilon_y, \epsilon_{xy}, K_x, K_y, K_{xy}$ are all functions of $(x, y; u, v, w)$. The total potential energy expression is :-

$$\Pi = \frac{1}{2}\int_0^L\int_0^{2\pi r}\left[\frac{Et}{1-\nu^2}\left\{\epsilon_x^2 + 2\nu\epsilon_x\epsilon_y + \epsilon_y^2 + 2(1-\nu)\epsilon_{xy}^2\right\}\right. \qquad 7.15$$
$$\left. + D\left\{K_x^2 + 2\nu K_x K_y + K_y^2 + 2(1-\nu)K_{xy}^2\right\} - 2pw\right]dx\,dy - \int_0^{2\pi r}(N_x)_{x=L}\,dy\int_0^L\frac{\partial u}{\partial x}\,dx$$

As outlined in chapter six, the equilibrium equations are provided by writing the Euler equations for the total potential energy, with respect to the three displacements. The resulting equations are :-

for u: $$-\frac{\partial}{\partial x}\left(2\epsilon_x.1 + 2\nu\epsilon_y.1\right) - \frac{\partial}{\partial y}\left(2\{1-\nu\}\epsilon_{xy}.1\right) = 0 \qquad 7.16$$

for v: $$-\frac{\partial}{\partial x}\left(2\{1-\nu\}\epsilon_{xy}.1\right) \quad -\frac{\partial}{\partial y}\left(2\epsilon_y.1 + 2\nu\epsilon_x.1\right) = 0 \qquad 7.17$$

for w: $$-2p + \frac{Et}{1-\nu^2}\left[2\nu\epsilon_x\left(-\frac{1}{r}\right) + 2\epsilon_y\left(-\frac{1}{R}\right) - \frac{\partial}{\partial x}\left\{2\epsilon_x\left(\frac{\partial w}{\partial x} + \frac{\partial w_0}{\partial x}\right)\right.\right.$$
$$\left. + 2\nu\epsilon_y\left(\frac{\partial w}{\partial x} + \frac{\partial w_0}{\partial x}\right) + 4(1-\nu)\epsilon_{xy}\left(\frac{\partial w}{\partial y} + \frac{\partial w_0}{\partial y}\right)\right\}$$
$$- \frac{\partial}{\partial y}\left\{2\nu\epsilon_x\left(\frac{\partial w}{\partial y} + \frac{\partial w_0}{\partial y}\right) + 2\epsilon_y\left(\frac{\partial w}{\partial y} + \frac{\partial w_0}{\partial y}\right) + 4(1-\nu)\epsilon_x\left(\frac{\partial w}{\partial x} + \frac{\partial w_0}{\partial x}\right)\right\}$$
$$+ 2D\left\{\frac{\partial^2}{\partial x^2}\left(\frac{\partial^2 w}{\partial x^2}\right) + 2(1-\nu)\frac{\partial^2}{\partial x\partial y}\left(\frac{\partial^2 w}{\partial x\partial y}\right) + \nu\frac{\partial^2}{\partial x^2}\left(\frac{\partial^2 w}{\partial y^2}\right) + \nu\frac{\partial^2}{\partial y^2}\left(\frac{\partial^2 w}{\partial x^2}\right)\right.$$
$$\left.\left. + \frac{\partial^2}{\partial y^2}\left(\frac{\partial^2 w}{\partial y^2}\right)\right\} = 0 \qquad 7.18$$

These simplify to :-

$$\frac{\partial N_x}{\partial x} + \frac{\partial N_{xy}}{\partial y} = 0 \qquad 7.19$$

$$\frac{\partial N_{xy}}{\partial x} + \frac{\partial N_y}{\partial y} = 0 \qquad 7.20$$

$$-p + \frac{Et}{1-\nu^2}\left[-\frac{1}{R}(\epsilon_y+\nu\epsilon_x) - \frac{\partial}{\partial x}\left\{(\epsilon_x+\nu\epsilon_y)\left(\frac{\partial w}{\partial x}+\frac{\partial w_0}{\partial x}\right)+\tfrac{1}{2}(1-\nu)\epsilon_{xy}\left(\frac{\partial w}{\partial y}+\frac{\partial w_0}{\partial y}\right)\right\}\right.$$

$$\left. - \frac{\partial}{\partial y}\left\{(\epsilon_y+\nu\epsilon_x)\left(\frac{\partial w}{\partial y}+\frac{\partial w_0}{\partial y}\right) + 2(1-\nu)\epsilon_{xy}\left(\frac{\partial w}{\partial x}+\frac{\partial w_0}{\partial x}\right)\right\}\right]$$

$$+ D\left[\frac{\partial^2}{\partial x^2}\left(\frac{\partial^2 w}{\partial x^2}+\nu\frac{\partial^2 w}{\partial y^2}\right)+2(1-\nu)\frac{\partial^2}{\partial x\partial y}\left(\frac{\partial^2 w}{\partial x\partial y}\right)+\frac{\partial^2}{\partial y^2}\left(\frac{\partial^2 w}{\partial y^2}+\nu\frac{\partial^2 w}{\partial x^2}\right)\right] = 0 \qquad 7.21$$

The <u>equilibrium equation</u> for the radial displacement, w, is given by equation 7.21 using equations 7.19 and 7.20.

i.e. $$D\nabla^4 w = p + N_x\left(\frac{\partial^2 w}{\partial x^2}+\frac{\partial^2 w_0}{\partial x^2}\right) + N_{xy}\left(\frac{\partial^2 w}{\partial x\partial y}+\frac{\partial^2 w_0}{\partial x\partial y}\right)$$

$$+ N_y\left(\frac{\partial^2 w}{\partial y^2}+\frac{\partial^2 w_0}{\partial y^2}+\frac{1}{R}\right) \qquad 7.22$$

Equations 7.19, 7.20 are satisfied by a stress function, $\phi(x,y)$, such that

$$N_x = \frac{\partial^2\phi}{\partial y^2} \;;\; N_y = \frac{\partial^2\phi}{\partial x^2} \;;\; N_{xy} = -\frac{\partial^2\phi}{\partial x\partial y}. \qquad 7.23$$

By using equations 7.1-7.6, 7.19, 7.20, equations 7.23 yield

$$\nabla^4\phi + \frac{Et}{R}\frac{\partial^2 w}{\partial x^2} = Et\left[\left(\frac{\partial^2 w}{\partial x\partial y}\right)-\frac{\partial^2 w}{\partial x}\frac{\partial^2 w}{\partial y^2}-\frac{\partial^2 w_0}{\partial x^2}\frac{\partial^2 w}{\partial y^2}-\frac{\partial^2 w}{\partial x^2}\frac{\partial^2 w_0}{\partial y^2}-2\frac{\partial^2 w_0}{\partial x\partial y}\frac{\partial^2 w}{\partial x\partial y}\right]$$

7.2

This is usually referred to as the <u>Compatibility equation</u>.

7.3 Choice of displacement functions.

Let the displacement function be represented by the general expression

$$w = \sum_m \sum_n a_{mn} \cos \frac{m\pi x}{l_x} \cos \frac{n\pi y}{l_y} + \text{constant term.}$$

Kempner (68) has shown how an 'improved' approximation for the displacement function can be determined from the single term used for the classical theory. This entails substitution into the compatibility equation to determine the stress function, ϕ, then substitution for ϕ and w in the right hand side of the equilibrium equation. The particular solution of this equation gives an 'improved' approximation for the displacement function.

Thus, by just using the term represented by the coefficient, a_{11}, Kempner found that the 'improved' form of the displacement function included the terms $a_{11}, a_{20}, a_{02}, a_{13}$ and a_{31}. However, he used only the first three terms for his solution. These three terms, together with the halfwavelengths l_x, and l_y, make up the five parameter displacement function used in this thesis.

By including all the terms $a_{11}, a_{20}, a_{02}, a_{13}$ and a_{31}, we have the seven parameter displacement as used in sectio 7.6. Since the term represented by a_{11} appears to be the dominant term in the displacement function, it was also decided to investigate the influence of the term a_{22}. This term, together with those of the five parameter function, gave the six parameter displacement function of section 7.5.

As can be seen from the above (and in what follows), the five parameter function contains only those terms for which $m+n = 2$. The six parameter function contains one, and the seven parameter function two terms for which $m+n = 4$. By including all

those terms for which $m+n = 4$, the ten parameter displacement function of section 7.7 is obtained.

As the number of terms taken in the displacementfunction increases, so do the number of terms that occur in the stress function. The terms that occur in the stress function corresponding to a particular displacement function, are as follows :-

a) Five parameters :

w :	a_{02}, a_{11}, a_{20}.	$(m+n = 2)$
ϕ :	A_{02}, A_{11}, A_{20};	$(m+n = 2)$
	A_{13}, A_{31}.	$(m+n = 4)$

b) Six parameters :

w :	a_{02}, a_{11}, a_{20};	$(m+n = 2)$
	a_{22}.	$(m+n = 4)$
ϕ :	A_{02}, A_{11}, A_{20};	$(m+n = 2)$
	$A_{04}, A_{13}, A_{22}, A_{31}, A_{40}$;	$(m+n = 4)$
	A_{24}, A_{42}.	$(m+n = 6)$

c) Seven parameters :

w :	a_{02}, a_{11}, a_{20};	$(m+n = 2)$
	a_{13}, a_{31}.	$(m+n = 4)$
ϕ :	A_{02}, A_{11}, A_{20};	$(m+n = 2)$
	$A_{04}, A_{13}, A_{22}, A_{31}, A_{40}$;	$(m+n = 4)$
	$A_{06}, A_{15}, A_{24}, A_{33}, A_{42}, A_{51}; A_{60}$;	$(m+n = 6)$
	A_{44}.	$(m+n = 8)$

d) Ten parameters :

w : a_{02}, a_{11}, a_{20} ; $(m+n = 2)$

$a_{04}, a_{13}, a_{22}, a_{31}, a_{40}$. $(m+n = 4)$

ϕ : A_{02}, A_{11}, A_{20} ; $(m+n = 2)$

$A_{04}, A_{13}, A_{22}, A_{31}, A_{40}$; $(m+n = 4)$

$A_{06}, A_{15}, A_{24}, A_{33}, A_{42}, A_{51}, A_{60}$; $(m+n = 6)$

$A_{17}, A_{26}, A_{35}, A_{44}, A_{53}, A_{62}, A_{71}$. $(m+n = 8)$

7.4 Five Parameter Displacement Function.

Assume the radial deflection, w, to be given by :-

$$w = a\left(\cos\frac{\pi x}{l_x}\cos\frac{\pi y}{l_y} + b\cos\frac{2\pi x}{l_x} + c\cos\frac{2\pi y}{l_y} + d\right) \qquad 7.25$$

$$= a\left(C_x C_y + b\,C_{2x} + c\,C_{2y} + d\right) \quad \text{for brevity.}$$

Substitution in the compatibility equation (7.24) gives :-

$$\nabla^4\phi = -Et\frac{a^2\pi^4}{l_x^2 l_y^2}\left[2(b+c)C_xC_y + \tfrac{1}{2}C_{2x} + \tfrac{1}{2}C_{2y} + 2cC_xC_{3y} + 2bC_{3x}C_y + 16\,bc\,C_{2x}C_{2y} - \frac{l_y^2}{4\pi^2 a}\left(C_xC_y + 4bC_{2x}\right)\right] \qquad 7.26$$

Let $\phi = K\left(A'C_xC_y + B'C_{2x} + C'C_{2y} + D'C_xC_{3y} + E'C_{3x}C_y + F'C_{2x}C_{2y}\right) - \tfrac{1}{2}Ny^2$ 7.27

$$\therefore \nabla^4\phi = K\frac{\pi^4}{l_y^4}\left[A'(1+\mu^2)^2C_xC_y + 16\mu^4B'C_{2x} + 16C'C_{2y} + (9+\mu^2)^2D'C_xC_{3y} + (1+9\mu^2)E'C_{3x}C_y + 16(1+\mu^2)^2F'C_{2x}C_{2y}\right] \qquad 7.28$$

where $\mu = l_y/l_x$

By equating the coefficients of equations 7.26 and 7.28, the coefficients in equation 7.27 can be determined in terms of the parameters a, b, c, d, l_x, and l_y, of equation 7.25.

$$\therefore \phi = -Et a^2\mu^2 [A_{11}C_xC_y + A_{20}C_{2x} + A_{02}C_{2y} + A_{13}C_xC_{3y} + A_{31}C_{3x}C_y + A_{22}C_{2x}C_{2y}] - \tfrac{1}{2}Ny^2 \qquad 7.29$$

where $A_{11} = \dfrac{2(b+c)\alpha\beta - 1}{\alpha\beta(1+\mu^2)^2}$; $A_{20} = \dfrac{\alpha\beta - 8b}{32\mu^4\alpha\beta}$; $A_{02} = \dfrac{1}{32}$;

$A_{13} = \dfrac{2c}{(9+\mu^2)^2}$; $A_{31} = \dfrac{2b}{(1+9\mu^2)^2}$; $A_{22} = \dfrac{bc}{(1+\mu^2)^2}$;

$\mu = \dfrac{l_y}{l_x}$; $\beta = \dfrac{\pi^2 R}{l_y^2}$.

$$\therefore N_x = \frac{\partial^2\phi}{\partial y^2} = Et a^2\mu^2 \frac{\beta}{R}[A_{11}C_xC_y + 4A_{02}C_{2y} + 9A_{13}C_xC_{3y} + A_{31}C_{3x}C_y + 4A_{22}C_{2x}C_{2y}] - N$$

$$N_{xy} = \frac{\partial^2\phi}{\partial x\partial y} = Eta^2\mu^3 \frac{\beta}{R}[A_{11}S_xS_y + 3A_{13}S_xS_{3y} + 3A_{31}S_{3x}S_y + 4A_{22}S_{2x}S_{2y}]$$

$$N_y = \frac{\partial^2\phi}{\partial x^2} = Eta^2\mu^4 \frac{\beta}{R}[A_{11}C_xC_y + 4A_{20}C_{2x} + A_{13}C_xC_{3y} + 9A_{31}C_{3x}C_y + 4A_{22}C_{2x}C_{2y}] \qquad 7.30$$

Extensional Strain Energy.

$$W_1 = \frac{1}{2Et}\int_0^L\int_0^{2\pi r}\left[N_x^2 + N_y^2 - 2\nu N_x N_y + 2(1+\nu)N_{xy}^2\right]dx\,dy$$

$$\therefore W_1 = \frac{1}{2Et}\int_0^L\int_0^{2\pi r}(Eta^2\mu^2\tfrac{\beta}{R})^2\Big[\Big\{A_{11}C_xC_y + 4A_{02}C_{2y} + 9A_{13}C_xC_{3y} + A_{31}C_{3x}C_y + 4A_{22}C_{2x}C_{2y}$$
$$-\tfrac{NR}{Eta^2\mu^2\beta}\Big\}^2 + \mu^4\Big\{A_{11}C_xC_y + 4A_{20}C_{2x} + A_{13}C_xC_{3y} + 9A_{31}C_{3x}C_y + 4A_{22}C_{2x}C_{2y}\Big\}^2$$
$$-2\nu\mu^2\Big\{A_{11}C_xC_y + 4A_{02}C_{2y} + 9A_{13}C_xC_{3y} + A_{31}C_{3x}C_y + 4A_{22}C_{2x}C_{2y} - \tfrac{NR}{Eta^2\mu^2\beta}\Big\}\times$$
$$\times\Big\{A_{11}C_xC_y + 4A_{20}C_{2x} + A_{13}C_xC_{3y} + 9A_{31}C_{3x}C_y + 4A_{22}C_{2x}C_{2y}\Big\}$$
$$+2(1+\nu)\mu^2\Big\{A_{11}S_xS_y + 3A_{13}S_xS_{3y} + 3A_{31}S_{3x}S_y + 4A_{22}S_{2x}S_{2y}\Big\}^2\Big]dx\,dy$$

In carrying out the above (and subsequent) integrations, it is assumed that the length L is sufficiently long that $L \approx m\lambda_x$, and that $2\pi r \approx n\lambda_y$, where m and n are integers. Then, only terms that do not contain cosine expressions will remain after integration.

$$\therefore W_1 = (\tfrac{1}{4}\pi RL)Eta^4\mu^4\frac{\beta^2}{R^2}\Big[A_{11}(1+\mu^2)^2 + 32\mu^4A_{20}^2 + 32A_{02}^2 + (9+\mu^2)^2A_{13}^2$$
$$+ 16(1+\mu^2)^2A_{22}^2 + \frac{4N^2R^2}{E^2t^2a^4\mu^4\beta^2}\Big] \qquad 7.31.$$

Bending Strain Energy.

$$W_2 = \frac{1}{2} D \int_0^L \int_0^{2\pi r} \left[\left(\frac{\partial^2 w}{\partial x^2}\right)^2 + 2\nu \frac{\partial^2 w}{\partial x^2}\cdot\frac{\partial^2 w}{\partial y^2} + \left(\frac{\partial^2 w}{\partial y^2}\right)^2 + 2(1-\nu)\left(\frac{\partial^2 w}{\partial x \partial y}\right)^2 \right] dx\,dy$$

$$= \frac{1}{2} D \int_0^L \int_0^{2\pi r} \left[a^2 \frac{\pi^4}{\ell_x^4} (C_x C_y + 4b C_{2x})^2 + 2\nu \frac{a^2\pi^4}{\ell_x^2 \ell_y^2} (C_x C_y + 4b C_{2x})(C_x C_y + 4c C_{2y}) \right.$$

$$\left. + a^2 \frac{\pi^4}{\ell_y^2} (C_x C_y + 4c C_{2y})^2 + 2(1-\nu) \frac{a^2\pi^4}{\ell_x^2 \ell_y^2} S_x^2 S_y^2 \right] dx\,dy$$

$$= (1/4\pi RL)\, D a^2 \frac{\beta^2}{R^2} \left[(H\mu^2)^2 + 32\mu^4 b^2 + 32 c^2 \right] \qquad 7.32$$

Potential of the external load.

$$W_3 = -\int_0^{2\pi r} (N_x)_{x=L}\, dy \int_0^L \frac{\partial u}{\partial x}\, dx$$

$$\frac{\partial u}{\partial x} = \epsilon_x - \frac{1}{2}\left(\frac{\partial w}{\partial x}\right)^2$$

$$= \frac{1}{Et}\left[N_x - \nu N_y \right] - \frac{1}{2}\left(\frac{\partial w}{\partial x}\right)^2$$

$$= \frac{1}{Et}\left[Et a^2 \mu^2 \frac{\beta}{R} \left\{ A_{11} C_x C_y + 4A_{02} C_{2y} + 9A_{13} C_x C_{3y} + A_{31} C_{3x} C_y + 4A_{22} C_{2x} C_{2y} \right\} - N \right.$$

$$\left. - \nu Et a^2 \mu^2 \frac{\beta}{R} \left\{ A_{11} C_x C_y + 4A_{20} C_{2x} + A_{13} C_x C_{3y} + 9A_{31} C_{3x} C_y + 4A_{22} C_{2x} C_{2y} \right\} \right] - \frac{1}{2} a^2 \frac{\pi^2}{\ell_x^2} (S_x C_y + 2b S_{2x})$$

$$\therefore \int_0^L \frac{\partial u}{\partial x}\,dx = a^2\mu^2\frac{\beta}{R}\left[4LA_{02}C_{2y}\right] - \frac{NL}{Et} - \frac{1}{2}a^2\mu^2\frac{\beta}{R}\left[\tfrac{1}{4}L + \tfrac{1}{4}L\,C_{4y} + 2b^2L\right]$$

Upon integrating around the circumference to obtain the average value, we get :-

$$\int_0^L \frac{\partial u}{\partial x}dx = -a^2\mu^2\frac{\beta}{R}L\left[\frac{1}{8}(1+8b^2) + \frac{NR}{Eta^2\mu^2\beta}\right]$$

$$\int_0^{2\pi r}(N_x)_{x=L}\,dy = \int_0^{2\pi r}\left[Eta^2\mu^2\frac{\beta}{R}\left\{A_{11}C_L C_y + 4A_{02}C_{2y} + 9A_{03}C_L C_{3y} + A_{31}C_{3L}C_y + 4A_{22}C_{2L}C_{2y} - \frac{NR}{Eta^2\mu^2\beta}\right]dy$$

$$= -2\pi RN$$

$$\therefore \quad W_3 = -(-2\pi RN)\left\{-a^2\mu^2\frac{\beta}{R}L\left[\frac{1}{8}(1+8b^2) + \frac{NR}{Eta^2\mu^2\beta}\right]\right.$$

$$= -\left(\tfrac{1}{4}\pi RL\right)N\,a^2\mu^2\frac{\beta}{R}\left[(1+8b^2) + \frac{8NR}{Eta^2\mu^2\beta}\right]$$

$$= -\left(\tfrac{1}{4}\pi RL\right)N\left[a^2\mu^2\frac{\beta}{R}(1+8b^2) + \frac{8N}{Et}\right] \qquad 7.33$$

For the case of controlled end-shortening, $W_3 = 0$.

$W_4 = 0$, for no internal or external pressure.

$\varepsilon' = -\frac{1}{L}\int_0^L \frac{\partial u}{\partial x}dx$ is referred to as the unit end-shortening.

$$\therefore \varepsilon' = \frac{1}{8}a^2\mu^2\frac{\beta}{R}(1+8b^2) + \frac{N}{Et} \qquad 7.34a$$

Alternatively, if ε' is specified

$$N = Et\left[\varepsilon' - \frac{1}{8}a^2\mu^2\frac{\beta}{R}(1+8b^2)\right] \qquad 7.34b$$

Total Potential Energy.

$$\Pi = W_1 + W_2 + W_3$$

$$= \left(\tfrac{1}{4}\pi RL\right)Eta^4\frac{\beta^2}{R^2}\left[A_{11}^2(1+\mu^2)^2 + 32\mu^4A_{20}^2 + 32A_{02}^2 + (9+\mu^2)^2A_{13}^2 + (1+9\mu^2)^2A_{31}^2 + 16(1+\mu^2)^2A_{22}^2 + \frac{4N^2R^2}{Et^2a^4\mu^4\beta^2}\right] + Da^2\frac{\beta^2}{R^2}\left[\tfrac{1}{4}\pi RL\right]\left[(1+\mu^2)^2 + 32\mu^4b^2 + 32c^2\right] - \left(\tfrac{1}{4}\pi RL\right)N\left[a^2\mu^2\frac{\beta}{R}(1+8b^2) + \frac{8N}{Et}\right]$$

$$\therefore \Pi^* = Eta^4\mu^4\frac{\beta^2}{R^2}\left[(1+\mu^2)^2\left\{A_{11}^2 + \frac{D}{Eta^2\mu^4}\right\} + 32\mu^4\left(A_{20}^2 + \frac{Db^2}{Eta^2\mu^4}\right) + 32\left(A_{02}^2 + \frac{Dc^2}{Eta^2\mu^4}\right) + (9+\mu^2)^2A_{13}^2 + (1+9\mu^2)^2A_{31}^2 + 16(1+\mu^2)^2A_{22}^2\right] - a^2\mu^2\frac{\beta}{R}(1+8b^2)N - \frac{4N^2}{Et}$$

where $\Pi = \tfrac{1}{4}\pi RL.\,\Pi^*$ 7.35

By separating out the terms in Π^*, we have

$$\Pi^* = \frac{Et\,a^2}{R^2}\left[\frac{\mu^4\{2(b+c)\alpha\beta-1\}^2}{(1+\mu^2)} + \frac{D(1+\mu^2)^2\beta^2}{Et} + \frac{2(\alpha\beta-8b)^2}{64} + \frac{32D\mu^4b^2\beta^2}{Et}\right.$$
$$+ \frac{2a^2\mu^4\beta^2}{64} + \frac{32Dc^2\beta^2}{Et} + \frac{4a^2c^2\mu^4\beta^2}{(9+\mu^2)^2} + \frac{4a^2b^2\mu^4\beta^2}{(1+9\mu^2)^2}$$
$$\left. + \frac{16\,a^2b^2c^2\mu^4\beta^2}{(1+\mu^2)^2}\right] - a^2\mu^2\frac{\beta}{R}(1+8b^2)N - \frac{4N^2}{Et}$$

$$= \frac{Et\,a^2}{R^2}\left[\left\{\frac{\{(b+c)^2+4b^2c^2\}.4\mu^4}{(1+\mu^2)^2} + \frac{4c^2\mu^4}{(9+\mu^2)^2} + \frac{4b^2\mu^4}{(1+9\mu^2)^2} + \frac{(1+\mu^4)}{32}\right\}a^2\beta^2\right.$$
$$- \left\{\frac{4(b+c)\mu^4}{(1+\mu^2)^2} + \frac{b}{4}\right\}a\beta + \left\{b^2 + \frac{\mu^4}{(1+\mu^2)^2}\right\}$$
$$\left. + \frac{D}{Et}\left\{(1+\mu^2)^2 + 32(b^2\mu^4+c^2)\right\}\beta^2 - \frac{R}{Et}\left\{\mu^2(1+8b^2)N\right\}\beta\right] - \frac{4N^2}{Et}$$

7.36

i.e. $$\pi^* = \frac{Eta^2}{R^2}\left[A_1 a^2\beta^2 - A_2 a\beta + A_3 + A_4 \frac{D}{Et}\beta^2 - \frac{RN}{Et}A_5\beta\right] - \frac{4N^2}{Et} \qquad 7.37.$$

where
$$A_1 = \frac{4\{(b+c)^2+4bc\}\mu^4}{(1+\mu^2)^2} + \frac{4c^2\mu^4}{(9+\mu^2)^2} + \frac{4b^2\mu^4}{(1+9\mu^2)^2} + \frac{(1+\mu^4)}{32}$$

$$A_2 = \frac{4(b+c)\mu^4}{(1+\mu^2)^2} + \frac{b}{2}$$

$$A_3 = 2b^2 + \frac{\mu^4}{(1+\mu^2)^2}$$

$$A_4 = (1+\mu^2)^2 + 32(b^2\mu^4+c^2)$$

$$A_5 = \mu^2(1+8b^2)$$

As outlined in Chapter Six, the Rayleigh-Ritz method enables the five unknown parameters, a, b, c, μ, β, to be determined by setting the differential of π^* with respect to each of them, equal to zero. This gives five nonlinear simultaneous equations from which it

may be possible to evaluate the parameters. Useful methods for obtaining a numerical solution are discussed in section 6.6, and the actual numerical solution is given in Chapter Eight.

By differentiating π^* with respect to a and β, the following equations can be obtained :-

$$\begin{aligned} 2A_1 a^2\beta^2 - A_2 a\beta + 2A_4 \frac{D}{Et}\beta^2 - A_5 \frac{RN}{Et}\beta &= 0 \\ - A_2 a\beta + 2A_3 - 2A_4 \frac{D}{Et}\beta^2 &= 0 \end{aligned}$$

Therefore, the five nonlinear simultaneous equations can be written as:-

$$\frac{Eta^2}{R^2} \begin{pmatrix} 2A_1 & A_2 & 0 & 2A_4 & A_5 \\ 0 & A_2 & 2A_3 & -2A_4 & 0 \\ B_1 & B_2 & B_3 & B_4 & B_5 \\ C_1 & C_2 & C_3 & C_4 & C_5 \\ D_1 & D_2 & D_3 & D_4 & D_5 \end{pmatrix} \begin{pmatrix} a^2\beta^2 \\ -a\beta \\ 1 \\ \frac{D}{Et}\beta^2 \\ -\frac{RN}{Et}\beta \end{pmatrix} = 0 \qquad 7.38$$

where $A_i = \phi(b, c, \mu)$

$B_i = \partial A_i / \partial \mu$

$C_i = \partial A_i / \partial b$

$D_i = \partial A_i / \partial c$

$$B_1 = \left\{(b+c)^2 + 4b^2c^2\right\} \frac{16\mu^3}{(1+\mu^2)^3} + \frac{144c^2\mu^3}{(9+\mu^2)^3} + \frac{16b^2\mu^3}{(1+9\mu^2)^3} + \frac{1}{8}\mu^3$$

$$B_2 = 16(b+c)\frac{\mu^3}{(1+\mu^2)^3}$$

$$B_3 = \frac{4\mu^3}{(1+\mu^2)^3}$$

$$B_4 = 4\mu(1+\mu^2) + 128b^2\mu^3$$

$$B_5 = 2\mu(1+8b^2)$$

$$C_1 = 4\left\{2(b+c) + 8bc^2\right\}\frac{\mu^4}{(1+\mu^2)^2} + \frac{8b\mu^4}{(1+9\mu^2)^2}$$

$$C_2 = \frac{4\mu^4}{(1+\mu^2)^2} + \frac{1}{2}$$

$$C_3 = 4b$$

$$C_4 = 64b\mu^4$$

$$C_5 = 16b\mu^2$$

$$D_1 = 4\left\{2(b+c) + 8b^2c\right\}\frac{\mu^8}{(1+\mu^2)^2} + \frac{8c\mu^4}{(9+\mu^2)^2}$$

$$D_2 = \frac{4\mu^4}{(1+\mu^2)^2}$$

$$D_3 = 0$$

$$D_4 = 64c$$

$$D_5 = 0$$

7.5 SIX PARAMETER DISPLACEMENT FUNCTION.

Assume the radial displacement, ω, to be given by :-

$$\omega = a\left(C_x C_y + b\,C_{2x} + c\,C_{2y} + d\,C_{2x}C_{2y} + e\right)$$

$$\text{i.e. } \omega = a\left(\cos\frac{\pi x}{l_x}\cos\frac{\pi y}{l_y} + b\cos\frac{2\pi x}{l_x} + c\cos\frac{2\pi y}{l_y} + d\cos\frac{2\pi x}{l_x}\cos\frac{2\pi y}{l_y} + e\right) \qquad 7.39$$

The stress function, ϕ, is then given by :-

$$\phi = -Et a^2\mu^2\left[A_{11}C_xC_y + A_{20}C_{2x} + A_{02}C_{2y} + A_{22}C_{2x}C_{2y} + A_{13}C_xC_{3y} + A_{31}C_{3x}C_y + A_{40}C_{4x} + A_{04}C_{4y} + A_{24}C_{2x}C_{4y} + A_{42}C_{4x}C_{2y}\right] - \tfrac{1}{2}Ny^2 \qquad 7.40$$

where $A_{11} = \dfrac{2(b+c)\alpha\beta - 1}{\alpha\beta(1+\mu^2)^2}$; $A_{02} = \dfrac{1}{32}$; $A_{40} = \dfrac{d^2}{32\mu^2}$; $A_{04} = \dfrac{d^2}{32}$;

$A_{20} = \dfrac{(\alpha\beta - 8b)}{32\alpha\beta\mu^4}$; $A_{13} = \dfrac{2(c+2d)}{(9+\mu^2)^2}$; $A_{24} = \dfrac{cd}{2(4+\mu^2)^2}$

$A_{22} = \dfrac{\{2(bd+cd+2bc)\alpha\beta - d\}}{4\alpha\beta(1+\mu^2)^2}$; $A_{31} = \dfrac{2(b+2d)}{(1+9\mu^2)^2}$; $A_{42} = \dfrac{bd}{2(1+4\mu^2)^2}$

Extensional Strain Energy.

$$W_1 = (1/4\pi RL)\, Et a^4 \mu^4 \frac{\beta^2}{R^2} \left[A_{11}^2 (1+\mu^2)^2 + 32\mu^4 A_{20}^2 + 32 A_{02}^2 + 16(1+\mu^2)^2 A_{22}^2 + A_{13}^2 (9+\mu^2)^2 \right.$$
$$\left. + A_{31}^2 (1+9\mu^2)^2 + 512\mu^4 A_{40}^2 + 512 A_{04}^2 + 16(\mu^2+4) A_{24}^2 + 16(1+4\mu^2)^2 A_{42}^2 + \frac{4N^2R^2}{E^3 t^2 a^6 \mu^6 \beta^2} \right.$$

Bending Strain Energy.

$$W_2 = (1/4\pi RL)\, D a^2 \frac{\beta^2}{R^2} \left[(1+\mu^2)^2 + 32\mu^4 b^2 + 32 c^2 + 16(1+\mu^2)^2 d^2 \right]$$

Potential of the External Load.

$$W_3 = -(1/4\pi RL) \left[\{1+4(2b^2+d^2)\} \frac{Na^2\mu^2\beta}{R} + \frac{8N^2}{Et} \right]$$

Total Potential Energy.

$$\Pi^* = \frac{Eta^2}{R^2} \left[A_1 a^2 \beta^2 - A_2 a\beta + A_3 + A_4 \frac{D}{Et} \beta^2 - A_5 \frac{RN}{Et} \beta \right] - \frac{4N^2}{Et} \qquad 7.41$$

where

$$A_1 = \frac{4\mu^4(b+c)^2}{(1+\mu^2)^2} + \frac{(1+\mu^4)}{32} + \frac{4(bd+cd+2bc)^2\mu^4}{(1+\mu^2)^2} + \frac{4\mu^2(c+2d)^2}{(9+\mu^2)^2} + \frac{4\mu^4(b+2d)^2}{(1+9\mu^2)^2}$$

$$+ \mu^4 d^2 + 4\mu^4 d \left\{ \frac{c}{(\mu^2+4)^2} + \frac{b}{(1+4\mu^2)^2} \right\}$$

$$A_2 = \frac{4\mu^4(b+c)}{(1+\mu^2)^2} + \frac{1}{2}b + \frac{4d(bd+cd+2bc)\mu^4}{(1+\mu^2)^2}$$

$$A_3 = \frac{\mu^4}{(1+\mu^2)^2} + 2b^2 + \frac{d^2\mu^4}{(1+\mu^2)^2}$$

$$A_4 = (1+\mu^2)^2 + 32b^2\mu^4 + 32c^2 + 16(1+\mu^2)^2 d^2$$

$$A_5 = \mu^2(1+4(2b^2+d^2))$$

By differentiating with respect to the six parameters, a, b, c, d, μ, and β, six nonlinear simultaneous equations are obtained, which must then be solved to determine the values of the six parameters.

7.6 SEVEN PARAMETER DISPLACEMENT FUNCTION.

The radial displacement, w, is taken to be:-

$$w = a\left(\cos\frac{\pi x}{l_x}\cos\frac{\pi y}{l_y} + b\cos\frac{2\pi x}{l_x} + c\cos\frac{2\pi y}{l_y} + e\cos\frac{\pi x}{l_x}\cos\frac{3\pi y}{l_y} + f\left(\cos\frac{3\pi x}{l_x}\cos\frac{\pi y}{l_y} + d\right)\right)$$

i.e $$w = a(C_x C_y + b C_{2x} + c C_{2y} + e C_x C_{3y} + f C_{3x} C_y + d) \qquad 7.42.$$

The stress function, ϕ, then becomes :-

$$\phi = -Et a^2\mu^2\left[A_{11} C_x C_y + A_{20} C_{2x} + A_{02} C_{2y} + A_{22} C_{2x} C_{2y} + A_{40} C_{4x} + A_{04} C_{4y} + A_{24} C_{2x} C_{4y} + A_{42} C_{4x} C_{2y} + A_{60} C_{6x} + A_{06} C_{6y} + A_{13} C_x C_{3y} + A_{31} C_{3x} C_y + A_{15} C_x C_{5y} + A_{51} C_{5x} C_y + A_{33} C_{3x} C_{3y} + A_{44} C_{4x} C_{4y}\right] - \tfrac{1}{2} N y^2 \qquad 7.43.$$

where

$$A_{11} = \frac{\{2(b+c+bf+ce)\alpha\beta - 1\}}{\alpha\beta(1+\mu^2)^2}\ ; \quad A_{20} = \frac{\{(1+9e^2+2f)\alpha\beta - 8b\}}{32\mu^4\alpha\beta}\ ; \quad A_{40} = \frac{f}{64\mu^4}\ ; \quad A_{04} = \frac{e}{64}\ ;$$

$$A_{02} = \frac{(1+2e+9f^2)}{32}\ ; \quad A_{22} = \frac{\{(e+f)+ef+4bc\}}{4(1+\mu^2)^2}\ ; \quad A_{60} = \frac{f^2}{288\mu^4}\ ; \quad A_{06} = \frac{e^2}{288}$$

$$A_{24} = \frac{e(1+25f)}{16(\mu^2+4)^2}\ ; \quad A_{42} = \frac{f(1+25e)}{16(1+4\mu^2)^2}\ ; \quad A_{15} = \frac{2ce}{(\mu^2+25)^2}\ ; \quad A_{51} = \frac{2bf}{(1+25\mu^2)^2}\ ;$$

$$A_{13} = \frac{\{2(c+9be)\alpha\beta - e\}}{(\mu^2+9)^2\,9\beta}; \qquad A_{31} = \frac{\{2(b+cf)\alpha\beta - 9f\}}{(9\mu^2+1)^2\,9\beta};$$

$$A_{33} = \frac{2(be+cf)}{9(1+\mu^2)^2}; \qquad A_{44} = \frac{ef}{16(1+\mu^2)^2}.$$

Extensional Strain Energy

$$W_1 = (\tfrac{1}{4}\pi RL)\,Et\,a^4\mu^4\frac{\beta^2}{R^2}\Big[A_{11}^2(1+\mu^2)^2 + 32\mu^4A_{20}^2 + 32A_{02}^2 + 16A_{22}^2(1+\mu^2)^2 + 512\mu^4A_{40}^2$$
$$+ 512A_{04}^2 + 16(\mu^2+4)^2A_{24}^2 + 16(1+4\mu^2)^2A_{42}^2 + 2592\mu^4A_{60}^2 + 2592A_{06}^2$$
$$+ (9+\mu^2)^2A_{13}^2 + (1+9\mu^2)A_{31}^2 + 81(1+\mu^2)^2A_{33}^2 + 256(1+\mu^2)^2A_{44}^2 + \frac{4N^2R^2}{E^2t^2a^4\mu^4\beta^2}\Big]$$

Bending Strain Energy.

$$W_2 = (\tfrac{1}{4}\pi RL)\,D\,a^2\frac{\beta^2}{R^2}\Big[(1+\mu^2)^2 + 32\mu^4b^2 + 32c^2 + (\mu^2+9)^2e^2 + (1+9\mu^2)^2f^2\Big]$$

Potential of the External Load.

$$W_3 = -(\tfrac{1}{4}\pi RL)\Big[N\{1+8b^2+e^2+3f^2\}\,a^2\mu^2\frac{\beta}{R} + \frac{8N^2}{Et}\Big]$$

Total Potential Energy.

$$\pi^* = \frac{Eta^2}{R^2}\left[A_1 a^2\beta^2 - A_2 a\beta + A_3 + A_4 \frac{D}{Et}\beta^2 - A_5 \frac{RN}{Et}\beta\right] - \frac{4N^2}{Et} \qquad 7.44$$

where

$$A_1 = \frac{4\mu^4(b+c+bf+ce)^2}{(1+\mu^2)^2} + \frac{(1+9e^2+2f)^2}{32} + \frac{(1+2e+9f^2)^2\mu^4}{32} + \frac{\{e+f+4ef+4bc\}^2\mu^4}{(1+\mu^2)^2}$$

$$+ \frac{f^2}{16} + \frac{e^2\mu^4}{16} + \frac{e^2(1+25f)^2\mu^4}{16(\mu^2+4)^2} + \frac{f^2(1+25e)^2\mu^4}{16(1+4\mu^2)^2} + \frac{f^4}{32} + \frac{e^4\mu^4}{32} + \frac{4\mu^4(c+9be)^2}{(\mu^2+9)^2}$$

$$+ \frac{4\mu^4(b+cf)^2}{(1+9\mu^2)^2} + \frac{4c^2e^2\mu^4}{(\mu^2+25)^2} + \frac{4b^2f^2\mu^4}{(1+25\mu^2)^2} + \frac{4(be+cf)^2\mu^4}{(1+\mu^2)^2} + \frac{\mu^4e^2f^2}{(1+\mu^2)^2}$$

$$A_2 = \frac{4\mu^4(b+c+bf+ce)}{(1+\mu^2)^2} + \frac{b(1+9e^2+2f)}{2} + \frac{4e(c+9be)\mu^4}{(\mu^2+9)^2} + \frac{36f(b+cf)\mu^4}{(1+9\mu^2)^2}$$

$$A_3 = \frac{\mu^4}{(1+\mu^2)^2} + 2b^2 + \frac{e^2\mu^4}{(\mu^2+9)^2} + \frac{81f^2\mu^4}{(1+9\mu^2)^2}$$

$$A_4 = (1+\mu^2)^2 + 32\mu^4b^2 + 32c^2 + e^2(9+\mu^2)^2 + f^2(1+9\mu^2)^2$$

$$A_5 = \mu^2(1+8b^2+e^2+3f^2)$$

7.7. TEN PARAMETER DISPLACEMENT FUNCTION.

For a radial displacement, w, taken to be:-

$$w = a\,(C_x C_y + a_{20}C_{2x} + a_{02}C_{2y} + a_{22}C_{2x}C_{2y} + a_{13}C_x C_{3y} + a_{31}C_{3x}C_y + a_{40}C_{4x} + a_{04}C_{4y} + k) \qquad 7.45$$

the stress function, ϕ, becomes :-

$$\phi = -Et a^2\mu^2\left[A_{11}C_xC_y + A_{20}C_{2x} + A_{02}C_{2y} + A_{22}C_{2x}C_{2y} + A_{13}C_xC_{3y} + A_{31}C_{3x}C_y + A_{33}C_{3x}C_{3y} + A_{40}C_{4x} + A_{04}C_{4y} + A_{24}C_{2x}C_{4y} + A_{42}C_{4x}C_{2y} + A_{44}C_{4x}C_{4y} + A_{15}C_xC_{5y} + A_{51}C_{5x}C_y + A_{35}C_{3x}C_{5y} + A_{53}C_{5x}C_{3y} + A_{60}C_{6x} + A_{06}C_{6y} + A_{26}C_{2x}C_{6y} + A_{62}C_{6x}C_{2y} + A_{17}C_xC_{7y} + C_{71}C_{7x}C_y\right] - \tfrac{1}{2}Ny^2 \qquad 7.46$$

where

$$A_{11} = \frac{\left[2\{a_{20}(1+a_{31}) + a_{02}(1+a_{13}) + 2a_{22}(a_{13}+a_{31}-1) + 4a_{40}a_{31} + 4a_{04}a_{13}\}\alpha\beta - 1\right]}{(1+\mu^2)^2\alpha\beta};$$

$$A_{20} = \frac{\left[(1+9a_{13}^2 + 2a_{31} + 16a_{02}a_{22})\alpha\beta - 8a_{20}\right]}{32\mu^4\alpha\beta}; \quad A_{02} = \frac{(1+2a_{13}+9a_{31}^2+16a_{20}a_{22})}{32};$$

$$A_{22} = \frac{\left[\{2(a_{13}+a_{31}) + 8(a_{13}a_{31}+a_{20}a_{02}) + a_{22} + 16a_{22}(a_{40}+a_{04})\}\alpha\beta - 2a_{22}\right]}{8(1+\mu^2)^2\alpha\beta}$$

$$A_{13} = \frac{[2\{a_{22}(1+8a_{31})+a_{02}+9a_{20}a_{13}+4a_{04}\}\alpha\beta - a_{13}]}{\alpha\beta(9+\mu^2)^2}; \quad A_{40} = \frac{[(2a_{22}^2+a_{31})\alpha\beta - 4a_{40}]}{64\alpha\beta\mu^4};$$

$$A_{31} = \frac{[2\{a_{22}(1+8a_{13})+a_{20}+a_{02}a_{31}+4a_{40}\}\alpha\beta - 9a_{31}]}{9\alpha\beta(1+9\mu^2)^2}; \quad A_{04} = \frac{-2a_{22}^2+a_{13}}{64};$$

$$A_{33} = \frac{2[-a_{22}+9a_{13}(a_{20}+4a_{40})+9a_{31}(a_{02}+4a_{04})]}{81(\mu^2+1)^2}; \quad A_{24} = \frac{[2a_{22}+a_{13}(1+25a_{31})+8a_{02}a_{22}+64a_{20}a_{04}]}{16(\mu^2+4)^2};$$

$$A_{42} = \frac{[2a_{22}+a_{31}+25a_{31}a_{13}+a_{20}a_{22}+64a_{02}a_{40}]}{16(1+4\mu^2)^2}; \quad A_{44} = \frac{(a_{22}+8a_{31}a_{13}+128a_{04}a_{40})}{128(1+\mu^2)^2};$$

$$A_{15} = \frac{2[a_{13}(8a_{22}+a_{02})+4a_{04}]}{(\mu^2+25)^2}; \quad A_{51} = \frac{2[a_{31}(8a_{22}+a_{20})+4a_{40}]}{(1+25\mu^2)};$$

$$A_{35} = \frac{4(a_{22}a_{13}+18a_{31}a_{04})}{(9\mu^2+25)^2}; \quad A_{53} = \frac{4(a_{22}a_{31}+18a_{40}a_{13})}{(25\mu^2+9)^2};$$

$$A_{60} = \frac{a_{31}^2}{288\mu^4}; \quad A_{06} = \frac{a_{13}^2}{288}; \quad A_{26} = \frac{2a_{22}a_{04}}{(\mu^2+9)^2};$$

$$A_{62} = \frac{2a_{22}a_{40}}{(9\mu^2+1)^2}; \quad A_{17} = \frac{8a_{13}a_{04}}{(\mu^2+49)^2}; \quad A_{71} = \frac{8a_{31}a_{40}}{(49\mu^2+1)^2}$$

Total Potential Energy

$$\pi^* = \frac{Eta^2}{R^2}\left[A_1 a^2\beta^2 - A_2 a\beta + A_3 + A_4 \frac{D}{Et}\beta^2 - A_5 \frac{RN}{Et}\beta\right] - \frac{4N^2}{Et} \qquad 7.47$$

where

$$A_1 = \frac{4\mu^4(a_{20}+a_{20}a_{31}+a_{02}+a_{02}a_{13}+2a_{22}a_{13}+2a_{22}a_{31}-2a_{22}+4a_{40}a_{31}+4a_{04}a_{13})^2}{(1+\mu^2)^2}$$

$$+ \frac{(1+9a_{13}^2+2a_{31}+16a_{02}a_{22})^2}{32} + \frac{\mu^4(1+2a_{13}+9a_{31}^2+16a_{20}a_{22})^2}{32} + \frac{(2a_{22}^2+a_{31})^2}{8} + \frac{\mu^4(2a_{22}^2+a_{13})^2}{8}$$

$$+ \frac{\mu^4(2a_{13}+2a_{31}+8a_{13}a_{31}+8a_{02}a_{20}+a_{22}+16a_{22}a_{40}+16a_{22}a_{04})^2}{4(1+\mu^2)^2} + \frac{a_{31}^4}{32} + \frac{\mu^4 a_{13}^4}{32}$$

$$+ \frac{4\mu^4(a_{22}+8a_{22}a_{31}+a_{02}+9a_{20}a_{13}+4a_{04})^2}{(\mu^2+9)^2} + \frac{4\mu^4(a_{22}+8a_{22}a_{13}+a_{20}+a_{02}a_{31}+a_{40})^2}{(9\mu^2+1)^2}$$

$$+ \frac{4\mu^4(-a_{22}+9a_{13}a_{20}+36a_{13}a_{40}+9a_{31}a_{02}+36a_{31}a_{04})^2}{81(1+\mu^2)^2} + \frac{\mu^4(2a_{22}+a_{13}+25a_{13}a_{31}+8a_{02}a_{22}+64a_{20}a_{04})^2}{16(\mu^2+4)^2}$$

$$+ \frac{\mu^4(2a_{22}+a_{31}+25a_{31}a_{13}+8a_{22}a_{20}+64a_{02}a_{40})^2}{16(1+4\mu^2)^2} + \frac{64\mu^4 a_{22}^2 a_{04}^2}{(\mu^2+9)^2} + \frac{64\mu^4 a_{22}^2 a_{40}^2}{(9\mu^2+1)^2} +$$

$$+\frac{\mu^4(a_{22}+8a_{13}a_{31}+128a_{04}a_{40})^2}{64(1+\mu^2)^2}+\frac{4\mu^4(8a_{13}a_{22}+a_{13}a_{02}+4a_{04})^2}{(\mu^2+25)^2}$$

$$+\frac{4\mu^4(8a_{31}a_{22}+a_{31}a_{20}+4a_{40})^2}{(25\mu^2+1)^2}+\frac{16\mu^4(a_{22}a_{13}+18a_{31}a_{04})^2}{(9\mu^2+25)^2}$$

$$+\frac{16\mu^4(a_{22}a_{31}+18a_{40}a_{13})^2}{(25\mu^2+9)}+\frac{64\mu^4a_{13}^2a_{04}^2}{(\mu^2+49)^2}+\frac{64\mu^4a_{31}^2a_{40}^2}{(49\mu^2+1)^2}$$

$$A_2=\frac{4\mu^4(a_{20}+a_{20}a_{31}+a_{02}+a_{02}a_{13}+2a_{22}a_{13}+2a_{22}a_{31}+4a_{40}a_{31}+4a_{04}a_{13}-a_{22})}{(1+\mu^2)^2}+\frac{a_{40}(a_{31}+2a_{22}^2)}{}$$

$$+\frac{a_{20}(1+a_{13}^2+2a_{31}+16a_{02}a_{22})}{2}+\frac{4\mu^4a_{22}(2a_{13}+2a_{31}+8a_{13}a_{31}+8a_{02}a_{20}+a_{22}+16a_{22}a_{40}+16a_{22}a_{04})}{(1+\mu^2)}$$

$$+\frac{4\mu^4a_{22}(a_{22}+8a_{22}a_{31}+a_{02}+9a_{20}a_{13}+4a_{04})}{(\mu^2+9)^2}+\frac{36\mu^4a_{31}(a_{22}+8a_{22}a_{13}+a_{20}+a_{02}a_{31}+4a_{40})}{(9\mu^2+1)^2}$$

$$A_3=\frac{\mu^4}{(1+\mu^2)^2}+2a_{20}^2+\frac{\mu^4a_{22}^2}{(1+\mu^2)^2}+\frac{\mu^4a_{13}^2}{(\mu^2+9)^2}+\frac{81\mu^4a_{31}^2}{(9\mu^2+1)^2}+a_{40}^2$$

$$A_4=(1+\mu^2)^2+32(\mu^4a_{20}^2+a_{02}^2)+16(1+\mu^2)^2a_{22}^2+(\mu^2+9)^2a_{13}^2+(9\mu^2+1)a_{31}^2+512(\mu^4a_{40}^2+a_{04}^2)$$

$$A_5=\mu^2(1+8a_{20}^2+4a_{22}^2+a_{13}^2+3a_{31}^2+32a_{40}^2)$$

CHAPTER EIGHT

RESULTS OF THEORETICAL WORK

8.1 Introduction

Altogether, four methods were considered and used in order to obtain numerical solutions to the theory. These were:

(i) an iterative method based on that used by Thielemann

(ii) the generalised Newton-Raphson method

(iii) the method of Rosenbrock

(iv) the method of Powell.

These methods are by no means equally successful. The previous methods of Kempner and of Thielemann are outlined for comparison.

The main part of the numerical work was performed on a digital computer - initially on "Mercury" and later on "Atlas" - at the London University Institute of Computer Science. All the programmes were written in CHLF3.

8.2 Previous Methods

Kempner and Thielemann had previously obtained solutions for the five parameter case, as reviewed in Section 3.4.4.1. Both of these were iterative methods and were similar, though not exactly the same. Neither appeared to be suitable for the general case. Since μ appears in the nonlinear equations arising from the minimisation of the total potential energy expression in a complicated manner,

both methods considered fixed values for μ^2 and sought to solve for the axial stress resultant (or the stress) instead of vice versa. The two methods are outlined in the following paragraphs.

(a) The method used by Kempner [68]

By elimination between the equations, it was possible to express each unknown in terms of at least two of the unknown parameters and the fixed parameter, μ. To begin with, approximations were assumed for the two least significant parameters in the deflection function. Corresponding values for the other three parameters could then be calculated. Substitution of these values in the expressions for the two least significant parameters provided new estimates of their values, and the iteration could be repeated until successive values for the two least significant parameters were the same. These values then determined the values of the other three parameters for that particular value of μ.

(b) The method used by Thielemann [129]

Here also, the values were assumed initially for the two least significant parameters. By elimination, and substitution for some of the parameters in terms of these two least significant parameters, two equations in these two unknowns were obtained. Since the assumed values did not render these equations identically zero, Thielemann used the residuals to calculate new values for the parameters, and continued the iteration until two successive values for the stress resultant, N, differed by less than a pre-assigned

amount. Thielemann claimed that his results were the same as Kempner's.

8.3 Partial Elimination Method (based on that of Thielemann)

The five equations of **Chapter Seven** that result for the five parameter case, can be written as:

$$\begin{pmatrix} 2A_1 & A_2 & 0 & 2A_4 & A_5 \\ 0 & A_2 & 2A_3 & -2A_4 & 0 \\ B_1 & B_2 & B_3 & B_4 & B_5 \\ C_1 & C_2 & C_3 & C_4 & C_5 \\ D_1 & D_2 & 0 & D_4 & 0 \end{pmatrix} \begin{pmatrix} a^2\beta^2 \\ -a\beta \\ 1 \\ \frac{D}{Et}\beta^2 \\ -\frac{rN}{Et}\beta \end{pmatrix} = 0 \qquad (8.1)$$

where $A_i = f(b,c,\mu)$

$$B_i = \frac{\partial A_i}{\partial \mu}$$

$$C_i = \frac{\partial A_i}{\partial b}$$

$$D_i = \frac{\partial A_i}{\partial c}$$

Eliminating $a\beta$ between equations two and five, gives $\beta(b,c)$.

i.e. $\quad - A_2 a\beta + 2A_3 - 2A'_4\beta^2 = 0$

Therefore

$$a\beta = \frac{2A_3 - 2A'_4\beta^2}{A_2} = K_1 \qquad (8.2)$$

$$D_1 a^2\beta^2 - 2D_2\, a\beta + 2D'_4\, \beta^2 = 0$$

Therefore

$$D_1 K^2_1 - 2D_2 K_1 + 2D'_4\, \beta^2 = 0 \qquad (8.3)$$

To eliminate N, we have from equations one and three:

$$2A_1 K^2_1 - 2A_2 K_1 + 2A_3 + 2A'_4\, \beta^2 - 2A_5\, \beta = 0$$

$$\mu B_1 K^2_1 - \mu B_2 K_1 + \mu B_3 + \mu B_4 \beta^2 - \mu\, B_5 \beta = 0$$

Now it happens that $2A_5 = \mu B_5$

Therefore:

$$(2A_1 - \mu B_1)\, K^2_1 - (2A_2 - \mu B_2)\, K_1 + (2A_3 - \mu B_3) + (2A_4 - \mu B_4)\, \beta^2 = 0 \qquad (8.4)$$

Eliminating N between equations three and four, we have:

$$8\mu b\, (B_1\, K^2_1 - B_2\, K_1 + B_3 + B_4\, \beta^2 - B_5 \beta) = 0$$

$$(1 + 8b^2)(C_1\, K^2_1 - C_2\, K_1 + C_3 + C_4\, \beta^2 - C_5\, \beta) = 0$$

Therefore:

$$\left\{8\mu bB_1 - (1 + 8b^2)\, C_1\right\} K^2{}_1 - \left\{8\mu bB_2 - (1 + 8b^2)\, C_2\right\} . K_1$$

$$+ 8\mu bB_3 - (1 + 8b^2)\, C_3$$

$$+ \left\{8\mu bB_4 - (1 + 8b^2)\, C_4\right\} \beta^2 = 0 \qquad (8.5)$$

For fixed values of μ , equations 9.4 and 9.5 become functions of the two parameters, b, c.

Thus we can write:

$$\phi_1 (b,c) = 0 \qquad (8.4a)$$

$$\phi_2 (b,c) = 0 \qquad (8.5a)$$

Unless b and c have the correct value corresponding to the particular value of μ , these equations will yield residuals, R_1 and R_2, respectively. The key to the usefulness of the method lies in how the residuals R_1 and R_2 can be used to provide better estimates for b and c. Various plots of b and c against changes in R_1 and R_2 seemed to be of little value in indicating in what direction or by how much b and c should be varied.

The next method for utilising R_1 and R_2 to guide the choice of b and c, used the generalised Newton-Raphson method. Here only variations in b and c were considered, and these lead to the following equations for evaluating the required corrections:-

$$\left.\begin{aligned} \Delta b.\ \frac{\partial \phi_1}{\partial b} + \Delta c\ .\ \frac{\partial \phi_1}{\partial c} + \phi_1 &= 0 \\ \Delta b.\ \frac{\partial \phi_2}{\partial b} + \Delta c\ .\ \frac{\partial \phi_2}{\partial c} + \phi_2 &= 0 \end{aligned}\right\} \qquad (8.6)$$

Unfortunately the method failed in a large number of cases, for when the new values of b and c were used in the next iteration, they produced imaginary values for β.

Due to the slow speed of hand computation, and the difficulties of determining corrections to b and c, as well as the difficulties of carrying sufficient significant figures in the computations, the method was finally abandoned in favour of digital computer methods for which a different approach was recommended.

8.4 Generalised Newton-Raphson Method

This has already been outlined in Section 6.6.3. It was available as a library programme (Programme 557) from the University of London Institute of Computer Science. It is illustrated by means of the flow diagram, Figure 8.1. The main disadvantage of this method is that unless the initial values that are assumed for the parameters are sufficiently close to the final solution, then the method either fails to converge, or it will diverge to a solution that is not a real solution to the problem. This latter case occurs when the solution is such that either α or β are found to be negative.

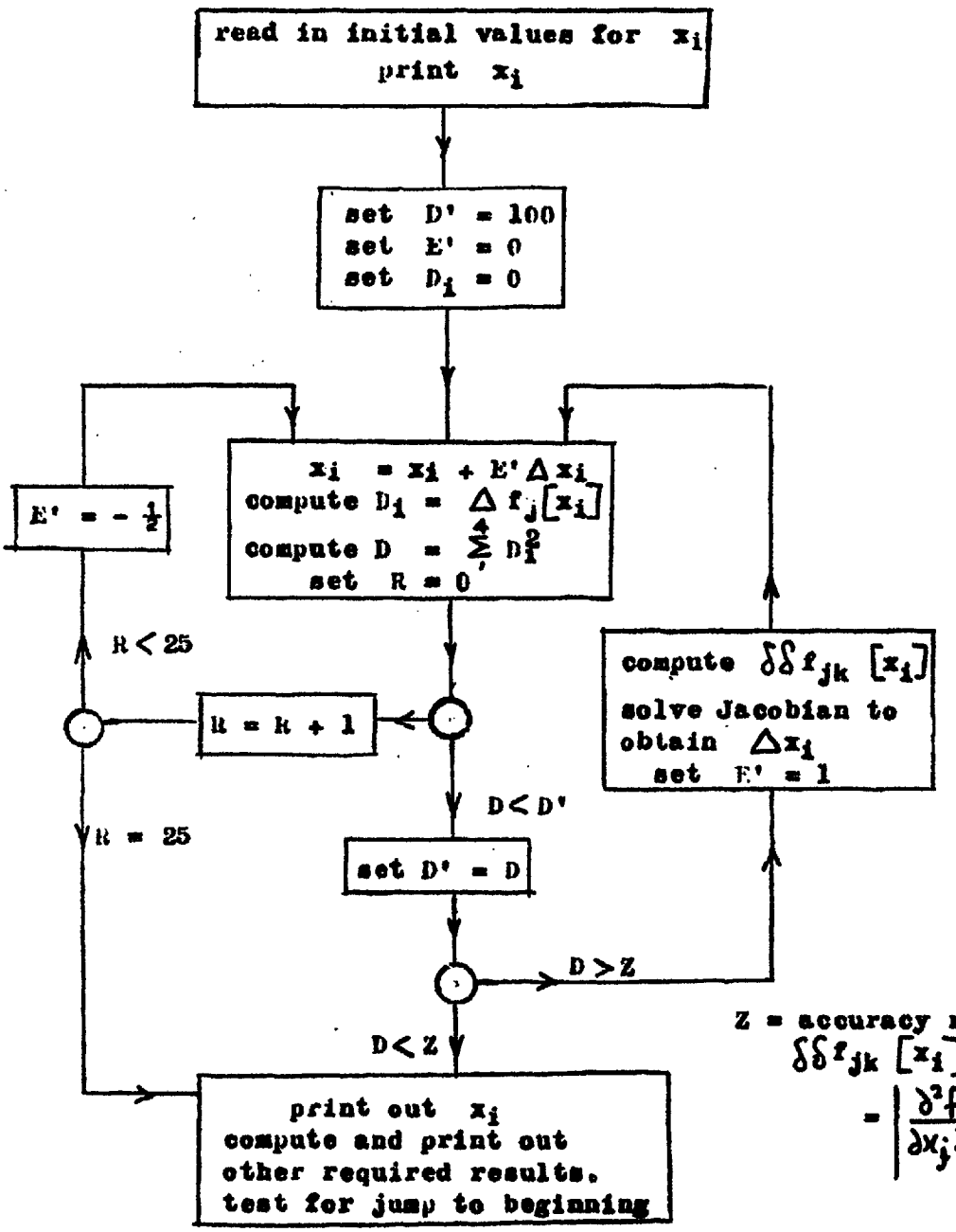


Fig. 8.1: Flow diagram for generalised Newton - Raphson method.

i.e. $\beta = \frac{\pi^2 R}{ly^2}$

Therefore, for positive R, and ly real,

$$\beta = \frac{\pi^2 R}{ly^2} \not< 0$$

When reasonable estimates are available for the set of parameters, then this method appears to be quite useful.

8.5 Rosenbrock Minimisation Method

The method is illustrated by means of the flow diagram (Figure 8.2) and was available as library routine (Routine 970) from the University of London Institute of Computer Science. This method, unlike the previous method, is a direct minimisation method. The gradient vector is not defined analytically, and is determined by a finite difference method.

Briefly, the method is initiated using an arbitrary step length that is then multiplied by α ($\alpha > 1$) each time a step successfully reduces the value of the function (or finds an equal value). If a step fails to reduce the value of the function, then the step length is multiplied by $-\beta$ ($0 < \beta < 1$). Searches are made in each of n coordinate directions initially, after which the gradient vector is then evaluated and the search continued in n orthogonal directions that are coordinates of the gradient vector. This search strategy down the line of steepest descent is uneconomical in computing time, and the method becomes inefficient

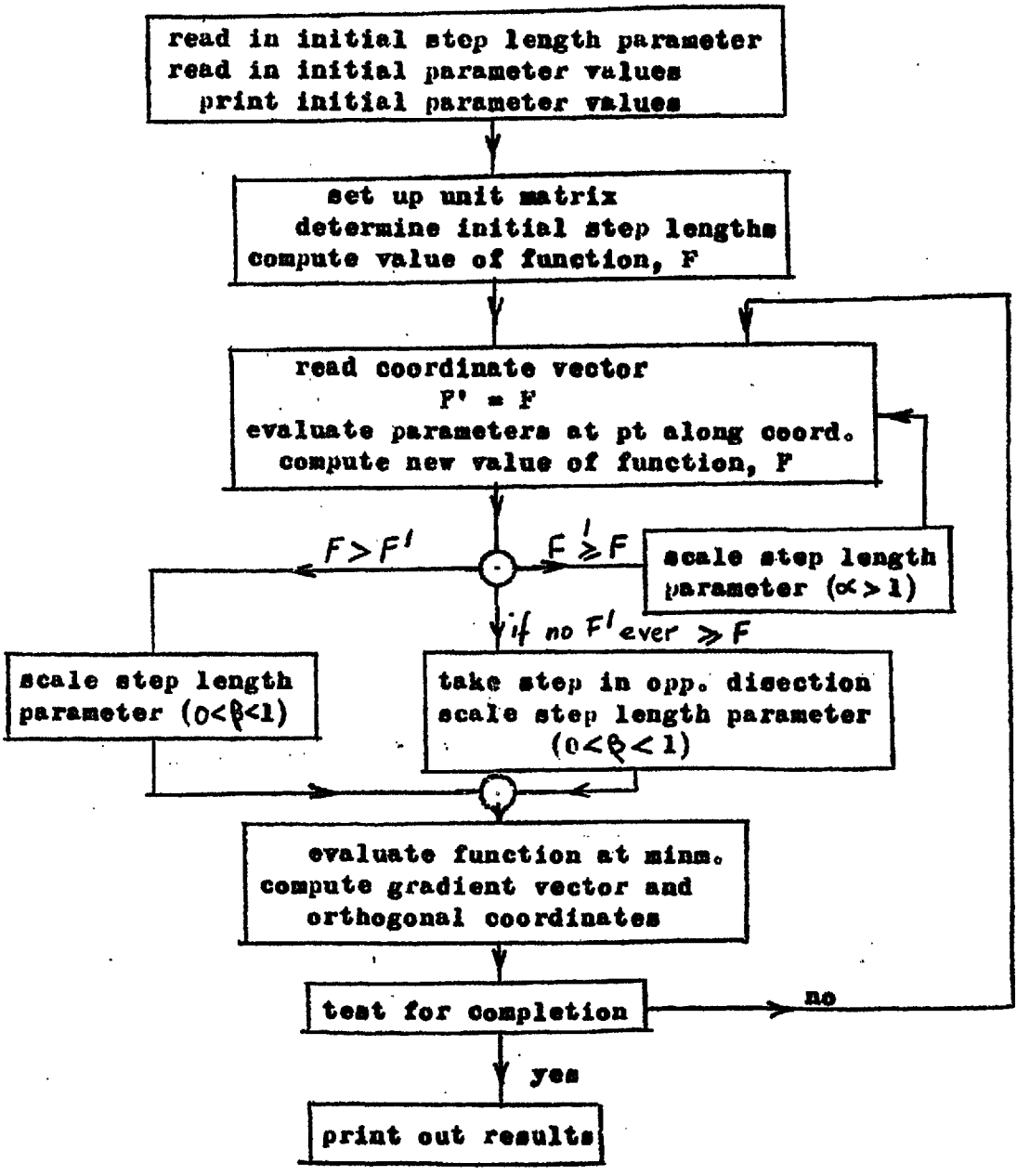


Fig. 8.2: Flow diagram for Rosenbrock's steepest descent method.

when the gradient becomes ill-defined near the minimum point. On this account, the method produced slightly different results to those obtained from the generalised Newton-Raphson method, even though both methods started with the same data. On other occasions, if one of the parameters in the set of parameters were slightly perturbed, then entirely different results would usually ensue.

8.6 Fletcher-Powell Minimisation Method

This is also a direct minimisation method, but unlike the Rosenbrock method, it relies on the gradient vector being defined analytically. Starting from a unit matrix, the method builds up successive approximations to the inverse of the matrix of the second derivatives of the function. This is used to define the directions of search for the method, and is modified after each step so that at the minimum point, the matrix is the inverse of the matrix of the second derivatives of the function. The process of computation is illustrated by the flow diagram, Figure 8.3.

Two different computer programmes were used for this method. The first was written by the Computer Unit staff, and closely followed the outline given by Fletcher and Powell [33]. Difficulties that were experienced with this programme appeared to be due to the method of interpolating along the gradient vector to locate the minimum. Before these difficulties could be resolved, a programme

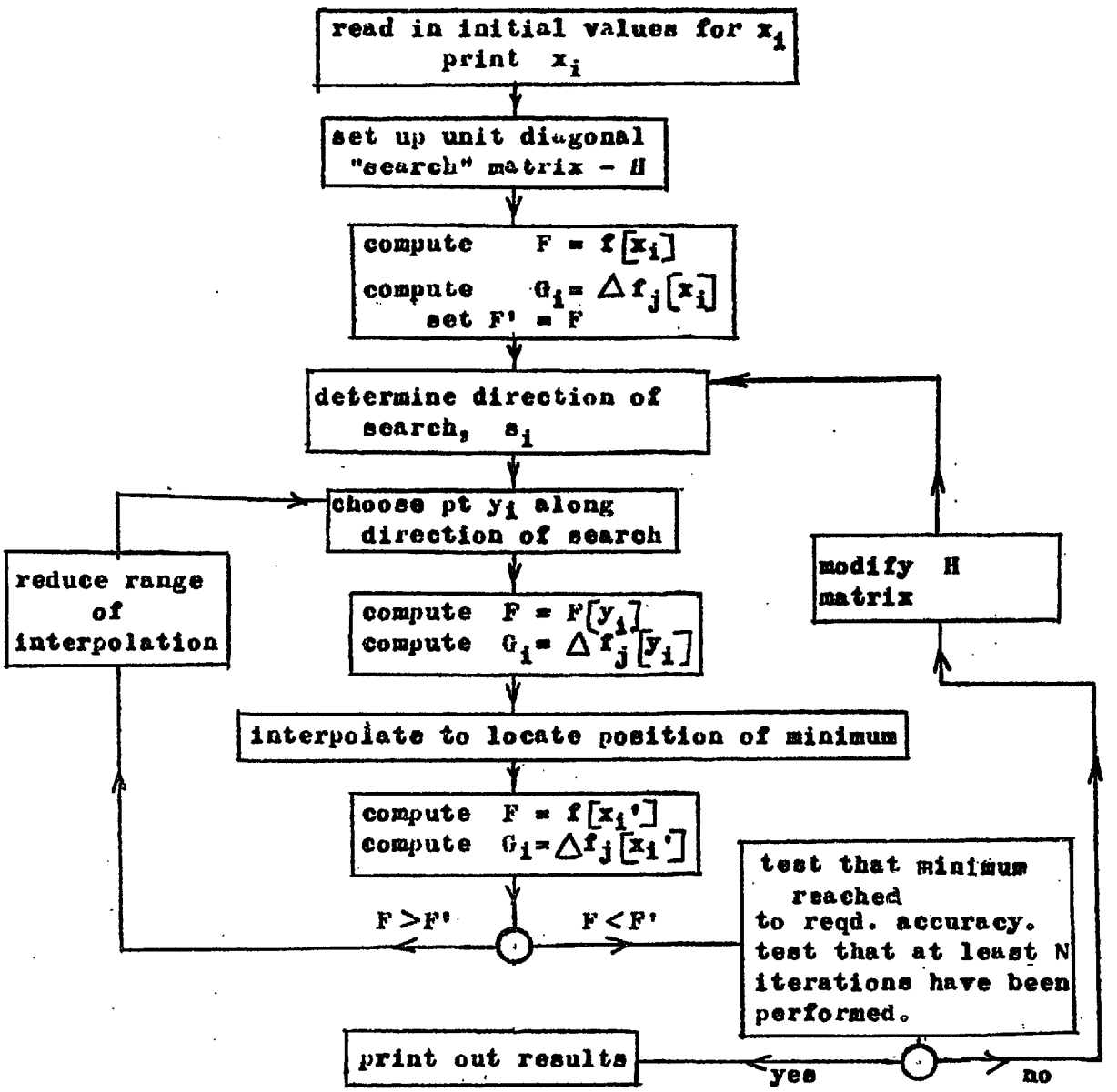


Fig. 8.3: Flow diagram for Fletcher - Powell Descent method.

written by Powell became available and after slight modification, this was subsequently used in the form of a routine.

8.7 Numerical Results - Five Parameter Case

The three methods that were used in connection with the Atlas computer, did not prove to be equally successful. A comparison of these methods is as follows:-

1) Newton-Raphson Method

If the initial parameter values were sufficiently close to the actual solution, then convergence was fast and only 2 - 3 iterations were required to reduce the residual of each equation below a value of 1×10^{-10}. For those cases where the initial parameter values were not sufficiently close to the solution, then the method diverged wildly in one iteration, or over a long series of iterations.

For the five parameter case, it was possible to process some fifty sets of data in approximately 12,000 computing instructions (50 seconds computing time on Atlas).

2) Rosenbrock Method

This was almost as fast as the previous method - providing the initial data was reasonably accurate. However, to the accuracy specified (i.e. to within 1×10^{-6} value of parameter, for each parameter), the final values were different from thise obtained from the previous method for the same initial data. When the data was not particularly accurate, convergence was much slower, and slight variations in the value of a parameter could lead to widely different

solutions.

3) Fletcher-Powell Method

This did not show the rapid convergence that was claimed for it. Even when data obtained by the Newton-Raphson method was tried, it failed to produce a final solution in 45,000 computing instructions (approximately 180 seconds). However, it could build up reasonable values of the parameters when starting from a very poor estimate. One of the main attractions of the method was its ability to compute solutions for a series of values of the load or of the end-shortening. Once the inverse Hessian matrix had been built up for one case, then the method offered the possibility of using the computed matrix and the parameter values for that case, as the starting data for the next case where the load (or end-shortening) had been altered slightly. However, starting difficulties for the first case meant that the full scope of the computer programme could not be tested, Sobey [161] found the method to be satisfactory, but he makes no reference to the length of computing time required to obtain any of his results.

The results for the five parameter case (three arbitrary constants in the assumed deflection function, together with the two half-wavelengths) are given in Table 8.1 and in Figures 8.4 and 8.5. These results were obtained using the Newton-Raphson method.

Considerable difficulty was experienced in obtaining compatible sets of values for the parameters, corresponding to a particular point on the load-end shortening diagram. After attempting to use the

TABLE 8.1

NUMERICAL RESULTS FOR FIVE PARAMETER CASE

N^*	c^*	μ	a	b	c	β
0.99988	8.7596	1.4140	0.095912	0.47342	-0.047023	23.674
0.9990	8.2705	1.3535	0.057691	0.44965	-0.047655	24.266
0.9934	7.4332	1.2395	0.061802	0.40831	-0.047694	25.045
0.9250	5.6661	1.0000	0.073121	0.33495	-0.0 3872	24.889
0.9237	5.6479	0.99786	0.073223	0.33437	-0.038555	24.879
0.91013	5.4666	0.9770	0.074195	0.3287	-0.036834	24.771
0.8036	4.3452	0.86256	0.078234	0.29898	-0.023382	24.151
0.6200	2.8668	0.72791	0.07819	0.26477	0.0037965	23.667
0.600	2.7218	0.71424	0.077869	0.26125	0.0073479	23.630
0.5896	2.6472	0.7071	0.077683	0.25940	0.009257	23.611
0.5844	2.6102	0.70352	0.077585	0.25848	0.010227	23.601
0.57929	2.5740	0.7000	0.077485	0.25756	0.011191	23.591
0.55771	2.4225	0.6850	0.077032	0.25367	0.015388	23.548
0.54	2.3000	0.67250	0.076622	0.25042	0.018986	23.509
0.52260	2.1812	0.6600	0.076187	0.24717	0.022663	23.467
0.49555	1.9995	0.6400	0.075451	0.24199	0.028660	23.392
0.490	1.9626	0.63579	0.075292	0.24091	0.029934	23.374
0.47601	1.8704	0.6250	0.074877	0.23814	0.033206	23.327
0.4572	1.7478	0.6100	0.074292	0.23432	0.037744	23.255
0.43918	1.6319	0.5950	0.073705	0.23056	0.042226	23.175
0.4220	1.5226	0.5800	0.073122	0.22686	0.046597	23.086
0.41	1.4470	0.56903	0.072703	0.22421	0.049696	23.015
0.4005	1.3874	0.5600	0.072364	0.22205	0.052159	22.953
0.38812	1.3100	0.5477	0.071913	0.21918	0.055377	22.864
0.3852	1.2949	0.54522	0.071824	0.21860	0.056004	22.845
0.38071	1.2638	0.5400	0.071639	0.21740	0.057297	22.804
0.37	1.1969	0.52834	0.071239	0.21477	0.060049	22.709
0.36274	1.1514	0.5200	0.070964	0.21292	0.061891	22.637
0.35	1.0709	0.50432	0.070478	0.20952	0.065045	22.492
0.34672	1.0498	0.5000	0.070353	0.20860	0.065838	22.450
0.34	1.0063	0.49074	0.070096	0.20665	0.067423	22.354
0.33	0.93951	0.47555	0.069719	0.20350	0.069671	22.183
0.32115	0.87691	0.4600	0.069399	0.20033	0.071585	21.986
0.32	0.86836	0.45776	0.069359	0.19987	0.071729	21.955
0.31625	0.83962	0.4500	0.069235	0.19831	0.072432	21.844
0.313	0.81320	0.44252	0.069137	0.19680	0.072996	21.730
0.31	0.78688	0.43468	0.06906	0.19521	0.073471	21.600
0.3065	0.75213	0.42364	0.06900	0.19297	0.073942	21.400
0.3044	0.72712	0.41512	0.069001	0.19123	0.074152	21.229
0.30122	0.67330	0.3950	0.069150	0.18707	0.074192	20.752
0.3016	0.64244	0.38102	0.069498	0.18402	0.073771	20.371

N^*	ε^*	μ	a	b	c	β
0.3029	0.61806	0.36884	0.069921	0.18131	0.073219	19.983
0.3031	0.61578	0.36762	0.069972	0.18103	0.073153	19.941
0.30391	0.60797	0.3633	0.070166	0.18005	0.072906	19.790
0.30420	0.60552	0.3619	0.070234	0.17973	0.072822	19.739
0.30449	0.60328	0.3606	0.070299	0.17943	0.072741	19.692
0.30482	0.60091	0.35920	0.070372	0.17910	0.072652	19.640
0.30861	0.5810	0.3464	0.071154	0.17609	0.071746	19.134
0.31	0.57530	0.34272	0.071321	0.17516	0.071437	18.988
0.32	0.55125	0.32151	0.073383	0.16994	0.069577	17.973
0.33	0.53828	0.30547	0.075499	0.16582	0.067984	17.095
0.3428	0.52916	0.28840	0.078431	0.16130	0.066176	16.057
0.35	0.52629	0.27980	0.080236	0.15899	0.06524	15.496
0.3560	0.52479	0.27302	0.081838	0.15716	0.064495	15.036
0.3615	0.52399	0.26700	0.083405	0.15553	0.063831	14.618
0.36822	0.52365	0.26000	0.085415	0.15364	0.063058	14.118
0.37314	0.52377	0.2550	0.086985	0.15229	0.062507	13.754
0.37816	0.52419	0.25000	0.088677	0.15095	0.061957	13.385
0.40602	0.53055	0.2236	0.10009	0.14397	0.059108	11.367
0.43199	0.54084	0.2000	0.11493	0.13802	0.056687	9.5208
0.46131	0.55576	0.1732	0.14048	0.13179	0.054141	7.4608
0.49404	0.57529	0.1414	0.19258	0.12518	0.051463	5.1858
of lesser accuracy						
0.5978	0.66364	0.14090	0.17999	0.11069	0.042589	4.9004
0.838	0.86098	0.099630	0.21109	0.070213	0.031164	2.6546

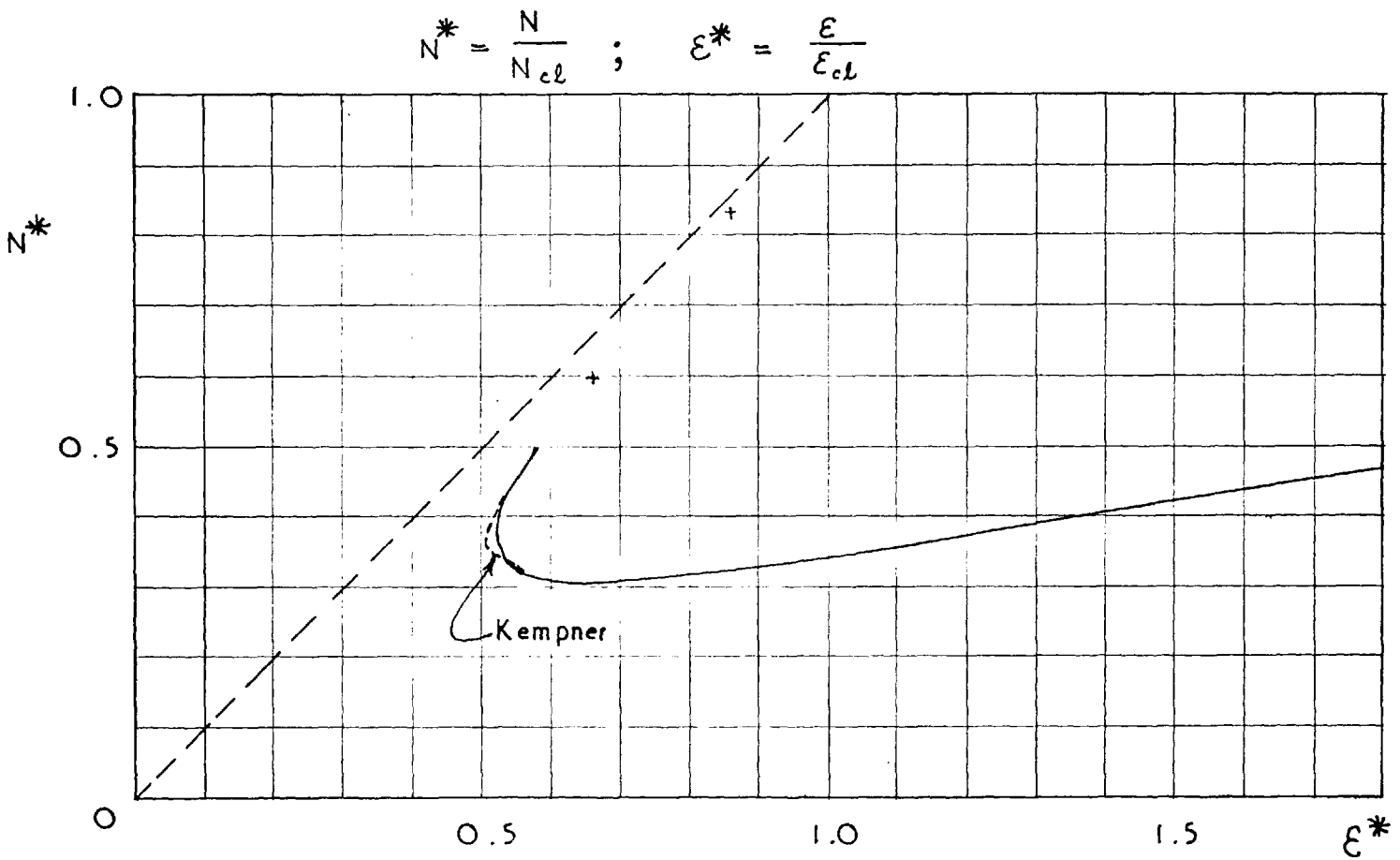


FIG. 8-4: LOAD - END SHORTENING DIAGRAM (linear plot).

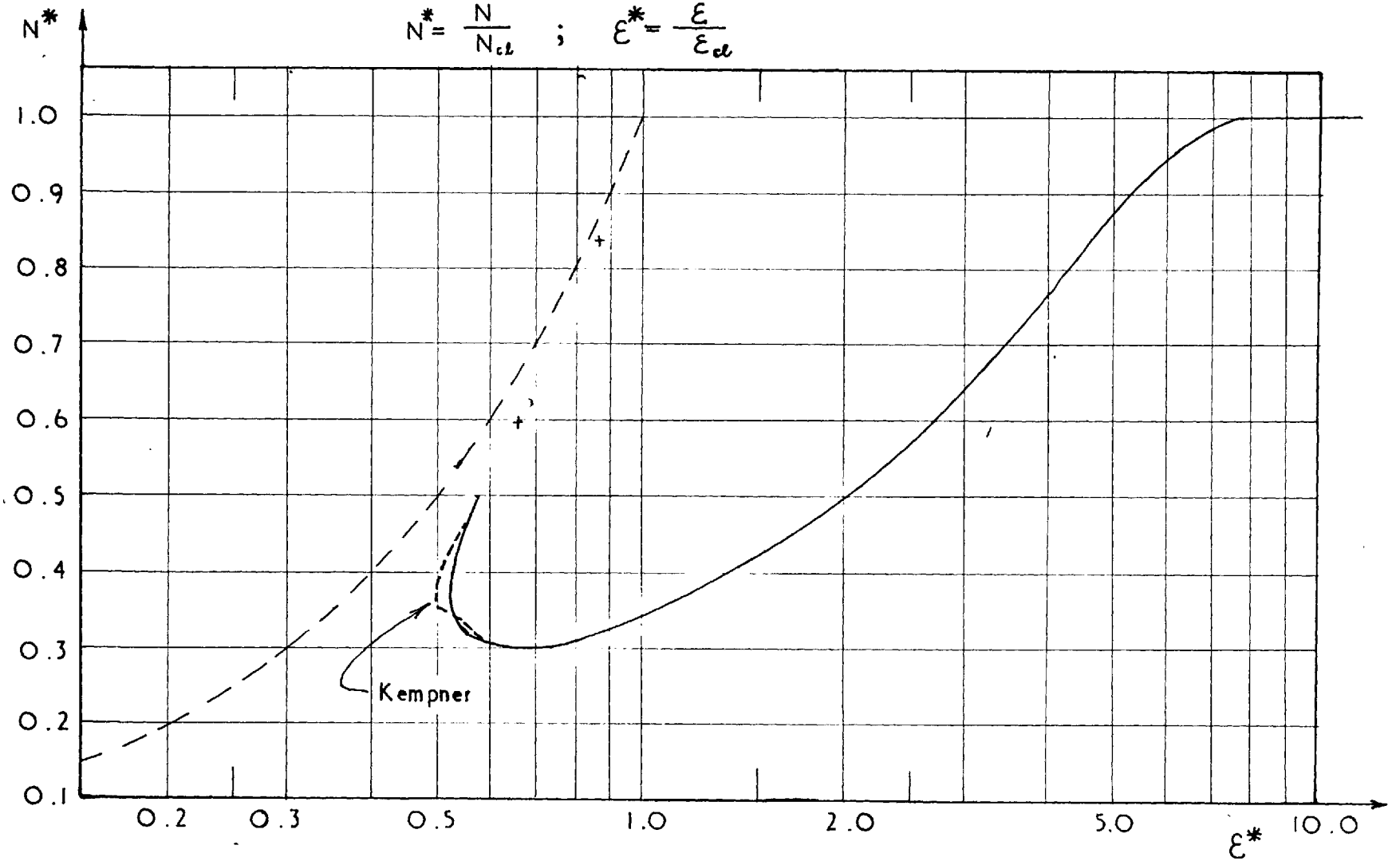


FIG. 8·5 : LOAD - END SHORTENING DIAGRAM (log. — linear plot)

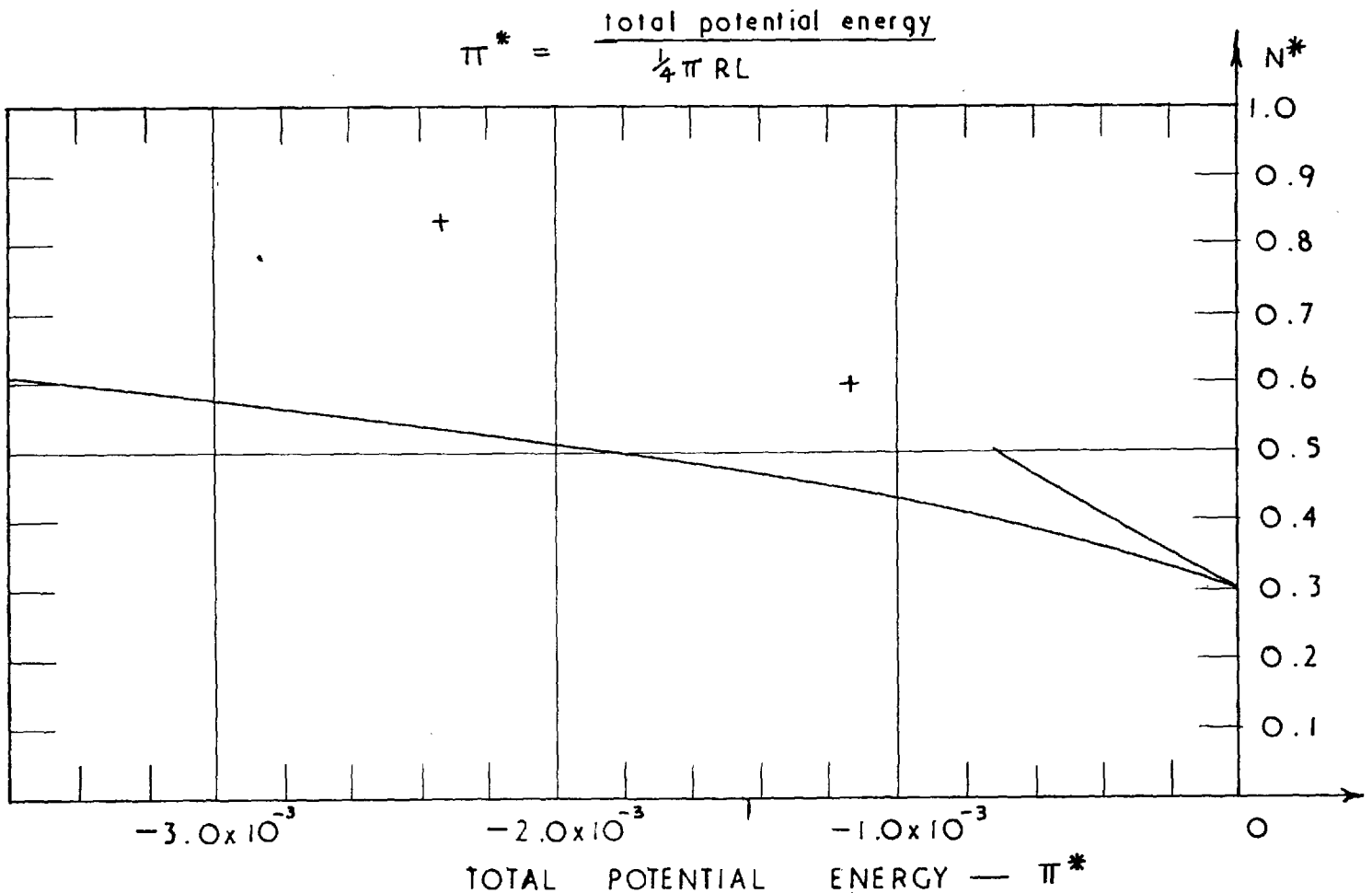


FIG. 8.6 : VARIATION OF TOTAL POTENTIAL ENERGY

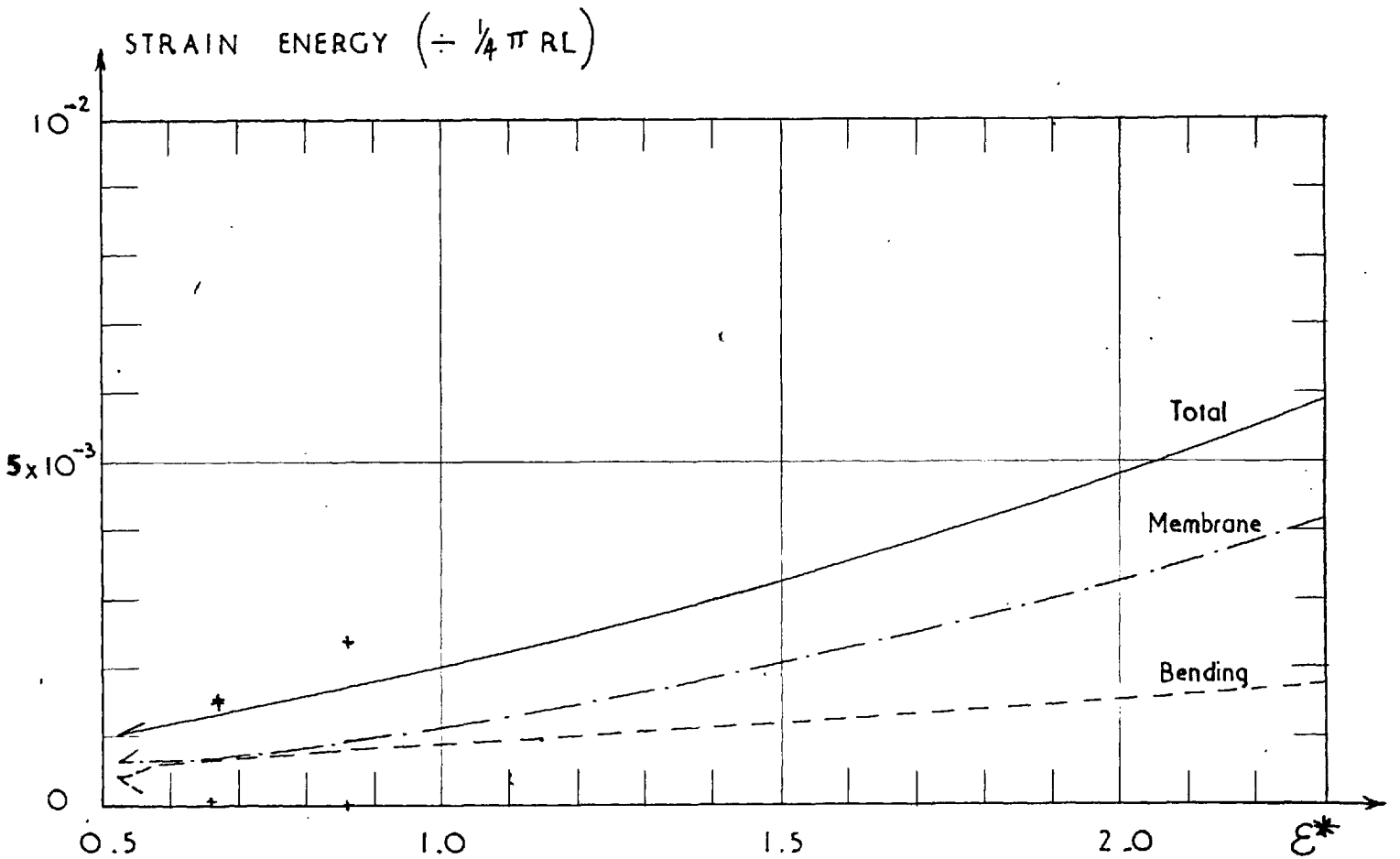


FIG. 8.7 : VARIATION OF STRAIN ENERGY.

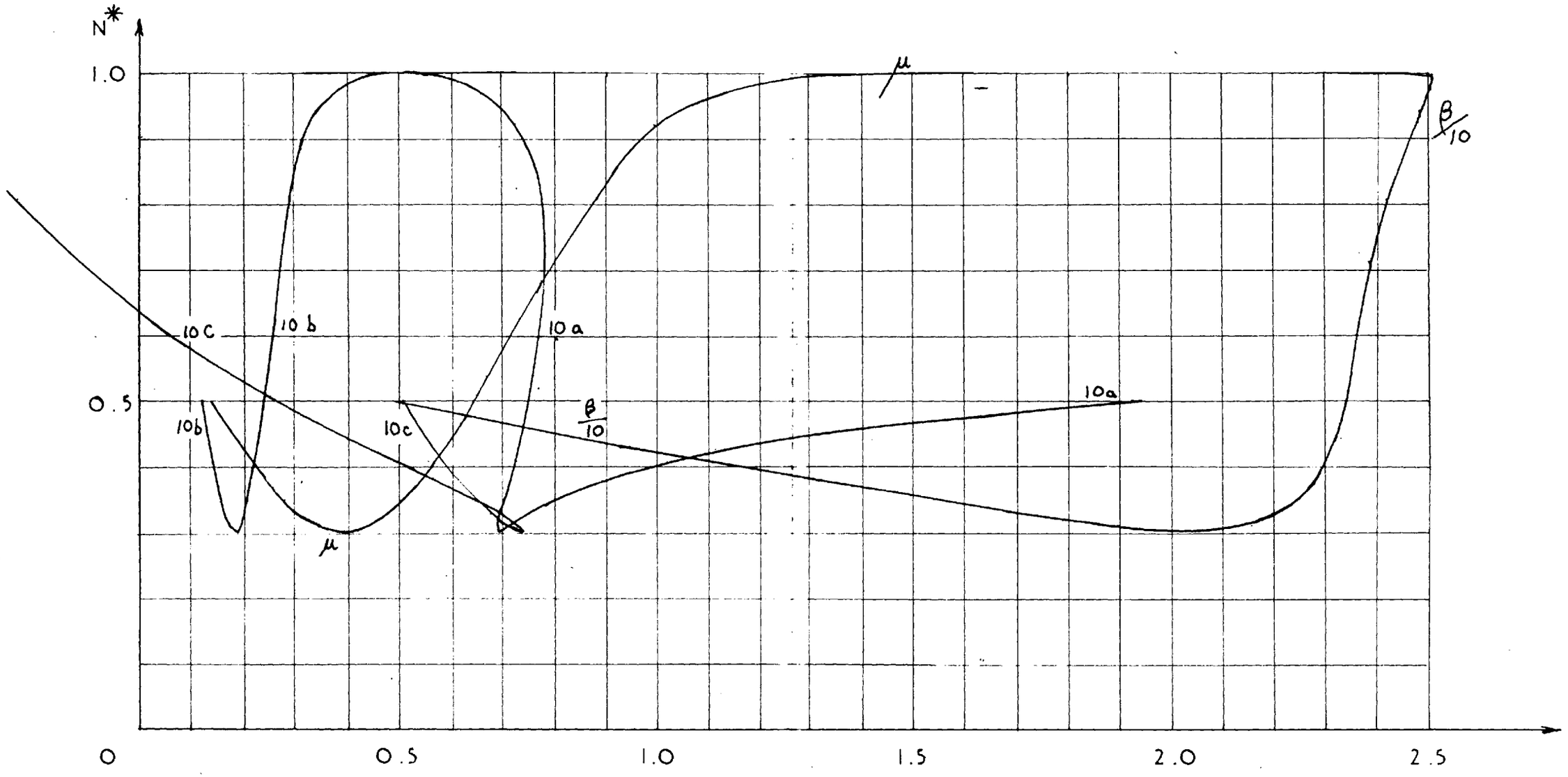


FIG. 8·8 : VARIATION OF PARAMETER VALUES FOR FIVE PARAMETER DEFLECTION FUNCTION .

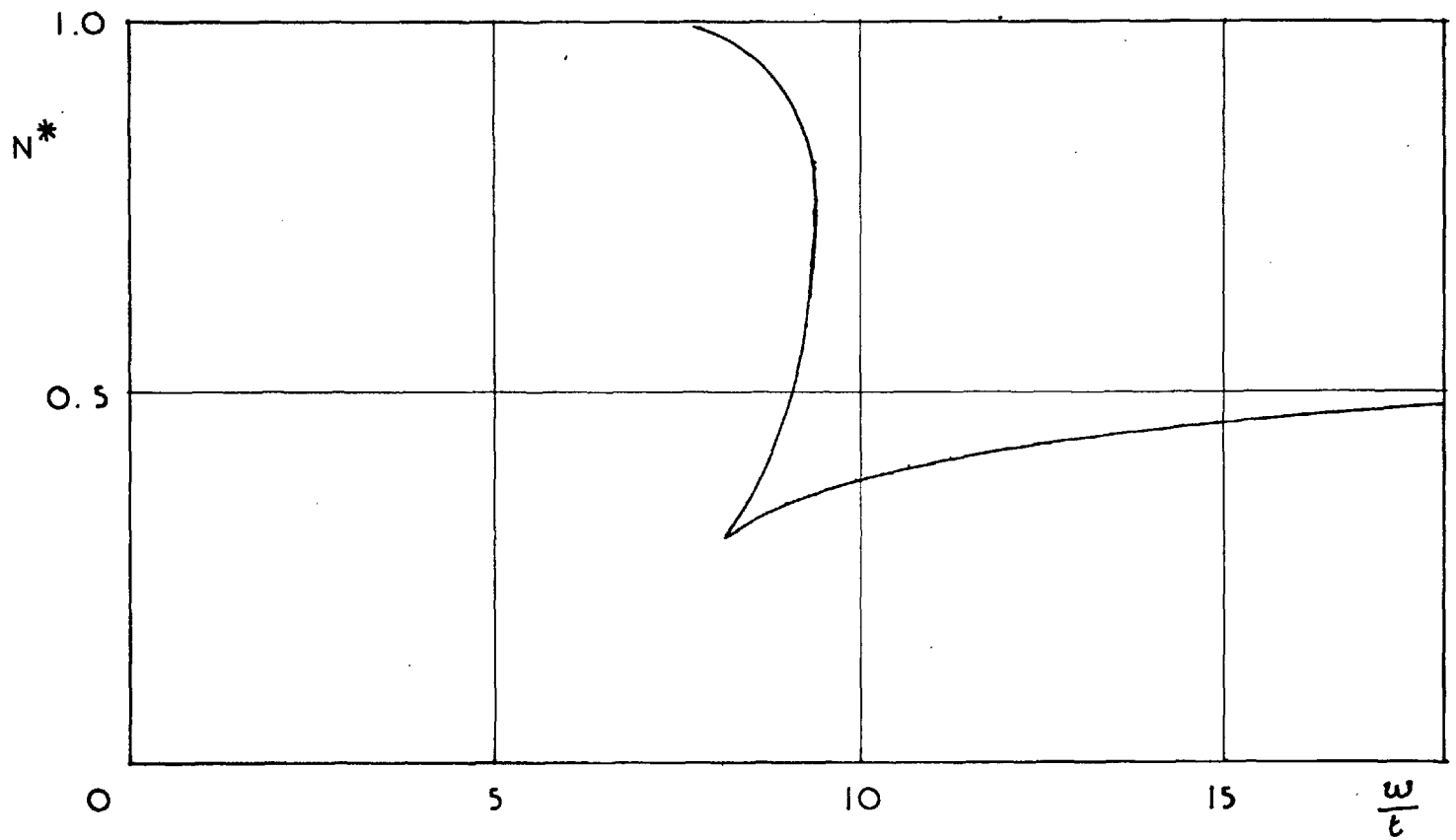


FIG. 8·9: VARIATION OF RADIAL DISPLACEMENT WITH STRESS

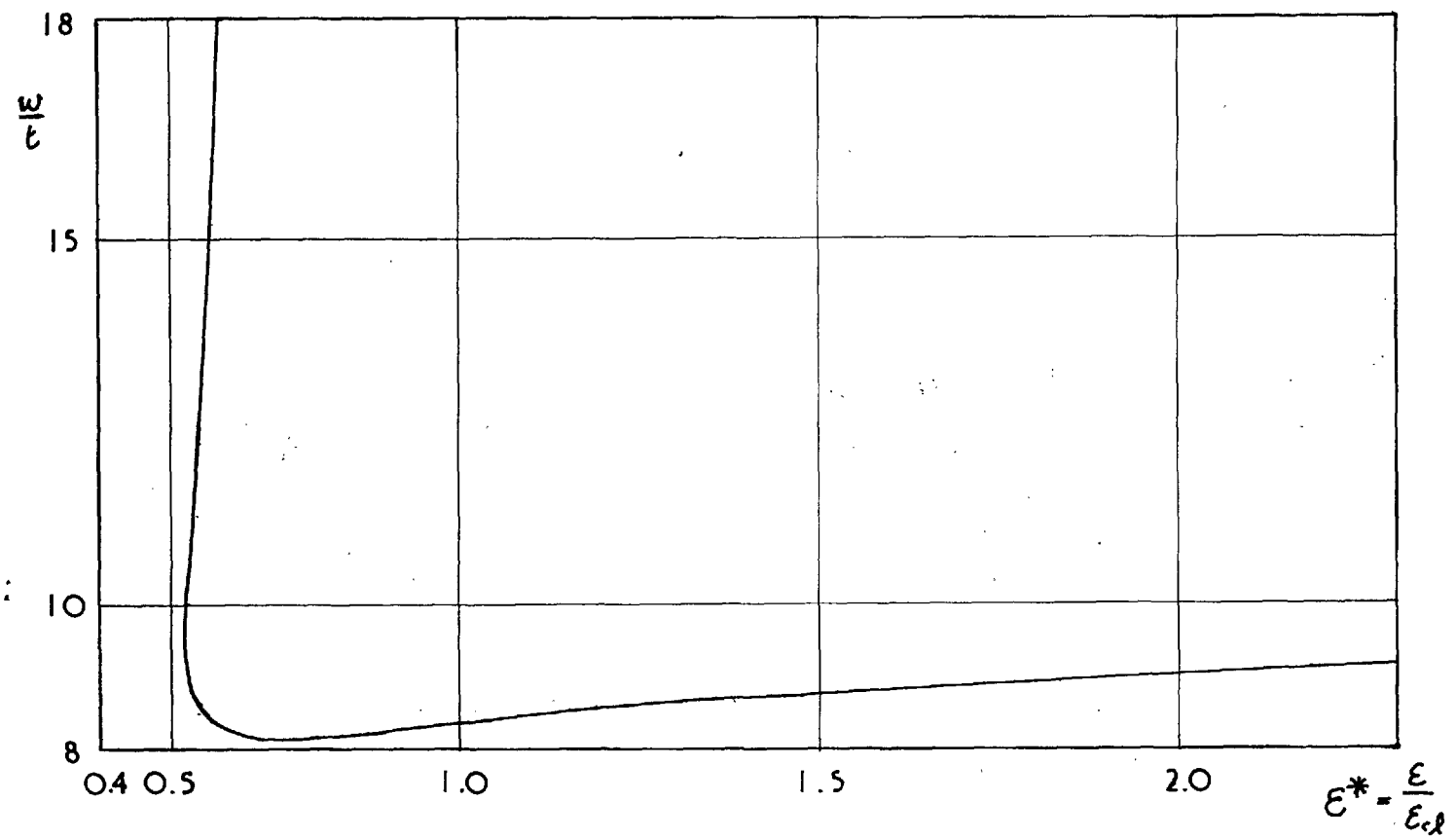


FIG. 8·10: VARIATION OF RADIAL DISPLACEMENT WITH END - SHORTENING.

Fletcher-Powell method, it was found that the sets of values generated by that method were useful for initial data for the Newton-Raphson method. Kempner's data was also used. To begin with, all sets of data were used twice: in one case with the load as the constant parameter, and with μ, the ratio of the two half wavelengths kept constant in the other. In approximately half the trials, no convergence was achieved for the solution. When the method had obviously diverged to an unreal solution, the results were discarded. Otherwise the "solution" was taken as initial data, this time treating the other of the two parameters mentioned previously, being kept constant. In this way, the number of solutions that converged to the required accuracy were multiplied to enable the load-end shortening curve to be plotted as given by the solid line in Figures 8.4 to 8.5.

It is to be noted that the curve in the post-buckling region that rises from the point of minimum post-buckling stress reaching the value of the classical buckling stress, is the mathematical solution to the problem. Experimental results do not show this same rise of stress with increasing end-shortening.

The variation of total potential energy with load, is shown in Figure 8.6, while the variation of strain energy with the end-shortening is shown in Figure 8.7. Figure 8.8 shows the variation in the value of the five parameters as a function of the load. The variation in the deflection with variation in load, and in end-shortening, is shown

in Figures 8.9 and 8.10.

The load-end shortening curve obtained in the theoretical work agrees with that obtained by Kempner except in the region between say the point ($N^* = 0.494$, $\varepsilon^* = 0.575$) on the unstable branch and the point of minimum post-buckling stress. A large number of points on the curve were obtained for this part of the curve and these produced the smooth curve of Figure 8.4 as against Kempner's curve, which is also shown in Figure 8.4 .

A comparison of Kempner's results and the results of this theory, for the points of minimum post-buckling end-shortening and minimum post-buckling stress is:-

	Minimum post buckling end-shortening		Stress	
	N^*	ε^*	N^*	ε^*
Kempner	0.3560	0.5077	0.3002	0.6020
this thesis	0.36822	0.52365	0.30122	0.67330

In order to determine the minimum post-buckling stress more accurately, the computer programme should have been recast so that the stress resultant (N, but also referred to here as the "load") was replaced by the end-shortening. Attempts to find a solution for $N^* = 0.3002$, the minimum obtained by Kempner, always resulted in a failure of the method to converge, suggesting that this might be lower than the true minimum.

Difficulties were experienced in obtaining solutions for the unstable branch of the curve (Figure 8.4) for $\varepsilon^* > 0.50$, and for the unbuckled branch, the latter being of interest for an idea of the

strain and total potential energies. Almroth[2] and Sobey [161] had also reported difficulties in obtaining solutions for the unbuckled part of the curve. In an attempt to obtain convergence of the solutions in this part of the curve, the chapter in the computer programme where the elements of the Jacobian were evaluated by finite differences, was replaced by the corresponding analytic expressions. While this did not yield the expected convergence, it did prevent the wild divergence that could occur in one iteration using the Jacobian evaluated from finite differences. The values obtained for $N^* \approx 0.60$, and $N^* = 0.838$ do give some indication of the trend of the curves for the unstable branch, even though the accuracy is low.

When a reasonable number of sets of parameter values had been obtained an attempt was made to provide more solutions by interpolation between those already obtained. It was found that interpolation from a graph was not of sufficient accuracy for the method diverged in nearly every case. For values obtained by interpolation from the numerical results, convergence was achieved in almost every case.

8.8 Numerical Results - Other Cases

The other cases for which solutions were sought were the six, seven, and ten parameter cases as outlined in the theory of Chapter Seven.

For these, both the Fletcher-Powell and the Newton-Raphson method were used. For these cases as well, the Fletcher-Powell method failed to obtain a solution for even one case, after 45,000 computing

instructions (3 minutes' computing time on "Atlas"). When sets of parameter values that had been obtained as improved approximations by the Fletcher-Powell method were used as initial data in the Newton-Raphson method, no cases of convergence were obtained. As a result, no numerical values for these additional cases are reported here.

8.9 Discussion

Arising out of the numerical work for the five parameter case, there are several suggestions relating to the method of obtaining sufficient numerical results for this and similar problems. The suggestions relate to the generalised Newton-Raphson method as it appears to be the most useful of the three computer methods considered.

(a) Initially, a few points must be located on the stress-end shortening curve by trial and error. The Fletcher-Powell method could be of use here, to provide compatible sets of parameter values, which it can do quite rapidly, even when starting from a poor initial approximation. In order to economise on computing time, it would seem sufficient to programme the Fletcher-Powell method so that it stops after evaluating the function a certain number of times, instead of stopping only when a certain accuracy is reached.

(b) From these few points many others can be determined by altering one of the parameters slightly in each set of parameters. Then by using this perturbed set of parameters as an initial set of data, with the perturbed parameter being taken as the constant parameter,

further solutions can be generated. The load appears to be the best parameter for perturbing, since perturbations with respect to it cause the least disturbance to the other parameters.

(c) Interpolation between the numerical values for a few points can also be used to extend the number of solutions. Graphical interpolation is not accurate enough.

(d) The particular computer programme used for the Newton-Raphson method of solution was not able to obtain solutions corresponding to part of the unstable branch of the curve. The use of analytic expressions for the Jacobian matrix may be sufficient to obtain convergent solutions for the five parameter case, but this will be an unsatisfactory method when the number of parameters is much greater than five. Then, either double-length arithmetic as used by Almroth [2] or the method used by Sobey [161], appear to be the only means of obtaining solutions for this part of the curve.

CHAPTER NINE

EXPERIMENTAL WORK

9.1 Introduction

The main details of the testing frame were decided upon after studying the few published descriptions of previous experimental work, and after taking into account the following considerations:-

1) the use of a screw-jack for applying the load would enable the end-shortening of the specimen to be controlled;

2) the size of the test specimens was chosen to be 12" diameter and 18" in length, giving L/R = 3;

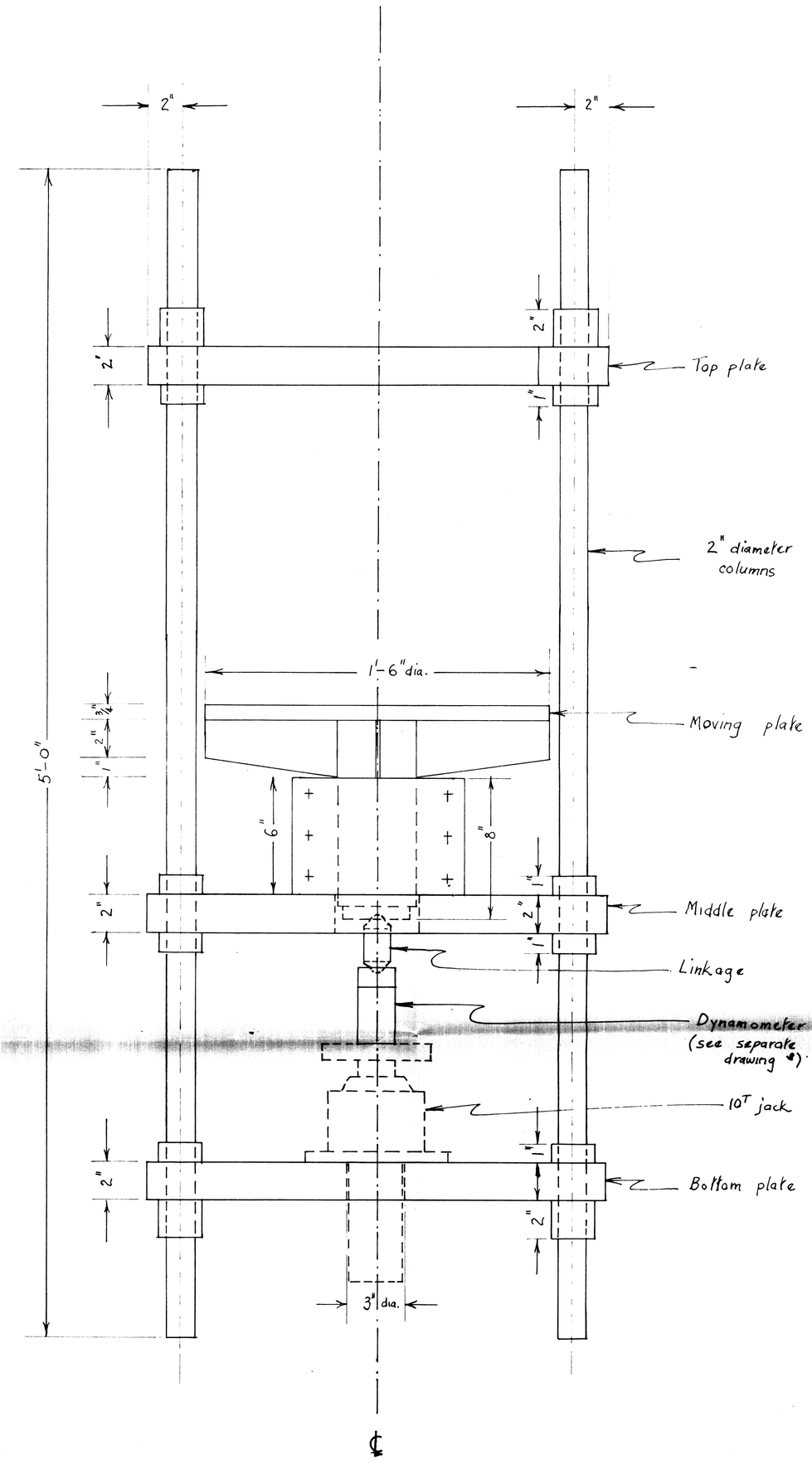
3) as it was intended to experiment with cylinders made from steel plate or shim with a welded seam, the range of likely wall thicknesses determined the load capacity of the frame and the screw-jack.

9.2 Testing Frame

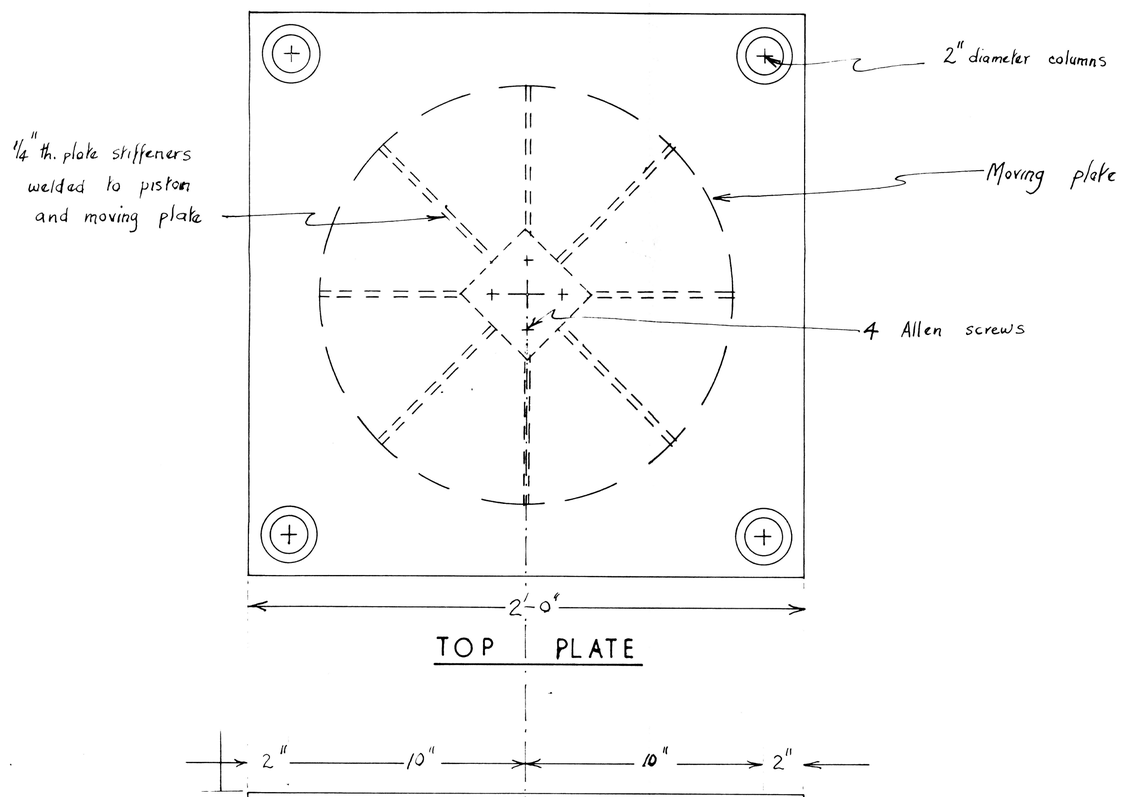
The details of the frame are shown in Figure 9.1 and Plate 9.1. The fabrication was carried out in the Departmental workshops.

The three horizontal plates were cut from 2" thick steel plate. The four 2" diameter steel columns were threaded for their whole length in order to permit the three plates to be adjusted to the required heights, and to permit their alignment into parallel planes. The thickness of the three plates and the diameter of the columns were selected in order to minimise as much as possible the energy stored in the frame. This was necessary if full use was to be made of the screw-jack to carry out controlled-end-shortening tests on the cylindrical shell

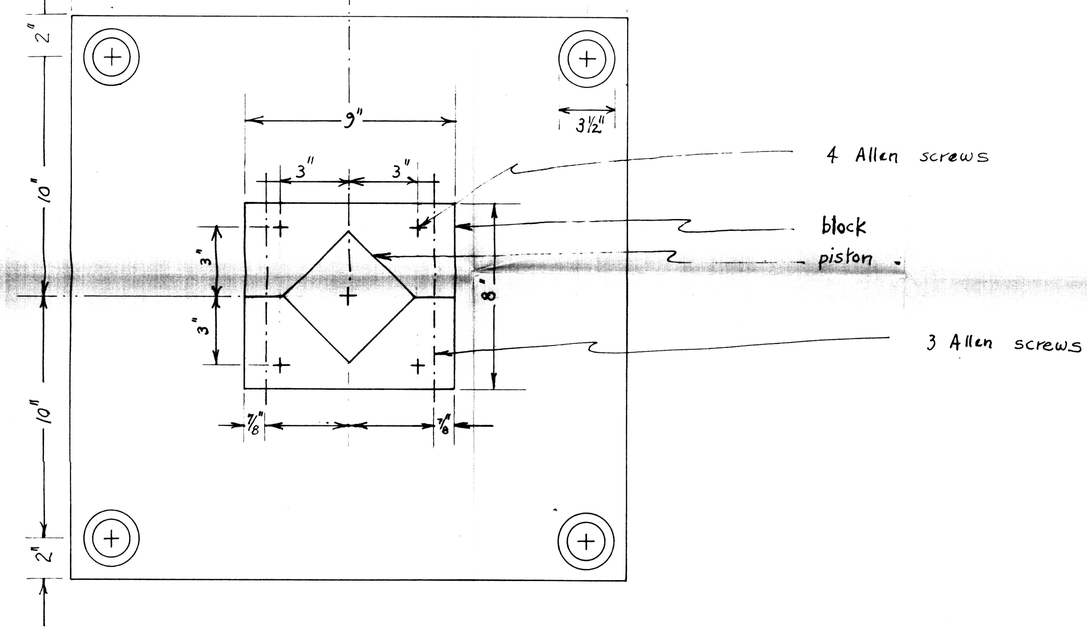
BOTTOM PLATE similar to top plate but with 3" diameter central hole.



ELEVATION



TOP PLATE



MIDDLE PLATE

SCALE : 3" = 1'-0"
i.e. 1/4 f.s.

FIG. 9.1 : DETAILS OF TESTING FRAME.

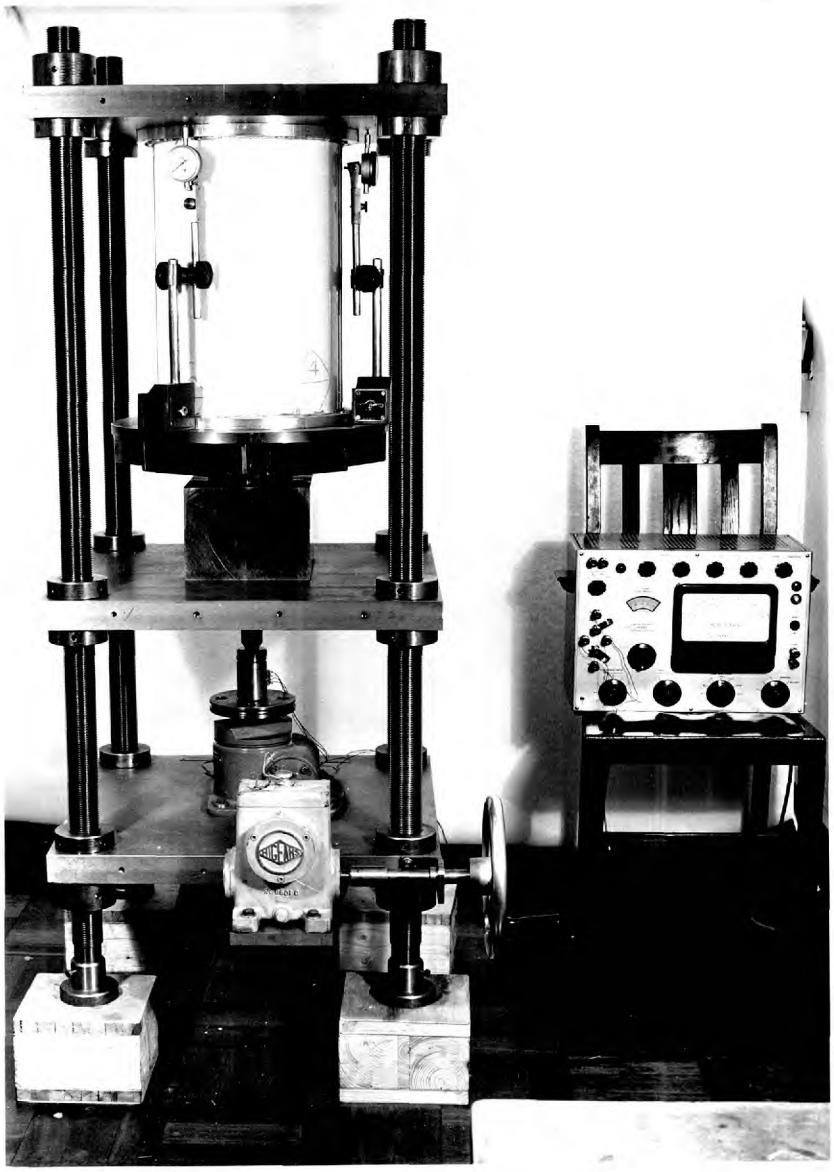


Plate 9.1. Testing Frame

Additional features that were incorporated into the frame include a block and piston arrangement, and a thrust linkage. The purpose of the former was to ensure that the thrust on the cylinder was axial, and to prevent tilting of the moving plate. The thrust linkage transferred the thrust from the screwjack to the piston, and could accommodate any deviation between the thrust lines of the jack and the piston.

In order to ensure that the block and piston would reduce any tilting of the moving plate to a minimum, the unit was made as in the following description. The piston itself was ground so that each face was smooth. The two halves of the block were then lapped and scraped until the piston just fitted. In the final assembly, the unit was packed with an anti-scuffing paste to prevent binding between the block and the piston. This paste also acted as a lubricant for the piston. From the dynamometer readings, it appeared that the friction in the block and piston was uniform - at least over the range of movement of the piston that was used in the tests reported later in this Chapter.

Screwjack

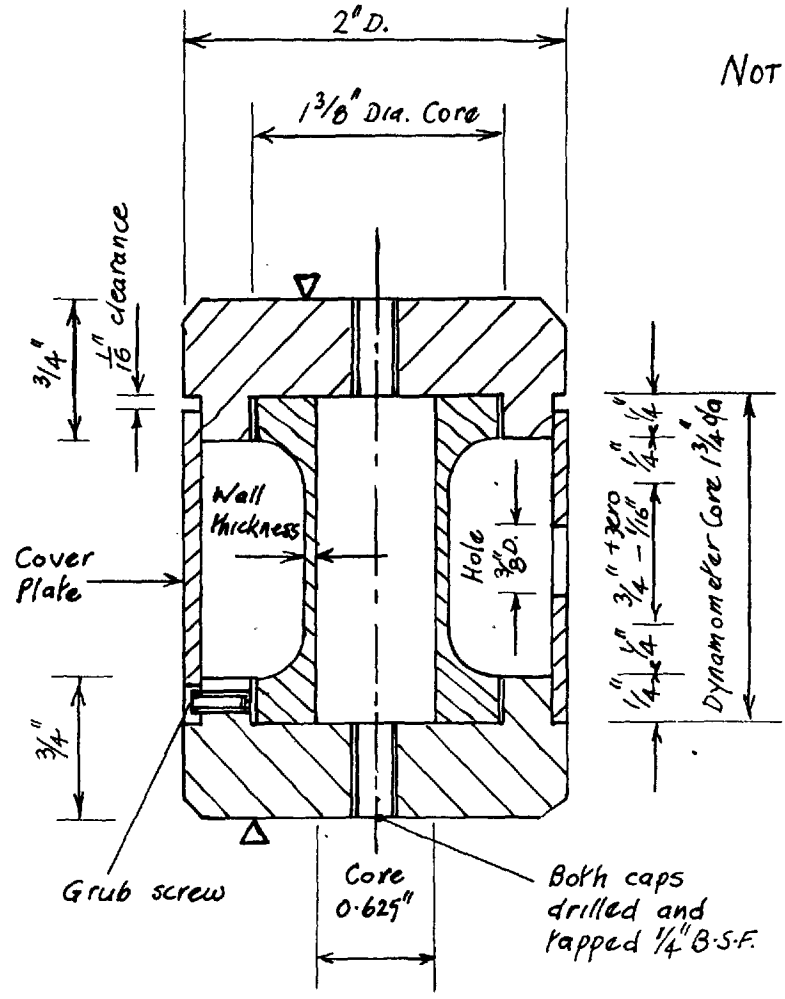
The jack that was used in conjunction with the test frame was a "Duff Norton" model 1810, rated at 10^{T} maximum load, and manufactured by Messrs. Consolidated Pneumatic Tool Co. Ltd. It had a maximum rise of 6", and was geared so that 48 turns of the drive shaft would raise the load one inch. A gearbox giving a 10 to 1 reduction gearing was connected to the main drive shaft of the jack. Thus one revolution

of the control handle corresponded to a 0.0025 in. rise of the load, and hence with this system it was possible to control the end-shortening of the specimen to 0.0001 in without difficulty, as measured on any one dial gauge. It was not possible to control the average end-shortening as given by the average reading of the three dial gauges, to this same accuracy, since variations of up to 0.0020" would occur between the three readings.

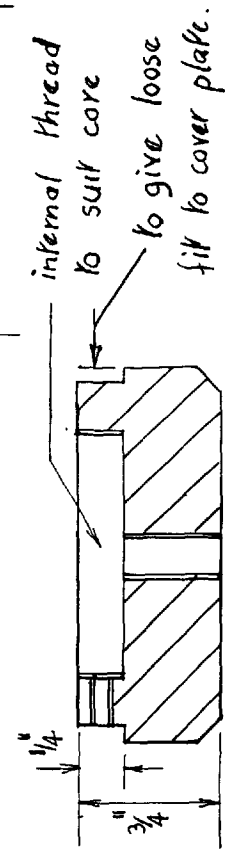
9.3 Dynamometers

Three dynamometers were made, to measure loads up to 5, 7.5 and 10 tons. The details of the dynamometers are shown in Figure 9.2 and Plate 9.2. Beryllium copper was used for the cores instead of the more usual duralumin, on account of its high elastic limit and its greater strain at the proportional limit. This latter property offered greater sensitivity for load determination. The cores could be easily machined prior to the heat treatment.

For the heat treatment of the cores, the recommendations of the manufacturer (Messrs. Johnson, Matthey and Co. Ltd.) were followed. This involved coating them in a refractory material, then heating for 2-1/2 hours at a temperature of 325° - 345°C, after which they were quenched in cold water. A pickle of hot sulphuric acid (one part of concentrated acid to four parts of water) was used to clean the surfaces of oxide scale produced during the heat treatment process. The cores were subsequently dipped into a chromic acid solution to give them a clean dry surface ready for taking the strain gauges.



SECTION THROUGH DYNAMOMETER ASSEMBLY



SECTION THROUGH END CAPS

DYNAMOMETER CORE Be. Cu.			END CAPS mild steel	COVER PLATE
Range Tons	Number required	Wall thickness	Number required	one cover plate with grub screw is required for each dynamometer
5·0	ONE	0·043"	ONE PAIR	
7·5	ONE	0·063"	ONE PAIR	
10·0	ONE	0·081"	ONE PAIR	

FIG. 9·2: DYNAMOMETER DETAILS.

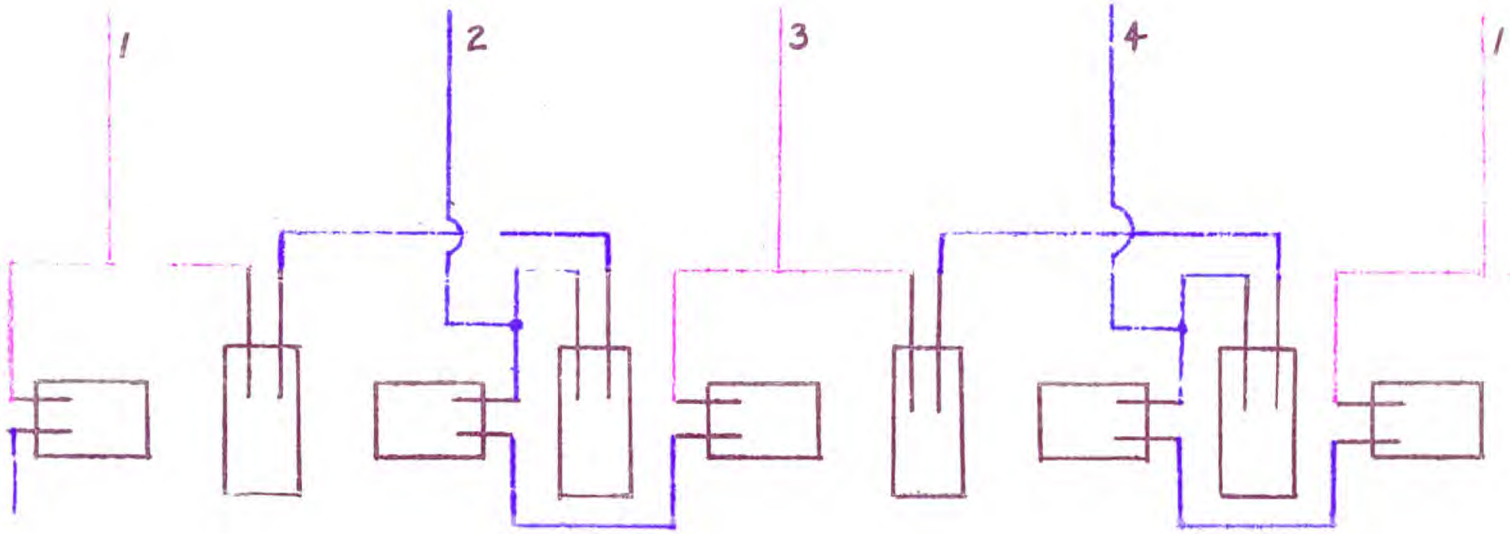
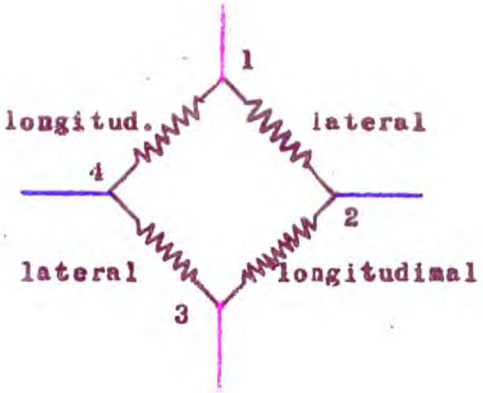


Fig. 9.3: Wiring diagram for 5T dynamometer to make four arm bridge.



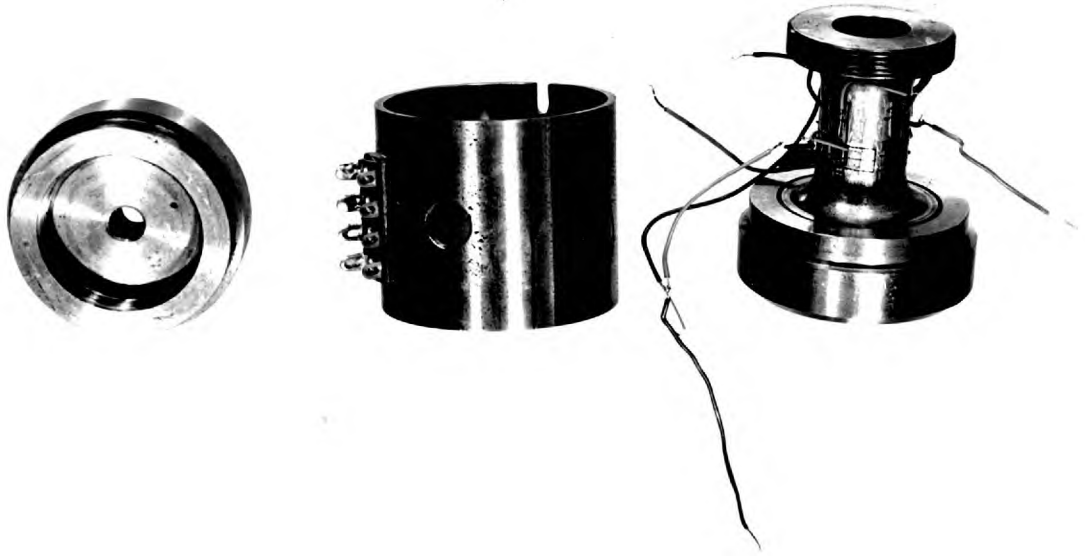


Plate 9.2. 5^{T}. Dynamometer.

The dynamometer cores had been designed to take eight strain gauges, i.e. four in each of the longitudinal and circumferential directions. This meant that opposite pairs of gauges could be connected together to form one arm of a Wheatstone bridge circuit. However, on the 5^T dynamometer this did not prove entirely satisfactory since it was difficult to make the connections in the restricted space, and the wiring arrangement of Figure 9.3 was adopted for the other two dynamometers.

The strain gauges used were of the resistance type and made by Messrs. Tokyo Sokki Kenkyijo Co. Ltd. They had a gauge length of 5 mm, a resistance of 120 $\pm$.3 ohm, and a gauge factor of 2.03. Small perspex clamps were used to hold the strain gauges in place while the adhesive (P-2: made by the manufacturers of the strain gauges) set. The setting time of the adhesive was about twenty minutes, but the gauges were left clamped for 1-1/2 hours.

After checking the stability of the dynamometers using a 10^T Buckton testing machine, they were then calibrated in the testing frame against a prooving ring. It was necessary to calibrate the dynamometer again when in the testing frame itself in order that the friction in the piston could be taken into account. Several calibration runs were carried out at different times and the resulting calibration curves were the same in each case. From this it appeared that the friction in the piston remained constant throughout the duration of the tests.

9.4 Cylinders

Originally it had been intended to experiment first with steel cylinders, and then with cylinders of other materials. Since it proved difficult to manufacture reliable cylinders from metal, however, the tests were carried out on cylinders made from plastic. A description of the types of cylinders made, together with some comment on the success of manufacture, is given in subsequent paragraphs.

1) Steel

Only one cylinder was made, with dimensions 12" diameter, 18" long and 0.035" wall thickness. This cylinder was arc welded along the seam (the wall thickness being the minimum that could be welded). However, the wall thickness was not thin enough and the cylinder buckled plastically.

2) Aluminium

These were turned in a lathe from extruded tubing that was of 9-3/4" internal diameter, and 1/8" wall thickness. In this way it was possible to produce cylinders of different wall thicknesses, ranging from 0.030" down to 0.010". Unfortunately the resulting cylinders were not reliable on account of variations of up to 0.005" in the wall thickness. This variation was due to the fact that initially the extruded tubing was some 0.005" out-of-round and the wooden mandril used during the turning-down process was unable to pull the tubing back into an exactly circular shape.

3) Plastics

Those used were "Flovic" and "Darvic", both manufactured by Messrs. Imperial Chemical Industries Ltd., and used in sheet form. They are manufactured from polyvinyl chloride (PVC) plastics.

(a) Flovic

Two layers of 0.010" nominal thickness were bonded together using a rubber based cement, to form a cylinder of 12" diameter, 18" long and of 0.020" nominal thickness.

The cement would not spread evenly and the resulting cylinders were of very poor shape. The thicker patches of cement tended to soften the Flovic locally and bulges in the cylinder resulted. For this reason - as well as for the effect of the end conditions, as described later - the experimental results for these cylinders were discarded.

(b) Darvic

This was used in two thicknesses - 0.020" and 1/32" - from which it was possible to make cylinders of three thicknesses, i.e. 0.020" and 1/32" from single thicknesses, and 0.040" from two layers of 0.020" material cemented together. Again, difficulties were encountered in cementing two layers together, and no satisfactory cylinders of 0.040" thickness were produced.

The 0.020" and 1/32" thick cylinders were formed with a 1" lap joint in the case of the first set of cylinders (white Darvic) and with a 1/2" lap joint for the second set (grey Darvic).

The cement used for joining the Darvic sheet was "Tensol 50", also made by Messrs. Imperial Chemical Industires Ltd., being a special cement

for bonding Darvic to itself. On account of the quick drying time of the cement compared with the time needed to spread the cement and then clamp the sheet on to the steel former, it was necessary to thin the cement with up to an equal amount of hexachloronone to increase the drying time.

9.5 Method of Testing

Aluminium end caps were used to hold the cylinders to the correct shape and to transfer the load from the testing machine to the cylinder. They consisted of 14" diameter circular discs cut from 3/4" plate and had two circular grooves cut in them, both 1/4" wide and 1/4" deep. These were machined in, and had inside diameters of 12" and of 9-3/4". It was thus possible to slip the ends of the cylinder into the grooves in each end plate and fill the groove with a sealing compound to hold the cylinder in place.

For the first series of tests, a low-temperature melting point alloy sold under the trade name "Cerrobend", was used. This material, on account of its low melting point, was easy to melt, set quickly when poured into the groove, and did not soften the plastic. It did not bond on to the Darvic, and its slight shrinkage on cooling caused it to draw away slightly from the cylinder.

For the second series of tests, two different adhesives were used. One was "Certite", and the other was "Araldite", manufactured by Messrs. Stuart B. Dickens Ltd., and by Messrs. CIBA (A.R.L.) Ltd., respectively. Certite did not bond to the Darvic, nor did it flow as readily as the Araldite. Its hardening time was about 20 minutes from

the time of mixing the two components. Araldite had the property of bonding on to the Darvic, and the advantage of this is described in the next section. Its hardening time was about six hours.

Testing Procedure

Since there was the possibility of the anti-scuffing paste used in the block and piston setting slightly when left undisturbed for a period of time, the piston was worked up and down several times before testing, the same being done when calibrating the dynamometer. The piston was then raised to bring the cylinder just into contact with the top plate of the machine. This could be judged easily by means of the strain reading measured on the 5v "Peekel" strain recorder. The cylinder was then rotated until the top plate and the end cap of the cylinder were as near parallel as possible. (Unfortunately, it proved impossible to ever make these parallel in the first place). When this was achieved, the dial gauges were zeroed, and the cylinder was ready for testing.

Loading was carried out in stages that corresponded to increments of 200 divisions in the strain reading for the dynamometers in the case of the 0.03" cylinders, and 100 division increments for the 0.02" thick cylinders. This loading stage took about 10 seconds, and the whole cycle - loading, reading and recording of dynamometer strain reading and deflection - was kept to 30 seconds. The maximum load sustained by the cylinder could be easily noted since the Peekel strain recorder used could be adjusted to read accurately over the whole range of the scale. After the first buckle appeared, loading could not be carried out in fixed increments due to the irregular occurance of

further buckles - and also the fact that the cylinder would not sustain any large increase in the load carried. On unloading, the stages were at 10 - 20 division increments to begin with, since the end-shortening decreased without a corresponding large decrease in load. After the disappearance of all buckles, the cylinder was unloaded completely in the same increments as used for loading. The zero readings could never be checked since there was always a slight inelastic straining in the material.

9.6 Results

The experimental results for the "Darvic" cylinders are summarised in Tables 9.1 and 9.2. Some typical load-end shortening curves are presented in Figures 9.4 to 9.7. Figure 9.4 showing the results for test three on cylinder 3 (test 3/3) is plotted non-dimensionally and the theoretical curve (shown dotted) is indicated for comparison. In the post-buckling region the experimental results are lower than the theoretical results, but show a similar increase in load with increasing end-shortening. This is also shown in the results for test 3/8 (Figure 9.5).

The main feature that has been shown by this series of tests concerns the influence of the end conditions on the buckling of the cylinder. This is shown clearly in the tests on cylinder five, where first "Cerrobend" and later "Araldite" were used as end fixing materials. A comparison of the results for cylinders 4, 5 and G3 with those for cylinders 3, 5 and G4 shows that, as as mentioned in Section 9.5, the value of the

TABLE 9.1

EXPERIMENTAL DATA

Cylinder No.	Length inches	Radius inches	Thickness inches	End Shortening ε_{c1} inches	End Fixing Material
3	17.92	5.965	0.034	619×10^{-4}	Araldite
4	18.00	5.964	0.034	619×10^{-4}	Cerrobend
5	17.93	5.958	0.034	619×10^{-4}	Cerrobend Araldite
G1	17.92	5.946	0.022	402×10^{-4}	Araldite
G2	17.915	5.950	0.022	400×10^{-4}	Araldite
G3	17.94	5.955	0.032	584×10^{-4}	Certite
G4	17.86	5.952	0.034	617×10^{-4}	Araldite

For cylinder 5,

Tests 1 to 5 used "Cerrobend"

Tests 6 to 12 used "Araldite"

Test No.	E lb/in^2	P_{cl} lb	Buckling Load	Maximum Load P_{max} lb		$\varepsilon_{M.L.}$ 10^{-4}ins	Minimum P.B.load P_{MPL} lb		ε_{MPL} 10^{-4}ins	No. of Buckles
3/1	546,000	1400	maximum	1700	0.71	475	635	0.28	415	7 - d.r.
3/2	514,000	2260		1660	0.73	475	655	0.29	465	7 - n.c.d.r.
3/3	523,000	2300		1555	0.68	450	540	0.23	400	7 - d.r.
3/4	516,000	2270		1555	0.68	440	550	0.24	395	7 - d.r.
3/5[1]	517,000	2275		1530	0.67	440	540	0.23	405	7 - d.r.
3/6	522,000	2295		1440	0.63	420	730	0.32	325	7 n.c.d.r.
3/7	512,000	2250		1550	0.69	445	490	0.22	430	7 - d.r.
3/8	498,000	2190		1489	0.68	445	495	0.22	420	7 - d.r.
3/9	502,000	2210		1440	0.65	410	495	0.22	405	7 - d.r.
4/1	403,000	1775		885	0.50	370				
4/2	417,000	1830		920	0.50	340				
4/3	417,000	1830	760	885	0.49	357				
4/4	432,000	1900		885	0.47	328				
4/5	(-)	(-)	250	975	( )	450				
4/6	417,000	1830		1000	0.55	387				
4/7	421,000	1850		1050	0.57	405				
4/8	437,000	1920		1160	0.61	427				
5/1	326,000	1435	190	840	0.59	408				
5/2	387,000	1705	250	820	0.48	338				
5/3	422,000	1860	120	915	0.49	356				
5/4	422,000	1860		910	0.49	361				
5/5	422,000	1860		900	0.48	353				
5/6	475,000	2085	maximum	1615	0.77	489	760	0.36	518	6 - S.r.
5/7	455,000	2000	440	1300	0.65	480	610	0.30	444	6 - S.r.
5/8	475,000	2085	maximum	1350	0.65	426	590	0.28	311	S.r.
5/9	494,000	2170	maximum	1360	0.63	414	570	0.26	339	S.r.
5/10	470,000	2060	maximum	1200	0.58	383	615	0.30	334	S.r.
5/11	485,000	2130		1170	0.55	379	545	0.26	296	S.r.
5/12				1125		362	(405)		(685)	S.r.

TABLE 9.2 EXPERIMENTAL RESULTS

Test No.	E lb/in^2	P_{cl} lb	Buckling Load	Maximum Load P_{max} lb		$\varepsilon_{M.L.}$ 10^{-4}in.	Minimum P.B.load lb/in^2		ε_{MPL} 10^{-4}in.	No. of Buckles	
G1/1[1]	430,000	790	125	350	0.44	235	180	0.23	414		
G1/2	397,000	730	125	400	0.55	256	140	0.19	425		
G1/3	485,000	890	maximum	530	0.59	270	210	0.22			
G1/4	464,000	855		530	0.62	270	170	0.20	400		
G1/5	483,000	890		495	0.56	250	(90)[2]	(0.10)	680		
G1/6	388,000	715		400	0.56	245	165	0.23	320		
G2/1	372,000	685	(300)	455	0.67	280	145	0.21	475		
G2/2	380,000	700	(310)	435	0.67	270	115	0.16	425		
G2/3	364,000	670	315	475	0.71	290	145	0.22	485		
G2/4	445,000	815	(400)	530	0.65	290	145	0.18	285		
G2/5	425,000	780	(340)	470	0.60	265	140	0.18	305		
G2/6	460,000	845	(370)	530	0.63	280	140	0.17	295		
G2/7[1]	383,000	705		480	0.68	270	130	0.18	395		
G2/8	383,000	705	340	470	0.67	265	140	0.20	345		
G2/9	383,000	705	340	505	0.72	285	145	0.21	315		
G2/10	383,000	705	340	470	0.67	270	155	0.22	390		
G2/11	435,000	800	370	500	0.63	300	135	0.17	430		
G2/12	395,000	725	340	480	0.66	270	125	0.17	400		
G3/1[1]	336,000	1395		930	0.67	423	435	0.31	520	6	
G3/2	327,000	1360	350	880	0.64	473	325	0.24	475	6	d.r.
G3/3	302,000	1260	560	895	0.71	463	340	0.27	520	5	
G3/4	327,000	1360	470	835	0.61	465	320	0.23	640		n.c.d.r.
G3/5	286,000	1190	455	800	0.67	447	430	0.36			n.c.d.r.
G3/6	284,000	1180	500	760	0.64	460	285	0.24	805		n.c.d.r.
G3/7	265,000	1100	430	720	0.65	550	295	0.27	730	5	n.c.d.r.
G3/8	281,000	1170	560	685	0.59	455	245	0.21		5	n.c.d.r.

TABLE 9.2 continued

Test No.	E lb/in^2	P_{cl} lb	Buckling Load	Maximum Load P_{max} lb		$\varepsilon_{M.L.}$ 10^{-4}in.	Minimum P.B.load lb/in^2		ε_{MPL} 10^{-4}in.	No. of Buckles	
G4/1	445,000	1960	maximum	1230	0.63	415	385	0.20	370		d.r.
G4/2	450,000	1980		1145*	0.58	375	285	0.14	480		
G4/3	445,000	1960		1090*	0.56	365	290	0.15	540	6	d.r.
G4/4	450,000	1980		1160	0.59		430	0.22	600	6	d.r.
G4/5[1]	445,000	1960		1200	0.61					7	d.r.
G4/6	445,000	1960		1140	0.58	400	370	0.19	560	7	d.r.
G4/7	450,000	1980		1120	0.57		365	0.18	720		d.r.

TABLE 9.2 continued

* splice opening up

n.c.d.r. = not complete double ring of buckles

d.r. = double ring of buckles

s.r. = single ring of buckles

1 = air holes in cylinder

2 = minimum load obtained after forming the buckling pattern by prodding the cylinder

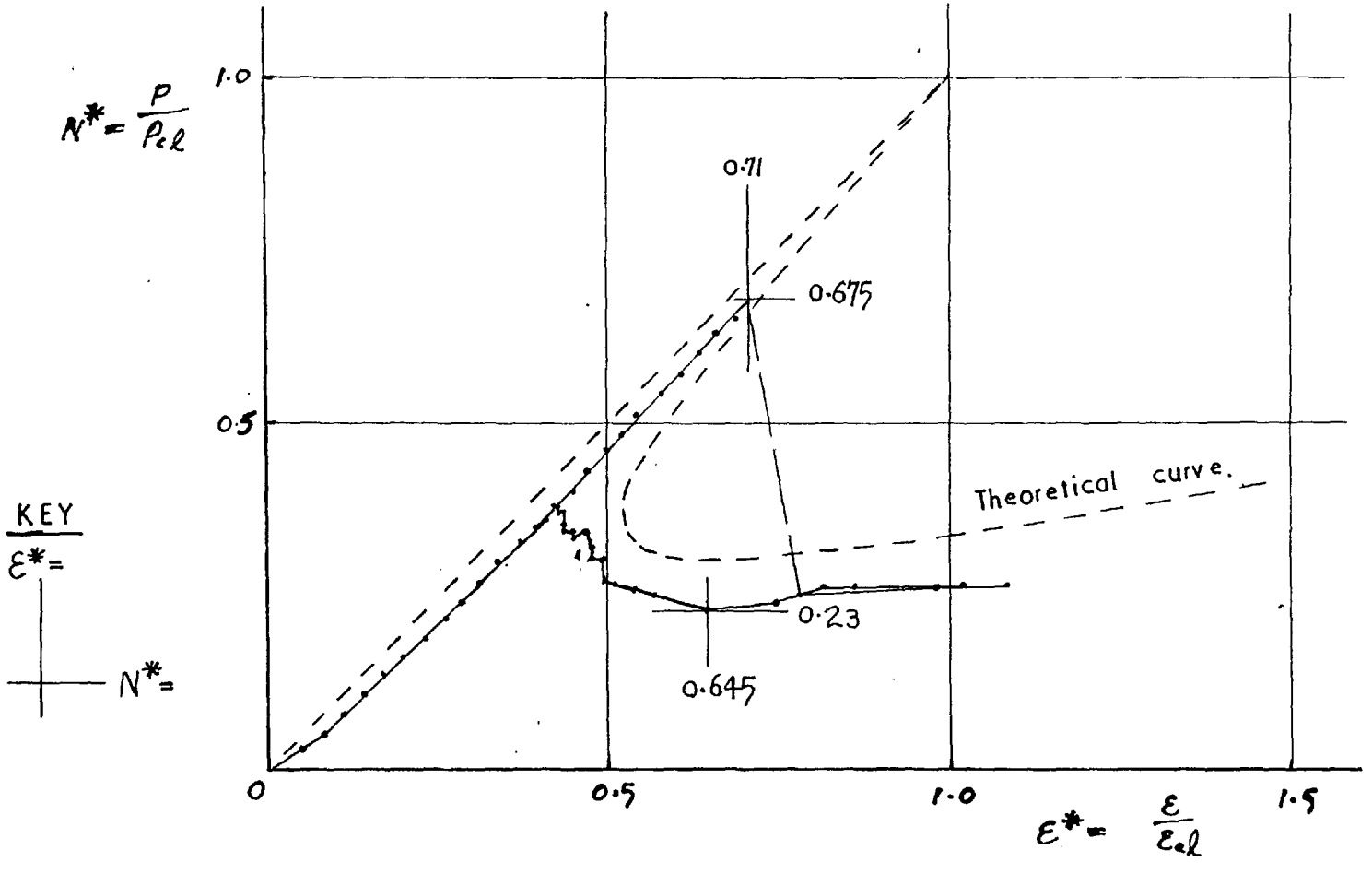


FIG. 9·4: RESULTS FOR TEST 3/3.

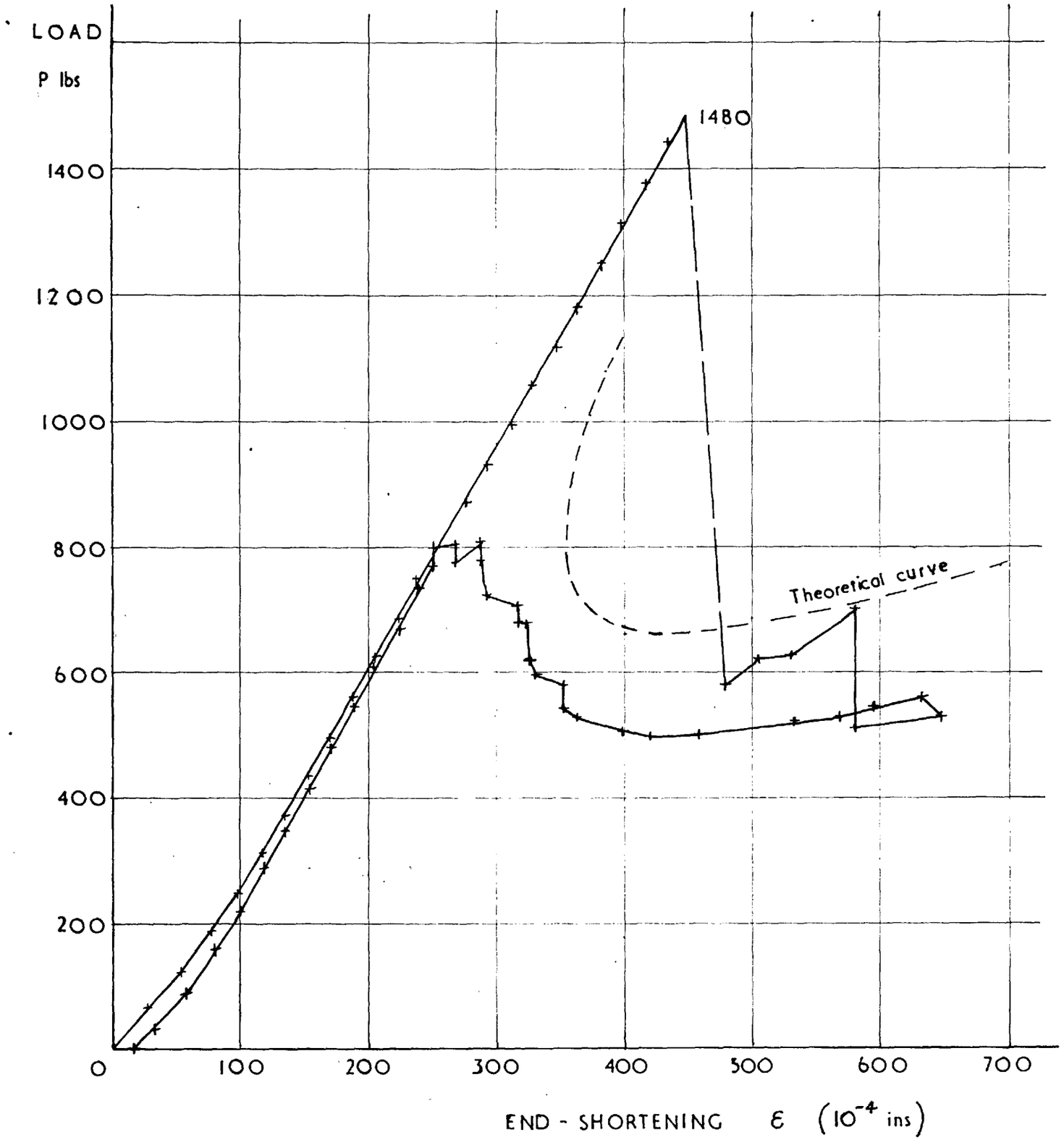


FIG. 9·5: EXPERIMENTAL RESULTS - CYLINDER 3, TEST 8.

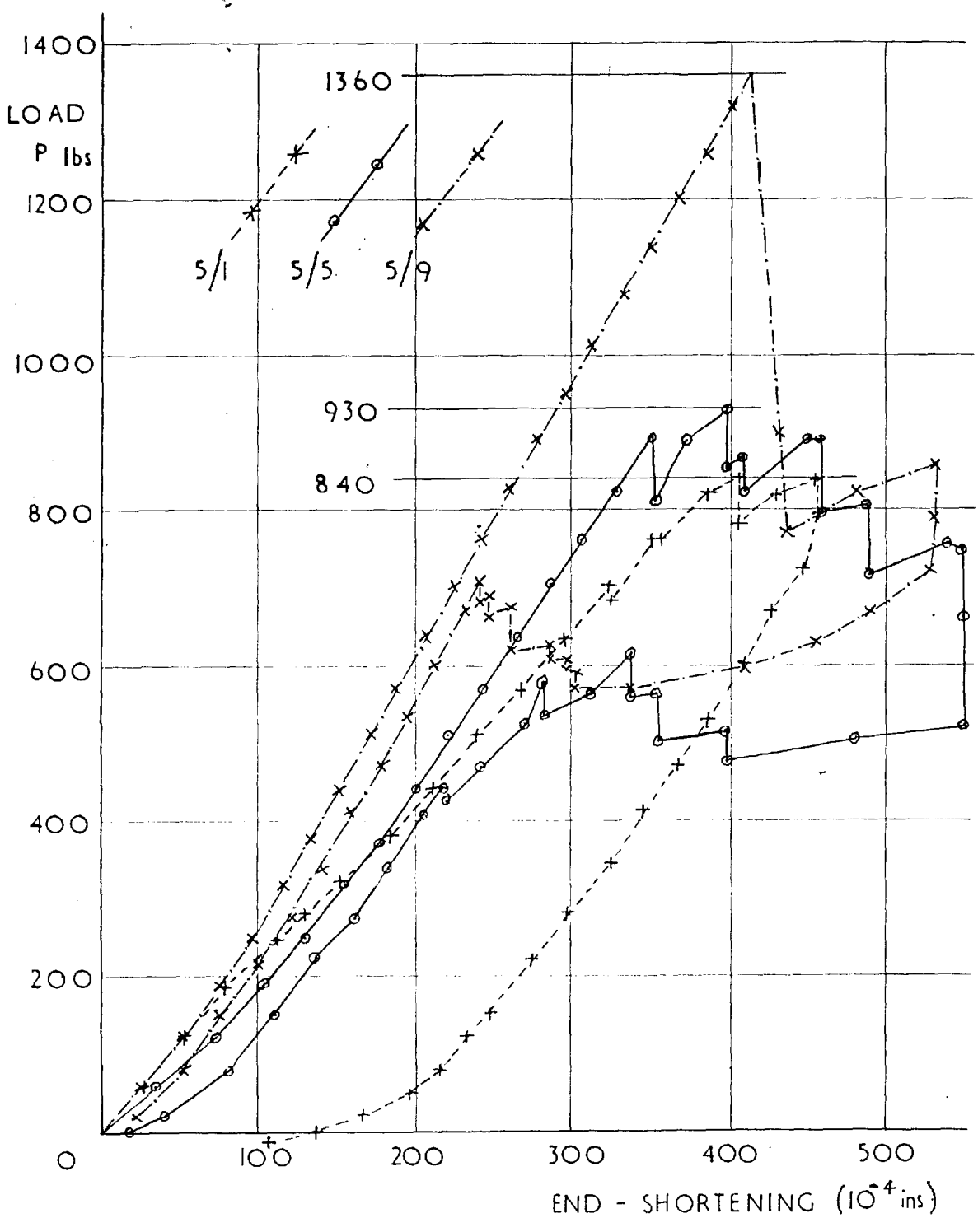


FIG. 9·6: EXPERIMENTAL RESULTS – CYLINDER 5

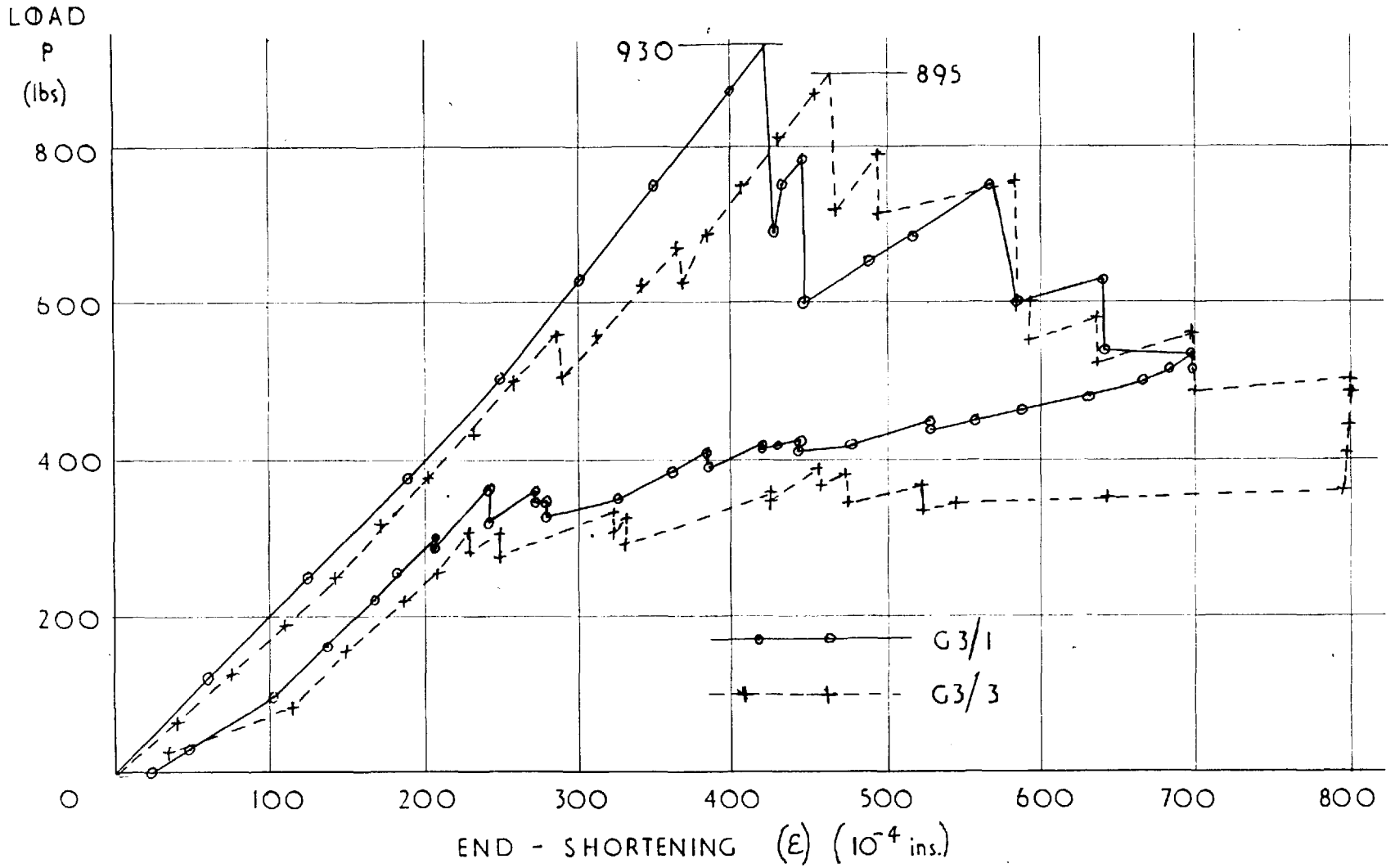


FIG. 9.7:
EXPERIMENTAL RESULTS - CYLINDER G3

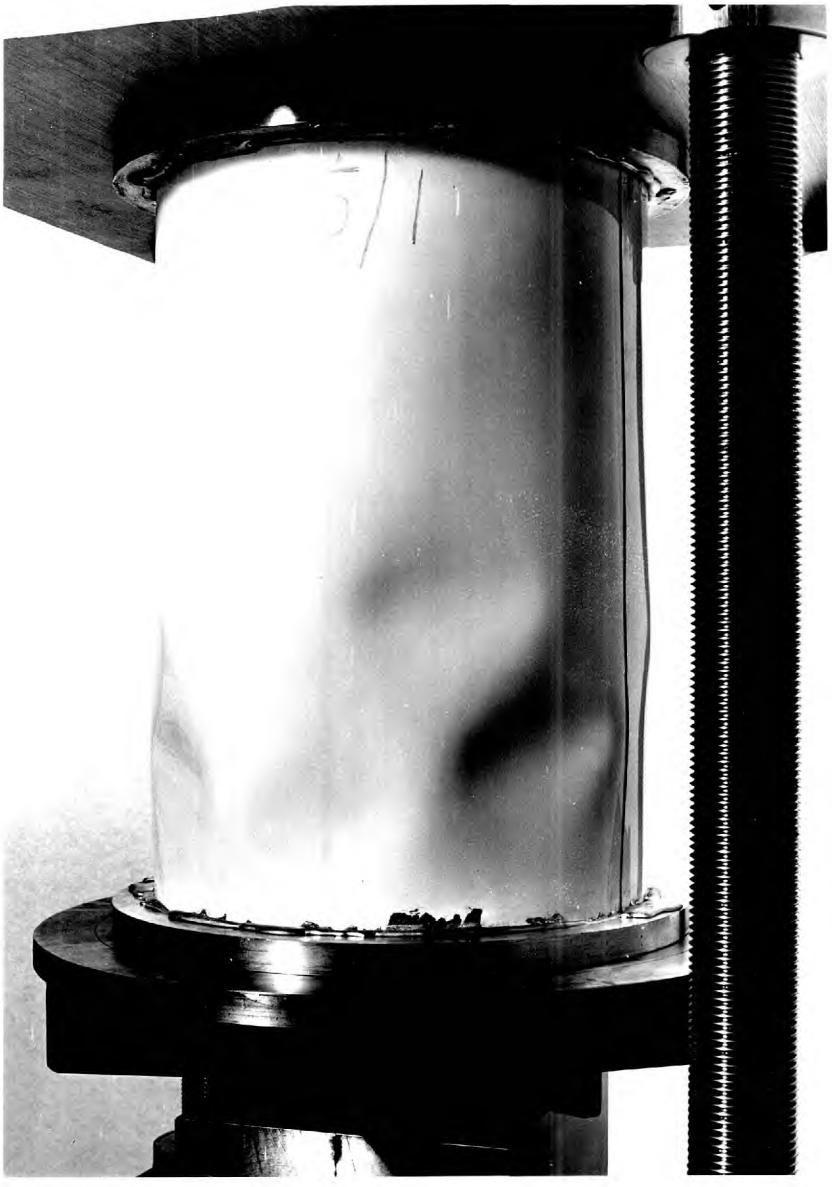


Plate 9.3. Buckle pattern - cylinder 5.



Plate 9.4. Buckle pattern - cylinder 9.



Plate 9.5. Buckle pattern - cylinder G4.

maximum load carried by the cylinder is influenced by the rigidity of the material used for holding it in the end plates. This is discussed further in the next section.

The maximum loads sustained by the cylinders were in the range 0.5 - 0.7 of the calculated classical buckling loads. The maximum loads sustained by each cylinder over the series of tests carried out on it, showed some variation.

Defining the buckling load as the load at which nonlinear displacements are initiated in the structure, it was found that some cylinders buckled at very low loads but continued to carry increasing load as the end-shortening was increased, until the maximum load was reached. (This neglects the initial nonlinearity that occurred in the initial stages of loading, caused by the end cap and the top plate of the machine not being parallel). After the maximum load has been reached, the load dropped suddenly and, while there might be further small increases in the load as the end-shortening was increased, the general trend was a reduction in the load-carrying capacity until a minimum was reached, usually at an end-shortening greater than that corresponding to the end-shortening for the classical buckling load of the cylinder. Not all the tests were carried out with the end-shortening becoming as great as (or greater than) the classical end-shortening value, but from those tests where it was, the minimum load carried by a cylinder at these large values of the end-shortening was approximately the same in all the tests on the same cylinder.

As the end-shortening of the cylinder was reduced, it was possible

in some tests to measure the minimum load carried by the cylinder while still fully buckled (see Figures 9.4 and 9.5). In these cases, the load would usually increase slightly again before the end-shortening had been reduced sufficiently to cause the buckles to snap out with a sudden increase in load. These minimum loads carried in the buckled state showed some scatter and were in the range 0.15 - 0.3 of the classical buckling load, though most of the results were close to 0.2 of the classical load. To some extent, the minimum post-buckling loads were dependent upon the development of the buckling process. When the buckles formed two complete rings, the minimum load was lower (in terms of the classical load) than when one complete and one partially complete ring were formed. For the case of only a single ring of buckles the minimum load would seem to be higher still.

The mimimum load carried in the buckled state, at approximately 0.2 of the classical load, is lower than the theoretical value of 0.301 obtained for the theory presented in this thesis. The shape of the experimental load-end shortening curve for the post-buckling region does resemble the shape of the theoretical curve.

The work of Thielemann [125] had suggested that even very small internal pressures might have a significant effect on the buckling of the cylinder. For this reason, small air holes were drilled in the cylinders for some tests. However, the tests did not show any significant effects that could be due to internal pressurisation, or lack of it.

However, the experimental curves did not go to sufficiently large values of end-shortening to check that the increase in load was as predicted by the theoretical curve. The minimum loads from these tests are higher than those reported by Thielemann [125] and by Almroth et al.[149], who obtained loads that were about 0.10 of the classical buckling load.

In the tests carried out, generally lower minimum post-buckling loads were obtained in the tests on the thinner cylinders (i.e. cylinders G1 and G2) than was the case for the thicker cylinders (i.e. cylinders 3, G3 and G4). This suggests that the thickness of the cylinder influences the buckling process. In these tests, the thinner cylinders were much more flexible than the thicker ones, and the end caps were not as effective in holding them to a circular shape. It is possible, that as has been observed in experiments on cylinders in torsion (see Figure 3.7) different materials do not buckle in an identical manner. This might explain the difference between the minimum post-buckling loads reported by Thielemann and by Almroth, and those of these thesis. Further tests on cylinders of different thicknesses and different materials would be desirable to check these suggestions.

9.7 Discussion

Previous experimental results appear to fall into two classes, for the case of controlled end-shortening of the cylinder. As mentioned in Section 3.4.2, the buckles that formed, appeared one by one around the surface of the cylinder, and their distribution was generally random to begin with. However, Almroth et al. [149] reported that for both controlled end-shortening and for deadweight loading, a ring of buckles formed around the cylinder at one value of the end-shortening.

In the tests reported in this thesis, both types of buckling were found to take place. Thecase of random, isolated buckling is illustrated by Plate 9.3. Here the individual buckles formed one after the other, with those near the bottom plate forming first. Plate 9.4 shows the way in which a 0.040" thick cylinder (not otherwise reported) buckled. (It should be noted that defects in manufacture have had an influence as well). The numbers on the buckles indicate the order in which they formed. The full lines indicate the size of the buckles when they first appeared, while the dotted lines show the extent of buckling at some later stage of loading. Buckling of this nature resulted when the cylinders were held to the end plates by means of "Cerrobend" or "Certite". For this type of end fixing, the maximum load was reached only after several buckles had formed around the cylinder. When "Araldite" was used as the end fixing material, then the buckling occurred suddenly with a very significant decrease in load, and took the form of a single or double ring of buckles within the central portion of the cylinder.

Only for this type of end fixing was it possible to measure the minimum post-buckling load as the end-shortening was reduced.

One difficulty in the tests occurred when setting the dial gauges to zero, at the beginning of each test. It proved impossible to fit the end plates on the cylinders so that both the end plates would be parallel to the plates of the machine (which had been set as nearly parallel to each other as possible). This meant that the cylinder was never loaded uniformly, and from the load-end shortening curves it appears that the results for the first few load stages were affected by this. In Figure 9.4 it can be seen that although the experimental results for the unbuckled cylinder do not follow the theoretical line as plotted, the slope of the line after the second load stage is very nearly the same as that of the theoretical results.

For each test, the value of the modulus of elasticity of the material was determined from the slope of the load-end shortening diagram. This method, however, only produced satisfactory results for those cases where Araldite was used as the end fixing material. The manufacturer's figure for the modulus of elasticity is 500,000 lb/in^2 approximately. From this, the average value for cylinder 3 of 517,000 lb/in^2 is somewhat high, while the average of 447,000 lb/in^2 for cylinder G4 is somewhat low. The justification for measuring the modulus of elasticity of the cylinder material in this way is that, as pointed out by the manufacturers [164] "Darvic" is a thermoplastic material whose mechanical properties are dependent on temperature, time, and strain. Consequently, since the cylinders: (i) were formed by bending from flat

sheet and may have undergone slight stretching while on the former; (ii) might undergo some inelastic straining during the buckling process; (iii) could not all be tested at the same controlled temperature; then it seemed preferable to measure the modulus of elasticity for each test from the load-end shortening diagram, rather than use the results from a standard test which may or may not relate to that of the actual cylinders. The values used for the comparison of the theoretical results are therefore more properly referred to as the "apparent" modulus of elasticity of the Darvic. Had a figure of 500,000 lb/in^2 been used throughout, then the maximum loads measured would have been lower and shown a much greater scattering when compared to the classical buckling load.

CHAPTER TEN

DISCUSSION AND CONCLUSIONS

10.1 Discussion

10.1.1 Experimental Work

From the tests carried out, it was found that the end conditions of the cylinder have a considerable influence on the development of the buckling process for the cylinder. When the cylinder ends were held rigidly (i.e. by "Araldite"), the buckles usually snapped in at least a single ring, though sometimes a double ring. For those cases where the end fixing was less rigid (i.e. "Cerrobend" or "Certite"), then the buckles formed singly and at random over the surface. The only reference in the literature to the influence of end conditions on the buckling process, is that of Kanemitsu and Nojima [156] who appear to have found that the end effects have no influence providing that $L > 1.5\ R$. For the tests reported in this thesis, $L = 3\ R$, and end conditions appeared to be quite important.

In the tests, there was difficulty in applying the loads uniformly around the circumference of the cylinder, since it was not possible to make the top plate of the frame and the end cap of the cylinder, actually parallel.

In order to provide more uniform end conditions than was possible in the tests reported here, and also to help in providing a more uniform loading distribution, it would be preferable to use end caps similar to those used by Almroth et al. [149]. With the centre

(detachable) portion being made a push fit on to each cylinder, all cylinders tested can be held as rigidly as is possible. If the groove between the centre portion of the cap and the remainder is filled with "Araldite", then the cylinder ends should be completely fixed. With a 1-1/2" - 2" thick end cap, it should then be reasonable to load the cylinder through a ball seating. Since a new centre portion for the end cap will be required for each cylinder, it would seem preferable to reduce the size of the cylinders to a diameter of between 6" and 9", with the length reduced accordingly.

10.1.2 Theoretical Work

The theoretical solution of this thesis is not completely identical with that of Kempner (see Figures 8.4, 8.5). The cause of this discrepancy is not obvious, though it may be due to the two different methods used for evaluating the solutions (see Chapter 8). The numerical solutions of this thesis were such that the residuals of the five nonlinear simultaneous equations were reduced to less than 1×10^{-10} but Kempner gives no indication as to the possible accuracy of his solutions. Many more solutions were obtained for this region than are given in Table 8.1, and they all confirm the indicated curve.

The curve showing the changes of total potential energy (Figure 8.6) has the same general trend as that given by Almroth [2] for the same displacement function.

The work of Almroth and of Sobey in obtaining solutions using displacement functions with more than five parameters in them, is no

mean achievement. However, while these solutions yield minimum post-buckling load than is in closer agreement with Thielemann's [125] and Almroth et al's[149] experimental minimum (0.10 Pcl) it is then much lower than the experimental minimum (0.20 Pcl) indicated by the tests reported in this thesis. Also, Sobey indicates the contours of the deflected cylindrical surface, for a load corresponding to the point of minimum post-buckling strain. These contours resemble a chequerboard pattern and not the observed diamond pattern of the buckled cylinder, and suggest that the mathematical solution using large numbers of parameters does not correspond to the physics of the problem. It has also been pointed out that Almroth's eleven parameter solution does not correspond to a diamond-pattern of buckling, either. Hence the complete solution to the buckling of cylindrical shells is not to be achieved solely by considering more and more parameters in the deflection function. Instead, work needs to be carried out using a more general function than used to date, which will satisfy boundary conditions for a cylinder of finite length, and which can treat mathematically a single or a double ring of buckling around the surface.

Sobey has expressed the opinion that the Fletcher-Powell method for obtaining a numerical solution has advantages over the other methods, and particularly the advantage that once a solution has been obtained for one case it can make use of information stored for this case as the starting point for the solution at a nearby point. This would enable all the information required to plot the load-end shortening curve to

be comuted at one time. This may be an advantage when sufficient computer time is available to enable the solution to be obtained for the first case, but when only limited computer time is available in each run, then the method is limited in use. In these latter conditions, the Newton-Raphson method is to be preferred even though many solutions may fail to converge.

10.2 Conclusions

1) The experimental results showed that for "Darvic" cylinders made as described, and tested with the ends held rigidly, the buckling loads were generally in the range 0.5 - 0.7 of the classical buckling load, while the minimum load carried in the buckled state was approximately 0.20 of the classical buckling load in each case.

2) The theoretical solution using the five parameter displacement function of this thesis, predicts the trend of the experimental results over a range of load and end-shortening near the point of minimum load for the buckled cylinder. There is, however, a discrepancy between the theoretically determined minimum load of 0.301 of the classical buckling load and the experimental value of approximately 0.20.

3) From the numerical solution for the five parameter displacement function, the generalised Newton-Raphson method proved to be the most useful method of solution.

REFERENCES

Abbreviations used are:-

A.F.O.S.R.	Air Force Office for Scientific Research
A.M.R.	Applied Mechanics Review
A.I.A.A.	American Institute for Aeronautics and Astronautics
B.A.R.C. R and M	British Aeronautical Research Committee Reports and Memoranda
G.A.L.C.I.T.	Guggenheim Aeronautical Laboratory, California Institute of Technology
I.A.S.S.	International Association for Shell Structures
I.U.T.A.M.	International Union of Theoretical and Applied Mechanics
N.A.C.A.	National Advisory Committee for Aeronautics
N.A.S.A.	National Aeronautics and Space Administration
N.A.S.A. T.M.	N.A.C.A. (N.A.S.A.) Technical Memoranda
N.A.S.A. T.N.	N.A.C.A. (N.A.S.A.) Technical Notes
P.M.M. (A.M.M.)	Prikladnaia Matematika i Mekhanika (Translated as: Applied Mathematics and Mechanics)
Proc. A.S.C.E.	Proceedings of American Society of Civil Engineers (New York)
Trans. A.S.M.E.	Transations of the American Society of Mechanical Engineers (New York)

(1) Almroth, B.O. "Buckling of orthotropic cylinders under axial compression" Rpt. LMSC-6-90-63-35, Lockheed Missiles and Space Company, June 1963.

(2) " "Post buckling behaviour of axially compressed circular cylinders" A.I.A.A. Journ. Vol.1, pp 630-3, 1963.

(3) Almroth, B.O. and Brush, D.O. "The buckling of axially loaded cylindrical shells" Rpt. LMSC-6-90-63-77, presented at Lockheed Missiles and Space Co. Conference on shell theory and analysis, August 21-23, 1963.

(4) Altshular, B. "Nonlinear buckling of a spherical shell" Thesis, New York University, 1953.

(5) Archer, R.R. "Stability limits for a clamped spherical shell segment under uniform pressure" Quart. Appl. Mech., V.15, p.355, 1958.

(6) Ar[illegible], A.E. and Herman[illegible], G. "Buckling of thin shells under external pressure" Proc.A.S.C.E., Vol.89, No.EM3, p.131, 1963.

(7) Batchelor, B. de V. "Stress distribution in some shells of negative Gaussian curvature, with particular reference to edge effects" Ph.D. Thesis, University of London, November 1963.

(8) Batdorf, S.B. "Simplified method of elastic stability analysis for thin cylindrical shells" N.A.C.A. T.N. 1341, 1947.

(9) Batdorf, S.B. "A simplified method of elastic stability analysis for thin cylindrical shells. pt. II - Modified equilibrium equation" N.A.C.A. T.N. 1342, 1947.

(10) Batdorf, S.B., Stein, M. and Schildcrout, M. (a) "The critical stress of thin walled cylinders in axial compression" N.A.C.A. T.N. 1343, 1947.

(b) "The critical stress of thin walled cylinders in torsion" N.A.C.A. T.N. 1344, 1947.

(c) "The critical combinations of torsion and direct axial stress for thin walled cylinders" N.A.C.A. T.N. 1345, 1947.

(11) Bijlaard, P.P. "The critical external pressure of conical shells that are simply supported at the edges" Bell Aircraft Coorp. Tech. Rpt. No.02-941-027, 1953.

(12) Booth, A.D. "Numerical methods" Butterworths, London, 1955.

(13) Bolotin, V.V. "Nonconservative problems of the theory of elastic stability" Pergamon Press, 1963.

(14) Bridget, F.J., Jerome, C.C. and Vosseller, A.B. "Some new experiments on the buckling of thin walled construction" Trans. A.S.M.E., Vol.56, pp 569-78, 1934.

(15) Bryan, G.H. "On the stability of elastic systems" Cambridge Phil. Soc., Vol.6, pp 199-210, 1888.

(16) Bryan, G.H. "On the stability of a plane plate under thrusts in its own plane, with applications to the 'buckling' of the sides of a ship" Lon. Maths. Soc. Vol.22, pp 54-67, 1891.

(17) Budiansky, B. "The buckling of clamped shallow spherical shells" Proc. I.U.T.A.M. symposium on the theory of thin elastic shells, Delft, p.64, North Holland Publishing Co., Amsterdam, 1960.

(18) Budiansky, B. and Hu, P. "The Lagrangian multiplier method of finding upper and lower limits to the critical stresses of clamped plates" N.A.C.A. T.N. 1103, 1946.

(19) Budiansky, B., Hu, P. and Conner, [illegible] "Notes on the Lagrangian multiplier method in elastic-stability analysis" N.A.C.A. T.N. 1558, 1948.

(20) Chaundy, T. "The differential calculus" Oxford University Press, Oxford, 1935.

(21) Chen, Wen, Liang "The effect of geometrical imperfections on the elastic buckling of thin shallow spherical shells" Thesis, Mass. Inst. of Techn. (M.I.T.) Dept. of Civil and Sanitary Engineering, January 1959.

(22) Crate, H., Batdorf, S.B. and Baab, G.W. "The effect of internal pressure on the buckling stress of thin-walled circular cylinders under torsion" N.A.C.A. W.R. L-67, 1944.

(23) Donnell, L.H. "The stability of thin walled tubes under torsion" N.A.C.A. Rpt. 479, 1933.

(24) Donnell, L.H. "A new bending theory for the buckling of thin cylinders under axial compression and bending" Trans. A.S.M.E., Vol. 56, pp 795-806, 1934.

(25) Donnell, L.H. "The effect of imperfections on the buckling of thin cylinders under external pressure" A pl. Mech. (A.S.M.E.) Vol. 23, pp 569-575, 1956.

(26) Donnell, L.H. "General shell displacement-strain relations" Lecture, Imperial College, 24th May, 1964.

(27) Donnell, L.H. and Wan, C.C. "The effect of imperfections on the buckling of thin cylinders and columns under axial compression" Appl. Mech. Vol. 17, pp 73-83, 1950.

(28) Elsgolc, L.E. "Calculus of Variations" Pergamon Press, London, 1961.

(29) Euler, L. "On the strength of columns" (1757) trans. in Am. J. Phys., p. 315, 1947.

(30) Evensen, D.A. "High speed photographic observation of the buckling of thin cylinders" Proc. Soc. for Exptl. Stress Anal. (Exptl. Mech.) Vol. 21, p. 110, 1964.

(31) Feodosiev, V.I. "On the stability of a spherical shell subjected to external pressure" P.M.M. (Leningrad) Vol. 18, p. 35, 1954.

(32) Feodosiev, V.I. "On a method of solution of the nonlinear problems of stability of deformable systems" P.M.M. (A.M.M.) Vol. 27, p. 392, 1963.

(33) Fletcher, R. and Powell, M.J.D. "A rapidly convergent descent method for minimisation" Computer Journal, Vol. 6, p. 163, 1963.

(34) Flügge, W. "Die stabilität der Kreiszylinderschale" Ing. Archiv, Vol. 3, pp 463-506, 1932.

(35) Forsythe, A.R. "Calculus of variations" Cambridge University Press, 1927.

(36) Fox, C. "An introduction to the calculus of variations" Oxford University Press, 1954.

(37) Friedrichs, K.O. "On the minimum buckling load for spherical shells" Theodore v. Karman Anniversary Volume, A.S.M.E., p. 258, 1941.

(38) Fung, Y.C. and Kaplan, A. "The buckling of low arches and curved beams of small curvature" N.A.C.A. T.N. 2840, 1952.

(39) Fung, Y.C. and Sechler, E.E. "The buckling of thin walled circular cylinders under axial compression and internal pressure" J. Aero. Sci., Vol. 24, pp 351-6, 1957.

(40) Fung, Y.C. and Sechler, E.E. "Instability of thin-elastic shells" 'Structural Mechanics' - Proc. 1st Symposium on Naval Structural mechanics (Pergamon), 1958.

(41) Gerard, G. "Introduction to structural stability theory" 1961.

(42) Gerard, G. and Becker, H. "Handbook of Structural Stability Pt. I - Buckling of flat plates" N.A.C.A. T.N. 3781, 1957.

(43) Gerard, G. and Becker, H. "Handbook of Structural Stability Pt. II - Buckling of composite elements" N.A.C.A. T.N. 3782, 1957.

(44) Gerard, G. and Becker, H. "Handbook of Structural Stability Pt. III - Buckling of curved plates and shells" N.A.C.A. T.N. 3783, 1957.

(45) Gjelsvik, A. and Bodner, S.R. "The energy criterion and snap buckling of arches" Proc. A.S.C.E., Vol. 88, No. EM5, pp 87-134, 1962.

(46) Gjelsvik, A. and Bodner, S.R. "Nonsymmetrical snap-buckling of spherical caps" Proc. A.S.C.E., Vol. 88, EM5, pp 135-165, 1962.

(47) Grigolyuk, E.I. "The stability of a closed double-layer conical shell under the action of a uniform normal pressure" Inz. Sborn. Akad. Nauk. SSSR, No. 19, p. 73, 1954. (trans. as D.W. Taylor Model Basin Transl. 265, March 1956)

(48) Grigolyuk, E.I. "Nonlinear vibrations and stability of shallow shells" Izvestia Akad. Nauk. SSSR, No. 3, pp 33-68, 1955 (trans. as Inst. of Eng. Research, Univ. of California, Berkeley, California, Appl. Mech. series 131, No. 7, January 1960)

(49) G.A.L.C.I.T. "Some investigations of the general instability of stiffened metal cylinders - Pt. I" N.A.C.A. T.N. 905, 1943.

(50) G.A.L.C.I.T. "Some investigations of the general instability of stiffened metal cylinders - Pt. IV" N.A.C.A. T.N. 908, 1943.

(51) Harris, L.A., Suer, H.S., Skene, W.T., and Benjamin, R.J. "The stability of thin walled unstiffened circular cylinders under axial compression including the effects of internal pressure" J. Aero. Sci., Vol. 24, p. 587, 1957.

(52) Harris, L.A., Suer, H.S. and Skene, W.T. "The effect of internal pressure on the buckling stress of thin walled circular cylinders under combined axial compression and torsion" J. Aero. Sci., Vol. 25, p. 142, 1958.

(53) Harris, L.A., Suer, H.S. and Skene, W.T. "Model investigations of unstiffened and stiffened circular cylinders" Experimental Mechanics, Vol. 1, pp 1-9, 1961. (Proc. Soc. Exptl. Stress Anal.)

(54) Ho, F.H. and Nash, W.O. "Dynamic buckling of spherical shells", presented at I.A.S.S. symposium on non-classical shell problems, Warsaw, 1963.

(55) Hoff, N.J. "Buckling and stability" J. Roy. Aero. Soc., Vol. 58, p. 3, 1954.

(56) Hoff, N.J. "Thin circular conical shells under arbitrary loads" J. Appl. Mech., Vol. 22, p. 557, 1955.

(57) Hoff, N.J. "The buckling of thin shells" A.F.O.S.R. T.N. 61-1422, 1961.

(58) Hoff, N.J. and Singer, J. "The buckling of circular conical shells under external pressure" Proc. I.U.T.A.M. symposium on the theory of thin elastic shells, Delft, Holland, pp 389-414, 1959.

(59) Homewood, R.H., Brine, A.C. and Johnson, A.E. "An experimental investigation of the buckling instability of monocoque shells" Proc. Soc. Exptl. Stress Anal., Vol. 18, p. 88, 1961.

(60) Hopkins, H.G. and Brown, E.H. "The effect of internal pressure on the initial buckling of thin walled circular cylinders under torsion" B.A.R.C. R. and M. 2423, 1951.

(61) Householder, A.S. "Principles of numerical analysis" McGraw-Hill, 1953.

(62) Humphreys, J.S. and Bodner, S.R. "Dynamic buckling of shallow shells under impulsive loading" Proc. A.S.C.E., Vol. 88, EM2, pp 17-36, 1962.

(63) Kantorovich, L.V. and Krylov, V.I. "Approximate methods of higher analysis" Noordhoff, Groningen, Holland, 1958.

(64) Kaplan, A. and Fung, Y.C. "A nonlinear theory of the bending and buckling of thin elastic shallow shells" N.A.C.A. T.N. 3212, 1954.

(65) Karman, T. and Tsien, H.S. "The buckling of spherical shells by external pressure" J. Aero. Sci., Vol. 7, pp 43-50, 1939.

(66) Karman, T. and Tsien, H.S. "The buckling of thin cylindrical shells under axial compression" J. Aero. Sci., Vol. 8, p.303-312, 1941.

(67) Keller, H.B. and Reiss, E.L. "Spherical cap snapping" J. Aero. Sci., Vol. 26, p. 643, 1959.

(68) Kempner, J. "Postbuckling behaviour of axially compressed circular cylindrical shells" J. Aero. Sci., Vol. 21, p. 329, 1954.

(69) Kempner, J. "Recent results in the theory of large deflections of cylindrical shells" Polytechnic Inst. of Brooklyn, PIBAL Rpt. 360, 1956.

(70) Kempner, J. "Stability equations for conical shells" J. Aero. Sci., Vol. 25, p. 137, 1958.

(71) Kempner, J., Pandalai, K.A., Patel, S.A. and Crouzet-Pascal, J. "Postbuckling behaviour of circular cylindrical shells under hydrostatic pressure" J. Aero. Sci., Vol. 24, p. 253, 1957.

(72) Kuranishi, M. and Niisawa, J. "An approach to the real buckling stress of thin cylindrical shells under axial compressive load" Proc. I.U.T.A.M. symposium on the theory of thin elastic shells, Delft, p. 189, 1959.

(73) Lackman, L. and Penzien, J. "The buckling of circular cones under axial compression" Trans. A.S.M.E. 81E (J. Appl. Mech.) pp 458-60, 1960.

(74) Langhaar, H.L. "A strain-energy expression for thin elastic shells" Trans. A.S.M.E. (J. Appl. Mech.) Vol. 71, pp 183-9, 1949.

(75) Langhaar, H.L. and Boresi, A.P. "Snapthrough and post buckling behaviour of cylindrical shells under the action of external pressure" Univ. Illinois Eng. Explt. Res. Station Bull. 443, 1957.

(76) Leggett, D.M.A. and Jones, R.P.N. "The behaviour of a cylindrical shell under axial compression when the buckling load has been exceeded" B.A.R.C. R. and M. 2190, 1942.

(77) Lo, H., Crate, H., and Schwartz, E.B. "The buckling of thin walled cylinders under axial compression and internal pressure" N.A.C.A. Rpt. 1027, 1951.

(78) Loo, T.T. "The effects of large deflections and imperfections on the elastic buckling of cylinders under torsion and axial compression" Proc. 2nd U.S. Nat. Cong. of Appl. Mech., A.S.M.E., New York, 1955.

(79) Lorenz, R. "Die nicht achenssymmetrische knickung dünnwandiger Hohlzylinder" Physikalische Zeitschrift, Vol. 13, p. 241, 1911.

(80) Lu, S.Y. and Nash, W.A. "Elastic instability of pressurised cylindrical shells under compression or bending" Proc. 4th U.S. Nat. Cong. Appl. Mech., 1962, A.S.M.E., p. 697, 1963.

(81) Lundquist, E.E. "Strength tests of thin walled Duralumin cylinders in compression" N.A.C.A. Rpt. 473, 1933.

(82) Lundquist, E.E. "Strength tests of thin walled Duralumin cylinders in torsion" N.A.C.A. T.N. 427, 1932.

(83) Michielson, H.F. "The behaviour of thin cylindrical shells after buckling under axial compression" J. Aero. Sci., Vol. 15, p. 738, 1948.

(84) v. Mises, R. "Der Kritische Aussendruck Zylindrische Rohre" V.D.I. Zeitschrift, Vol. 58, p. 750, 1914.

(85) Murray, F.J. and Wright, F.W. "The buckling of thin spherical shells" J. Aero, Sci., Vol. 28, p. 223, 1961.

(86) Mushtari, K.M. "On the theory of stability of a spherical shell subject to external pressure" P.M.M., Vol. 19, p. 251, 1955.

(87) Mushtari, K.M. and Sachenkov, A.V. "The stability of cylindrical and conical shells of circular cross-section subjected to simultaneous action of axial compression and normal external pressure" P.M.M., Vol. 18, pp 667-674, 1954. (also N.A.C.A. T.M. 1433, 1958)

(88) Mushtari, K.M. and Surkin, R.G. "On the nonlinear stability theory of elastic equilibrium of a thin spherical shell under the influence of a uniformly distributed normal external pressure" P.M.M., Vol. 14, p. 573, 1950.

(89) Nachbar, W. and Hoff, N.J. "The buckling of a free edge of an axially compressed circular cylindrical shell" Quart. of Appl. Maths., Vol. 20, p. 267, 1962.

(90) Nash, W.A. "The effect of large deflections and initial imperfections on the buckling of cylindrical shells subjected to hydrostatic pressure" J. Aero. Sci., Vol. 22, p. 264, 1955.

(91) Nash, W.A. "Buckling of initially imperfect cylindrical shells subject to torsion" J. Appl. Mech., Vol. 24, p. 12, 1957.

(92) Niordson, F.I.N. "The buckling of conical shells subjected to uniform external lateral pressure" Trans. Royal Inst. of Technology, Sweden, No. 10, 1947.

(93) Pflügger, A. "Stabilität dünner Kegelschalen" Ing. Arch., Vol. 8, p. 151, 1937.

(94) Poincaré, H. "Sur l'equilibre d'une masse fluide animée d'un mouvement de rotation" Acta Math. Vol. 7, pp 259-380, 1885.

(95) Prager, W. "The general variational principle of the theory of structural stability" Quart. Appl. Maths., Vol. 4, p. 378, 1947.

(96) Radkowsky, P.P. "Buckling of thin single and multi-layer conical and cylindrical shells with rotationally symmetric stresses" Proc. 3rd U.S. Nat. Cong. Appl. Mech., A.S.M.E., 1958.

(97) Reiss, E.L. "Axially symmetric buckling of shallow spherical shells under external pressure" J. Appl. Mech., Vol. 25, p. 556, 1958.

(98) Reiss, E.L., Greenberg, H.J. and Keller, H.B. "Nonlinear deflections of shallow spherical shells" J. Aero, Sci., Vol. 24, p. 533, 1957.

(99) Reissner, E. and Weinitschke, H.J. "Finite pure bending of circular cylindrical tubes" Quart. Appl. Maths., Vol. 20, p. 305, 1963.

(100) Ritz, W. "Über eine neue methode zur lösung gewisser variations probleme der mathematischen physik" J. Reine Angrew Math., Vol. 135, p.1, 1909.

(101) Robertson, A. "The strength of tubular struts" Proc. Roy. Soc. Lond. (Series A) Vol. 121, p. 558, 1925.

(102) Robertson, A. "The strength of tubular struts" B.A.R.C. R. and M. Tech. Rpts., Vol. 56, 1934.

(103) Rosenbrock, H.H. "An automatic method for finding the greatest or least value of a function" Computer Journ., Vol. 3, p. 175, 1960.

(104) Seide, P. "Axisymmetric buckling of circular cones under axial compression" J. Appl. Mech., Vol. 23, p. 625, 1956.

(105) Seide, P. "A Donnell type theory for the assymmetrical bending and buckling of thin conical shells" J. Appl. Mech., Vol. 24, p. 547, 1957.

(106) Seide, P. "A note on the stability equations for conical shells" J. Aero. Sci., Vol. 25, p. 342, 1958.

(107) Seide, P. "On the buckling of truncated conical shells under uniform hydrostatic pressure" Proc. I.U.T.A.M. symposium on theory of thin elastic shells, Delft, p. 363, 1959.

(108) Seide, P. "On the buckling of truncated conical shells in torsion" Trans. A.S.M.E., Vol. 84E (J. Appl. Mech., Vol. 2[illegible]) p. 321, 1962.

(109) Seide, P. "Calculations for the stability of thin conical frustrums subjected to external uniform hydrostatic pressure and axial load" J. Aero. Sci., Vol. 29, p. 951, 1962.

(110) Seide, P. "A survey of buckling theory and experiment for circular conical shells of constant thickness" N.A.C.A. T.N. D-1510, p. 401, 1962.

(111) Seide, P. "The stability of internally pressurised conical shells under axial compression" 4th U.S. Nat. Cong. Appl. Mech., 1962, A.S.M.E., 1963.

(112) Simons, R.M. "A power series solution of the nonlinear equations for the axisymmetric bending of shallow spherical shells" J. Maths. Phys., Vol. 35, p. 164, 1956.

(113) Singer, J. "Simplified equations for thin circular conical shells under arbitrary loads and arbitrary temperature distribution" Technion, Israel Inst. of Technology, Dept. of Aero. Eng., Rpt. 4, 1959.

(114) Singer, J. "The effect of axial constraint on the instability of thin circular cylindrical shells under external pressure" A.F.O.S.R. T.N. 60-165, 1959.

(115) Singer, J. and Eckstein, A. "An experimental investigation of the instability of conical shells under external pressure" Bull. Research Council, Israel, Vol. 11c, p. 97, 1962.

(116) Singer, J., Eckstein, A. and Baruch, M. "Recent experimental studies of the buckling conical shells under external pressure" Proc. 5th Israel Conf. on Aeronautics and Astronautics, Jerusalem Academic Press, 1963.

(117) Singer, J., Eckstein, A. and Baruch, M. "The buckling of conical shells under external pressure, torsion, and axial compression" A.F. 61(052)-339, 1962.

(118) Sokolnikoff, I.S. "The mathematical theory of elasticity" McGraw-Hill, 1956.

(119) Southwell, R.V. "The general theory of elastic stability" Phil. Trans. Roy. Soc. (Lond.) Series A, Vol. 213, p. 187, 1913.

(120) Southwell, R.V. "The collapse of tubes" Phil. Mag., May 1913, September 1913, January 1915.

(121) Sturm, R.G. "A study of the collapsing pressure of thin walled cylinders" Univ. of Illinois Eng. Exptl. Research Stn. Bull., 329, 1941.

(122) Suer, H.S., Harris, L.A., Skene, W.T. and Benjamin, R.J. "The bending stability of thin walled unstiffened circular cylinders including the effect of internal pressure" J. Aero. Sci., Vol. 25, p. 281, 1958.

(123) Surkin, R.G. "The problem of the loss of strength of a spherical shell subjected to an external evenly distributed pressure" Izvestia Kazan. Fil. Akad. Nauk., SSSR, Phys. ser., Vol. 10, p. 51, 1956.

(124) Taylor, C.E. "The elastic stability of a conical shell loaded by uniform external pressure" Proc. 3rd Midwestern Conf. on Solid Mech., Univ. of Michigan, p. 86, 1957.

(125) Thielemann, W. "New developments in the nonlinear theories of the buckling of thin cylindrical shells" Proc. Durand Centenial Conf., Stanford Univ., (ed. Hoff, N.J. and Vinecat,W.G.) 1959.

(126) Thompson, J.M.T. "Elastic buckling of thin spherical shells" Symposium on Nuclear Reactor Containment Buildings and Pressure Vessels, Glasgow, 1960. Butterworths, London, 1961.

(127) Thompson, J.M.T. "Basic principles in the general theory of elastic stability" J. Mech. Phys. Solids, Vol. 11, p. 13, 1963.

(128) Thurston, C.A. "A numerical solution of the non-linear equations for axisymmetric bending of shallow spherical shells" J. Appl. Mech., Vol. 28, p. 557, 1961.

(129) Timoshenko, S.P. and Gere, J.M. "Theory of elastic stability" McGraw-Hill, 1961.

(130) Tokugawa, T. "An approximate method for calculating the collapse pressure of thin cylindrical, conical, and spherical shells under uniform external pressure" Read before the Zösen Kyokai Ship-building Assn. of Japan, November 17th, 1940.

(131) Trefftz, E. "Konvergenz und Fehlerschätzung beim Ritzschen Verfahren" Math. Ann., Vol. 100, p. 503, 1928.

(132) Trefftz, E. "Zur theorie der Stabilität des elastischen Gleichgewichts" Z.A.M.M., Vol. 13, p. 160, 1933.

(133) Tsien, H.S. "The buckling of columns with non-linear supports" J. Aero. Sci., Vol. 9, p. 119, 1942.

(134) Tsien, H.S. "A theory for the buckling of thin shells" J. Aero. Sci., Vol. 10, p. 373, 1942.

(135) Tsien, H.S. "Lower building loads in the non-linear theory for thin shells" Quart. Appl. Maths., Vol. 3, p. 236, 1947.

(136) Volmir, A.S. "On the influence of initial imperfections on the stability of cylindrical shells under external pressure" Dokladi Akad. Nauk. SSSR (N.S.), Vol. 113, p. 291, 1957. (see also A.M.R. Vol. 11, 1948, review 3063)

(137) Volmir, A.S. "On the stability of dynamically loaded cylindrical shells" Soviet Physics Doklady, Vol. 3, p. 1287, 1958.

(138) Weingarten, V.I. "The effects of internal pressure on the buckling of circular cylindrical shells under bending" J. Aero. Sci., Vol. 29, p. 804, 1962.

(139) Weingarten, V.I. "The effect of internal pressure and axial tension on the buckling of cylindrical shells under torsion" 4th U.S. Nat. Cong. Appl. Mech., A.S.M.E., p. 827, 1963.

(140) Weinitschke, H. "On a stability problem for shallow spherical shells" J. Maths. Phys., Vol. 38, p. 209, 1960.

(141) v. Willich, G.P.R. "The elastic stability of thin spherical shells" Proc. A.S.C.E., Vol. 85, E.M.1., p. 51, 1959.

(142) Wilson, W.M. and Newmark, N.M. "The strength of thin cylindrical shells" Bull. 255, Univ. of Illinois, 1933.

(143) Windenburg, D.F. and Trilling, C. "The collapse by instability of thin cylindrical shells under external pressure" Trans. A.S.M.E., Vol. 56, p. 819, 1934.

(144) Yao, J.C. "The dynamics of elastic buckling of cylindrical shells" 4th U.S. Nat. Cong. Appl. Mech., 1962, A.S.M.E., p. 427, 1963.

(145) Yoshimura, Y. "On the mechanism of buckling of a circular cylindrical shell under axial compression" N.A.C.A. T.M., 1390, 1955.

(146) Yoshimura, Y. and Niisawa, J. "The lower buckling stress of circular cylindrical shells subjected to torsion" J. Aero. Sci., Vol. 24, p. 211, 1957.

(147) Yoshimura, Y. and Uemura, M. "The buckling of spherical shells due to external pressure" Rpt. Inst. Sci., Tokyo, Pt. I, Vol. 3, p. 316, 1949 Pt. II, Vol. 6, p. 367, 1952. Aero. Eng. Pt. III, Vol. 2, p. 113, 1954.

(148) Ziegler, H. "On the concept of elastic stability" Advances in Appl. Mech., IV, Academic Press, New York, 1956.

ADDITIONAL REFERENCES

(148a) Babcock, C.D. and Sechler, E.E. "The effect of initial imperfections on the buckling stress of cylindrical shells" NACA TN D-1510, 1962.

(149) Almroth, B.O. Holmes, A.M.C. and Brush, D.O. "An experimental study of the buckling of cylinders under axial compression" Experimental Mechanics, V.4, p.263, 1964.

(150) Bradshaw, R.R. "Some aspects of concrete shell buckling" Journ. A.C.I., V.60, No.3, 1963.

(151) Donnell, L.H. "Effect of imperfections on the buckling of thin cylinders with fixed edges under external pressure" 3rd U.S. Nat. Cong. Appl. Mech., A.S.M.E., p. 305, 1958.

(152) Donnell, L.H. "Shell theory" 4th Midwestern Conf. on Solid Mech., Univ. Texas, Texas, 1959.

(153) Donnell, L.H. "General thin shell displacement-strain relations" 4th U.S. Nat. Cong. Appl. Mech., A.S.M.E., p.529, 1962.

(154)

(155) Hoff, N.J.
Proc. 5th Int. Appl. Mech. Congress Munich, 1964.

(156) Kanemitsu, S. and Nojima, N.M. "Axial compression tests on thin circular cylinders" M.Sc. Thesis, Calif. Inst. Tech., 1939.

(157) Kloppel, K. and Jungbluth, O. "A contribution to the Durschlag problem of thin wall spherical shells" (in German) Stahlbau, V.22, p.121, 1953.

(158) Lundgren, H. "Stability tests on cylindrical reinforced concrete shells" (in Danish) Ingeniøruidenskabelige Shrifter, No.5, Copenhagen, 1945.

(159) Morice, P.B. "Research on shell structures" Proc. Shell Roof Symposium, 1952, London, 1954.

(160) Novozhilov, V.V. "The theory of thin shells"

(161) Sobey, A.J. "The buckling of an axially loaded circular cylinder with initial imperfections" R.A.E. Tech. Rpt., 64016, Sept. 1964.

(162) Tennyson, R.C. "A note on the classical buckling load of circular cylindrical shells under axial compression" J. A.I.A.A., Vol.1, p.475, 1963.

(163) Vlason, V.S. (Wlassow, W.S.) "Allgemeine Schalen theorie und ihre Anwendung in der Technik" Academie-Verlag, Berlin, 1958.

(164) "'Darvic' and 'Flovic' vinyl foil and sheets" Imperial Chemical Industries Ltd., May 1963.